Carderock Division
Naval Surface Warfare Center
Bethesda, MD 20084-5000

CRDKNSWC-TR-61-CR-94/06 September 1994

Survivability, Structures, and Materials Directorate
Technical Report

Deformation Limits on Two-Parameter Fracture Mechanics in Terms of Higher Order Asymptotics

by
D.L. Crane and T.L. Anderson, Texas A&M University

DTIC
ELECTE
DEC 2 8 1994
S D
F

19941223 060

Approved for public release; distribution is unlimited.

DTIC QUALITY INSPECTED 1

CARDIVNSWC-TR-61-CR-94/06 Deformation Limits on Two-Parameter Fracture Mechanics in Terms of Higher Order Asymptotics

ABSTRACT

Loss of constraint, which has been observed in various laboratory specimens, is caused by the interaction of crack tip plasticity with free boundaries. When this occurs, toughness is geometry dependent, and classical single-parameter fracture mechanics is no longer valid. A number of researchers have addressed constraint loss by introducing a second parameter into fracture mechanics methodologies. There are instances, however, when even two-parameter fracture theory breaks down.

This report addresses the limitations of two-parameter fracture mechanics. We performed an asymptotic analysis of the general power series representation of the crack tip stress potential in an elastic plastic material that obeys a Ramberg-Osgood constitutive law. Expansion of the power series over a substantial number of terms yields only three independent coefficients for low- and medium-hardening materials. The first independent coefficient is uniquely related to the J-integral, as Hutchinson, Rice and Rosengren discovered over 25 years ago. The second and third independent coefficients, K_2 and K_4, are a function of geometry and loading level. A two-parameter theory implies that the crack tip stress fields have two degrees of freedom, but the asymptotic analysis implies that *three* parameters are required to characterize near-tip conditions. Thus two-parameter fracture theory is a valid engineering model only when there is an approximately unique relationship between K_2 and K_4.

We performed elastic-plastic finite element analyses on several geometries and evaluated K_2 and K_4 as a function of deformation level. A reference two-parameter solution (which gives a unique relationship between K_2 and K_4) was provided by the modified boundary layer (MBL) geometry with an applied Mode I stress intensity factor, K_I, and various T stress values. The MBL configuration simulates a crack in an infinite body. The finite geometries we considered were the single edge notched bend (SENB), single edge notched tension (SENT), double edge notched tension (DENT), and center cracked tension (CCT) specimens. Crack length-to-width (a/W) ratios of 0.1, 0.5 and 0.9 were studied.

Results indicate that the near tip stresses in all but the deeply cracked SENB (a/W = 0.5, 0.9) and SENT (a/W = 0.9) lend themselves to a two-parameter characterization. However, the deeply cracked SENB and SENT specimens maintain a high level of constraint to relatively large deformation levels. Thus single-parameter fracture mechanics is fairly robust for these high constraint geometries, but two-parameter theory is of little value when constraint loss eventually occurs. On the other hand, in low constraint geometries such as the CCT panel and shallow notched SENB specimens, the departure from single-parameter theory is almost immediate, but the deformation evolves according to two-parameter theory (i.e., K_2 and K_4 maintain a nearly unique relationship).

Codes

Dist | Avail and / or Special

A-1

TABLE OF CONTENTS

TABLE OF CONTENTS (continued)

LIST OF FIGURES

LIST OF FIGURES (continued)

LIST OF FIGURES (continued)

LIST OF FIGURES (continued)

LIST OF FIGURES (continued)

LIST OF FIGURES (continued)

LIST OF TABLES

ADMINISTRATIVE INFORMATION

The work reported herein was funded under the Elastic-Plastic Fracture Mechanics of LWR Alloys Program at the Annapolis Detachment, Carderock Division, Naval Surface Warfare Center, Contract number N61533-92-K-0030. The Program is funded by the U.S. Nuclear Regulatory Commission under Interagency Agreement RES-93-002, FIN J6036. The Technical Program monitor is Dr. S.N. Malik at the USNRC. Technical monitoring of the contract was performed by Dr. Richard E. Link (CDNSWC 614).

CHAPTER I

INTRODUCTION

Since the introduction of what is known today as single parameter linear elastic fracture mechanics (LEFM) in the early to mid twentieth century [1-6], the focus of research in this discipline has had two primary objectives. First, it was necessary to apply the methodology known as fracture mechanics to real world problems. Standards have evolved to ensure that this was done in a systematic way. Second, within the original methodology, simplifying assumptions (e.g. linear elastic, single parameter, boundaries far removed from crack-tip, etc.) were made to make the problems mathematically more tractable. As issues such as plasticity, crack growth, and finite geometries came to being, the theory behind the original methodology had to be changed to include effects that result as a consequence of these issues.

Through the nineteen-sixties and early seventies, much attention was focused on the aspect of crack-tip plasticity. Several works [7-9] were completed which extended the idea of single parameter fracture mechanics to materials that exhibit nonlinear constitutive relations.

The combination of improved computer hardware and computerized finite element techniques in the seventies to mid-eighties enabled numerical modeling of elastic and limited plastic crack-tip problems. It was at this time that the previously pure analytic techniques could be compared with numerical results.

The increase in both speed of central processing units (CPU's) and accessible memory of computers in the late eighties and early nineties made it possible to numerically model complex geometries and include plasticity aspects. Although the theoretical methodology seemed to benefit from the increased computational capabilities developed through the eighties, the majority of the test standards are based on the original analytical work of the forties through the sixties [10-12].

Constraint has become an important issue in the transfer of fracture

---

The Journal Model is *Theoretical and Applied Fracture Mechanics.*

mechanic laboratory results to structural applications. The loss of constraint resulting from the development of plastic fields and their interaction with near tip finite boundaries found in many laboratory specimens and structures has led to studies whose objectives were to quantify the loss.

The original theoretical work in fracture mechanics avoided these issues by assuming a field characterized by a single parameter in which structural boundaries were far removed from the crack-tip. Most recently, attempts have been made to account for the constraint issue by introducing a second parameter to the methodology [13-20]. Several studies [21-30] had for their objectives, the idea of quantifying the limits of the single parameter methodology, but to the author's knowledge, no attempt has been made to determine the limits of the two-parameter methodology. It is the author's intent to quantify the applicability of the present two-parameter methodologies by means of higher order terms in the general power series representation of the stress potential.

1.1 Present Status of Problem

The original work of Williams [4] was based on an asymptotic analysis of the general power series representation for the stress potential near the tip of an infinitely sharp notch,

$$\hat{\chi}(\hat{r},\theta,\lambda)=\hat{r}^{\lambda+1}\Big[c_1\sin\{(\lambda+1)\theta\}+c_2\cos\{(\lambda+1)\theta\} +c_3\sin\{(\lambda-1)\theta\}+c_4\cos\{(\lambda-1)\theta\}\Big] \tag{1.1}$$

where $\hat{}$ indicates the dimensional quantity. This, combined with a linear constitutive relation, was used with small strain theory to obtain the pseudo eigenvalue λ. The boundary conditions for the crack problem are satisfied for the infinite sequence of values $\lambda = n/2$ where $n = 1, 2, 3, \ldots$. Williams was able to determine the series representation of the stress field from the potential as given by

$$\hat{\sigma}_{ij}(\hat{r},\theta)=\sum_{n=-1}^{\infty}A_n\hat{\sigma}_{ij}^{n}(\theta)\hat{r}^{\frac{n}{2}} \tag{1.2}$$

where $\hat{\sigma}_{ij}^{n}$ are angular functions and A_n are related to the multiplicative constants c_i. Williams was able to characterize the stress field up the multiplicative constants A_n.

At the same time Williams was performing his asymptotic analysis, Irwin [5] was also analyzing crack-tip fields in linear media. Irwin's approach utilized the complex stress potential of Westergaard [6],

$$F=\mathrm{Re}\,\bar{\bar{Z}}(z)+y\,\mathrm{Im}\,\bar{Z}(z). \tag{1.3}$$

By taking

$$Z(z)=\frac{\sigma}{\left[1-(a/z)^2\right]^{1/2}} \tag{1.4}$$

the stress field for a central straight crack located on the x-axis in an infinite plate with a biaxial field of tension, σ, could be determined. The corresponding Cartesian components for the first symmetric term in the near tip stress fields for this and Williams method are given as

$$\begin{aligned}
\sigma_{xx}(r,\theta)&=\frac{c_1}{\sqrt{2\pi r}}\cos\left\{\frac{\theta}{2}\right\}\left[1-\sin\left\{\frac{\theta}{2}\right\}\sin\left\{\frac{3\theta}{2}\right\}\right];\\
\sigma_{yy}(r,\theta)&=\frac{c_1}{\sqrt{2\pi r}}\cos\left\{\frac{\theta}{2}\right\}\left[1+\sin\left\{\frac{\theta}{2}\right\}\sin\left\{\frac{3\theta}{2}\right\}\right];\\
\sigma_{xy}(r,\theta)&=\frac{c_1}{\sqrt{2\pi r}}\cos\left\{\frac{\theta}{2}\right\}\sin\left\{\frac{\theta}{2}\right\}\sin\left\{\frac{3\theta}{2}\right\}.
\end{aligned} \tag{1.5}$$

Although the angular variation of the crack-tip stress fields found by Irwin were identical to those obtained by Williams, Irwin was able to relate the first multiplicative constant in the stress potential to the far field boundary conditions. This constant known today as the stress intensity factor (K) is the

basis for single parameter linear elastic fracture mechanics and is given here as $K = \sigma\sqrt{\pi a}$ for the central crack in an infinite plate.

Since the initiation of LEFM, the framework for a multi-parameter methodology was available but practitioners chose to ignore the higher order terms in the stress field. Irwin was the first to notice empirically the importance of the higher order terms. When comparing photo elastic representations of stress fields to his analytic predictions, a discrepancy was found in the stress parallel to the crack. This discrepancy, as shown by Sih [31] theoretically, is now known as the *T*-stress. It is the second term in the Williams general power series expansion. This term gives zero contribution to the opening mode stress but exists as a constant, hence no angular variation in the stress parallel to the crack plane.

Hutchinson [7] used the asymptotic approach of Williams in his analysis of a Ramberg-Osgood power-law hardening material,

$$\frac{\hat{\varepsilon}_{ij}}{\varepsilon_o} = (1+\nu)\frac{\hat{\sigma}_{ij}}{\sigma_o} - \nu\frac{\hat{\sigma}_{kk}}{\sigma_o}\delta_{ij} + \frac{3}{2}\alpha\left(\frac{\hat{\sigma}_e}{\sigma_o}\right)^{n-1}\frac{\hat{S}_{ij}}{\sigma_o}. \tag{1.6}$$

Here ν is poisson's ratio, σ_o is the yield stress, $\hat{\sigma}_e$ is the effective stress, $\hat{S}$ is the deviatoric stress, ε_o is the 2% offset yield strain, and α is a fitting parameter. Hutchinson was able to numerically determine the angular variation of the first term in the series representation of the stress field as it is derived from the stress potential and given by

$$\hat{\sigma}_{ij}(r,\theta) = A_1\hat{\sigma}_{ij}^1(\theta)r^{s_1}. \tag{1.7}$$

Concurrently, Rice and Rosengren [8] were using the asymptotic approach in power-law hardening materials. The first multiplicative constant was related to the far field boundary conditions through Rice's [9] path independent *J*-integral and is given by

$$A_1 = \sigma_o\left(\frac{\alpha\sigma_o\varepsilon_o I_n}{J}\right)^{s_1}. \tag{1.8}$$

This work extended the methodology of single parameter fracture mechanics from linear elastic materials to those that behave according to deformation type plasticity.

The main assumption of this theory was the description of the crack-tip stress field by a single parameter, namely the first multiplicative factor in the general power series representation of the stress potential.

The first attempt to account for higher order asymptotic terms in power-law hardening materials was provided by Yaochen and Wang [13]. They carried out a complete two term asymptotic analysis and were able to determine using a fourth order numerical Runge-Kutta method the angular variation of the second term in the stress potential. Yaochen et al. were able to determine the second multiplicitive constant by comparing the two term analytic solution to finite element results obtained by Shih and German [24] and Needleman and Tvergaard [25] for a single edge notched bend bar (SENB), single edge crack panel (SECP), and a center cracked panel (CCP) having a/W ratios from 0.5 to 0.9 and hardening exponents of 3, 10, and ∞.

Yaochen et al. concluded that the second coefficient of the asymptotic field changes with specimen geometry and development of the plastic zone. As a direct result, the second multiplicative factor K_2 was proposed as a second parameter, necessary in some instances to characterize the stress field at the crack-tip. In so doing, Yaochen et al. introduced the idea of two-parameter fracture mechanics.

Sharma and Aravas [14] expanded on the work of Yaochen et al. by solving for the second asymptotic term in both plane strain and plane stress. Sharma et al. solved the problem in a different manner then that of Yaochen. The two in-plane equilibrium equations and the three linear strain displacement relations were solved using finite elements. The asymptotic results were verified with full field finite element calculations. The full field calculations were based on the boundary layer method outlined by McMeeking [21], and Rice and Tracey [32]. In their work, they applied displacements corresponding to the first Williams term to the annular boundary of the crack-tip region. The plastic fields that result correspond to those which would be expected at the tip of a crack under high constraint for which all boundaries were far removed. These results have become known as

the small scale yielding solution (SSY). The plane strain results obtained for the second asymptotic term were identical to those of Yaochen.

O'Dowd and Shih [15,16] address what has become known as the difference field in an alternate manner. O'Dowd et al. argue that the crack-tip stress field could be expressed as

$$\sigma_{ij}(r,\theta) = \sigma_{ij}^{SSY}(r,\theta) + Q\delta_{ij}. \tag{1.9}$$

Here the stress field has been normalized by σ_o. They show the difference field represented here by Q to be hydrostatic in nature in the forward sector of the crack out to a normalized radius $\left(i.e.,\ r = \frac{\hat{r}\sigma_o}{J}\right)$ of about ten. The magnitude of Q is determined by taking the difference in the opening mode stress on the crack plane between a finite body and that for the SSY solution. The difference between these fields is taken at a predetermined location in the forward sector generally, $\theta = 0$ and $r = 2$. Although strictly speaking this is not theoretically rigorous, it seems to be somewhat robust.

Xia, Wang and Shih [17] and Yang, Chao and Sutton [18,19] expand the asymptotic analysis for a power hardening material to the fifth term. In each study, the strain hardening exponent was varied to determine which term would contain the first elastic field. In the analysis, only three amplitudes could be prescribed independently. For the appropriate choice of the independent amplitudes, it was possible to reproduce near tip fields representative of a broad range of crack-tip constraints. The higher order terms obtained in the studies collectively describe an approximately spatially uniform hydrostatic stress field. These results lend support to the suggestion given by O'Dowd and Shih [15,16] that Q could be introduced as a second fracture parameter that quantifies the near tip triaxiality.

Anderson and Dodds [33], Dodds, Anderson and Kirk [34], and Anderson and Dodds [35] use a micro mechanics approach to address the constraint issue. Unlike the afore mentioned work generally based on continuum mechanics, Anderson et al. base their model on a local criterion for cleavage failure. The model assumes that cleavage fracture is controlled by the volume of material at the crack-tip that is subject to a high stress level; the

larger the stressed volume, the higher the probability that cleavage will initiate from a critical microstructural feature. The loss of constraint in finite bodies tends to reduce the volume over which the higher stresses preside. As a result, one finds it necessary to apply a higher J value to a finite body to obtain the same stressed volume found in an infinite body at a lower J value.

The ratio of the finite body J value to the corresponding infinite body value defined as J_o is determined by the ratio of volumes contained within similar principle stress contours. This ratio can be thought of as a scaling factor that enables one to obtain a fracture toughness from one size specimen and then scale it so it corresponds to that which would be obtained from an infinite body or some other geometry. This approach has enabled the correction of fracture data which was affected by the loss of constraint common in many laboratory specimens.

Why should one be interested in the deformation limits on two-parameter fracture mechanics? The stress field characterization by a single parameter breaks down, for example, when free boundaries impinge on the crack-tip. The reduced crack-tip constraint associated with these free boundaries results in a lowering of the crack-tip stresses. Data presented by Sorem [36] shows an increase in the apparent elastic-plastic fracture toughness (J_C) for specimens with shallow cracks when tested in the transition region.

In the transition region, the fracture mechanism is changing from fracture by cleavage which is predominately stress controlled to that by ductile rupture which tends to be strain controlled. The apparent increase in toughness results from the loss of crack-tip constraint. Cleavage failure occurs when the stress over some small but measurable crack-tip volume attains a value sufficient to trigger the failure mechanism. Therefore, for structures that exhibit lower crack-tip constraint, the applied loading must be greater to produce the same critical crack-tip stresses. The associated increase in toughness is analogous to the increase observed when changing from plane strain to plane stress.

On the opposite end of the transition region and on the upper shelf were ductile rupture governs failure, Joyce [37] has shown that the loss of constraint associated with near tip finite boundaries has little influence on the toughness measured at the initiation of ductile crack growth (J_{Ic}). The data

does indicate that the loss of constraint influences the shape of the R-curve, or more specifically the apparent tearing modulus. The data shows a somewhat linear relation between the tearing modulus (measured at a fixed crack extension) and constraint measured in terms of the Q parameter introduced by O'Dowd and Shih [15,16].

The initiation of ductile fracture occurs as a result of void nucleation around second phase particles and is followed by void growth until the voids coalesce. Argon, Im and Safoglu [38] have argued that the initiation of voids around second phase particles occur at a critical combination of the hydrostatic and effective stress. Since the loss of constraint has little effect on the value of J_{Ic}, one could postulate the effective stress which depends on the maximum differences in the principle stresses is more important than the hydrostatic stress in the void nucleation process. A simple examination of Mohr's circle demonstrates that the effective stress can remain constant for any value of the hydrostatic component of the stress field.

Rice and Tracy [39] have also shown that void growth is dependent on the principle stresses and strain rate. Here the absolute magnitude of the principle stress components are decreased with a reduction of the hydrostatic stress. Since the void growth process appears to be dependent on the magnitude of the principle stresses, this could account for the dependence of the R-curve shape on the degree of crack tip constraint associated with a given specimen geometry. It would appear that the effective stress ahead of the crack-tip is sufficient (even with small decreases in the hydrostatic stress associated with loss of constraint) to initiate void nucleation and therefore void growth and coalescence are the important stages of ductile fracture as it relates to crack-tip constraint.

1.2 Research Objective

As is apparent, fracture toughness measures are dependent on the degree of constraint to which a crack-tip is subjected. The current method for dealing with the issue of constraint is to introduce a second parameter which corrects the stress level on the crack plane to agree with that measured numerically. The second parameter, along with the first represent, a two

dimensional failure locus. Stress states that correspond to points within the locus are safe while points outside the locus are subject to fracture.

There are three two-parameter methodologies at present. Each of the methodologies use the *J*-integral to quantify the deformation of fracture. The difference in the three methodologies is in the definition of the second parameter. The second parameter in one sense or another is a measure of the hydrostatic shift in the crack plane stresses associated with changes in the degree of constraint relative to that of high constraint or the small scale yielding model. One approach uses the value of the elastic *T*-stress just outside the plastic zone to measure constraint, while another method uses the difference between the normal stress to the crack plane for small scale yielding and the stress measured in a finite body at a fixed location on the crack plane. This difference is known as the *Q*-stress. Although the *Q*-stress is not theoretically rigorous in nature it appears to be somewhat robust in its application. The third two-parameter methodology is based on the second coefficient in the general power series expansion of the stress field. This method although being more theoretically rigorous suffers because it is only applicable for a Ramberg-Osgood constitutive law. The definition of the second parameter is in itself not that important as long as it is applied in a self consistent manner. However, the *T*-stress methodology breaks down with increased plasticity.

The objective of this proposed dissertation research is to evaluate the deformation limits on two-parameter fracture mechanics as defined by higher order asymptotic terms in nonlinear crack-tip stress fields that are influenced by geometric and/or material constraints.

1.3 Proposed Research Program

The deformation limits of two-parameter elastic-plastic fracture mechanics will be studied by comparing the amplitudes in the general elastic-plastic power series representations for stresses within the plastic zones for two-parameter plastic fields with those for multi-parameter plastic fields.

The two-parameter plastic field which will be used for this study is based on the solution of the modified boundary layer (MBL). Consider a

cracked body in which the plastic zone is well contained within an elastic region. If the plastic zone is small relative to any physical dimensions, the stresses in an annulus outside the plastic zone can be characterized by the general elastic power series representation developed by Williams [4]. The stresses in an annulus within the plastic zone but outside the finite strain zone can also be characterized by the general elastic-plastic power series representation developed by Hutchinson [7], Rice and Rosengren [8]. If we assume initially that the conditions in the far field lend to the characterization of the stresses in the elastic annulus by the first two terms in the Williams solution, then the fields in the plastic zone by definition are only dependent on the same two parameters. The amplitudes of the elastic-plastic power series themselves are dependent on these two parameters also. The amplitudes in the elastic-plastic series will be determined by matching the series with the numerical results obtained for the plastic zone in the MBL for a given pair of amplitudes in the elastic power series. Rice [9] has shown the first amplitude, K_1, in the elastic-plastic series is completely determined using the *J*-integral. Yang, Chao and Sutton [19] have shown that there are only two independent amplitudes (K_2, K_4) remaining in the first five terms of the series. The third and fifth amplitudes depend on the independent amplitudes in the following manner $K_3 = \frac{K_2^2}{K_1}$, $K_5 = \frac{K_2^3}{K_1^2}$. Therefore a unique relation between the two independent amplitudes $K_4 = K_4(K_2)$ can be established as a function of deformation level since the plastic fields are two-parameter fields and the first amplitude is determined completely by the *J*-integral.

The relationship between K_2 and K_4 for the two-parameter plastic field will be compared with a similar relationship obtained for several finite bodies. The characterization of the stress field in the finite bodies can depend in general on a number of parameters. Comparison of the K_2 and K_4 relation for the modified boundary layer with that for the finite bodies as shown schematically in Fig. 1.1 will indicate when a two-parameter characterization of the stress field is no longer appropriate. It is possible to construct a difference field between the two-parameter results and the finite body results as given by

$$\Delta\sigma_{ij}^{Error}(r,\theta) = \sigma_{ij}^{Finite\ Body}(r,\theta) - \sigma_{ij}^{MBL}(r,\theta)$$
$$= \Delta K_4 \sigma_{ij}^{4}(\theta) r^{s_4} + \frac{K_2 \Delta K_4}{K_1} \sigma_{ij}^{6}(\theta) r^{s_6} \tag{1.10}$$

where

$$\Delta K_4 = K_4^{Finite\ Body} - K_4^{MBL}. \tag{1.11}$$

When the error defined by this relation is greater then a set value the two-parameter solution is deemed no longer acceptable. The procedures which will be used to construct this comparison are outlined in the following section.

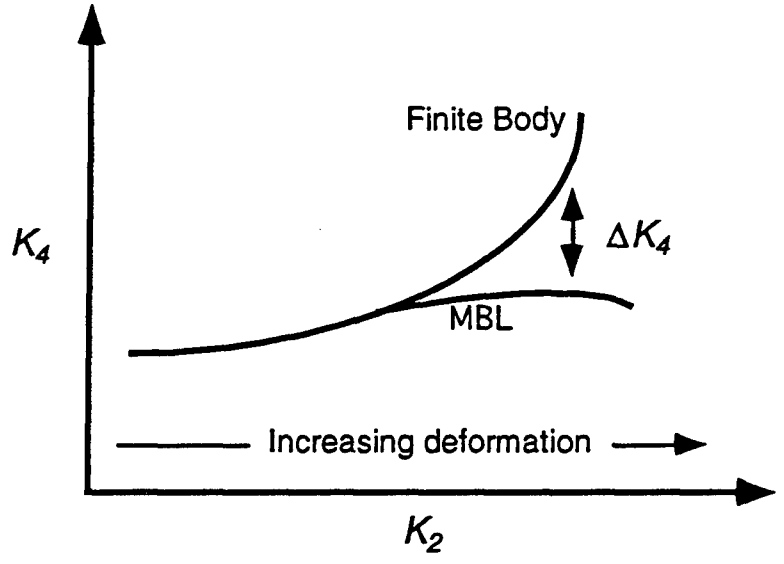

FIG. 1.1— Schematic relationship between K_2 and K_4.

CHAPTER II

PROCEDURES

The following sections contain the procedures that were followed to obtain the data necessary to compare the two-parameter fields with those of the finite geometries. The constitutive models for the analytic and numerical analysis are presented. The procedures used to solve the analytic problem are given as well as the numerical methods used to determine the finite geometry results.

2.1 Constitutive Models

The total strain at the tip of a crack in an elastic-plastic material is generally dominated by the plastic component. When unloading is insignificant, deformation plasticity has proved to be acceptable in crack-tip modeling. In the present work, deformation plasticity is used. The constitutive law used in the analytical study is based on Ramberg-Osgood behavior. The material for numerical studies is based on a linear plus power-law behavior (Ramberg-Osgood). The transition between the two segments is elliptic in nature. In the analytic study, the elastic strains in the Ramberg-Osgood relation do not enter the solution. Hence, the dominate strain at the crack-tip is assumed to be power-law in nature. Since the region of interest is near the crack-tip, both the Ramberg-Osgood and the linear plus power-law give equivalent results. The use of the linear plus power-law material is necessary in the modified boundary layer analysis to prevent premature yielding of material in the far field as well as material next to the boundary.

2.1.1 Analytical Constitutive Model

The Ramberg-Osgood total strain is assumed to be the sum of the elastic and plastic components as given by

$$\frac{\hat{\varepsilon}_{ij}^{Total}}{\varepsilon_o} = \frac{\hat{\varepsilon}_{ij}^{Elastic}}{\varepsilon_o} + \frac{\hat{\varepsilon}_{ij}^{Plastic}}{\varepsilon_o}. \tag{2.1}$$

Unless otherwise stated, ^ indicates the full dimensional quantity while the absence of the ^ indicates a normalized value. The elastic strain is assumed to follow Hooke's law and is given as

$$\frac{\hat{\varepsilon}_{ij}^{Elastic}}{\varepsilon_o} = (1+\nu)\frac{\hat{\sigma}_{ij}}{\sigma_o} - \nu\frac{\hat{\sigma}_{mm}}{\sigma_o}\delta_{ij}. \tag{2.2}$$

The plastic strain is given by the associative flow rule

$$\frac{\hat{\varepsilon}_{ij}^{Plastic}}{\varepsilon_o} = \frac{3}{2}\frac{\sigma_o}{\hat{\sigma}_e}\frac{\bar{\varepsilon}^{Plastic}}{\varepsilon_o}\frac{\hat{S}_{ij}}{\sigma_o} \tag{2.3}$$

where $\bar{\varepsilon}^{\text{Plastic}}$ is the equivalent effective plastic strain given by

$$\frac{\bar{\varepsilon}^{Plastic}}{\varepsilon_o} = \sqrt{\frac{2}{3}\frac{\hat{\varepsilon}_{ij}^{Plastic}}{\varepsilon_o}\frac{\hat{\varepsilon}_{ij}^{Plastic}}{\varepsilon_o}} \tag{2.4}$$

and $\hat{\sigma}_e$ is the effective stress (Mises stress) determined from

$$\frac{\hat{\sigma}_e}{\sigma_o} = \sqrt{\frac{3}{2}\frac{\hat{S}_{ij}}{\sigma_o}\frac{\hat{S}_{ij}}{\sigma_o}} \tag{2.5}$$

where $\hat{S}_{ij}$ is the deviatoric component of stress written as

$$\frac{\hat{S}_{ij}}{\sigma_o} = \frac{\hat{\sigma}_{ij}}{\sigma_o} - \frac{1}{3}\frac{\hat{\sigma}_{mm}}{\sigma_o}\delta_{ij}. \tag{2.6}$$

Substitution of Eq. (2.2-2.6) into Eq. (2.1) results in

$$\frac{\hat{\varepsilon}_{ij}^{Total}}{\varepsilon_o} = (1+\nu)\frac{\hat{\sigma}_{ij}}{\sigma_o} - \nu\frac{\hat{\sigma}_{mm}}{\sigma_o}\delta_{ij} + \frac{3}{2}\frac{\sigma_o}{\hat{\sigma}_e}\frac{\bar{\varepsilon}^{Plastic}}{\varepsilon_o}\frac{\hat{S}_{ij}}{\sigma_o}. \tag{2.7}$$

Noting that the normalized hydrostatic stress can be expressed as

$$\frac{p}{\sigma_0} = -\frac{1}{3}\frac{\hat{\sigma}_{mm}}{\sigma_0} = -\frac{1}{3(1-2\nu)}\frac{\hat{\varepsilon}_{mm}}{\varepsilon_0} \tag{2.8}$$

and the total deviatoric strain is given by

$$\frac{\hat{e}_{ij}^{Total}}{\varepsilon_o} = \frac{\hat{\varepsilon}_{ij}^{Total}}{\varepsilon_o} - \frac{1}{3}\frac{\hat{\varepsilon}_{mm}^{Total}}{\varepsilon_o}\delta_{ij}. \tag{2.9}$$

The deviatoric stress/strain relation can be expressed as

$$\frac{\hat{e}_{ij}^{Total}}{\varepsilon_o} = \left[(1+\nu) + \frac{3}{2}\frac{\sigma_o}{\hat{\sigma}_e}\frac{\bar{\varepsilon}^{Plastic}}{\varepsilon_o}\right]\frac{\hat{S}_{ij}}{\sigma_o} \tag{2.10}$$

and the equivalent effective deviatoric stress/strain relation is obtained by taking the inner product of the above relation to give

$$\frac{\bar{e}^{Total}}{\varepsilon_o} = \frac{2}{3}\left[(1+\nu) + \frac{3}{2}\frac{\sigma_o}{\hat{\sigma}_e}\frac{\bar{\varepsilon}^{Plastic}}{\varepsilon_o}\right]\frac{\hat{\sigma}_e}{\sigma_o} \tag{2.11}$$

where the total effective deviatoric strain is given by

$$\frac{\bar{e}^{\text{Total}}}{\varepsilon_o} = \sqrt{\frac{2}{3}\frac{\hat{e}_{ij}^{\text{Total}}}{\varepsilon_o}\frac{\hat{e}_{ij}^{\text{Total}}}{\varepsilon_o}}. \tag{2.12}$$

The equivalent plastic strain $\bar{\varepsilon}^{\text{Plastic}}$ is assumed to obey a power-law relation given by

$$\frac{\bar{\varepsilon}^{Plastic}}{\varepsilon_o} = \alpha \left(\frac{\hat{\sigma}_e}{\sigma_o} \right)^n \tag{2.13}$$

where n is the strain hardening exponent and α is a fitting parameter. Combining the above expressions results in the following expression for the total deviatoric Ramberg-Osgood strain in terms of stresses

$$\frac{\hat{e}_{ij}^{Total}}{\varepsilon_o} = \left[(1+\nu) + \frac{3}{2} \alpha \left(\frac{\hat{\sigma}_e}{\sigma_o} \right)^{n-1} \right] \frac{\hat{S}_{ij}}{\sigma_o}. \tag{2.14}$$

This constitutive relation is used in the asymptotic analysis.

2.1.2 Numerical Constitutive Model

The constitutive model used for the numerical study in the present research is a linear plus power-law (Ramberg-Osgood) with an elliptic transition region. The linear segment is necessary in the modified boundary layer to prevent boundary plasticity. The elliptic transition region provides continuity through the first derivative. The constitutive model is as follows

$$\frac{\hat{e}_{ij}^{Total}}{\varepsilon_0}=\begin{cases}[1+\nu]\dfrac{\hat{S}_{ij}}{\sigma_o} & for\ \dfrac{\hat{\sigma}_e}{\sigma_o}\le k_1;\\ \left[\dfrac{3}{2}\dfrac{\sigma_o}{\hat{\sigma}_e}\left\{\dfrac{\varepsilon_c}{\varepsilon_o}-R_1\sqrt{1-\left\{\dfrac{\dfrac{\hat{\sigma}_e}{\sigma_o}-\dfrac{\sigma_c}{\sigma_o}}{R_2}\right\}^2}\right\}+\dfrac{(2\nu-1)}{2}\right]\dfrac{\hat{S}_{ij}}{\sigma_o} & for\ k_1\le\dfrac{\hat{\sigma}_e}{\sigma_o}\le k_2;\\ \left[(1+\nu)+\dfrac{3}{2}\alpha\left(\dfrac{\hat{\sigma}_e}{\sigma_o}\right)^{n-1}\right]\dfrac{\hat{S}_{ij}}{\sigma_o} & for\ k_2\le\dfrac{\hat{\sigma}_e}{\sigma_o}.\end{cases}$$

(2.15)

where (ε_c,σ_c) are the coordinates of the center of the ellipse representing the transitional region in the effective stress/strain space and (R_1,R_2) are the ellipse's major and minor axis as shown in Fig. 2.1. These four degrees of freedom are determined by forcing continuity between segments up to the first derivative in the effective stress/strain space for fixed values of (k_1,k_2). The relation for the transition region is derived in a manner similar to that given in the previous section for the Ramberg-Osgood material except the equivalent effective plastic strain is derived from the equation of an ellipse given by

$$\left(\frac{\dfrac{\hat{\varepsilon}^{Total}}{\varepsilon_o}-\dfrac{\varepsilon_c}{\varepsilon_o}}{R_1}\right)^2+\left(\frac{\dfrac{\hat{\sigma}}{\sigma_o}-\dfrac{\sigma_c}{\sigma_o}}{R_2}\right)^2=1 \qquad (2.16)$$

from which the total uniaxial strain is obtained as

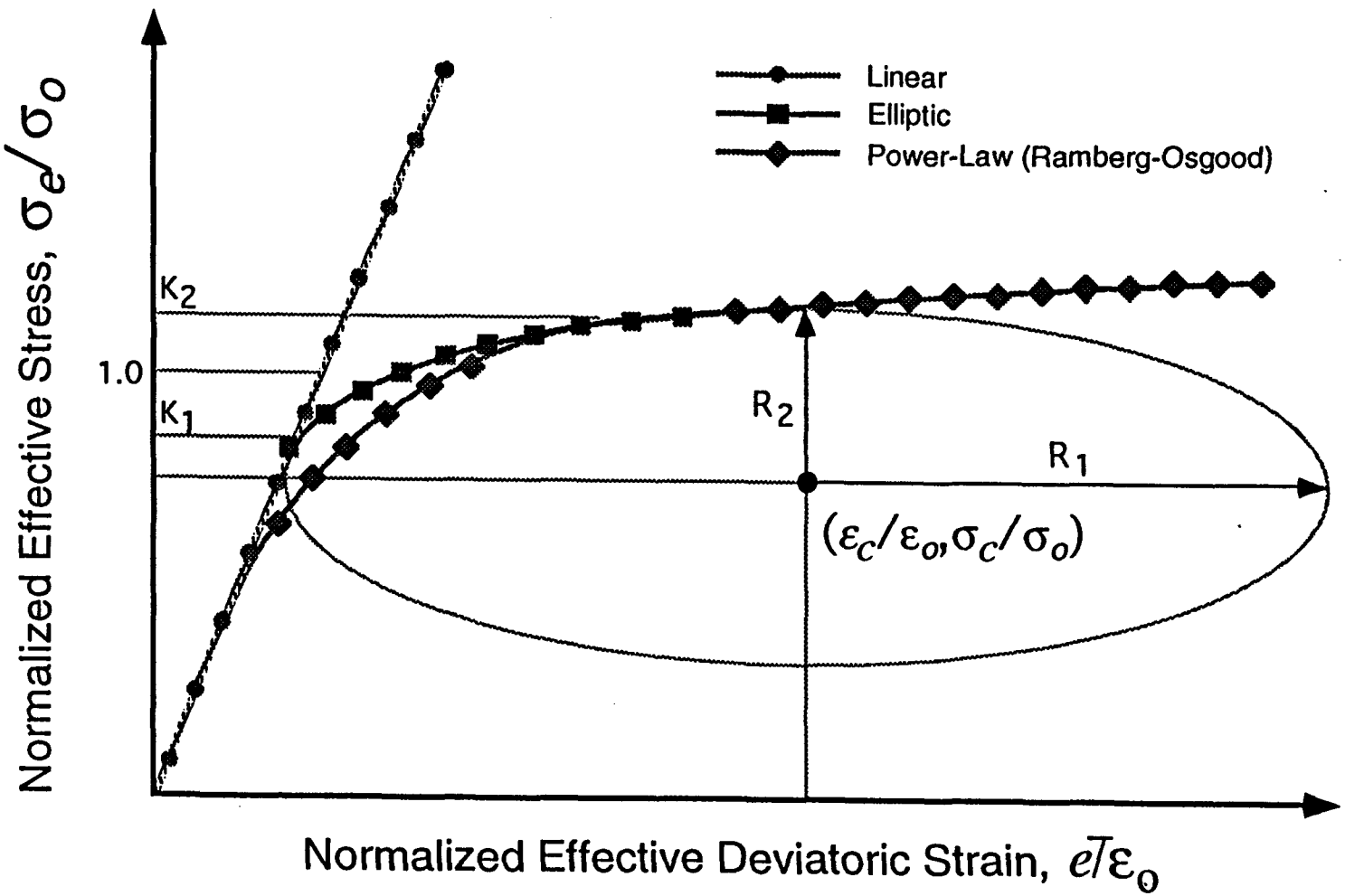

FIG. 2.1— Schematic of the effective linear, elliptic, and power-law constitutive relation.

$$\frac{\hat{\varepsilon}^{\text{Total}}}{\varepsilon_o} = \frac{\varepsilon_c}{\varepsilon_o} - R_1\sqrt{1-\left(\frac{\frac{\hat{\sigma}}{\sigma_o}-\frac{\sigma_c}{\sigma_o}}{R_2}\right)^2}\,. \tag{2.17}$$

The plastic strain is obtained by subtracting off the elastic portion of the strain

$$\frac{\hat{\varepsilon}^{\text{Plastic}}}{\varepsilon_o} = \frac{\varepsilon_c}{\varepsilon_o} - R_1\sqrt{1-\left(\frac{\frac{\hat{\sigma}}{\sigma_o}-\frac{\sigma_c}{\sigma_o}}{R_2}\right)^2} - \frac{\hat{\sigma}}{\sigma_o} \tag{2.18}$$

assuming the multiaxial plastic strain behaves similar in nature to the uniaxial relation, the following is obtained for the effective plastic strain

$$\frac{\bar{\varepsilon}^{\text{Plastic}}}{\varepsilon_o} = \frac{\varepsilon_c}{\varepsilon_o} - R_1\sqrt{1-\left(\frac{\frac{\hat{\sigma}_e}{\sigma_o}-\frac{\sigma_c}{\sigma_o}}{R_2}\right)^2} - \frac{\hat{\sigma}_e}{\sigma_o}. \tag{2.19}$$

Substitution of the previous expression into the deviatoric stress/strain relation derived in the preceding section based on the effective plastic strain results in the deviatoric stress/strain relation for the elliptic transition region as given above.

The displacement-based theory of finite elements as the name implies results in the determination of the displacements from which the strains are readily available. Given the strains, the stresses must be determined from the above constitutive equation. Since the elliptic and the power-law segments of the deviatoric stress/strain relations are nonlinear with respect to the deviatoric stress they must be solved numerically.

The solution of the constitutive equations is cast into the equivalent effective stress/strain space by taking the individual inner products as follows

$$\frac{2}{3}\frac{\hat{e}_{ij}^{Total}}{\varepsilon_o}\frac{\hat{e}_{ij}^{Total}}{\varepsilon_o}=\frac{4}{9}\beta^2\frac{3}{2}\frac{\hat{S}_{ij}}{\sigma_o}\frac{\hat{S}_{ij}}{\sigma_o} \tag{2.20}$$

where β is the expression in the square brackets in the constitutive equations. The equivalent effective deviatoric strain is obtained from the above expression and is given by

$$\frac{\bar{e}^{Total}}{\varepsilon_o}=\frac{2}{3}\beta\frac{\hat{\sigma}_e}{\sigma_o} \tag{2.21}$$

where $\hat{\sigma}_e$ is as previously defined and the effective deviatoric strain is given by

$$\frac{\bar{e}^{Total}}{\varepsilon_o}=\sqrt{\frac{2}{3}\frac{\hat{e}_{ij}^{\text{Total}}}{\varepsilon_o}\frac{\hat{e}_{ij}^{\text{Total}}}{\varepsilon_o}}. \tag{2.22}$$

The equivalent effective deviatoric stress/strain relations are given by

$$\frac{\bar{e}^{Total}}{\varepsilon_0}=\begin{cases}\dfrac{2}{3}[1+\nu]\dfrac{\hat{\sigma}_e}{\sigma_o} & for\ \dfrac{\hat{\sigma}_e}{\sigma_o}\le k_1;\\[2ex] \dfrac{2}{3}\left[\dfrac{3}{2}\dfrac{\sigma_o}{\hat{\sigma}_e}\left\{\dfrac{\varepsilon_c}{\varepsilon_o}-R_1\sqrt{1-\left\{\dfrac{\dfrac{\hat{\sigma}_e}{\sigma_o}-\dfrac{\sigma_c}{\sigma_o}}{R_2}\right\}^2}\right\}+\dfrac{(2\nu-1)}{2}\right]\dfrac{\hat{\sigma}_e}{\sigma_o} & for\ k_1\le\dfrac{\hat{\sigma}_e}{\sigma_o}\le k_2;\\[2ex] \dfrac{2}{3}\left[(1+\nu)+\dfrac{3}{2}\alpha\left(\dfrac{\hat{\sigma}_e}{\sigma_o}\right)^{n-1}\right]\dfrac{\hat{\sigma}_e}{\sigma_o} & for\ k_2\le\dfrac{\hat{\sigma}_e}{\sigma_o}.\end{cases} \tag{2.23}$$

The linear equation is solved directly and the nonlinear equations are solved using Newton's method. The above equations are rearranged to obtain

$$f\left(\frac{\hat{\sigma}_e}{\sigma_o}\right)=\frac{2}{3}\beta\frac{\hat{\sigma}_e}{\sigma_o}-\frac{\bar{e}^{Total}}{\varepsilon_o} \tag{2.24}$$

with the Jacobian given by

$$\frac{\partial f\left(\frac{\hat{\sigma}_e}{\sigma_o}\right)}{\partial\left(\frac{\hat{\sigma}_e}{\sigma_o}\right)}=\begin{cases}\dfrac{2}{3}[1+\nu] & for\ \dfrac{\hat{\sigma}_e}{\sigma_o}\le k_1;\\[2ex] \left[\left\{\dfrac{R_1}{R_2}\left(1-\left\{\dfrac{\frac{\hat{\sigma}_e}{\sigma_o}-\frac{\sigma_c}{\sigma_o}}{R_2}\right\}^2\right)^{-\frac{1}{2}}\left\{\dfrac{\frac{\hat{\sigma}_e}{\sigma_o}-\frac{\sigma_c}{\sigma_o}}{R_2}\right\}\right\}+\dfrac{(2\nu-1)}{3}\right] & for\ k_1\le\dfrac{\hat{\sigma}_e}{\sigma_o}\le k_2;\\[2ex] \left[\dfrac{2}{3}(1+\nu)+n\alpha\left(\dfrac{\hat{\sigma}_e}{\sigma_o}\right)^{n-1}\right] & for\ k_2\le\dfrac{\hat{\sigma}_e}{\sigma_o}.\end{cases} \tag{2.25}$$

Once the equivalent stress has been determined, the deviatoric stress can be calculated by inverting the deviatoric form of the constitutive equations

$$\frac{\hat{S}_{ij}}{\sigma_o}=\frac{1}{\beta}\frac{\hat{e}_{ij}^{\text{Total}}}{\varepsilon_o} \tag{2.26}$$

and finally, the total stress is calculated using

$$\frac{\hat{\sigma}_{ij}}{\sigma_o}=\frac{\hat{S}_{ij}}{\sigma_o}+\frac{1}{3(1-2\nu)}\frac{\hat{\varepsilon}_{ij}^{\text{Total}}}{\varepsilon_o}\delta_{ij}. \tag{2.27}$$

2.1.2.1 Material Stiffness

The material stiffness is calculated by differentiating the deviatoric stresses with respect to each of the deviatoric strains. It should be noted that from the above expression, the following relation may be obtained

$$\beta = \frac{3}{2}\frac{\bar{e}^{\text{Total}}}{\varepsilon_o}\frac{\sigma_o}{\hat{\sigma}_e}. \tag{2.28}$$

Substituting this expression for beta and differentiating the deviatoric stress with respect to the deviatoric strain results in

$$\partial \hat{S}_{ij} = \frac{2}{3}\partial\left\{\frac{\hat{\sigma}_{\text{e}}}{\bar{e}^{\text{Total}}}\hat{e}_{ij}^{\text{Total}}\right\} = \frac{2}{3}\left[\frac{\hat{\sigma}_{\text{e}}}{\bar{e}^{\text{Total}}}\partial\hat{e}_{ij}^{\text{Total}} + \left\{\frac{\partial\hat{\sigma}_{\text{e}}}{\bar{e}^{\text{Total}}} - \frac{\hat{\sigma}_{\text{e}}}{\left(\bar{e}^{\text{Total}}\right)^2}\partial\bar{e}^{\text{Total}}\right\}\hat{e}_{ij}^{\text{Total}}\right] \tag{2.29}$$

Using the effective stress/strain relations, the following may be obtained

$$\partial\hat{\sigma}_e = \gamma\partial\bar{e}^{\text{Total}} \tag{2.30}$$

where

$$\gamma = \begin{cases} \dfrac{3E}{2(1+\nu)} & for\ \dfrac{\hat{\sigma}_e}{\sigma_o} \le k_1; \\ E\left[\left\{\dfrac{R_1}{R_2}\left(1-\left\{\dfrac{\dfrac{\hat{\sigma}_e}{\sigma_o}-\dfrac{\sigma_c}{\sigma_o}}{R_2}\right\}^2\right)^{-\frac{1}{2}}\left\{\dfrac{\dfrac{\hat{\sigma}_e}{\sigma_o}-\dfrac{\sigma_c}{\sigma_o}}{R_2}\right\}\right\}+\dfrac{(2\nu-1)}{3}\right]^{-1} & for\ k_1 \le \dfrac{\hat{\sigma}_e}{\sigma_o} \le k_2; \\ E\left[\dfrac{2}{3}(1+\nu)+n\alpha\left(\dfrac{\hat{\sigma}_e}{\sigma_o}\right)^{n-1}\right]^{-1} & for\ k_2 \le \dfrac{\hat{\sigma}_e}{\sigma_o}. \end{cases} \tag{2.31}$$

Differentiating the effective deviatoric strain results in

$$\partial \overline{e}^{\text{Total}} = \frac{2}{3}\frac{\hat{e}_{ij}^{Total}}{\overline{e}^{\text{Total}}}\partial \hat{e}_{ij}^{Total}. \tag{2.32}$$

Substitution into the previous expression and then into the derivative of the deviatoric stresses gives

$$\partial \hat{S}_{ij} = \frac{2}{3}\frac{\hat{\sigma}_e}{\overline{e}^{\text{Total}}}\left[\delta_{im}\delta_{jn}+\frac{2}{3}\frac{1}{\overline{e}^{\text{Total}}}\left\{\frac{\gamma}{\hat{\sigma}_e}-\frac{1}{\overline{e}^{\text{Total}}}\right\}\hat{e}_{mn}^{\text{Total}}\hat{e}_{ij}^{\text{Total}}\right]\partial \hat{e}_{mn}^{\text{Total}}. \tag{2.33}$$

The derivative of the deviatoric stress and strain may be written as

$$\begin{aligned} \partial \hat{S}_{ij} &= \partial \hat{\sigma}_{ij} - \frac{E}{3(1-2\nu)}\delta_{op}\delta_{ij}\partial \hat{\varepsilon}_{op}^{\text{Total}}, \\ \partial \hat{e}_{mn}^{\text{Total}} &= \left(\delta_{mo}\delta_{np}-\frac{\delta_{op}\delta_{mn}}{3}\right)\partial \hat{\varepsilon}_{op}^{\text{Total}}. \end{aligned} \tag{2.34}$$

Substitution of the previous results into the stiffness relation gives

$$\partial\hat{\sigma}_{ij} = \left\{ \frac{2}{3}\frac{\hat{\sigma}_e}{\bar{e}^{\text{Total}}} \left[\delta_{io}\delta_{jp} + \frac{2}{3}\frac{1}{\bar{e}^{\text{Total}}} \left\{ \frac{\gamma}{\hat{\sigma}_e} - \frac{1}{\bar{e}^{\text{Total}}} \right\} \hat{e}_{op}^{\text{Total}} \hat{e}_{ij}^{\text{Total}} \right] + \frac{1}{3}\left[\frac{E}{(1-2\nu)} - \frac{2}{3}\frac{\hat{\sigma}_e}{\bar{e}^{\text{Total}}} \right] \delta_{ij}\delta_{op} \right\} \partial\hat{e}_{op}^{\text{Total}}. \tag{2.35}$$

The material stiffness is updated incrementally in the user material subroutine.

2.1.2.2 Strain Energy Density

The strain energy density is computed for use in the *J*-integral calculations. The total strain energy density is obtained by integrating the increment of work per unit volume produced during deformation.

$$Strain\,Energy\,Density = SED = \int \hat{\sigma}_{ij} d\hat{\varepsilon}_{ij}^{Total}. \tag{2.36}$$

This may be rewritten in deviatoric form as

$$SED = \int \hat{\sigma}_{ij} d\hat{e}_{ij}^{Total} + \frac{3(1-2\nu)}{2E} p^2 \tag{2.37}$$

where p is the hydrostatic pressure as defined previously. The deviatoric stress/strain relations may be substituted into the above expression to obtain

$$SED = \begin{cases} \Omega_1(q)\Big|_0^p + \Omega_2(q)\Big|_0^{\hat{\sigma}_e} & for\ \dfrac{\hat{\sigma}_e}{\sigma_o} \le k_1; \\ \Omega_1(q)\Big|_0^p + \Omega_2(q)\Big|_0^{k_1\sigma_o} + \Omega_3(q)\Big|_{k_1\sigma_o}^{\hat{\sigma}_e} & for\ k_1 \le \dfrac{\hat{\sigma}_e}{\sigma_o} \le k_2; \\ \Omega_1(q)\Big|_0^p + \Omega_2(q)\Big|_0^{k_1\sigma_o} + \Omega_3(q)\Big|_{k_1\sigma_o}^{k_2\sigma_o} + \Omega_4(q)\Big|_{k_2\sigma_o}^{\hat{\sigma}_e} & for\ k_2 \le \dfrac{\hat{\sigma}_e}{\sigma_o}. \end{cases}$$

(2.38)

where the integrated quantities are given by

$$\Omega_i(q) = \frac{1}{E}\begin{cases} \dfrac{3(1-2\nu)}{2}q^2; \\ \dfrac{(1+\nu)}{3}q^2; \\ R_1R_2\sigma_o^2\left[\dfrac{1}{2}\sin^{-1}\left(\dfrac{\dfrac{q}{\sigma_o}-\dfrac{\sigma_c}{\sigma_o}}{R_2}\right) - \dfrac{1}{4}\sin\left\{2\sin^{-1}\left(\dfrac{\dfrac{q}{\sigma_o}-\dfrac{\sigma_c}{\sigma_o}}{R_2}\right)\right\}\right. \\ \qquad \left. -\dfrac{1}{R_2}\dfrac{\sigma_c}{\sigma_o}\sqrt{1-\left(\dfrac{\dfrac{q}{\sigma_o}-\dfrac{\sigma_c}{\sigma_o}}{R_2}\right)^2}\right] + \dfrac{(2\nu-1)}{6}q^2; \\ \dfrac{(1+\nu)}{3}q^2 + \dfrac{n}{n+1}\sigma_o^2\left(\dfrac{q}{\sigma_o}\right)^{n+1}. \end{cases}$$

(2.39)

The constitutive model, material stiffness and the strain energy density have be coded in FORTRAN user subroutine called UMAT. The user subroutine is included in Appendix A.

2.2 *Asymptotic Analysis*

The following section contains the procedures for the analytical solution for the potential, stress, strain, and displacement fields for a crack in an elastic-plastic material. The governing field equations are derived and then the solution technique is outlined.

2.2.1 *Derivation of Governing Field Equation*

A general power series expansion was chosen for the analytical representation of the near tip fields in the present work. The coordinate system of choice is of cylindrical type and is centered at the crack-tip as shown in Fig. 2.2. In the equations that follow, we nondimensionalize the radial distance from the crack-tip by means of the *J*-integral and material flow properties:

$$r \equiv \frac{\alpha \varepsilon_0 \sigma_0 \hat{r}}{J} \tag{2.40}$$

where $\hat{r}$ is the dimensional radial distance and r is the normalized distance. Note that J is the actual dimensional quantity—we do not nondimensionalize J in this derivation unless otherwise stated. Also, the stress potential, stress, strain, displacements, and strain energy density are normalized as follows:

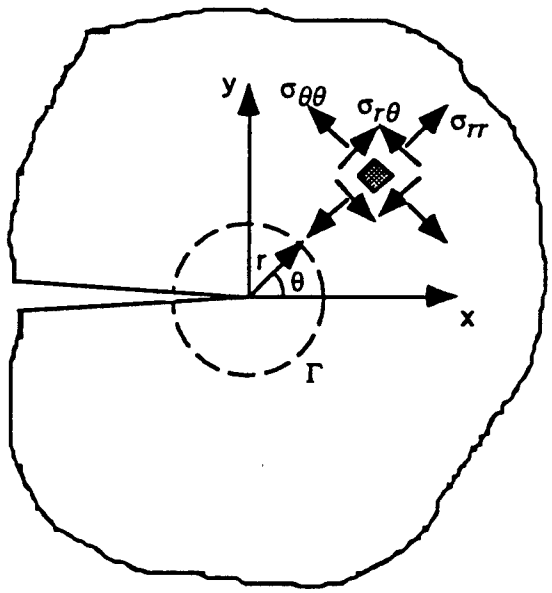

FIG. 2.2— Crack tip coordinate system.

$$\Phi(r,\theta)\equiv\frac{\hat{\Phi}(r,\theta)}{\sigma_o};\qquad \sigma_{ij}(r,\theta)\equiv\frac{\hat{\sigma}_{ij}(r,\theta)}{\sigma_o};$$

$$\varepsilon_{ij}(r,\theta)\equiv\frac{\hat{\varepsilon}_{ij}(r,\theta)}{\alpha\varepsilon_o};\qquad u_i(r,\theta)\equiv\frac{\hat{u}_i(r,\theta)}{\alpha\varepsilon_o};\tag{2.41}$$

$$W(r,\theta)\equiv\frac{\hat{W}(r,\theta)}{\alpha\sigma_o\varepsilon_o}$$

where σ_o is the flow stress, ε_o is the yield strain (σ_o/E) and α is a material constant that appears in the Ramberg-Osgood stress strain constitutive law, Eq. (2.14). Note that the dimensional stresses and actual strains are barred; unbarred stresses and strains are nondimensional unless otherwise specified.

The stress potential is expanded in powers of the radial coordinate as follows:

$$\Phi(r,\theta)=\sum_{m=1}^{\infty}K_m\phi^m(\theta)\,r^{s_m+2}\tag{2.42}$$

where K_m is the unknown amplitude of the m^{th} term, $\phi^m(\theta)$ is a dimensionless angular function to be determined, and s_m+2 is the unknown exponent of r. The term s_m can be thought of as a pseudo-eigenvalue in the sense that the formulation of this problem does not result in the traditional eigenvalue type. Here each term of the series is assumed to be separable in r and θ, but when combined in their totality, the resulting expression is no longer separable in the two in-plane coordinates. At this point it should also be mentioned that no formal proof exists establishing the completeness of this set of functions. In the case that the functions are complete, the series expansion represents the exact stress potential. Conversely, if the functions are not complete, the series is an approximation for the stress potential.

The stress components are derived to satisfy the polar form of the equilibrium equations

$$\frac{\partial \sigma_{rr}(r,\theta)}{\partial r} + \frac{1}{r}\frac{\partial \sigma_{r\theta}(r,\theta)}{\partial \theta} + \frac{\sigma_{rr}(r,\theta) - \sigma_{\theta\theta}(r,\theta)}{r} = 0$$
$$\frac{\partial \sigma_{r\theta}(r,\theta)}{\partial r} + \frac{1}{r}\frac{\partial \sigma_{\theta\theta}(r,\theta)}{\partial \theta} + \frac{2\,\sigma_{r\theta}(r,\theta)}{r} = 0 \qquad (2.43)$$

for the plane problem from the potential as

$$\sigma_{rr}(r,\theta) = \frac{1}{r}\frac{\partial \Phi(r,\theta)}{\partial r} + \frac{1}{r^2}\frac{\partial^2 \Phi(r,\theta)}{\partial \theta^2}$$
$$\sigma_{\theta\theta}(r,\theta) = \frac{\partial^2 \Phi(r,\theta)}{\partial r^2} \qquad (2.44)$$
$$\sigma_{r\theta}(r,\theta) = -\frac{\partial}{\partial r}\left(\frac{1}{r}\frac{\partial \Phi(r,\theta)}{\partial \theta}\right) = \frac{1}{r^2}\frac{\partial \Phi(r,\theta)}{\partial \theta} - \frac{1}{r}\frac{\partial^2 \Phi(r,\theta)}{\partial r \partial \theta}.$$

Substituting the power series expansion of the stress potential into Eq. (2.44) results in the following stresses

$$\sigma_{ij}(r,\theta) = \sum_{m=1}^{\infty} K_m \sigma_{ij}^m(\theta)\; r^{s_m} \qquad (2.45)$$

where

$$\sigma_{rr}^m(\theta) = \frac{d^2\phi_m(\theta)}{d\theta^2} + (s_m + 2)\,\phi_m(\theta)$$
$$\sigma_{\theta\theta}^m(\theta) = (s_m + 2)(s_m + 1)\,\phi_m(\theta) \qquad (2.46)$$
$$\sigma_{r\theta}^m(\theta) = -(s_m + 1)\frac{d\phi_m(\theta)}{d\theta}.$$

The expressions obtained for the stress field are then used to determine the Mises or effective stress

$$\sigma_e(r,\theta) = \left[\frac{3}{2} S_{ij}(r,\theta)\; S_{ij}(r,\theta)\right]^{\frac{1}{2}} \qquad (2.47)$$

where $S_{ij}(r,\theta)$ are the deviatoric stresses and are defined as follows

$$S_{ij}(r,\theta) = \sigma_{ij}(r,\theta) - \frac{1}{3}\sigma_{kk}(r,\theta)\delta_{ij}. \tag{2.48}$$

Here repeated indices are understood to be summed and δ_{ij} is the well known Kronecker delta whose value is $\delta_{ij}=1$ for $i=j$ and $\delta_{ij}=0$ when $i\neq j$. After substitution of the series representation of the stress fields, the deviatoric stresses may be written as

$$S_{ij}(r,\theta) = \sum_{m=1}^{\infty} K_m S_{ij}^m(\theta)\ r^{sm} \tag{2.49}$$

where

$$S_{ij}^m(\theta) = \sigma_{ij}^m(\theta) - \frac{1}{3}\sigma_{kk}^m(\theta)\delta_{ij}. \tag{2.50}$$

The deviatoric stresses are dependent on the out-of-plane normal stress $\sigma_{zz}(r,\theta)$ at this point so the third constitutive equation is solved to obtain the following relation for the out-of-plane normal stress

$$\sigma_{zz}(r,\theta) - \frac{\alpha}{\left[1 + \alpha\sigma_e^{n-1}(r,\theta)\right]}\varepsilon_{zz}(r,\theta) = \lambda(r,\theta)\left[\sigma_{rr}(r,\theta) + \sigma_{\theta\theta}(r,\theta)\right] \tag{2.51}$$

where

$$\lambda(r,\theta) = \frac{\left[\nu + \frac{\alpha}{2}\sigma_e^{n-1}(r,\theta)\right]}{\left[1 + \alpha\sigma_e^{n-1}(r,\theta)\right]}. \tag{2.52}$$

Here lambda is bounded by $\nu \le \lambda(r,\theta) \le 0.5$. At this point it is worth examining the situations for which the limiting values of λ are approached. First, for the case of an elastic material, $\alpha \to 0$ and $\lambda \to \nu$. Second, when a material is incompressible, $\nu \to 0.5$ and $\lambda \to 0.5$. Finally, when $\nu << \sigma_e^{n-1}$ as in a fully developed plastic region, $\lambda \to 0.5$. The use of the above expression

for the out-of-plane normal stress in the remaining analysis results in the ability to solve both the plane stress as well as the plane strain problem. In both cases σ_{zz} is taken as λ times the sum of the in-plane normal stresses. For the case of plane stress we set λ equal to zero and for plane strain we assume λ is 0.5. The latter is an assumption which makes the analysis somewhat neater, but will be checked after the full field results are obtained.

Introducing the deviatoric stresses in the effective stress, the following series representation is obtained

$$\sigma_e^2(r,\theta) = K_1^2 \sigma_{e_{11}}(\theta) r^{2s_1} \left[1 + \sum_{\ell=1}^{\infty} \left[\frac{2K_\ell}{K_1} \frac{\sigma_{e_{1\ell}}(\theta)}{\sigma_{e_{11}}(\theta)} r^{\Delta s_\ell} + \sum_{m=1}^{\infty} \frac{K_\ell K_m}{K_1^2} \frac{\sigma_{e_{\ell m}}(\theta)}{\sigma_{e_{11}}(\theta)} r^{\Delta s_\ell + \Delta s_m} \right] \right] \tag{2.53}$$

where

$$\sigma_{e_{\ell m}}(\theta) = \frac{3}{2} S_{ij}^{\ell}(\theta)\, S_{ij}^{m}(\theta). \tag{2.54}$$

Note that the above expression represents the coupling angular functions for the effective stress and have units of stress squared.

The next step in the analysis is to express the strains in terms of a power series by substituting the stresses into the constitutive relation. First, before this can be accomplished, the effective stress must be raised to the power *(n-1)*. Application of the binomial expansion

$$\left[1+f(r,\theta)\right]^n = 1 + nf(r,\theta)^1 + \frac{n(n-1)}{2!} f(r,\theta)^2 + \frac{n(n-1)(n-2)}{3!} f(r,\theta)^3 + \cdots \tag{2.55}$$

results in the following series representation for the expanded effective stress

$$\sigma_e^{n-1}(r,\theta) = K_1^{n-1}\sigma_{e_1}^{n-1}(\theta)r^{(n-1)s_1}\Big[1 + \sum_{\ell=2}^{\infty}\frac{K_\ell}{K_1}r^{\Delta s_\ell}\Big[F_\ell(\theta) + \sum_{m=2}^{\infty}\frac{K_m}{K_1}r^{\Delta s_m}$$
$$\Big[F_{\ell m}(\theta) + \sum_{n=2}^{\infty}\frac{K_n}{K_1}r^{\Delta s_n}\Big[F_{\ell mn}(\theta) + \sum_{o=2}^{\infty}\frac{K_o}{K_1}r^{\Delta s_o}[\cdots]\,]\,]\,]\,]\,] \tag{2.56}$$

where $F_{\ell mn\ldots}(\theta)$ are angular functions dependent on $\sigma_{e_{ij}}(\theta)$. The strains are obtained by introducing the above series expansions of the stress components into the constitutive equation. The series representation of the strains becomes

$$\varepsilon_{ij}(r,\theta) = \sum_{\ell=1}^{\infty}K_\ell\varepsilon_{ij}^{E(\ell)}(\theta)r^{t_\ell^E} + \sum_{\ell=1}^{\infty}\tilde{K}_\ell\varepsilon_{ij}^{P(\ell)}(\theta)r^{\tilde{t}_\ell^P} \tag{2.57}$$

where E indicates the term results from an elastic field and P from a plastic field. $\tilde{K}_\ell$ are functions of K_ℓ and the hardening exponent n. The exponents $t_\ell^{E,P}$ are functions of the stress exponents s_ℓ and the hardening exponent in the plastic case.

The displacement fields are readily available from the strain/displacement relations

$$\varepsilon_{rr}(r,\theta) = \frac{\partial u_r(r,\theta)}{\partial r}$$
$$\varepsilon_{\theta\theta}(r,\theta) = \frac{u_r(r,\theta)}{r} + \frac{1}{r}\frac{\partial u_\theta(r,\theta)}{\partial\theta} \tag{2.58}$$
$$\varepsilon_{r\theta}(r,\theta) = \frac{1}{2}\left[\frac{1}{r}\frac{\partial u_r(r,\theta)}{\partial\theta} + \frac{\partial u_\theta(r,\theta)}{\partial r} - \frac{u_\theta(r,\theta)}{r}\right].$$

The first relation can be integrated directly to obtain the expression for the radial displacement. The expression for the shearing strain can be rearranged by multiplying by two and dividing by r such that the terms containing the angular displacement may be combined under one common partial with

respect to the radial coordinate, $\frac{\partial(\ )}{\partial r}$. The resulting expression can then be integrated with respect to r to obtain the angular displacement. The resulting expressions for the displacement field are

$$u_r(r,\theta)=\int \varepsilon_{rr}(r,\theta)dr$$
$$u_\theta(r,\theta)=r\int\frac{1}{r}\left[2\varepsilon_{r\theta}(r,\theta)-\frac{1}{r}\frac{\partial u_r(r,\theta)}{\partial\theta}\right]dr. \tag{2.59}$$

The above series representation of the strain field can be substituted into the integrals to obtain

$$\begin{aligned} u_r(r,\theta) &= \sum_{\ell=1}^{\infty} K_\ell u_r^{E(\ell)}(\theta) r^{t_\ell^E+1} + \sum_{\ell=1}^{\infty} \tilde{K}_\ell u_r^{P(\ell)}(\theta) r^{\tilde{t}_\ell^P+1} \\ u_\theta(r,\theta) &= \sum_{\ell=1}^{\infty} K_\ell u_\theta^{E(\ell)}(\theta) r^{t_\ell^E+1} + \sum_{\ell=1}^{\infty} \tilde{K}_\ell u_\theta^{P(\ell)}(\theta) r^{\tilde{t}_\ell^P+1} \end{aligned} \tag{2.60}$$

where

$$u_r^{E,P(\ell)}(\theta)=\frac{\varepsilon_{rr}^\ell(\theta)}{t^{E,P(\ell)}+1}$$
$$u_\theta^{E,P(\ell)}(\theta)=\frac{1}{t^{E,P(\ell)}}\left[2\varepsilon_{r\theta}^\ell(\theta)-\frac{1}{t^{E,P(\ell)}+1}\frac{d\varepsilon_{r\theta}^\ell(\theta)}{d\theta}\right]. \tag{2.61}$$

The above expressions for the displacement field ignore rigid body displacements.

The final equation to be satisfied in the field problem is the polar form of the compatibility equation

$$\frac{1}{r}\frac{\partial^2}{\partial r^2}[r\varepsilon_{\theta\theta}(r,\theta)]+\frac{1}{r^2}\frac{\partial^2}{\partial\theta^2}[\varepsilon_{rr}(r,\theta)]-\frac{1}{r}\frac{\partial}{\partial r}[\varepsilon_{rr}(r,\theta)]-\frac{2}{r^2}\frac{\partial^2}{\partial r\partial\theta}[r\varepsilon_{r\theta}(r,\theta)]=0 \tag{2.62}$$

Substituting the series expansion of the strains into the Eq. (2.62) results in the following second order power series differential equation:

$$\sum_{\ell=1}^{\infty} K_\ell \Pi_\ell^E(\theta) r^{t_\ell^E - 2} + \sum_{\ell=1}^{\infty} \tilde{K}_\ell \Pi_\ell^P(\theta) r^{t_\ell^P - 2} = 0 \tag{2.63}$$

where

$$\begin{aligned} \Pi_\ell^{E,P}(\theta) = \frac{d^2}{d\theta^2}\varepsilon_{rr}^{E,P(\ell)}(\theta) - 2\left(t_\ell^{E,P}+1\right)\frac{d}{d\theta}\varepsilon_{r\theta}^{E,P(\ell)}(\theta) \\ + t_\ell^{E,P}\left(t_\ell^{E,P}+1\right)\varepsilon_{\theta\theta}^{E,P(\ell)}(\theta) - t_\ell^{E,P}\varepsilon_{rr}^{E,P(\ell)}(\theta). \end{aligned} \tag{2.64}$$

The second order differential equation is satisfied asymptotically (term by term) by solving the individual eigenvalue problems $\Pi_\ell^{E,P}(\theta) = 0$. Each of these second order equations is transformed into a fourth order ordinary differential equation in terms of $\phi^m(\theta)$:

$$\begin{aligned} C_4^m(\theta)\frac{d^4\phi^m(\theta)}{d\theta^4} + C_3^m(\theta)\frac{d^3\phi^m(\theta)}{d\theta^3} + C_2^m(\theta)\frac{d^2\phi^m(\theta)}{d\theta^2} \\ + C_1^m(\theta)\frac{d\phi^m(\theta)}{d\theta} + C_0^m\phi^m(\theta) + C_P^m(\theta) = 0 \end{aligned} \tag{2.65}$$

where

$$C_i^m(\theta) = L_i^m(\theta) + N_i^m(\theta) \tag{2.66}$$

and the coefficients are

$$\begin{aligned} N_i^m(\theta) &= N_i^m\left\{n, s_m, \phi^m(\theta), \phi^m(\theta)', \phi^m(\theta)'', \phi^m(\theta)'''\right\} \quad \text{(nonlinear)} \\ L_i^m(\theta) &= L_i^m\left\{n, s_m, s_\ell, \phi^\ell(\theta), \phi^\ell(\theta)', \phi^\ell(\theta)'', \phi^\ell(\theta)'''\right\} \quad \text{(linear)}. \end{aligned} \tag{2.67}$$

$C_P^m(\theta) = C_P^m\left\{n, s_\ell, \phi^\ell(\theta), \phi^\ell(\theta)', \phi^\ell(\theta)'', \phi^\ell(\theta)'''\right\}$ is the particular part of the differential equation and depends on the solution to previous fields as

designated by the indices ℓ. The differential equation corresponding to the first term of the series (*HRR* field) is homogeneous in $\phi^1(\theta)$ and s_1, and is nonlinear. The fields that follow are inhomogeneous (i.e. include coefficients that depend on solutions to previous fields) but are linear (i.e. $N_i^m(\theta)=0$ for $m>1$).

The solution to the above differential equation is subject to the following boundary conditions. Loading of the Crack in mode I results in the following four conditions. The first two are symmetry conditions on the crack plane. Since the stress state on either side of the crack plane must be identical, the stress potential must be an even function about $\theta=0$ and therefore odd derivatives of the potential are odd functions as given by

$$\frac{\partial^\ell \Phi(r,+\theta)}{\partial\theta^\ell} = (-1)^\ell \frac{\partial^\ell \Phi(r,-\theta)}{\partial\theta^\ell} \tag{2.68}$$

where $\ell = 0,1,2,3,\ldots$. This results in the conditions that

$$\begin{aligned} &\frac{\partial\Phi(r,0)}{\partial\theta} = 0 \quad \rightarrow \quad \sigma_{r\theta}(r,0)=0 \\ &\frac{\partial^3\Phi(r,0)}{\partial\theta^3} = 0. \end{aligned} \tag{2.69}$$

The second set of boundary conditions result from the stress free surface on the crack flank

$$\begin{aligned} &\sigma_{\theta\theta}(r,\pi)=0 \quad \rightarrow \quad \frac{\partial^2\Phi(r,\pi)}{\partial r^2}=0 \\ &\sigma_{r\theta}(r,\pi)=0 \quad \rightarrow \quad \frac{\partial\Phi(r,\pi)}{\partial\theta}=0. \end{aligned} \tag{2.70}$$

The above conditions on the stress potential put the following restrictions on the angular functions in its series representation:

$\theta = 0$:

$$\frac{d\phi^m(0)}{d\theta} = 0 \rightarrow \sigma^m_{r\theta}(0) = 0$$
$$\frac{d^3\phi^m(0)}{d^3\theta} = 0 \rightarrow \text{symmetry} \tag{2.71}$$

$\theta = \pi$:

$$\phi^m(\pi) = 0 \rightarrow \sigma^m_{\theta\theta}(\pi) = 0$$
$$\frac{d\phi^m(\pi)}{d\theta} = 0 \rightarrow \sigma^m_{r\theta}(\pi) = 0. \tag{2.72}$$

Combining these conditions with the above differential equations reduces the problem to determining the pseudo eigenvalues and corresponding angular functions (pseudo eigen functions) which satisfy the above boundary conditions. The solution of this problem leaves only the coefficients in the series expansion of the stress potential to be determined.

2.2.2 Numerical Solution of Governing Field Equation

The fourth order differential equation derived in the previous section (Eq. 2.65) was solved using a multiple shooting technique. The first step in the solution of the differential equation was to write it as a set of four equivalent first order equations coupled with a single first order equation for the eigenvalue as follows

$$
\begin{aligned}
\phi^{\ell}(\theta) &= Y_1^{\ell}(\theta) \\
\frac{d\phi^{\ell}(\theta)}{d\theta} &= \frac{dY_1^{\ell}(\theta)}{d\theta} = Y_2^{\ell}(\theta) \\
\frac{d^2\phi^{\ell}(\theta)}{d\theta^2} &= \frac{dY_2^{\ell}(\theta)}{d\theta} = Y_3^{\ell}(\theta) \\
\frac{d^3\phi^{\ell}(\theta)}{d\theta^3} &= \frac{dY_3^{\ell}(\theta)}{d\theta} = Y_4^{\ell}(\theta) \\
\frac{d^4\phi^{\ell}(\theta)}{d\theta^4} = \frac{dY_4^{\ell}(\theta)}{d\theta} &= -\frac{\left[\begin{array}{c} C_3^{\ell}(\theta)Y_4^{\ell}(\theta)+C_2^{\ell}(\theta)Y_3^{\ell}(\theta)+C_1^{\ell}(\theta)Y_2^{\ell}(\theta) \\ +C_0^{\ell}(\theta)Y_1^{\ell}(\theta)+C_P^{\ell}(\theta) \end{array}\right]}{C_4^{\ell}(\theta)}
\end{aligned}
\tag{2.73a}
$$

and

$$
\begin{aligned}
s_{\ell} &= Y_5^{\ell}(\theta) \\
\frac{ds_{\ell}}{d\theta} &= \frac{dY_5^{\ell}(\theta)}{d\theta} = 0.
\end{aligned}
\tag{2.73b}
$$

These equations were then integrated from the left ($\theta = 0$) and right ($\theta = \pi$) boundaries using DIVPRK a sixth order explicit Runge-Kutta-Verner integration method in the IMSL MATH/LIBRARY [40]. The solution at $\theta + h$ is estimated by

$$
\begin{aligned}
Y_i^{\ell}(\theta+h) \approx Y_i^{\ell}(\theta) + \Bigg(& \frac{3}{40}k_i^{\ell,1} + 0k_i^{\ell,2} + \frac{875}{2244}k_i^{\ell,3} + \frac{23}{72}k_i^{\ell,4} \\
& + \frac{264}{1955}k_i^{\ell,5} + 0k_i^{\ell,6} + \frac{125}{11592}k_i^{\ell,7} + \frac{1}{160}k_i^{\ell,8} \Bigg)
\end{aligned}
\tag{2.74}
$$

where the indices ℓ is the field number, i is the first order equation number. The coefficients $k_i^{\ell,j}$ are defined in Appendix B. The value h in these constants is the step size for integration. An initial step size of 0.01 was selected and was adjusted between $0.000001 \le h \le 0.2$ to keep the global error ≤ 0.00001.

The boundary conditions imposed on the above system are shown in the Fig. 2.3. The homogeneous boundary conditions are a result of the symmetry and stress free boundary discussed above. The magnitude of the angular fields in the stress potential were arbitrary set to one at $\theta = 0$ for the purpose of integration but were later scaled such that the corresponding angular field associated with the equivalent stress would have a maximum value of one. It was possible to do the scaling because the coefficients in the series expansion are yet to be determined and will scale the fields to their appropriate magnitudes. The boundary conditions designated by g_i^ℓ were initially unknown. It was possible to determine their appropriate values by initially guessing values. The correct values were then arrived at by systematically adjusting them in successive iterations until all the differences between the corresponding functions $Y_i^\ell(\theta)$ integrated from $\theta = 0$ and those integrated from $\theta = \pi$ had differences defined as

$$F_i^\ell(g_j^\ell) = \lim_{\theta \to \pi/2^-} \left[Y_i^\ell(\theta)\right] - \lim_{\theta \to \pi/2^+} \left[Y_i^\ell(\theta)\right] \tag{2.75}$$

that were less than 0.0000001. The adjustment of the five unknown boundary conditions were determined through a first order Taylor series expansion of the difference functions $F_i^\ell(g_j^\ell)$ as follows

$$\left\{g_i^{\ell,n+1}\right\} = \left\{g_i^{\ell,n}\right\} + \left[\frac{\partial F_i^\ell\left(g_k^{\ell,n}\right)}{\partial g_j^\ell}\right]^{-1} \left\{F_j^\ell\left(g_k^{\ell,n}\right)\right\} \tag{2.76}$$

where the indices n and n+1 indicate the current and next iterations, respectfully. The Jacobian of $F_i^\ell(g_j^\ell)$ was evaluated numerically for each iteration by varying g_k^ℓ individually by an increment of $\Delta g_k = 0.000001\ \delta_{km}$ $(m = 1,2,3,4,5)$ to determine $\Delta F_i^\ell\left(g_k^{\ell,n} + \Delta g_k\right)$. After obtaining these values, the Jacobian was estimated as follows

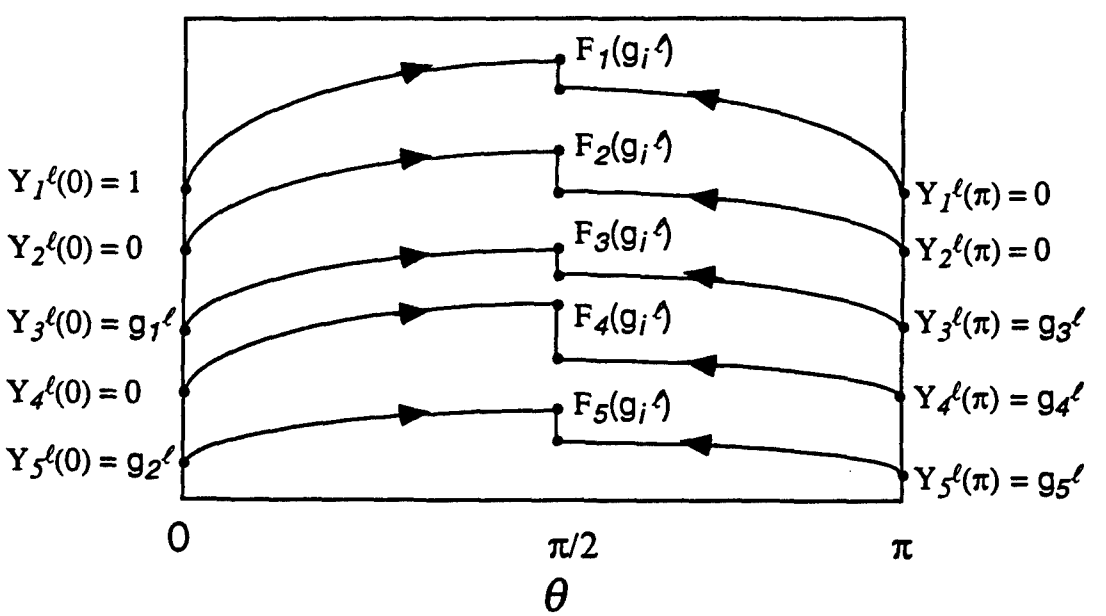

FIG. 2.3— Schematic of multiple shooting technique.

$$\frac{\partial F_i^{\ell}\left(g_k^{\ell,n}\right)}{\partial g_j^{\ell}} \approx \frac{\Delta F_i^{\ell}\left(g_k^{\ell,n}\right)}{\Delta g_j}. \tag{2.77}$$

The increments of the unknown boundary conditions Δg_k^{ℓ} were obtained using the IMSL subroutine DLINRG. This subroutine computes the solution of a linear system using the LU decomposition method. First, an upper and lower triangular matrix whose product returns the coefficient matrix are determined using Crout's algorithm.

$$Ax = LUx = b. \tag{2.78}$$

The solution of the system is then obtained by forward substitution of the lower triangular matrix and the right hand side vector to obtain an intermediate vector.

$$Ux = L^{-1}b = c. \tag{2.79}$$

Next, back substitution of the upper triangular matrix and the intermediate vector is performed.

$$x = U^{-1}c = U^{-1}L^{-1}b. \tag{2.80}$$

As stated before, the differential equations were integrated successively each time adjusting the values of g_i^{ℓ} until the differences in the right and left functions $Y_i^{\ell}(\theta)$ evaluated at $\theta = \pi/2$ were less than 0.0000001.

The angular functions for the potential were then used to determine the angular functions for the stress, strain and displacement fields using the relations given earlier. The fields were considered correct if the *J*-integral was path independent. The programs and input files developed to solve the differential equations are included in Appendix C.

2.3 Finite Element Analysis

Crack tip fields were obtained for the modified boundary layer and finite geometry specimens using the commercial finite element program ABAQUS 5.2 [41]. Specimen modeling and post processing of the results was accomplished using the solid modeler PATRAN 2.5 [42]. Data was translated between the two programs using PATABA and ABAPAT versions 3.1A.

2.3.1 Solution Methods

The field problem was solved using the procedures of the method of virtual work rate. The principle is derived from equilibrium as follows: First, the partial differential equations of equilibrium in the deformed configuration are multiplied by a test function (virtual velocity)

$$\left[\frac{\partial \bar{\tau}}{\partial \bar{x}} + \bar{f}\right] \cdot \delta \bar{v} = 0. \tag{2.81}$$

In this section arrows are used over tensors to indicate their order. Second, the residual is integrated over the domain of interest

$$\int_V \left[\frac{\partial \bar{\tau}}{\partial \bar{x}} + \bar{f}\right] \cdot \delta \bar{v} dV = 0. \tag{2.82}$$

Third, the product rule is used to rewrite the first term

$$\frac{\partial}{\partial \bar{x}}(\bar{\tau} \cdot \delta \bar{v}) = \frac{\partial \bar{\tau}}{\partial \bar{x}} \cdot \delta \bar{v} + \bar{\tau} \cdot \frac{\partial \delta \bar{v}}{\partial \bar{x}}$$

$$\int_V \left[\frac{\partial}{\partial \bar{x}}(\bar{\tau} \cdot \delta \bar{v}) - \bar{\tau} \cdot \frac{\partial \delta \bar{v}}{\partial \bar{x}} + \bar{f} \cdot \delta \bar{v}\right] dV = 0. \tag{2.83}$$

Fourth, the divergence theorem is used on the first term to obtain

$$\int_V \left[\bar{\tau} \cdot \frac{\partial \delta \bar{v}}{\partial \bar{x}}\right] dV - \int_S \left[\bar{\tau} \cdot \hat{n} \delta \bar{v}\right] dS - \int_V \left[\bar{f} \cdot \delta \bar{v}\right] dV = 0. \tag{2.84}$$

Finally, the gradient of the virtual velocity is related to the virtual rate of deformation by

$$\frac{\partial \delta \bar{v}}{\partial \bar{x}} = \delta \bar{L} = \delta \bar{D}_{sym} + \delta \bar{W}_{skew} \tag{2.85}$$

where

$$\delta \bar{D}_{sym} = \frac{\delta \bar{L} + \delta \bar{L}^T}{2} \quad \text{and} \quad \delta \bar{W}_{skew} = \frac{\delta \bar{L} - \delta \bar{L}^T}{2}. \tag{2.86}$$

Here $\delta \bar{D}$ is the rate of deformation tensor and $\delta \bar{W}$ is the rate of spin tensor.

Substituting these results into the above expression and taking the Cauchy stress tensor $\bar{\tau}$ to be symmetric and thus when multiplied by a skew matrix $\delta \bar{W}$ results in the zero matrix the weak form of equilibrium is obtained

$$\int_V \bar{\tau} \cdot \delta \bar{D} dV - \int_S \bar{t} \cdot \delta \bar{v} dS - \int_V \bar{f} \cdot \delta \bar{v} dV = 0. \tag{2.87}$$

The statement of the principle is as follows:

> *The rate at which the external applied loads do work must balance the rate at which the internal forces do work..*

The first integral in the above expression contains the conjugate work pair of stress and strain rate. The integral can be transformed so its evaluation may be taken over the original configuration provided the appropriate conjugate work pair are used. The conjugate pairs of interest are as follows

Stress	Strain Rate	Domain
Cauchy, $\bar{\tau}$	Deformation Rate Tensor, $\bar{D}$	current
Kirchhoff, $\bar{\sigma}$	Deformation Rate Tensor, $\bar{D}$	original
2nd Piola-Kirchhoff, $\bar{S}$	Green -Lagrange Strain Rate, $\dot{\bar{\varepsilon}}$	original

Since the rate behavior of materials is generally modeled with constitutive relations using the deformation rate tensor, and we expect the elastic behavior

to be derivable from a thermodynamic potential defined over the original configuration, the Kirchhoff stress ($\bar{\sigma}$) and the deformation rate tensor ($\bar{D}$) are used in ABAQUS. The Kirchhoff stress is related to the Cauchy stress ($\bar{\tau}$) by

$$\bar{\tau} = \frac{\bar{\sigma}}{\det|\bar{F}|} \tag{2.88}$$

where $\bar{F}$ is the deformation gradient $\frac{\partial \bar{x}}{\partial \bar{X}}$ and $\bar{x}$ are the deformed coordinates while $\bar{X}$ are the undeformed coordinates. Although the Kirchhoff stress is used in the constitutive model, the final stress output is the Cauchy stress.

The finite element form of the principle of virtual work rate is obtained by discretizing the original domain into a finite number of subdomains called elements. The displacement formulation interpolates the displacement field within each element from locations (nodes) where the displacements are sought. The principle of the virtual work rate is applied over each element in the following form

$$\int_{V_o} \bar{B}_M \cdot \bar{\sigma} dV_o - \int_S \bar{N}_M^T \cdot \bar{t} dS - \int_V \bar{N}_M^T \cdot \bar{f} dV = 0 \tag{2.89}$$

where N_M are the interpolation (shape functions) and B_M is the displacement to strain transformation matrix containing spatial derivatives of the interpolation functions. The contributions of all elements are then summed. The above equation is in general nonlinear in nature and can be written as

$$F^M\left(u^P\right) = 0 \tag{2.90}$$

where u^P are the unknown displacements. The nonlinearities result from four sources; material nonlinearity, large displacement gradients, large displacements and rotations, and boundary conditions. The nonlinear system is solved incrementally. First, the equation is expanded in a Taylor's series about the approximate solution u_i^P as

$$F^M\left(u_i^P\right)+\frac{\partial F^M\left(u_i^P\right)}{\partial u^N}\left(u_{i+1}^P-u_i^P\right)+\cdots = 0. \tag{2.91}$$

The second term contains the Jacobian (stiffness) matrix for the nonlinear system and is given by

$$K_{MN}=\int_{V_o}\bar{B}_M:\bar{\bar{H}}:\bar{B}_N dV_o+\int_{V_o}\bar{\sigma}:\partial_N\bar{B}_M dV_o-\int_S\bar{N}_M^T\cdot\bar{Q}_N^S dS-\int_V\bar{N}_M^T\cdot\bar{Q}_N^V dV \tag{2.92}$$

where $\bar{\bar{H}}$ is the current material tangent stiffness tensor. The integrals containing $\bar{Q}_N^S$ and $\bar{Q}_N^V$ result from what are termed follower forces and are generally called the load stiffness matrix and are defined as

$$\begin{aligned}\bar{Q}_N^S&=\frac{\partial\bar{t}}{\partial u_N}+\frac{\bar{t}}{A_r}\frac{\partial A_r}{\partial u_N}\\ \bar{Q}_N^V&=\frac{\partial\bar{f}}{\partial u_N}+\frac{\bar{f}}{J}\frac{\partial J}{\partial u_N}\end{aligned} \tag{2.93}$$

where A_r is the ratio of surface areas between the current and reference configurations and J is the ratio of the volume between the current and reference configurations.

Successive corrections are made to the nodal displacements by solving the linear system

$$u_{i+1}^M = u_i^M-\left[K_{MN}\right]^{-1}F^N\left(u_i^M\right). \tag{2.94}$$

After each iteration, the updated displacement vector is used to determine the residual in the nonlinear system. When the residual is below some predetermined convergence tolerance, the system has been solved for that increment.

After convergence is obtained, the strain increment is calculated from the rate of deformation using the following relation

$$\Delta\bar{e} = \bar{e} - \bar{e}_0 = \int_{\bar{e}_0}^{\bar{e}} d\bar{e} = \int_t^{t+\Delta t} \mathrm{D}\,dt \tag{2.95}$$

and is related to the velocity gradient through

$$\Delta e = \int_0^{\Delta t} \left[\frac{\breve{\mathrm{L}}(t+\tau) + \breve{\mathrm{L}}(t+\tau)^{\mathrm{T}}}{2} \right] d\tau \tag{2.96}$$

where $\breve{\mathrm{L}}$ is the velocity gradient defined over the increment of time Δt as

$$\breve{\mathrm{L}}(t+\tau) = \Delta R(t+\Delta t)\left[\Delta R(t+\tau)^{\mathrm{T}}\ \mathrm{L}\ \Delta R(t+\tau)\right]\Delta R(t+\Delta t)^{\mathrm{T}}. \tag{2.97}$$

Using the polar decomposition of the deformation gradient increment, the part in brackets in the previous expression once substituted in the integral can be rewritten in terms of the increment of the right stretch tensor

$$\Delta R^{\mathrm{T}}\left(\mathrm{L} + \mathrm{L}^{\mathrm{T}}\right)\Delta R = \Delta\dot{U}\Delta U^{-1} + \Delta U^{-1}\Delta\dot{U}. \tag{2.98}$$

Now assuming that the incremental stretch has the same principle directions throughout the increment we can write the increment of stretch as

$$\begin{aligned} \Delta U = \left(1 + \left\{\Delta\lambda_I - 1\right\}\frac{\tau}{\Delta t}\right)\bar{N}_I \cdot \bar{N}_I + \left(1 + \left\{\Delta\lambda_{II} - 1\right\}\frac{\tau}{\Delta t}\right)\bar{N}_{II} \cdot \bar{N}_{II} \\ + \left(1 + \left\{\Delta\lambda_{III} - 1\right\}\frac{\tau}{\Delta t}\right)\bar{N}_{III} \cdot \bar{N}_{III}. \end{aligned} \tag{2.99}$$

Substituting into the integral and integrating results in the logarithmic strain increment given by

$$\Delta e = \ln(\Delta\lambda_I)\mathrm{n}_I \cdot \mathrm{n}_I + \ln(\Delta\lambda_{II})\mathrm{n}_{II} \cdot \mathrm{n}_{II} + \ln(\Delta\lambda_{III})\mathrm{n}_{III} \cdot \mathrm{n}_{III} \tag{2.100}$$

where λ_i are the eigenvalues of the left stretch tensor $\mathrm{F} \cdot \mathrm{F}^{\mathrm{T}}$ and N_i, n_i are the eigen vectors at the beginning and end of the increment, respectfully (i.e. different by ΔR). The strain increment is sent along with all necessary variables to the constitutive routine to obtain the increment of Kirchhoff

stress. This stress is then transformed to the Cauchy stress in the deformed configuration.

All specimens were modeled using continuum plane strain eight node isoparametric elements (CPE8). These elements are displacement based and use the same order shape functions for both variable interpolation within the element and coordinate mapping between the local (master) and global spaces. The mapping of coordinates and interpolation of displacements are given as follows

$$\begin{aligned} x_i(\xi_\ell) &= \sum_{j=1}^{8} \bar{x}_i^j N_j(\xi_\ell) \\ u_k(x_i(\xi_\ell)) &= \sum_{j=1}^{8} \bar{u}_k^j N_j(\xi_\ell) \end{aligned} \tag{2.101}$$

where j is an indices over the number of nodes in the element, $\bar{x}_i^j$ are the global coordinates of the nodes, $\bar{u}_i^j$ are the nodal displacements, N_j are the shape functions defined over the master element given in Appendix D, ξ_ℓ are the local coordinates, and x_i and u_k are the global coordinates and displacements, respectfully. A 3×3 Gauss quadrature with nine integration points was used for integrating over the master element. Full integration was deemed necessary to capture the complete effect of plasticity near the crack-tip. Reduced integration which is used frequently to reduce the effect of over estimating the stiffness matrix in the displacement formulation was not used. The calculations where conducted with the following expression

$$\int_\Omega I(\xi_1, \xi_2) d\xi_1 d\xi_2 \approx \sum_{m=1}^{3} \left[\sum_{n=1}^{3} I(\xi_1^n, \xi_2^m) w_n \right] w_m = \sum_{\ell=1}^{9} I(\xi_1^\ell, \xi_2^\ell) \bar{w}_\ell \tag{2.102}$$

where ξ_i^ℓ are the coordinates of the nine quadrature points and $\bar{w}_\ell$ are the nine quadrature weights their values are given in Appendix D. A schematic of the CPE8 element is given in Fig. 2.4 with both its node and integration point numbering.

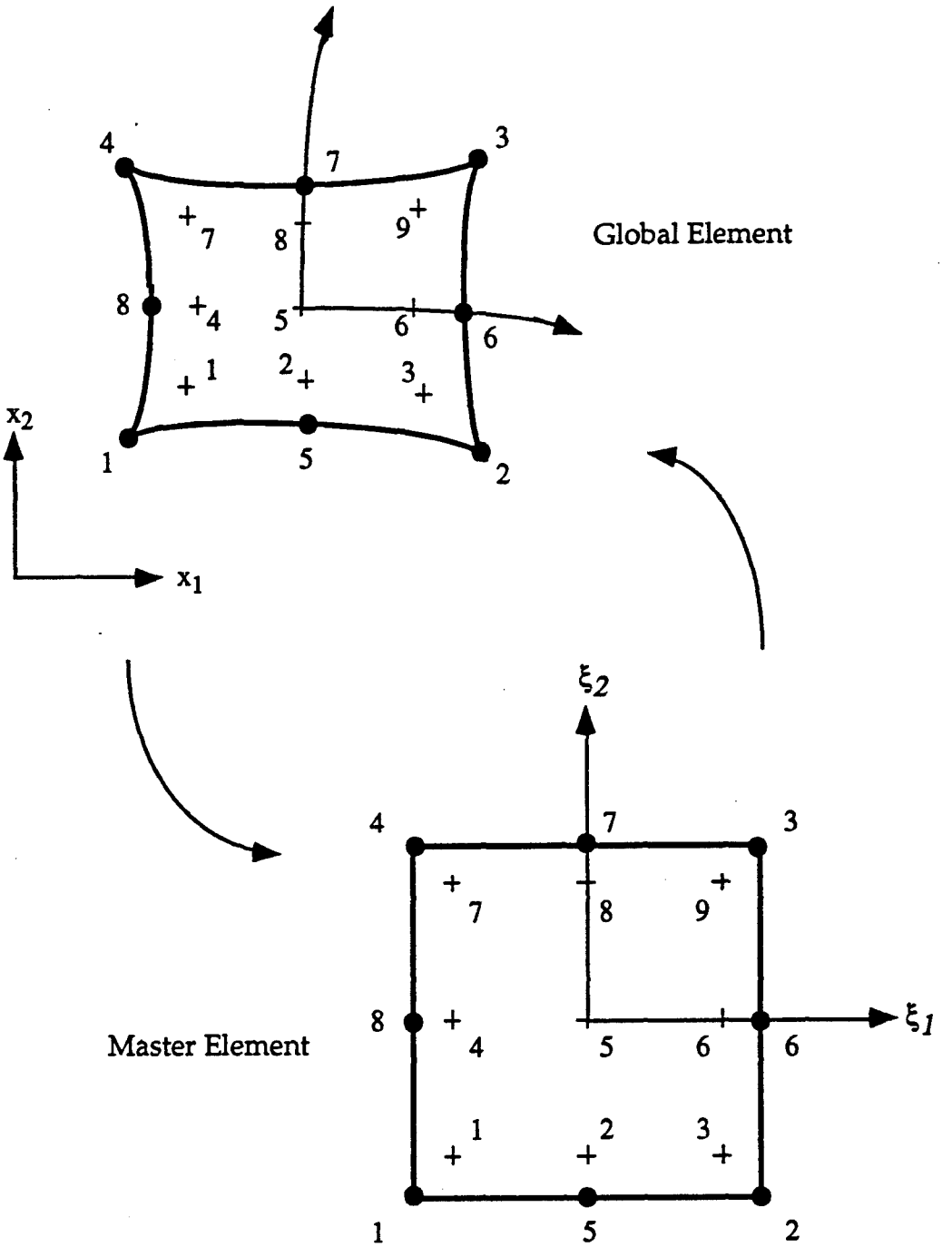

FIG. 2.4— Node and quadrature point numbering for the CPE8 element.

2.3.2 Modified Boundary Layer Models

A modified boundary layer as shown in Fig. 2.5 with a displacement field corresponding to the first three Williams terms (K_I,T and S) was constructed using

$$\hat{u}_x(\hat{r},\theta)=\frac{K_I(1+\nu)}{\sqrt{2\pi}\,E}\left[\cos\left(\frac{\theta}{2}\right)\left\{3-4\nu-\cos(\theta)\right\}\right]\hat{r}^{\frac{1}{2}}+\frac{T\left(1-\nu^2\right)}{E}\cos(\theta)\hat{r}$$
$$+S\left[\frac{(1+\nu)}{E}\begin{Bmatrix}\cos(\theta)\left\langle\left(\frac{3}{2}-4\nu\right)\cos\left(\frac{\theta}{2}\right)+\frac{1}{2}\cos\left(\frac{5\theta}{2}\right)\right\rangle\\ -\sin(\theta)\left\langle\left(\frac{9}{2}-4\nu\right)\sin\left(\frac{\theta}{2}\right)-\frac{1}{2}\sin\left(\frac{5\theta}{2}\right)\right\rangle\end{Bmatrix}\right]\hat{r}^{\frac{3}{2}} \quad (2.103a)$$

$$\hat{u}_y(\hat{r},\theta)=\frac{K_I(1+\nu)}{\sqrt{2\pi}\,E}\left[\sin\left(\frac{\theta}{2}\right)\left\{3-4\nu-\cos(\theta)\right\}\right]\hat{r}^{\frac{1}{2}}-\frac{T\nu(1-\nu)}{E}\sin(\theta)\hat{r}$$
$$+\ S\left[\frac{(1+\nu)}{E}\begin{Bmatrix}\sin(\theta)\left\langle\left(\frac{3}{2}-4\nu\right)\cos\left(\frac{\theta}{2}\right)+\frac{1}{2}\cos\left(\frac{5\theta}{2}\right)\right\rangle\\ +\cos(\theta)\left\langle\left(\frac{9}{2}-4\nu\right)\sin\left(\frac{\theta}{2}\right)-\frac{1}{2}\sin\left(\frac{5\theta}{2}\right)\right\rangle\end{Bmatrix}\right]\hat{r}^{\frac{3}{2}}. \quad (2.103b)$$

The first two terms (K_I and T)of the Williams solution was chosen as our two-parameter field, Larsson and Carlsson [43]. All higher order coefficients where set to zero. The evolution of the plastic field in this model by definition depends only on two parameters K_I and T , excluding material properties. For this reason, the second and third independent coefficients in the nonlinear asymptotic analysis must only depend on the same two parameters K_I and T when the analytical representation for the stress field is matched with the full field finite element results. A separate model was constructed to study the influence of the third Williams term on the stress field near the crack-tip. Displacements corresponding to K_I and S where applied to the boundary in this model.

The region was modeled as a 25.4 cm semi-circle, 2.54 cm thick. There are 54 rings of elements which geometrically degenerate towards the crack-tip. The ratio of the radial dimension of the outermost element ring to the

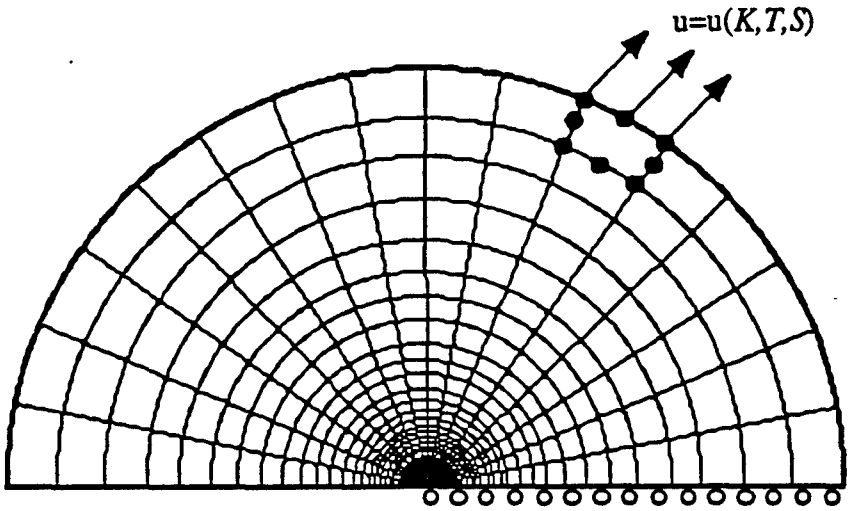

FIG. 2.5— Modified boundary layer mesh and boundary conditions.

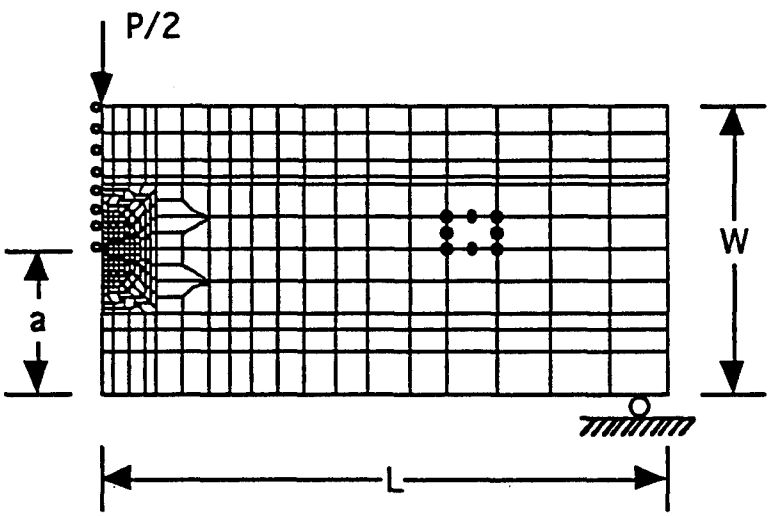

FIG. 2.6— Single edge notch bend specimen mesh and boundary conditions.

inner most ring is 3.21251 cm / 0.001145 cm = 2805.69. There are 16 rays of elements centered at the crack-tip with an angular measure of 0.19634 radians. The crack-tip elements were degenerated to triangles. The mid-side nodes where left in place and the crack-tip nodes were not tied, resulting in a $1/r$ strain singularity. The analysis was based on small strain theory.

The boundary displacements in the first model were applied by first applying displacements associated with a K_I value of $54.96\text{MPa}\sqrt{\text{m}}$ and then displacements associated with T/σ_0 varying from -1 to +1 in 0.1 increments. It was confirmed by using $27.48\text{MPa}\sqrt{\text{m}}$ as an alternate value of K_I that the stress distribution depends only on the value of T/σ_0 when the radial distance is normalized by J/σ_0. Small scale yielding *(SSY)* was maintained by insuring that the value of the numerically measured J was at least 99% of J determined from K_I applied at the boundary. This was accomplished in two ways. First, the plastic zone r_p was restricted to ten percent of the radius of the model and second a constitutive model was used which behaved in a linear elastic manner up to $\approx 0.95\sigma_0$ and then became nonlinear so that at large strains the stress/strain curve corresponded to the Ramberg-Osgood curve.

The boundary displacements in the second model were applied in a manner similar to that of the first model. The applied K_I value was reduce to $27.48\text{MPa}\sqrt{\text{m}}$ to maintain small scale yielding. T/σ_0 was set to zero and S/σ_0 was varied from -1 to +1 in 0.1 increments. J-integrals were calculated by the domain integral method in both models and showed path independence for contours taken outside the finite strain zone. A sample ABAQUS input file is included in Appendix E.

2.3.3 Finite Geometry Specimen Models

The finite geometry specimens are the single edge notch bend (SENB), single edge notch tension (SENT), center cracked tension (CCT), and double edge notch tension (DENT). Figs. 2.6 and 2.7 show the mesh and boundary conditions for each of these geometries. Since the three specimens could be modeled using a similar geometry by only changing the boundary conditions, the following dimensions apply to all of the specimens; the depth of the specimens (W) was 5.08 cm, a crack length to width ratio (a/W) of 0.1, 0.5,

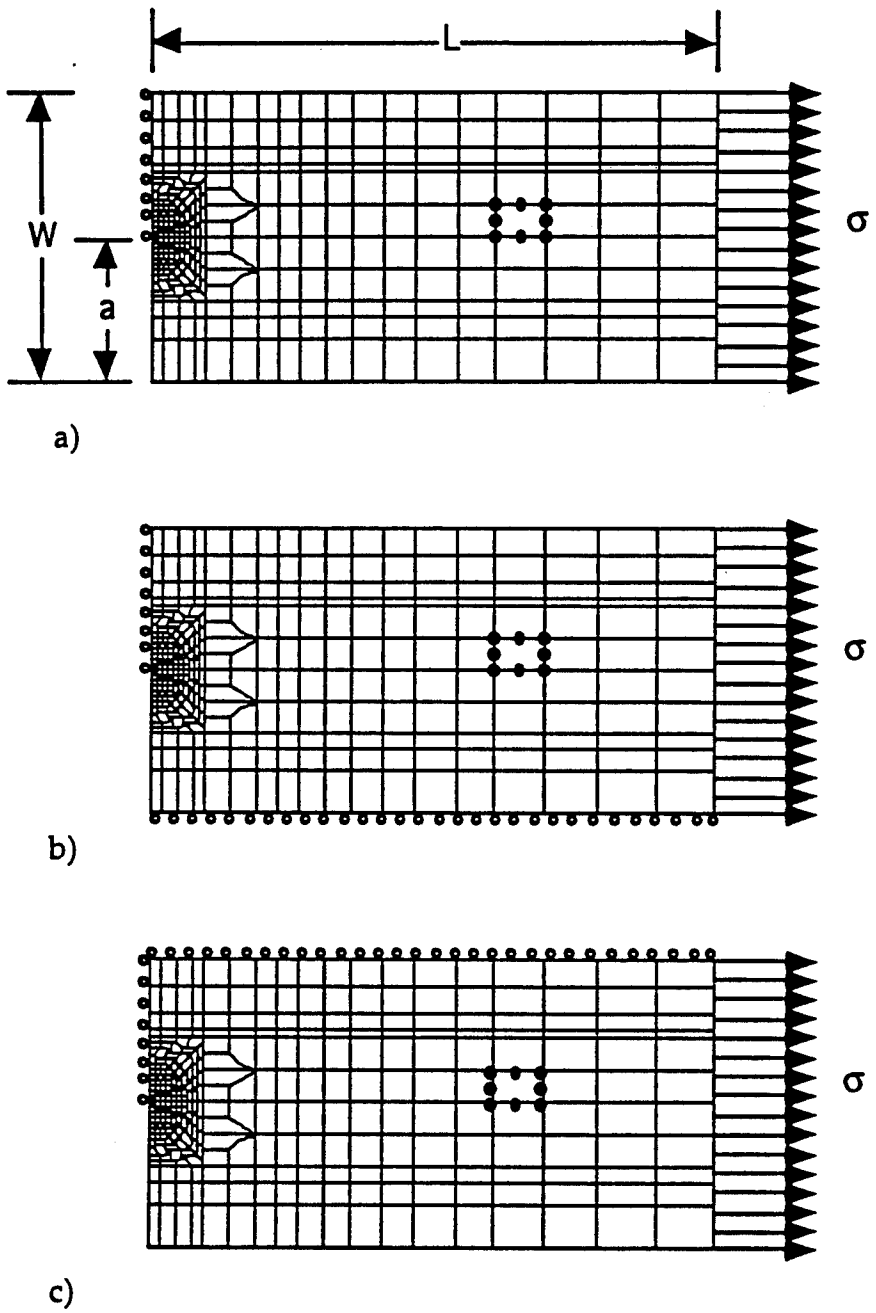

FIG. 2.7— Mesh and boundary conditions for a) Single edge notched tension, b) Center cracked tension, c) Double edge notched tension.

and 0.9 were used, the width to thickness ratio (W/B) was 2.0, and the half length (L) of the specimen was 10.16 cm. The focused mesh used in the modified boundary layer analysis was scaled and inserted for the crack-tip region.

Loads were applied to the specimens such that the plastic J values, as determined by the EPRI method [44], were given as $J_{pl} = a\sigma_o/\beta$. The coefficient β was chosen to be 20 for all geometries except the CCT which was loaded to a β value of 50. The resulting loads were calculated with the following expression

$$P=P_o\left[\frac{a}{\beta\alpha\varepsilon_o b h_1}\right]^{\frac{1}{n+1}} \tag{2.104}$$

where P_o is the specimens limit load, n, ε_o, α, are material constants from the Ramberg-Osgood constitutive relation, b is the uncracked ligament length, and h_1 is the EPRI coefficient for a given geometry. The load was applied incrementally in twenty equal steps. In all but the SENB specimen this load was distributed evenly over the surface on which it was applied. Stresses were determined for a cylindrical coordinate system centered at the crack-tip. J-integrals were calculated by the domain integral method and showed path independence for contours taken outside the finite strain zone. A sample ABAQUS input file is included in Appendix E.

2.4 J-Integral Analysis

The J-integral is a well known parameter used to characterize nonlinear material behavior ahead of a crack, it was first discovered as a general conservation integral by Eshelby [45] and was then applied independently to the crack problem by Rice [9]. The value of the J-integral gives a measure of the energy flux focused on the crack-tip. It is derived here from an integral over a two dimension area (shown in Fig. 2.8) containing no singular behavior given by

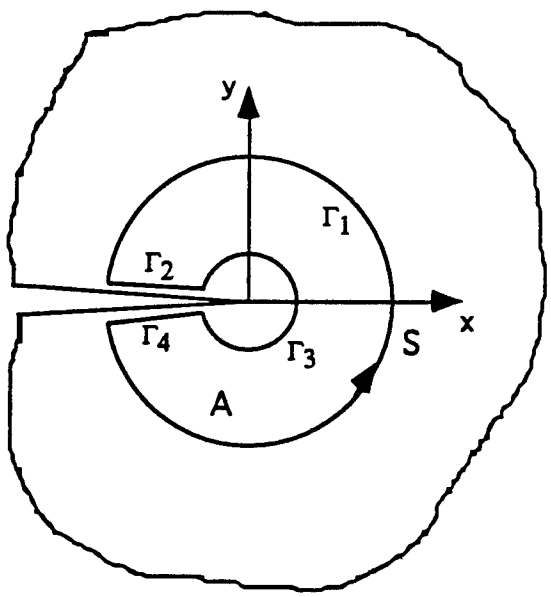

FIG. 2.8— Crack tip coordinate system and contours for the *J*-integral evaluation.

$$\int_A 0 dA = 0. \tag{2.105}$$

This expression holds for any area of interest. Substituting for the integrand a seemingly arbitrary term results in

$$\int_A \left[\frac{\partial}{\partial \hat{x}_j} \left(\hat{\sigma}_{ij} \frac{\partial \hat{u}_i}{\partial \hat{x}_1} \right) - \frac{\partial}{\partial \hat{x}_j} \left(\hat{\sigma}_{ij} \frac{\partial \hat{u}_i}{\partial \hat{x}_1} \right) \right] dA = 0. \tag{2.106}$$

Passing the differential operator through the brackets on the first term results in

$$\int_A \left[\frac{\partial \hat{\sigma}_{ij}}{\partial \hat{x}_j} \frac{\partial \hat{u}_i}{\partial \hat{x}_1} + \hat{\sigma}_{ij} \frac{\partial}{\partial \hat{x}_j} \frac{\partial \hat{u}_i}{\partial \hat{x}_1} - \frac{\partial}{\partial \hat{x}_j} \left(\hat{\sigma}_{ij} \frac{\partial \hat{u}_i}{\partial \hat{x}_1} \right) \right] dA = 0. \tag{2.107}$$

Noting the first term contains the equations of equilibrium and using the symmetry of the stress tensor along with changing the order of integration on the displacements in the second term the expression can be rewritten as

$$\int_A \left[\hat{\sigma}_{ij} \frac{\partial}{\partial \hat{x}_1} \left\{ \frac{1}{2} \left\langle \frac{\partial \hat{u}_i}{\partial \hat{x}_j} + \frac{\partial \hat{u}_j}{\partial \hat{x}_i} \right\rangle \right\} - \frac{\partial}{\partial \hat{x}_j} \left(\hat{\sigma}_{ij} \frac{\partial \hat{u}_i}{\partial \hat{x}_1} \right) \right] dA = 0. \tag{2.108}$$

The first term may be rewritten as $\hat{\sigma}_{ij} \frac{\partial \hat{\varepsilon}_{ij}}{\partial \hat{x}_1}$ which for materials whose stress/strain relation can be derived from a strain energy potential, $\frac{\partial \hat{W}}{\partial \hat{\varepsilon}_{ij}} = \hat{\sigma}_{ij}$, the entire expression can be written as

$$\int_A \left[\frac{\partial \hat{W}}{\partial \hat{x}_1} - \frac{\partial}{\partial \hat{x}_j} \left(\hat{\sigma}_{ij} \frac{\partial \hat{u}_i}{\partial \hat{x}_1} \right) \right] dA = 0. \tag{2.109}$$

Using the divergence theorem to convert the area integral to a line integral results in

$$\int_S \left[\hat{W} n_1 - \hat{\sigma}_{ij} n_j \frac{\partial \hat{u}_i}{\partial \hat{x}_1} \right] dS = 0 \tag{2.110}$$

and finally eliminating the direction cosines gives

$$\int_S \left[\hat{W} d\hat{x}_1 - \hat{t}_i \frac{\partial \hat{u}_i}{\partial \hat{x}_1} dS \right] = 0. \tag{2.111}$$

Taking the contour S to be that shown in Fig. 2.8 the integral can be split into four separate integrals along Γ_i where $S=\Gamma_1+\Gamma_2+\Gamma_3+\Gamma_4$. Noting that the paths along the crack faces do not contribute because dy and t_i are both zero results in

$$\int_{\Gamma_1} \left[\hat{W} d\hat{x}_1 - \hat{t}_i \frac{\partial \hat{u}_i}{\partial \hat{x}_1} d\Gamma_1 \right] + \int_{\Gamma_3} \left[\hat{W} d\hat{x}_2 - \hat{t}_i \frac{\partial \hat{u}_i}{\partial \hat{x}_1} d\Gamma_3 \right] = 0. \tag{2.112}$$

Therefore when the contour is taken as an open contour intersecting the crack surfaces, the expression for the *J*-integral is path independent and can be expressed as

$$J = \int_\Gamma \left(\hat{W} d\hat{x}_2 - \hat{T}_i \frac{\partial \hat{u}_i}{\partial \hat{x}_1} dS \right). \tag{2.113}$$

The *J*-integral was used in the analytic as well as the numerical portions of the present work.

2.4.1 Analytic J-integral

The *J*-integral was used in the analytic analysis to nondimensionalize the radial coordinate as well as to check the angular stress and displacement

fields. The power-law representations for the stress, strain and displacement field were substituted into the equation for J given above to obtain a general expression. The result is a series expansion of J in which all the terms but the first have exponents on the radial coordinate other then zero. For J to be path independent the coefficients of these terms must be zero. Each of the coefficients contain an integral with limits of $-\pi \le \theta \le \pi$ whose integrand contains the angular functions of stress, strain, and displacement. The angular fields were considered correct if the integrals were zero. The following is the method by which J was determined for the analytic work.

The expression for the J-integral can be expressed in polar form by first substituting for the traction vector $\hat{T}_i = \hat{\sigma}_{ij} n_j$ and then expanding to obtain

$$J = \int_{\Gamma} \left[\hat{W} d\hat{x}_2 - \left\{ \left(\hat{\sigma}_{11} \frac{\partial \hat{u}_1}{\partial \hat{x}_1} + \hat{\sigma}_{21} \frac{\partial \hat{u}_2}{\partial \hat{x}_1} \right) n_1 + \left(\hat{\sigma}_{12} \frac{\partial \hat{u}_1}{\partial \hat{x}_1} + \hat{\sigma}_{22} \frac{\partial \hat{u}_2}{\partial \hat{x}_1} \right) n_2 \right\} ds \right]. \tag{2.114}$$

where the term with $\hat{\sigma}_{33}$ has been omitted because $n_3 = 0$. The field variables are transformed following the rules for tensor transformations as follows

$$\begin{Bmatrix} \hat{u}_1(\hat{r},\theta) \\ \hat{u}_2(\hat{r},\theta) \end{Bmatrix} = \begin{bmatrix} \cos\theta & -\sin\theta \\ \sin\theta & \cos\theta \end{bmatrix} \begin{Bmatrix} \hat{u}_r(\hat{r},\theta) \\ \hat{u}_\theta(\hat{r},\theta) \end{Bmatrix} \tag{2.115}$$

$$\begin{Bmatrix} \hat{\sigma}_{11}(\hat{r},\theta) \\ \hat{\sigma}_{22}(\hat{r},\theta) \\ \hat{\sigma}_{12}(\hat{r},\theta) \end{Bmatrix} = \begin{bmatrix} \cos^2\theta & \sin^2\theta & -2\sin\theta\cos\theta \\ \sin^2\theta & \cos^2\theta & 2\sin\theta\cos\theta \\ \sin\theta\cos\theta & -\sin\theta\cos\theta & \cos^2\theta - \sin^2\theta \end{bmatrix} \begin{Bmatrix} \hat{\sigma}_{rr}(\hat{r},\theta) \\ \hat{\sigma}_{\theta\theta}(\hat{r},\theta) \\ \hat{\sigma}_{r\theta}(\hat{r},\theta) \end{Bmatrix}. \tag{2.116}$$

The gradient in the displacement field may be expressed in polar form using the chain rule

$$\frac{\partial \hat{u}_1(\hat{r},\theta)}{\partial \hat{x}_1} = \frac{\partial \hat{u}_1(\hat{r},\theta)}{\partial \theta}\frac{\partial \theta}{\partial \hat{x}_1} + \frac{\partial \hat{u}_1(\hat{r},\theta)}{\partial \hat{r}}\frac{\partial \hat{r}}{\partial \hat{x}_1}$$
$$\frac{\partial \hat{u}_2(\hat{r},\theta)}{\partial \hat{x}_1} = \frac{\partial \hat{u}_2(\hat{r},\theta)}{\partial \theta}\frac{\partial \theta}{\partial \hat{x}_1} + \frac{\partial \hat{u}_2(\hat{r},\theta)}{\partial \hat{r}}\frac{\partial \hat{r}}{\partial \hat{x}_1} \qquad (2.117)$$

where

$$\theta = \tan^{-1}\left(\frac{\hat{x}_2}{\hat{x}_1}\right); \qquad r = \sqrt{\hat{x}_1^{\,2} + \hat{x}_2^{\,2}} \qquad (2.118)$$

$$\frac{\partial \theta}{\partial \hat{x}_1} = \frac{-\sin\theta}{\hat{r}}; \quad \frac{\partial \hat{r}}{\partial \hat{x}_1} = \cos\theta \qquad (2.119)$$

$$d\hat{x}_1 = -\sin\theta \; ds; \quad d\hat{x}_2 = \cos\theta \; ds. \qquad (2.120)$$

The polar form of the *J*-integral for a circular contour is obtained by substituting the above expressions into the Cartesian form of the integral. After simplification, we obtain

$$\begin{aligned}\frac{J}{\alpha\sigma_o\varepsilon_o} = \int_\Gamma \Bigg[& \hat{W}(\hat{r},\theta)\cos\theta - \cos\theta \; \hat{\sigma}_{rr}(\hat{r},\theta)\frac{\partial \hat{u}_r(\hat{r},\theta)}{\partial \hat{r}} \\ & - \cos\theta \; \hat{\sigma}_{r\theta}(\hat{r},\theta)\frac{\partial \hat{u}_\theta(\hat{r},\theta)}{\partial \hat{r}} \\ & - \frac{\sin\theta}{\hat{r}}\hat{\sigma}_{rr}(\hat{r},\theta)\left\{\hat{u}_\theta(\hat{r},\theta) - \frac{\partial \hat{u}_r(\hat{r},\theta)}{\partial \theta}\right\} \\ & + \frac{\sin\theta}{\hat{r}}\hat{\sigma}_{r\theta}(\hat{r},\theta)\left\{\hat{u}_r(\hat{r},\theta) - \frac{\partial \hat{u}_\theta(\hat{r},\theta)}{\partial \theta}\right\}\Bigg]\hat{r}\,d\theta\end{aligned} \qquad (2.121)$$

where the field variables are the dimensional values. The strain energy density was obtained by integrating for the area under each of the stress/strain relations and summing the results as follows

$$\hat{W}(\hat{r},\theta)=\hat{\sigma}_{ij}(\hat{r},\theta)\hat{\varepsilon}_{ij}(\hat{r},\theta)-\int_0^{\hat{\sigma}_{ij}(\hat{r},\theta)}\hat{\varepsilon}_{ij}(\hat{r},\theta)\,d\hat{\sigma}_{ij}(\hat{r},\theta). \qquad (2.122)$$

The strain energy density for the Ramberg-Osgood constitutive model can be expressed as follows

$$\hat{W}(\hat{r},\theta) = \frac{1}{2}\hat{\sigma}_{ij}(\hat{r},\theta)\hat{\varepsilon}_{ij}^{Elastic}(\hat{r},\theta) + \frac{n}{n+1}\left\{\hat{\sigma}_e(\hat{r},\theta)\right\}^{n+1}. \qquad (2.123)$$

Substituting the series expansion of the stress, strain, and displacement fields into the strain energy density and then into the polar expression for the *J*-integral one obtains the following relation

$$\frac{J}{\alpha\sigma_o\varepsilon_o}=I_1\hat{r}^{\Delta s_1}+I_2\hat{r}^{\Delta s_2}+I_3\hat{r}^{\Delta s_3}+I_4\hat{r}^{\Delta s_4}+I_5\hat{r}^{\Delta s_5}+I_6\hat{r}^{\Delta s_6}+\cdots \qquad (2.124)$$

where $\Delta s_i = s_i - s_1$ and I_i are constants shown in Appendix F. The magnitude of the exponents increase with the first exponent being zero. Hence, as stated above, for *J* to be path independent (i.e. for any value of $\hat{r}$), the constants I_i must be zero for i >1. The angular fields were checked by evaluating each of the constants I_i .

2.4.2 Numerical J-Integral

The *J*-integral was evaluated for the modified boundary layer and finite body specimens using the domain integral technique. This method is implemented within ABAQUS. The domain integral form of the *J*-integral is obtained by multiplying the integrand by a function *q* as follows

$$J=\int_{\Gamma_3}\left(\hat{W}n_1-\hat{T}_i\frac{\partial\hat{u}_i}{\partial\hat{x}_1}\right)q\left(\hat{x}_i\right)dS. \qquad (2.125)$$

The magnitude of q(S) is dependent on the position along the contour. It is equal to one on Γ_3 and zero on the rest of the contour. The function q must transition between the value of one and zero smoothly over the enclosed domain. In the general case, Γ_3 must be taken vanishingly small. This is not conducive to numerical algorithms. For this reason, the above expression is transformed into an integral over the enclosed domain in which q is defined.

The above expression is converted by applying the divergence theorem. The resulting equation for the *J*-integral is

$$J = \int_A \frac{\partial}{\partial \hat{x}_i}\left[\left(\hat{W}\delta_{1i} - \hat{\sigma}_{ij}\frac{\partial \hat{u}_j}{\partial \hat{x}_1}\right) q\left(\hat{x}_i\right)\right] dA. \qquad (2.126)$$

The next step is to use the product rule on the integrand which results in the following

$$J = \int_A \left[\left(\hat{W}\delta_{1i} - \hat{\sigma}_{ij}\frac{\partial \hat{u}_j}{\partial \hat{x}_1}\right)\frac{\partial q(S)}{\partial \hat{x}_i} + \left(\frac{\partial \hat{W}}{\partial \hat{x}_1} - \frac{\partial}{\partial \hat{x}_i}\left\{\hat{\sigma}_{ij}\frac{\partial \hat{u}_j}{\partial \hat{x}_1}\right\}\right) q\left(\hat{x}_i\right)\right] dA. \qquad (2.127)$$

The second term in the integral is equal to zero as shown previously. The final expression for the *J*-integral is given by

$$J = \int_A \left[\left(\hat{W}\delta_{1i} - \hat{\sigma}_{ij}\frac{\partial \hat{u}_j}{\partial \hat{x}_1}\right)\frac{\partial q\left(\hat{x}_i\right)}{\partial \hat{x}_i}\right] dA. \qquad (2.128)$$

The integral is now evaluated numerically using Gauss quadrature. Each of the terms in the integrand is defined in the finite element formulation by interpolation from nodal points using element shape functions. The function q is given the value one at nodes along Γ_3 and zero at nodes along the rest of the contour. The magnitude of q at interior nodes is set at one.

Numerical values of the *J*-integral were obtained for twenty contours around the crack-tip. The first several contours were not path independent

which results from high distortion of elements near the tip of the crack in what is known as the finite strain zone. After the first six to ten contours, the value of J was path independent.

2.5 Analytic/Numerical Field Matching

The coefficients in the general power series representation of the stress field are determined by matching the analytic solution with the full field finite element solutions. The stress from the analytical solution was matched on a point by point bases with the modified boundary layer and finite body results. The following section contains an outline of the procedures used to determine the coefficients.

The series expansion of the stress field in normalized coordinates is given by

$$\sigma_{ij}(r,\theta) = K_1\sigma_{ij}^1(\theta)r^{s_1} + K_2\sigma_{ij}^2(\theta)r^{s_2} + K_3\sigma_{ij}^3(\theta)r^{s_3} + K_4\sigma_{ij}^4(\theta)r^{s_4} + K_5\sigma_{ij}^5(\theta)r^{s_5} + K_6\sigma_{ij}^6(\theta)r^{s_6} + \cdots. \tag{2.129}$$

The third, fifth and sixth coefficients for the values of the hardening coefficients used in the present study are not independent but depend on previous coefficients as will be discussed in the results section. The relation between these coefficients and the previous are given by

$$K_3 = \frac{K_2^2}{K_1}, \quad K_5 = \frac{K_3^2}{K_1^2}, \text{ and } \quad K_6 = \frac{K_2 K_4}{K_1}. \tag{2.130}$$

Substitution of the above into the equation for the stress gives

$$\sigma_{ij}(r,\theta) = K_1\sigma_{ij}^1(\theta)r^{s_1} + K_2\sigma_{ij}^2(\theta)r^{s_2} + \frac{K_2^2}{K_1}\sigma_{ij}^3(\theta)r^{s_3} + K_4\sigma_{ij}^4(\theta)r^{s_4} + \frac{K_3^2}{K_1^2}\sigma_{ij}^5(\theta)r^{s_5} + \frac{K_2 K_4}{K_1}\sigma_{ij}^6(\theta)r^{s_6} + \cdots. \tag{2.131}$$

In the first six terms, only three independent coefficients remain. The first is determined from the *J*-integral. The remaining two must be computed from matching with the finite element results. The expression for the stress may be rewritten as

$$\sigma_{ij}(r,\theta) = L_{ij}^{1} + L_{ij}^{2}K_2 + L_{ij}^{3}K_2^2 + L_{ij}^{4}K_4 + L_{ij}^{5}K_2^3 + L_{ij}^{6}K_2K_4 + \cdots \qquad (2.132)$$

where L_{ij}^{k} depends on the first coefficient, the angular stress fields, and the radial coordinate. The solution of the two remaining coefficients requires an independent equation for each. In this work, the radial and tangential stresses from the finite element results were used. The following equations were obtained

$$\begin{aligned}\sigma_{rr}^{FEA}(r,\theta) &= L_{rr}^{1} + L_{rr}^{2}K_2 + L_{rr}^{3}K_2^2 + L_{rr}^{4}K_4 + L_{rr}^{5}K_2^3 + L_{rr}^{6}K_2K_4 \\ \sigma_{\theta\theta}^{FEA}(r,\theta) &= L_{\theta\theta}^{1} + L_{\theta\theta}^{2}K_2 + L_{\theta\theta}^{3}K_2^2 + L_{\theta\theta}^{4}K_4 + L_{\theta\theta}^{5}K_2^3 + L_{\theta\theta}^{6}K_2K_4.\end{aligned} \qquad (2.133)$$

The fourth coefficient was eliminated from these equations resulting in the equation for K_2 as follows

$$G_1K_2^4 + G_2K_2^3 + G_3K_2^2 + G_4K_2 + G_5 = 0 \qquad (2.134)$$

where

$$\begin{aligned}G_1 &= L_{\theta\theta}^{6}L_{rr}^{5} - L_{\theta\theta}^{5}L_{rr}^{6} \\ G_2 &= L_{\theta\theta}^{4}L_{rr}^{5} + L_{\theta\theta}^{6}L_{rr}^{3} - L_{\theta\theta}^{5}L_{rr}^{4} - L_{\theta\theta}^{3}L_{rr}^{6} \\ G_3 &= L_{\theta\theta}^{4}L_{rr}^{3} + L_{\theta\theta}^{6}L_{rr}^{2} - L_{\theta\theta}^{3}L_{rr}^{4} - L_{\theta\theta}^{2}L_{rr}^{6} \\ G_4 &= L_{\theta\theta}^{4}L_{rr}^{2} + L_{\theta\theta}^{6}L_{rr}^{1} - L_{\theta\theta}^{2}L_{rr}^{4} - L_{\theta\theta}^{1}L_{rr}^{6} - L_{\theta\theta}^{6}\sigma_{rr}^{FEA}(r,\theta) + L_{rr}^{6}\sigma_{\theta\theta}^{FEA}(r,\theta) \\ G_5 &= L_{\theta\theta}^{4}L_{rr}^{1} - L_{\theta\theta}^{1}L_{rr}^{4} - L_{\theta\theta}^{4}\sigma_{rr}^{FEA}(r,\theta) + L_{rr}^{4}\sigma_{\theta\theta}^{FEA}(r,\theta).\end{aligned} \qquad (2.135)$$

K_2 was determined from Eq. (2.134) using Newton's method. The FORTRAN listing is given in Appendix G.

CHAPTER III

RESULTS

The analytic, numerical and comparison results are given in the following sections. First, the method for determining the exponents in the general power series expansion of the stress potential is reviewed and then the exponents are presented. The angular fields for stress, strain, and displacement corresponding to the first six exponents are introduced.

Second, the full field finite element results are presented. The stresses obtained from the finite element method for the geometries of this study are given along the crack plane and as a function of theta at a normalized radius of approximately two. The six term analytical representation of the stress field is also presented with the numerical results. Comparisons are made between the stress fields of the MBL for two different applied K valves. The influence of second and third Williams term on the stresses within the plastic region are reviewed. Next, the assumption made in the third constitutive equation of the analytical work, namely that $\lambda(r,\theta) = 0.5$ for plane strain is addressed.

Finally, the evaluations of the second and third independent coefficients in the general power series representation of the stress field are compared between the MBL and the finite body specimens. These results are used to determine when the stress field within the plastic region of the finite bodies may no longer be characterized by a two-parameter field.

3.1 Exponents

The angular fields and their corresponding exponents are obtained by satisfying the series representation of the compatibility equation (Eq. 2.63) asymptotically term by term. After using the binomial expansion of the effective stress in the plastic part of the strain and substituting into the compatibility equation, the exponents of the radial coordinate become integer combination of preceding exponents (i.e., $t_i = ns_1 + \alpha_k^i \Delta s_k$ where $\Delta s_k = s_k - s_1$ and α_k^i are positive integers). The corresponding ordinary differential

equation is given by $\pi_\ell^p(\theta)$, Eq. (2.63). the angular plastic stress/strain relation is given by

$$\dot{\varepsilon}_{ij}^{p(k)}(\theta)=\frac{3}{2}\sigma_{e_1}^{n-1}(\theta)\left[S_{ij}^k(\theta)+(n-1)\frac{\sigma_{e_{1k}}(\theta)S_{ij}^1(\theta)}{\sigma_{e_1}^2(\theta)}\right] \tag{3.1}$$

for terms where $t_i = ns_1 + \Delta s_i$. The fourth order ODE (Eq. 2.65) corresponding to these terms is homogeneous in nature. The corresponding exponents are independent of any preceding fields. The terms associated with exponents of the form $t_i = ns_1 + \alpha_k^i \Delta s_k$ where α_k^i is greater than one for single Δs_k or k takes on two or more values are not satisfied directly by the solution of the homogeneous equations. Hence, these terms are satisfied by grouping homogeneous terms with what are considered the particular terms. This reordering of terms results in the exponents being independent if the value is obtained from the homogeneous equation or dependent if the exponent on a homogeneous equation is forced to be some combination of previous exponents to satisfy a particular solution.

The exponents (s_i) in the general power series expansion of the stress potential are used to satisfy the boundary conditions at $\theta = \pi$, Eq. (2.72b). At $\theta = 0$ the first and third derivative of the angular potential function must be identically zero to satisfy the symmetry conditions. This leaves two unspecified boundary conditions, the value of the angular potential field and its second derivative, and the exponent. Either of the two boundary conditions can be fixed at $\theta = 0$ to make the problem well posed. Here we chose to fix the magnitude of the angular potential field to a magnitude of one. Subsequent to solving for the field the angular functions are rescaled such that the value of the angular equivalent stress function does not exceed unity. The second derivative of the angular potential function and the exponent are then selected to satisfy the two boundary conditions at $\theta = \pi$.

The first independent exponent is determined by solving for the leading nonlinear angular field. This was first solved by Hutchinson [7], Rice and Rosengren [8]. The angular functions associated with the first term have been coined the HRR field. The solution to the first term was obtained using a

multiple shooting technique as outlined in the procedures. The numerical value obtained for the leading exponent was compared to that derived by Rice who used the *J*-integral, $s_1 = -1/n+1$. The numerical values agreed with Rice's expression up to 8 significant figures.

Once the leading term was obtained, the higher order independent exponents were determined. The differential equations governing the higher order independent exponents are linear and similar in nature. The fourth order governing equations are obtained by substituting the plastic strains in Eq. (3.1) into Eq. (2.64). Since all higher order plastic strains depend exclusively on the present field and the leading (HRR) field in the same manner, the higher order independent exponents can be determined from the same equation.

The higher order independent exponents were determined in the following manner. Since the governing equation is linear, two elementary solutions are sought which satisfy the following boundary conditions at $\theta = 0$

$$\begin{aligned} &(1) \quad \phi_1^m(0) = 1, \quad \frac{d^2\phi_1^m(0)}{d\theta^2} = 0, \\ &(2) \quad \phi_2^m(0) = 0, \quad \frac{d^2\phi_2^m(0)}{d\theta^2} = 1, \end{aligned} \tag{3.2}$$

respectfully. The elementary solutions for the above conditions were obtained by integrating the governing equation with the sixth order explicit Runge-Kutta-Verner integration method outlined in the procedure section for a fixed valve of the exponent s_m. The general solution is then given by combining the elementary solutions as follows

$$\phi^m(\theta) = C_1\phi_1^m(\theta) + C_2\phi_2^m(\theta) \tag{3.3}$$

were C_1 and C_2 are real constants. Boundary conditions at $\theta = \pi$ must also be satisfied. Hence,

$$\begin{aligned} &\phi^m(\pi) = 0 = C_1\phi_1^m(\pi) + C_2\phi_2^m(\pi) \\ &\frac{d\phi^m(\pi)}{d\theta} = 0 = C_1\frac{d\phi_1^m(\pi)}{d\theta} + C_2\frac{d\phi_2^m(\pi)}{d\theta}. \end{aligned} \tag{3.4}$$

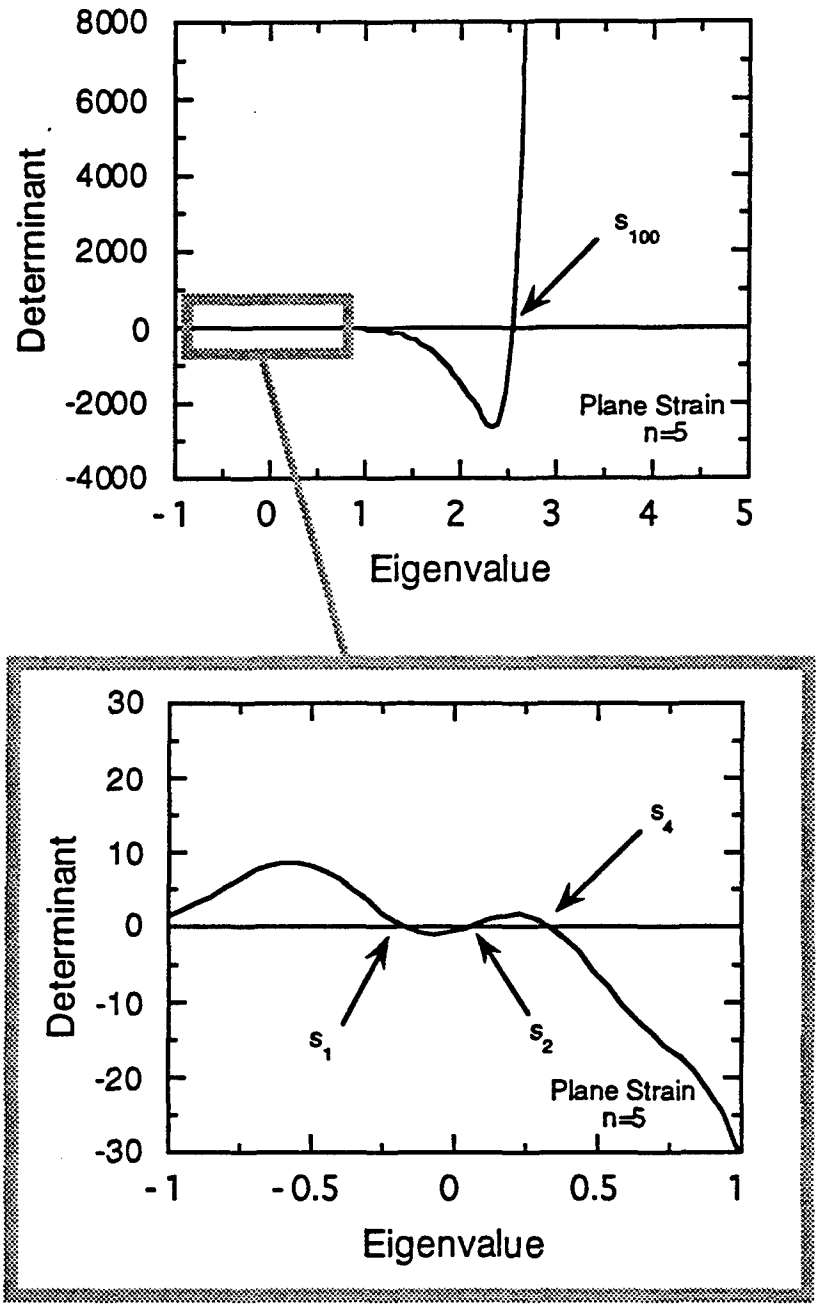

FIG. 3.1— Determination of independent eigenvalues for plane strain with a hardening coefficient of n=5.

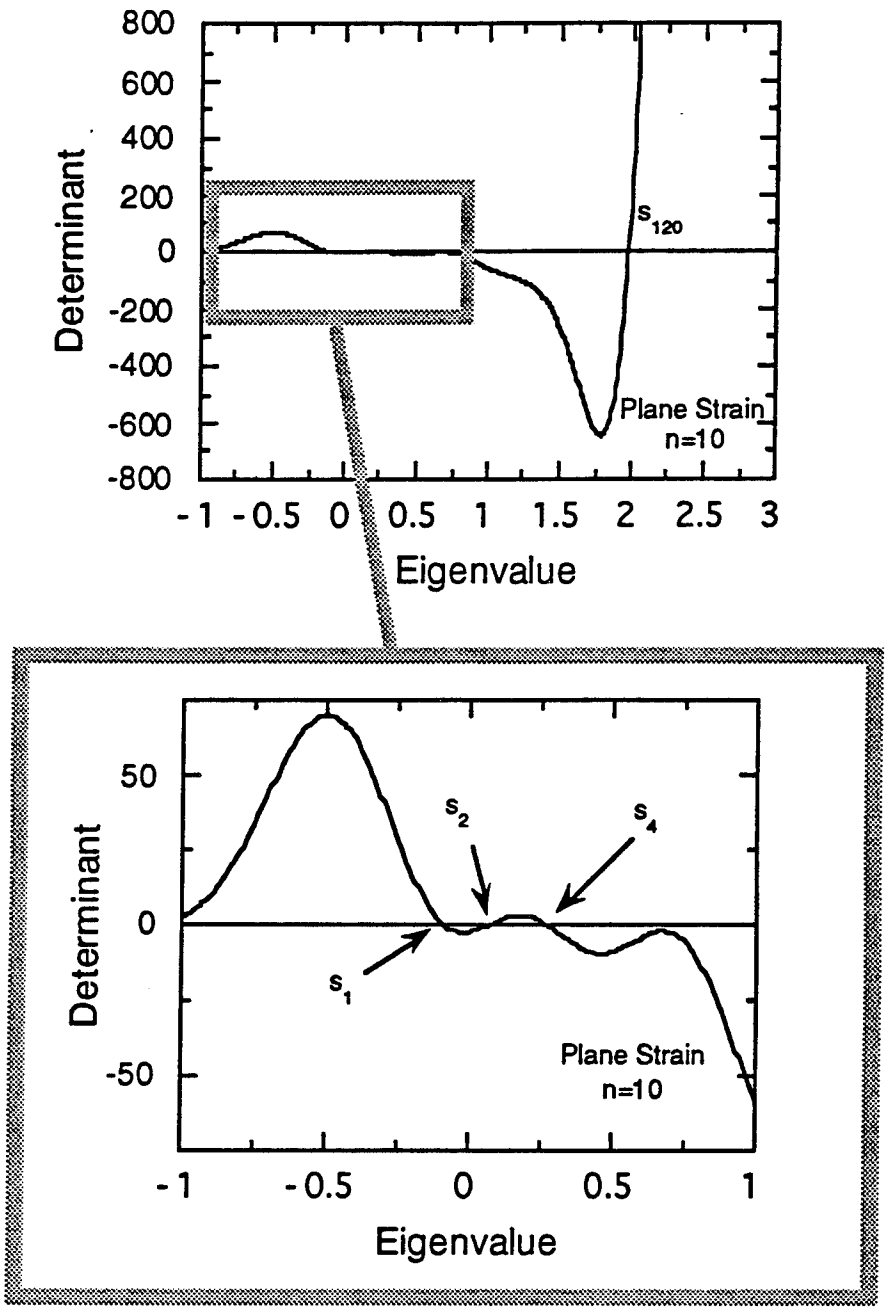

FIG. 3.2— Determination of independent eigenvalues for plane strain with a hardening coefficient of n=10.

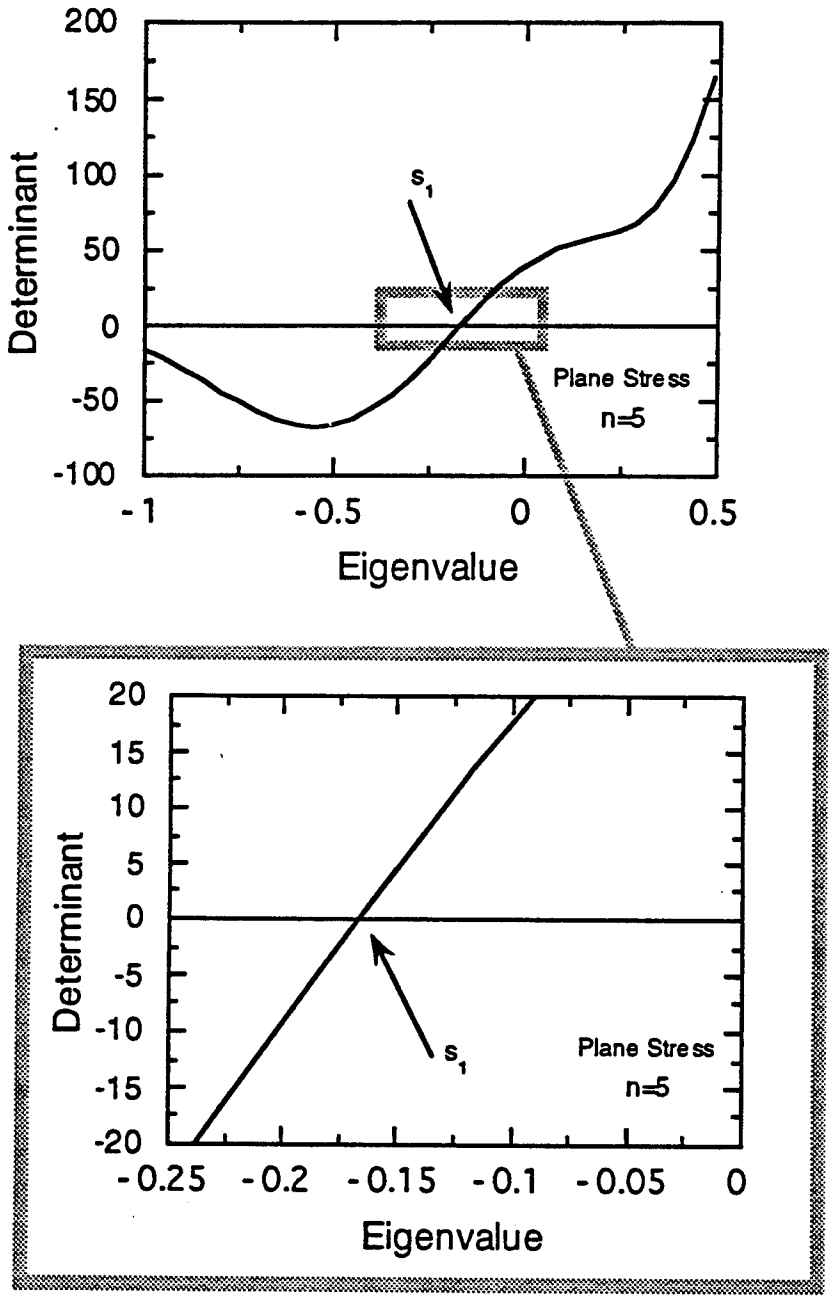

FIG. 3.3— Determination of independent eigenvalues for plane stress with a hardening coefficient of n=5.

These relations can be rearranged in matrix form to obtain

$$\begin{bmatrix} \phi_1^m(\pi) & \phi_2^m(\pi) \\ \dfrac{d\phi_1^m(\pi)}{d\theta} & \dfrac{d\phi_2^m(\pi)}{d\theta} \end{bmatrix} \begin{Bmatrix} C_1 \\ C_2 \end{Bmatrix} = \begin{Bmatrix} 0 \\ 0 \end{Bmatrix}. \tag{3.5}$$

A non-trivial solution for the vector $\{C\}$ exists if and only if the determinant of the matrix of the coefficients vanishes, i.e.

$$\phi_1^m(\pi)\frac{d\phi_2^m(\pi)}{d\theta} - \frac{d\phi_1^m(\pi)}{d\theta}\phi_2^m(\pi) = 0. \tag{3.6}$$

This is satisfied for discrete values of the exponent which correspond to the independent exponents s_m. Figs. 3.1-3.3 show Eq. (3.6) plotted as a function of the exponent value. Figs. 3.1 and 3.2 are the results for the case of plane strain with hardening exponents of 5 and 10, respectfully. Fig. 3.3 shows the results for the case of plane stress with a hardening exponent of 5. The locations were the determinant passes through zero represent the independent exponents. In the figures, the independent exponents are numbered by the order in which they appear in the series. The first cross over point corresponds to the HRR exponent $s_1 = -1/n + 1$. The first four independent exponents were obtained for the case of plane strain while only the first exponent could be determined for the plane stress case. Xia, et al. [17] and Yang, et al. [18,19] have reported similar findings for exponents up to the fourth field.

The dependent exponents were determined by grouping terms in the series representation of the compatibility equation. Some of the homogeneous terms were grouped with those that do not have coefficients that vanish (coefficients and exponents depend on solutions of earlier fields and hence provide a particular solution to a homogeneous equation) with independent terms. The asymptotic analysis is carried out by ordering the exponents on the radial coordinate in increasing order. The ordinary differential equation that results from the grouping is linear in nature and is associated with a particular solution. The solution of these fields was obtained by combining the two elementary solutions for the homogeneous equation with the solution for the particular part, i.e.

$$\phi^m(\theta) = C_1\phi_1^m(\theta) + C_2\phi_2^m(\theta) + \phi_p^m(\theta). \tag{3.7}$$

The coefficients were determined by satisfying the boundary conditions at $\theta = \pi$ by solving the system

$$\begin{bmatrix} \phi_1^m(\pi) & \phi_2^m(\pi) \\ \dfrac{d\phi_1^m(\pi)}{d\theta} & \dfrac{d\phi_2^m(\pi)}{d\theta} \end{bmatrix} \begin{Bmatrix} C_1 \\ C_2 \end{Bmatrix} = \begin{Bmatrix} -\phi_p^m(\pi) \\ -\dfrac{d\phi_p^m(\pi)}{d\theta} \end{Bmatrix}. \tag{3.8}$$

The exponents, their type and ordering are listed in Tables 3.1-3.3. Plane strain results for hardening exponents of 5 and 10 are given in Tables 3.1 and 3.2, respectively. Table 3.3 contains the results for plane stress with a hardening exponent of 5.

3.2 Angular Fields

The corresponding angular stress, strain, displacement, and *J*-integral fields derived from the first six angular potential functions for plane strain with hardening coefficients of 10 and 5 are given in Figs. 3.4-3.9 and Figs. 3.10-3.15, respectively. Each of the angular fields were evaluated for errors by checking for path independence of the *J*-integral. The angular integration constants I_i as given in Appendix F are shown in Figs. 3.9 and 3.15. The constants in all but the first term integrate to zero which preserved the path independence of the *J*-integral. The first four angular stress fields agree with those reported by Yang et al. [18,19]. All but the third field agree with those reported by Wang et al. [17] who recently have indicated there was an error in their third angular stress fields.

3.3 Finite Element and Analytic Comparisons

The HRR or first term of the stress series is plotted in Fig. 3.16 for a hardening exponent of n=10. The first term is given to compare the influence the higher order terms have on the results. The full field finite element results for each specimen are given along with the six term analytic solution in Figs. 3.17-3.28 for a hardening exponent of n=10. Tables 3.4-3.8 contain the general power

Table 3.1— Eigenvalue ordering for plane strain and a hardening exponent of n=5.

Eigenvalue Order	Eigenvalue s_i	Difference $\Delta s_i = s_i - s_1$	Particular Solutions	Type of Differential Equation
1	-0.166670	0.000000	---	HOMOGENEOUS-PLASTIC
2	0.054558	0.221220	---	HOMOGENEOUS-PLASTIC
3	0.275780	0.442450	1	PARTICULAR-PLASTIC
4	0.340720	0.507380	---	HOMOGENEOUS-PLASTIC
5	0.497010	0.663670	2	PARTICULAR-PLASTIC
6	0.500000	0.666670	1	PARTICULAR-ELASTIC
7	0.561940	0.728610	1	PARTICULAR-PLASTIC
8	0.718230	0.884900	4	PARTICULAR-PLASTIC
9	0.721220	0.887890	1	PARTICULAR-ELASTIC
⋮	⋮	⋮	⋮	⋮
~100	2.547700	2.714400	---	HOMOGENEOUS-PLASTIC

Table 3.2— Eigenvalue ordering for plane strain and a hardening exponent of n=10.

Eigenvalue Order	Eigenvalue s_i	Difference $\Delta s_i = s_i - s_1$	Particular Solutions	Type of Differential Equation
1	-0.090909	0.000000	---	HOMOGENEOUS-PLASTIC
2	0.069766	0.160680	---	HOMOGENEOUS-PLASTIC
3	0.230440	0.321350	1	PARTICULAR-PLASTIC
4	0.269590	0.360500	---	HOMOGENEOUS-PLASTIC
5	0.391120	0.482030	2	PARTICULAR-PLASTIC
6	0.430270	0.521180	1	PARTICULAR-PLASTIC
7	0.551790	0.642700	4	PARTICULAR-PLASTIC
8	0.590950	0.681850	3	PARTICULAR-PLASTIC
9	0.630100	0.721010	7	PARTICULAR-PLASTIC
10	0.712470	0.803380	6	PARTICULAR-PLASTIC
11	0.727270	0.818180	1	PARTICULAR-ELASTIC
⋮	⋮	⋮	⋮	⋮
~120	2.065909	1.975000	---	HOMOGENEOUS-PLASTIC

Table 3.3— Eigenvalue ordering for plane stress and a hardening exponent of n=5.

Eigenvalue Order	Eigenvalue s_i	Difference $\Delta s_i = s_i - s_1$	Particular Solutions	Type of Differential Equation
1	-0.166670	0.000000	---	HOMOGENEOUS-PLASTIC
2	0.500000	0.666670	1	PARTICULAR-ELASTIC
3	1.166700	1.333300	1	PARTICULAR-ELASTIC
4	1.833300	2.000000	1	PARTICULAR-ELASTIC
5	2.500000	2.666700	1	PARTICULAR-ELASTIC
6	3.166700	3.333300	1	PARTICULAR-ELASTIC
7	3.833300	4.000000	1	PARTICULAR-ELASTIC
8	4.500000	4.666700	1	PARTICULAR-ELASTIC
9	4.500000	4.666700	7	PARTICULAR-PLASTIC
10	5.166700	5.333300	1	PARTICULAR-ELASTIC
⋮	⋮	⋮	⋮	⋮

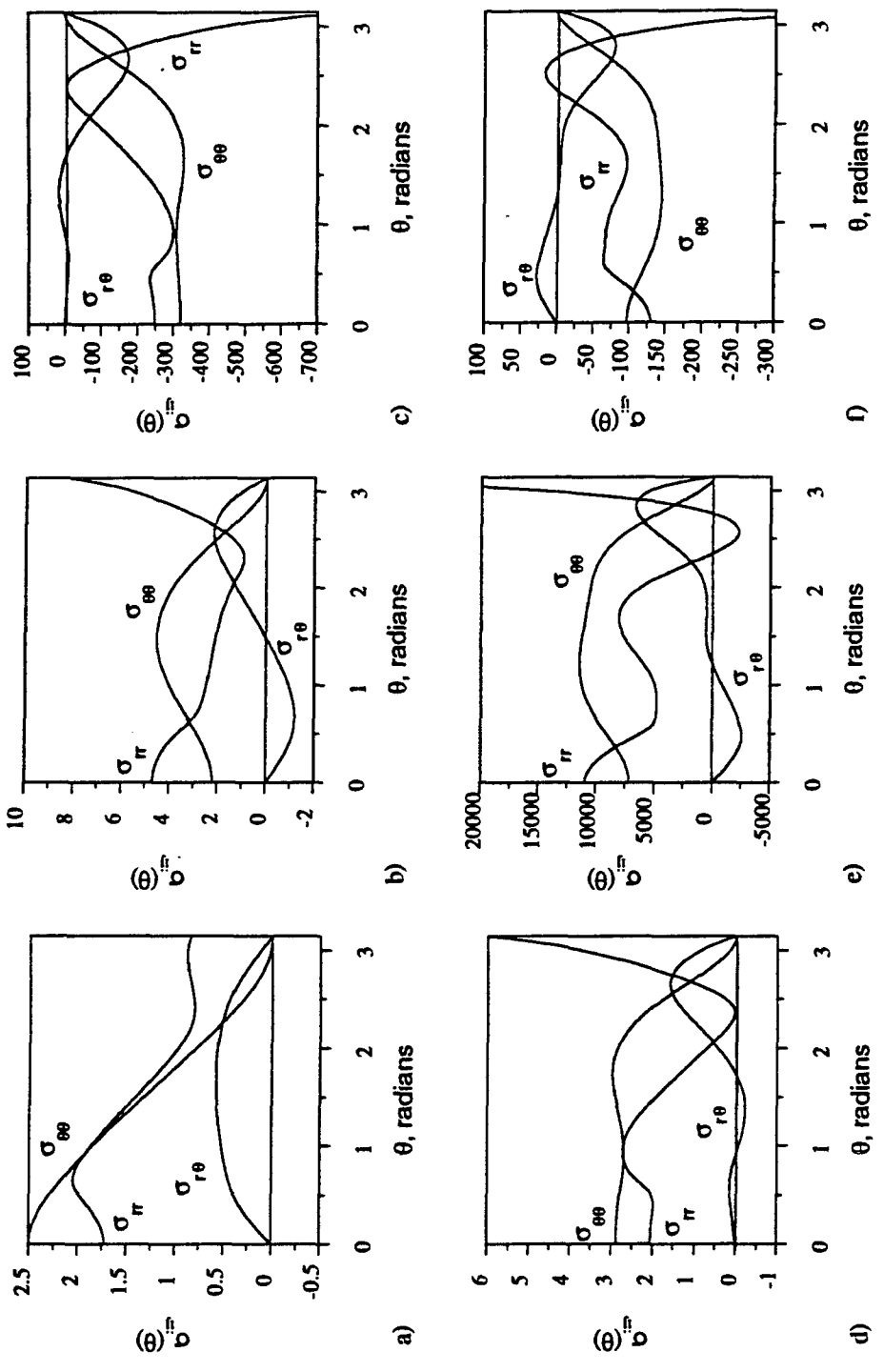

FIG. 3.4— Angular stress functions for n=10: a) field 1, b) field 2, c) field 3, d) field 4, e) field 5, f) field 6.

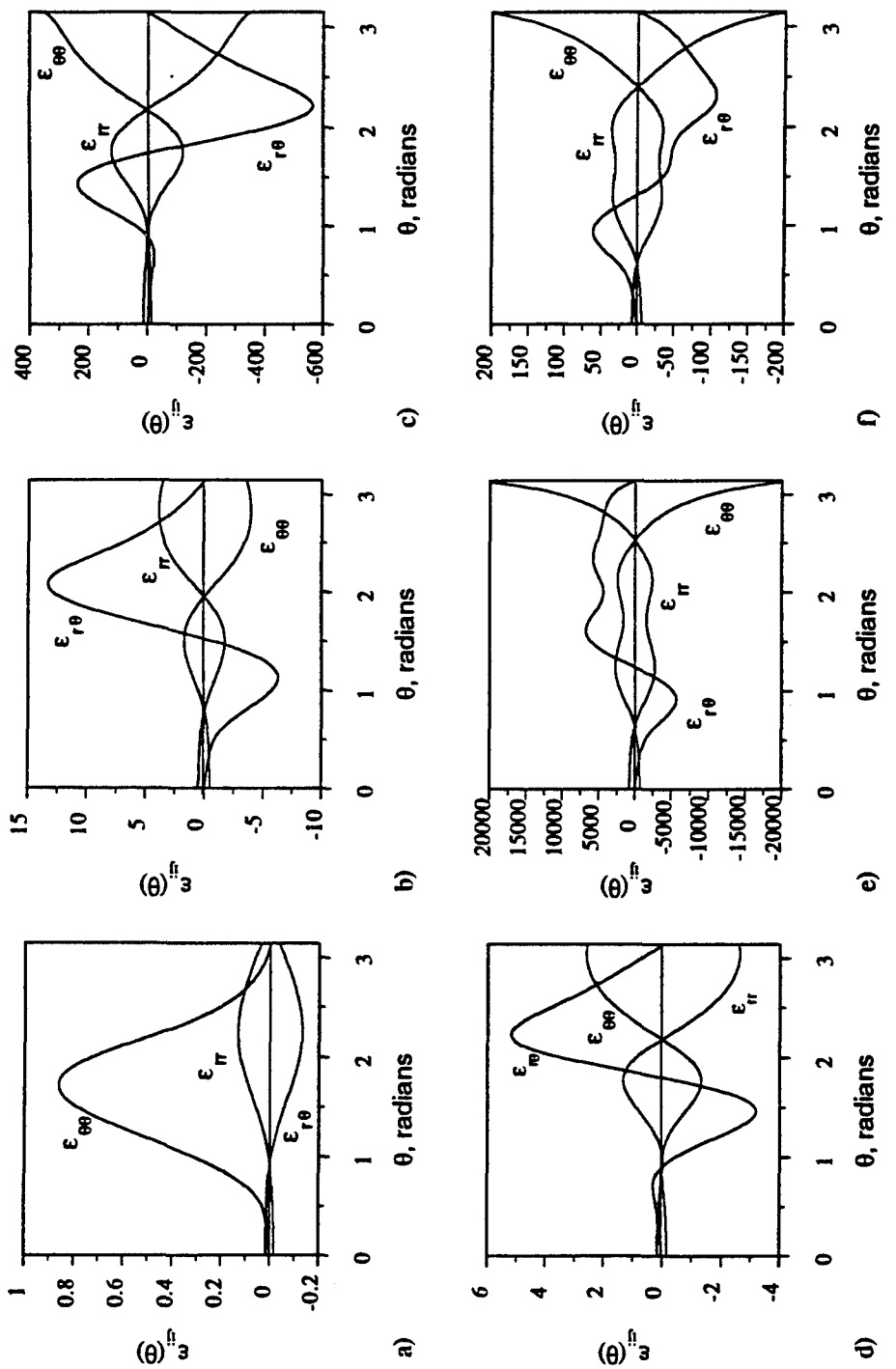

FIG. 3.5— Angular strain functions for n=10: a) field 1, b) field 2, c) field 3, d) field 4, e) field 5, f) field 6.

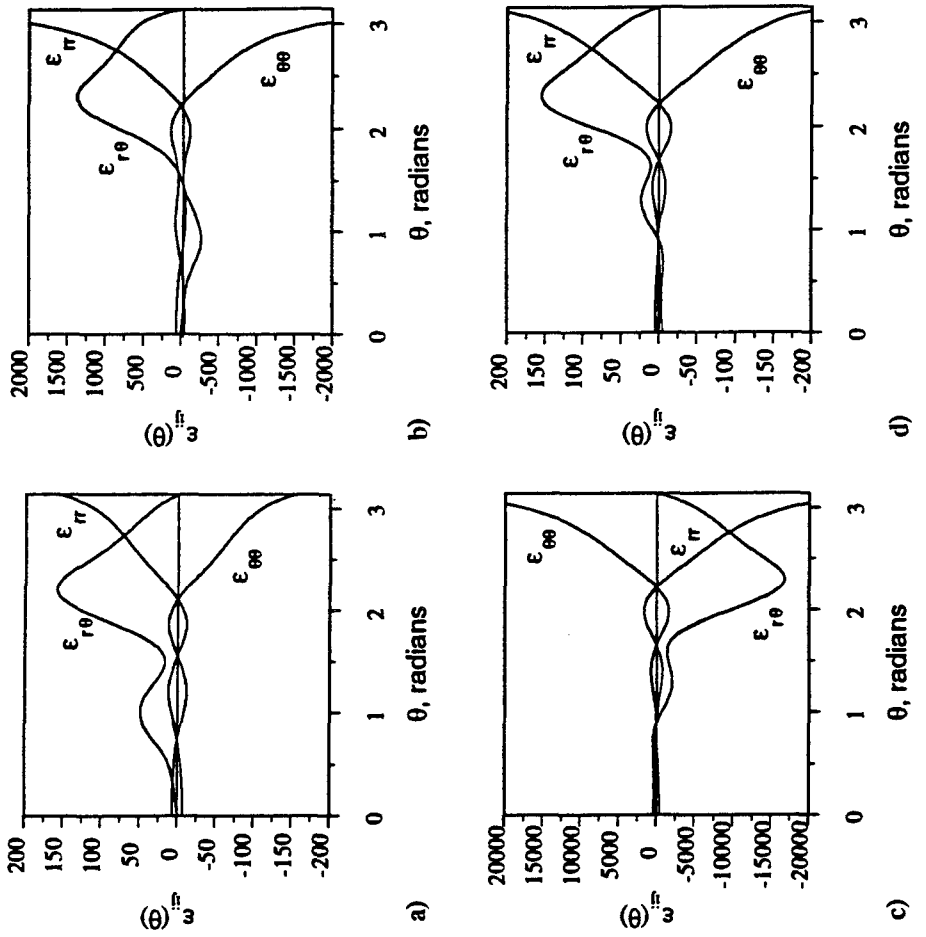

FIG. 3.6— Angular strain functions for particular solutions to differential equations:
a) field 22, b) field 222, c) field 23, d) field 24.

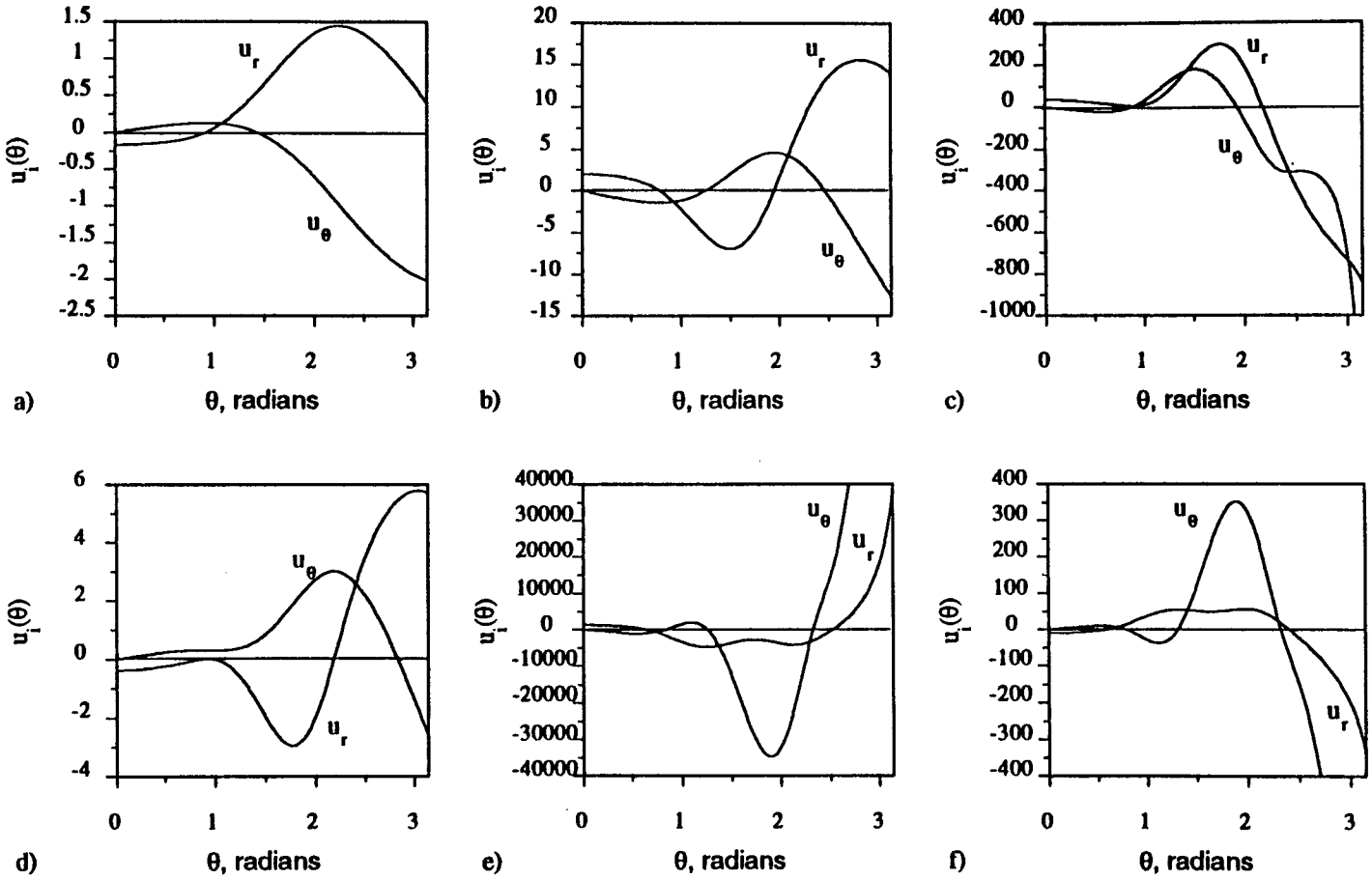

FIG. 3.7— Angular displacement functions for n=10: a) field 1, b) field 2, c) field 3, d) field 4, e) field 5, f) field 6.

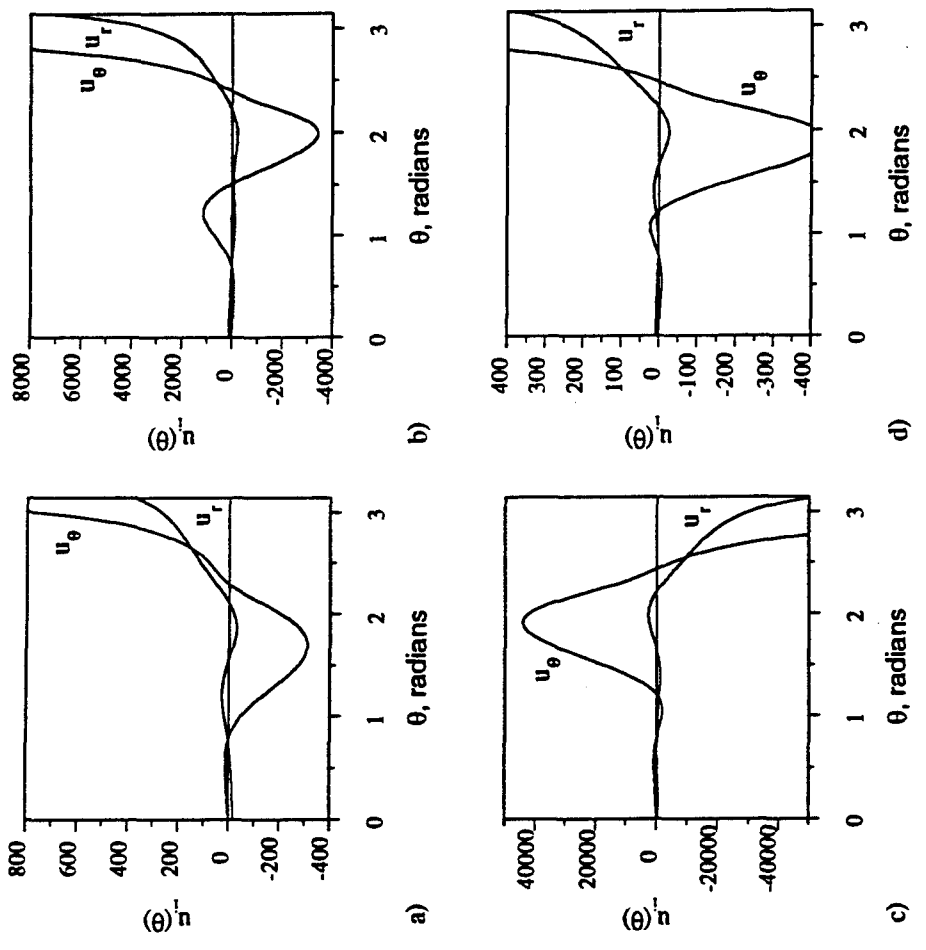

FIG. 3.8— Angular displacement functions for particular solutions to differential equations: a) field 22, b) field 222, c) field 23, d) field 24.

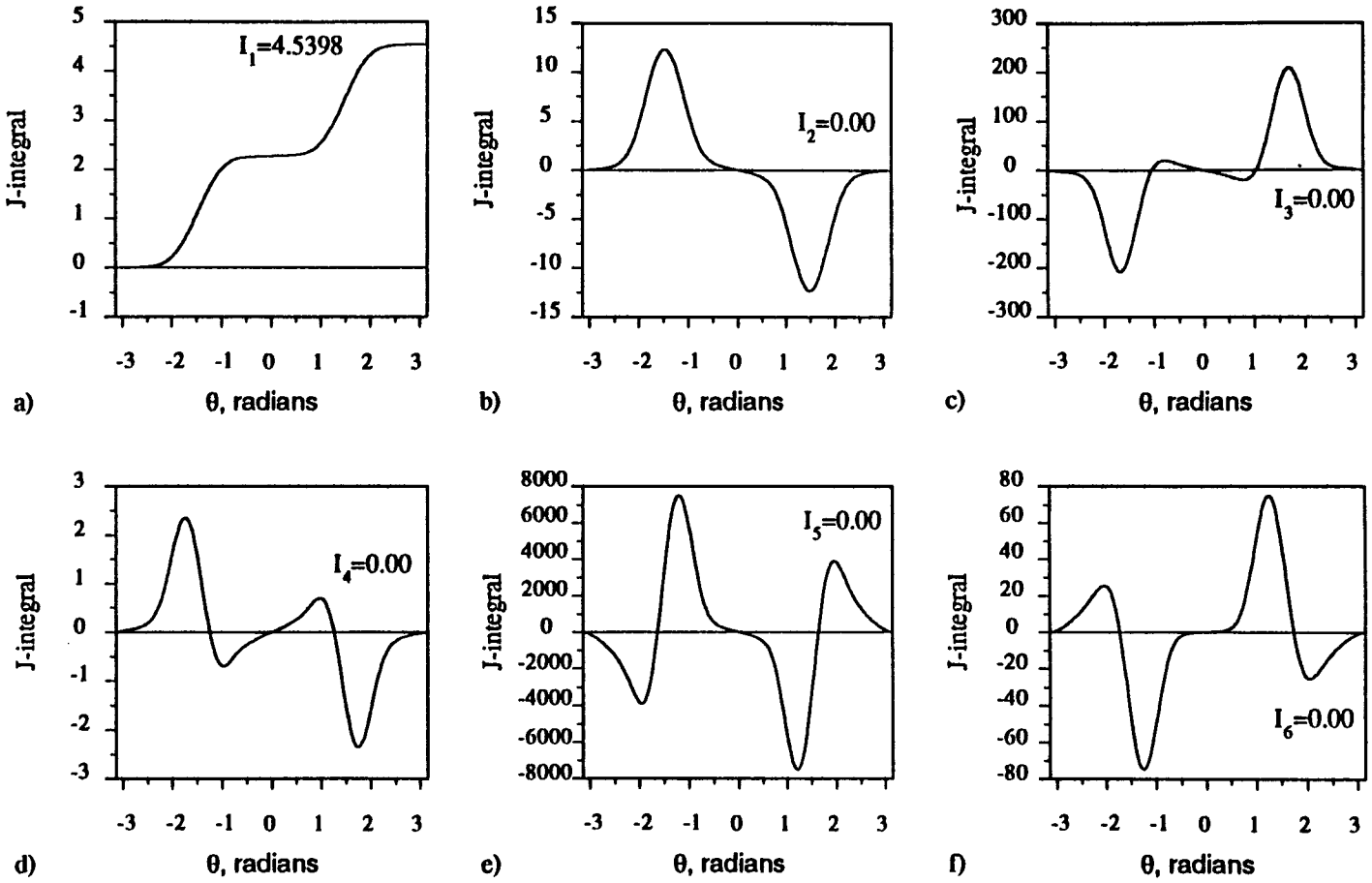

FIG. 3.9— Integration constants for the *J* - integral: a) field 1, b) field 2, c) field 3, d) field 4, e) field 5, f) field 6.

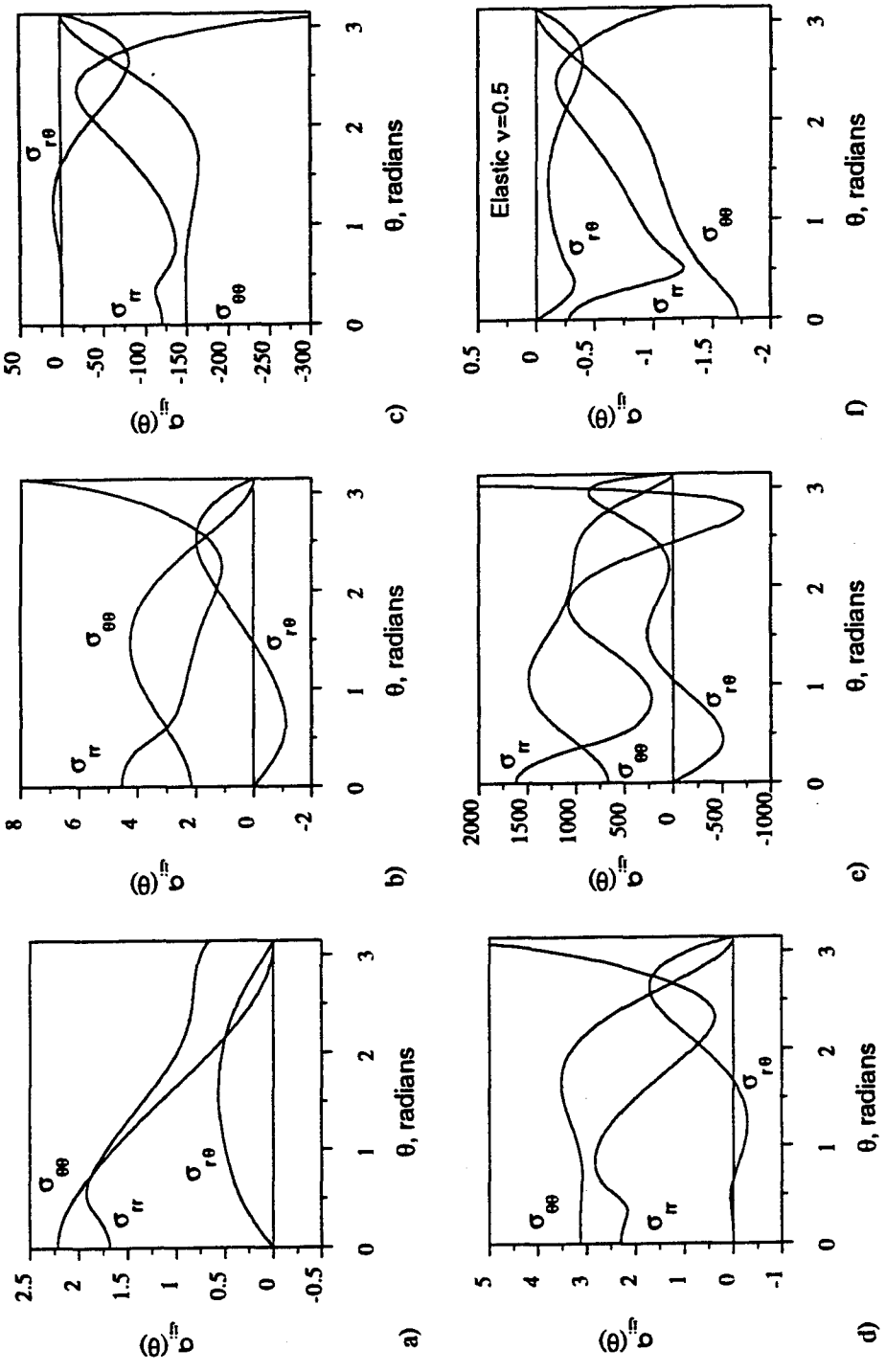

FIG. 3.10— Angular stress functions for n=5: a) field 1, b) field 2, c) field 3, d) field 4, e) field 5, f) field 6.

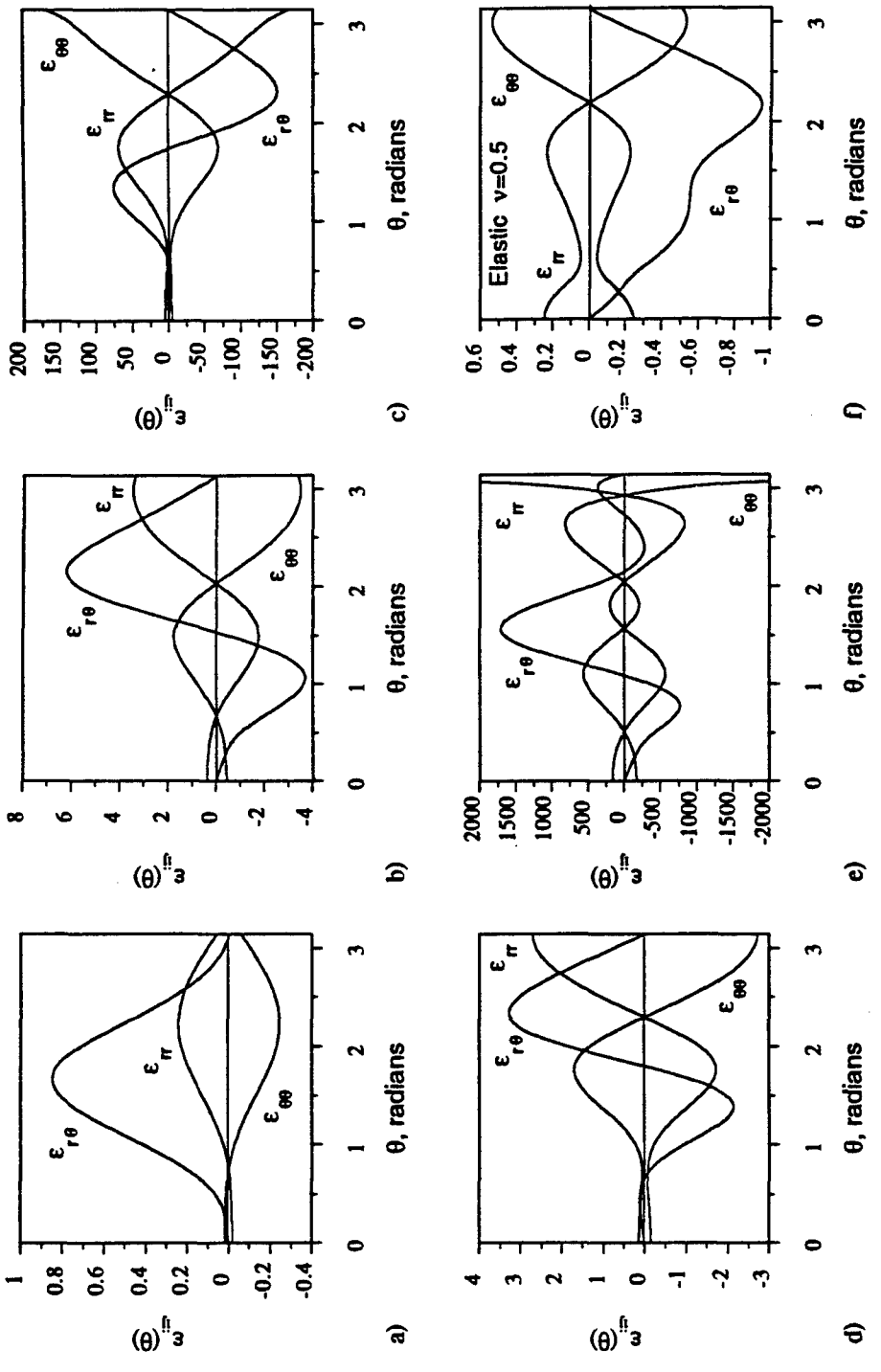

FIG. 3.11— Angular strain functions for n=5: a) field 1, b) field 2, c) field 3, d) field 4, e) field 5, f) field 6.

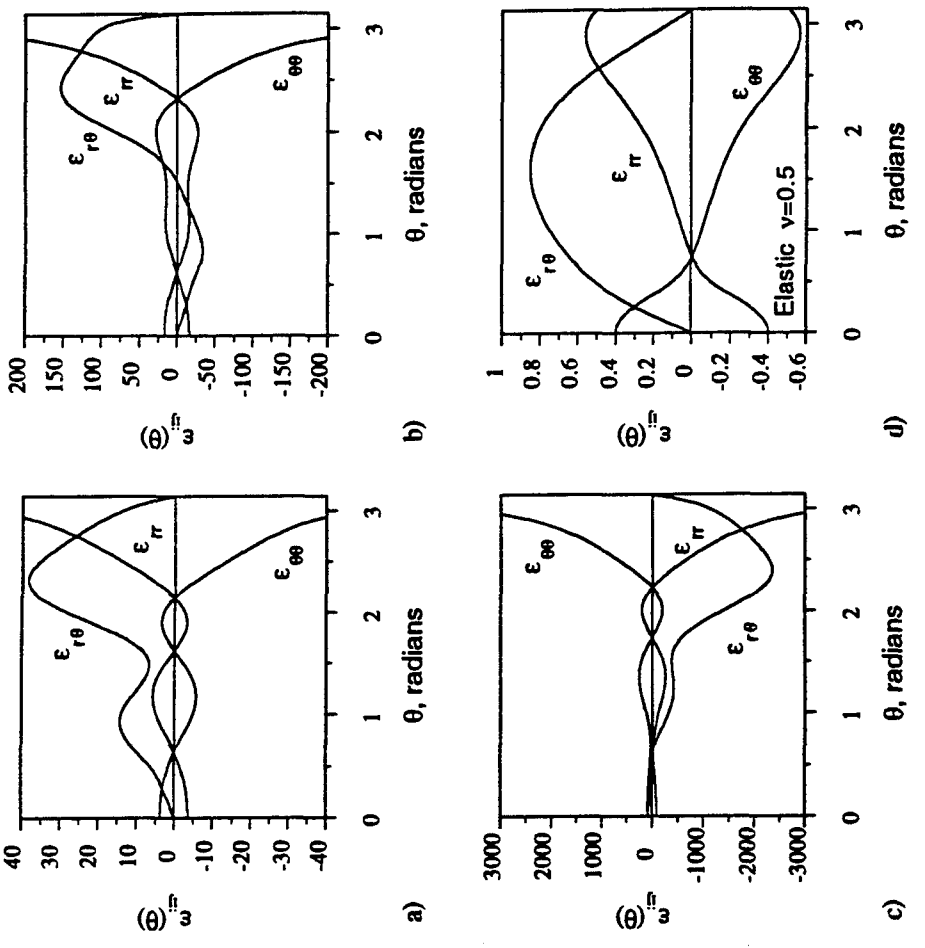

FIG. 3.12— Angular strain functions for particular solutions to differential equations: a) field 22, b) field 222, c) field 23, d) field e1.

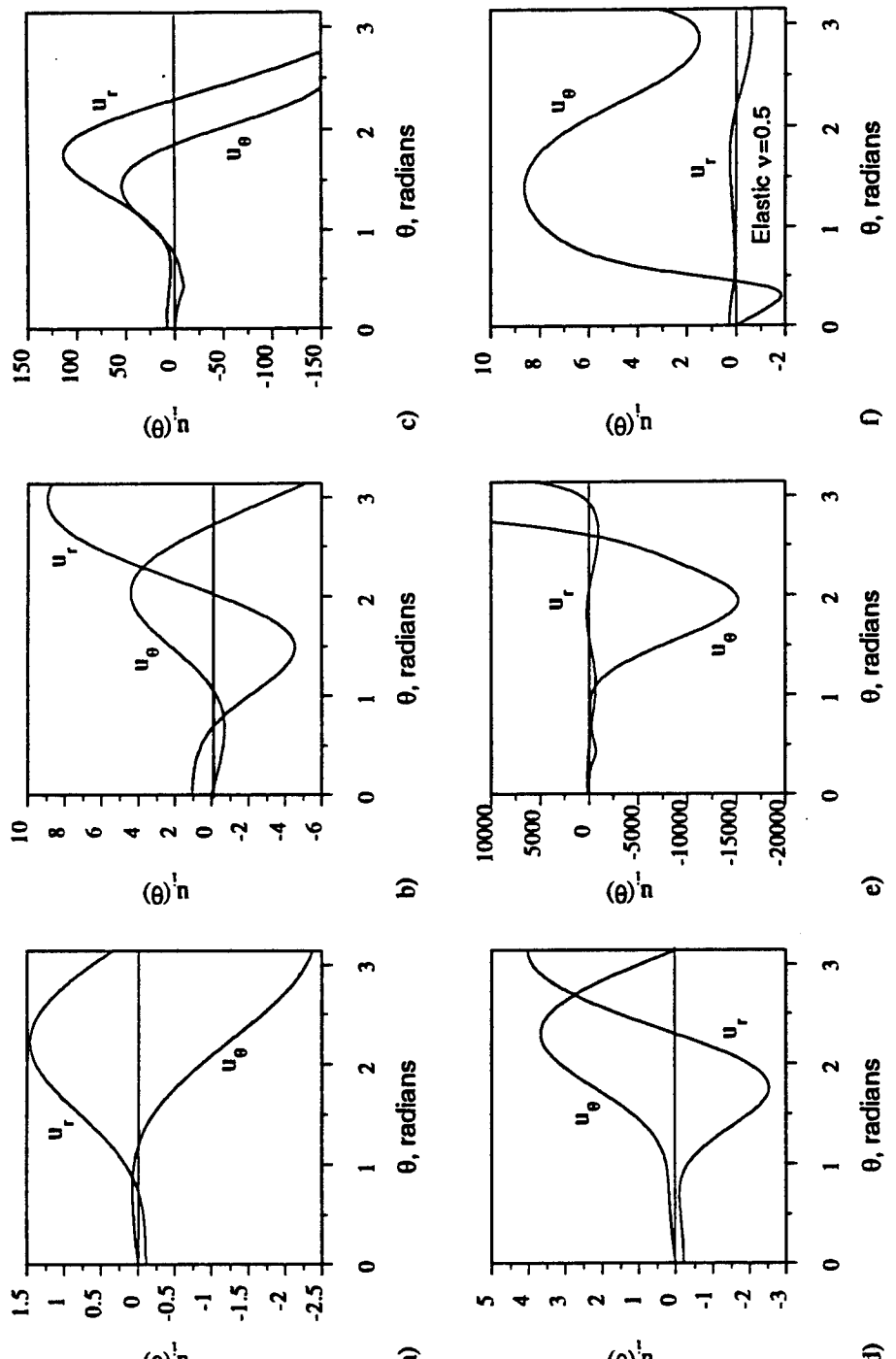

FIG. 3.13— Angular displacement functions for n=5: a) field 1, b) field 2, c) field 3, d) field 4, e) field 5, f) field 6.

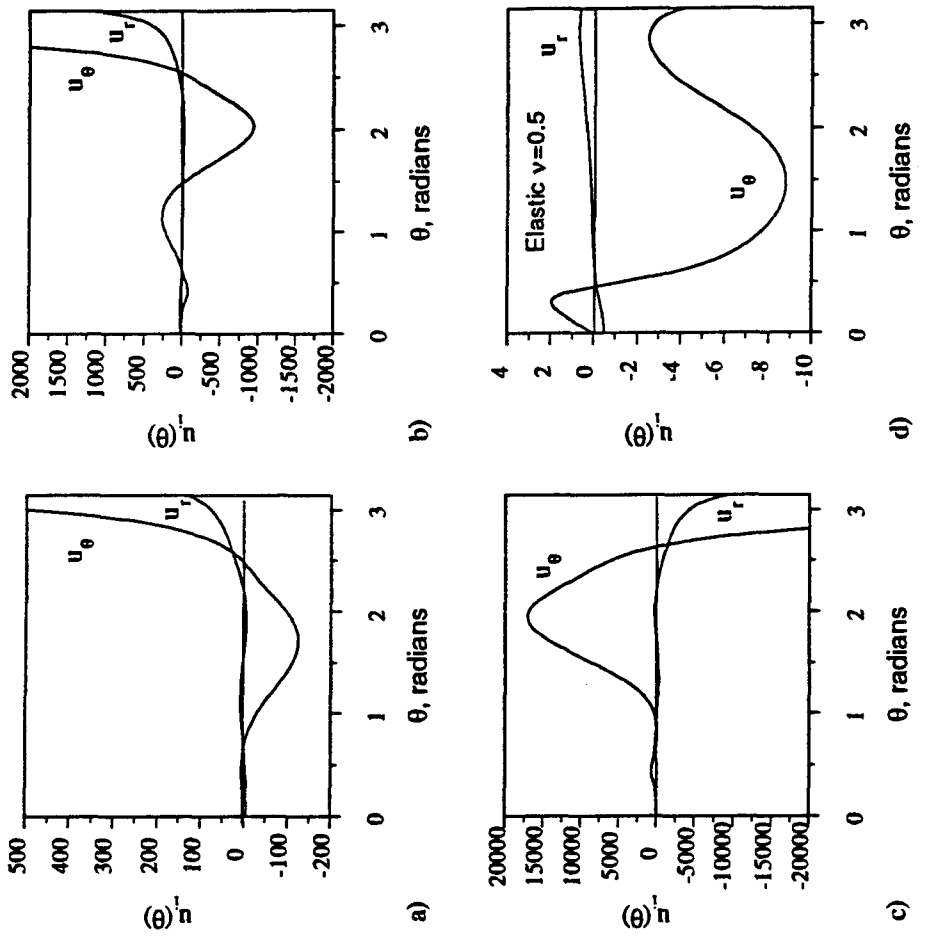

FIG. 3.14— Angular displacement functions for particular solutions to differential equations: a) field 22, b) field 222, c) field 23, d) field e1.

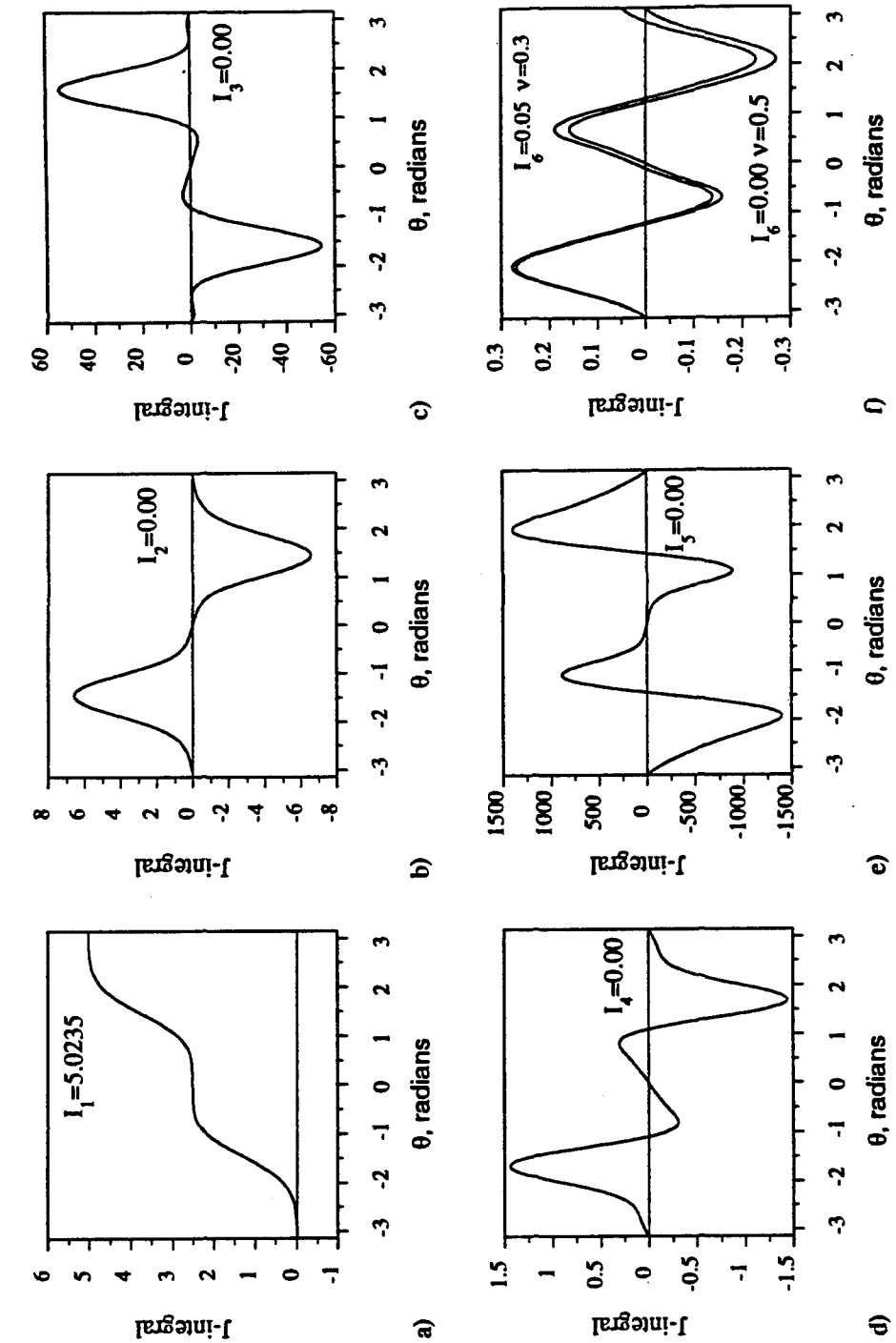

FIG. 3.15— Integration constants for the J - integral: a) field 1, b) field 2, c) field 3, d) field 4, e) field 5, f) field 6.

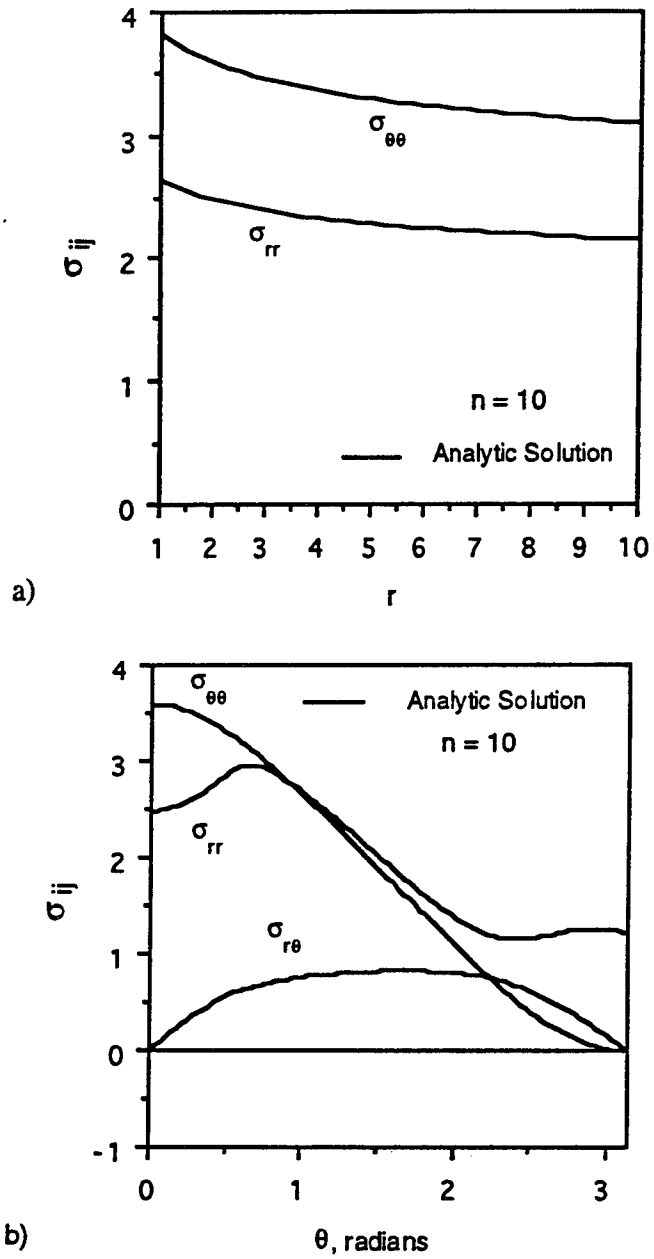

FIG. 3.16— Stress field for the single term (HRR) representation of the stress potential: a) radial variation, b) angular variation.

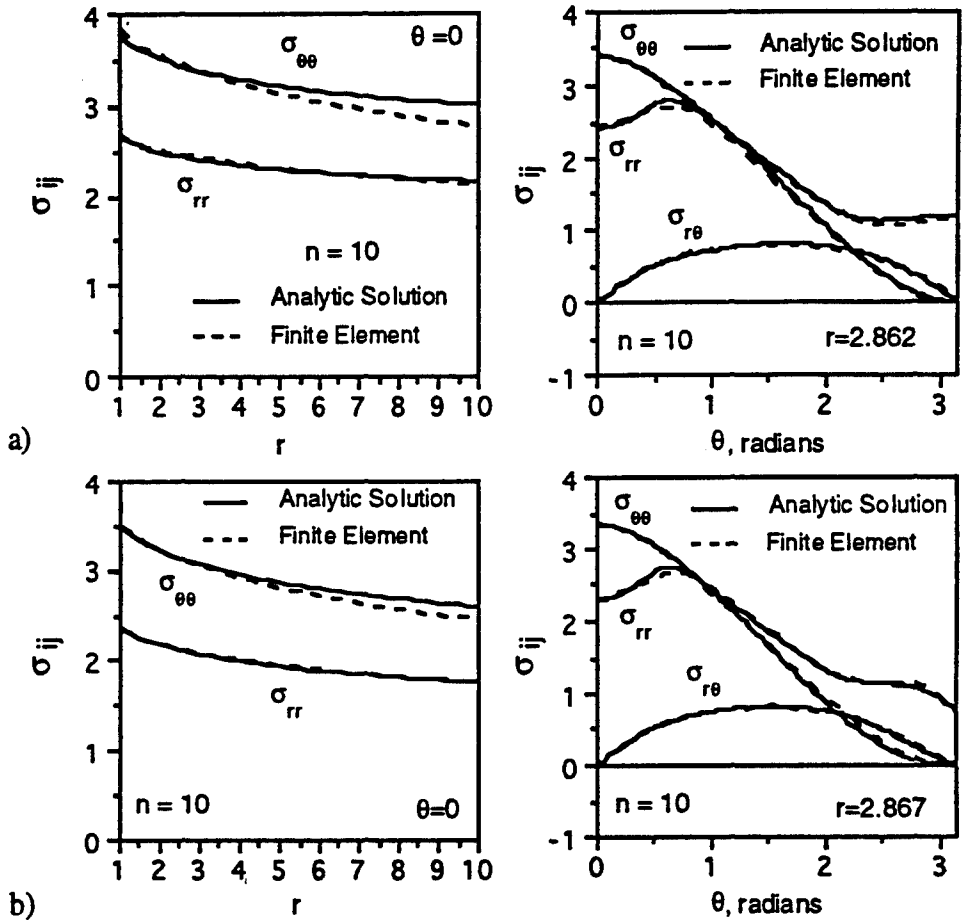

FIG. 3.17— Comparison of a six term analytic solution with finite element predictions for the in-plane stresses of the MBL: a) $T/\sigma_o = +0.3, \sigma_{PL} = 0.95\sigma_o$, b) $T/\sigma_o = -0.4, \sigma_{PL} = 0.95\sigma_o$.

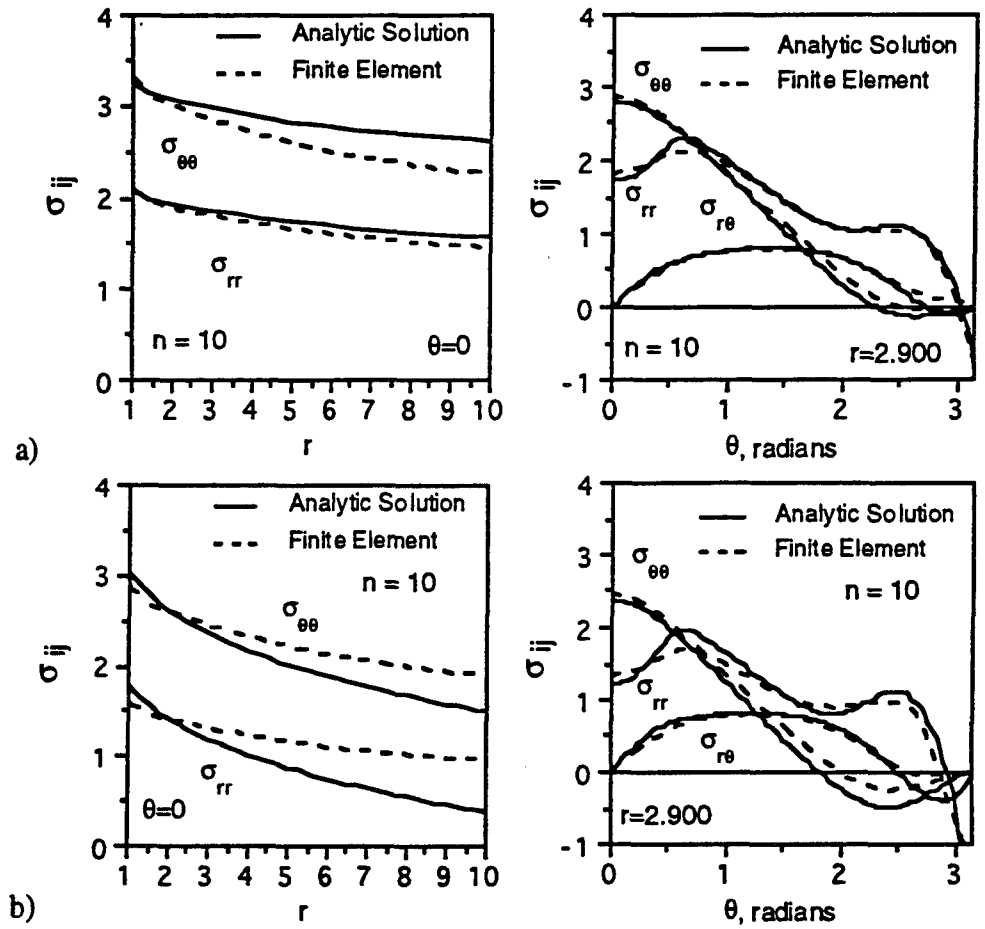

FIG. 3.18— Comparison of a six term analytic solution with finite element predictions for the in-plane stresses of the MBL: a) $T/\sigma_o = -0.7$, $\sigma_{PL} = 0.95\sigma_o$, b) $T/\sigma_o = -0.7$, $\sigma_{PL} = 0.85\sigma_o$.

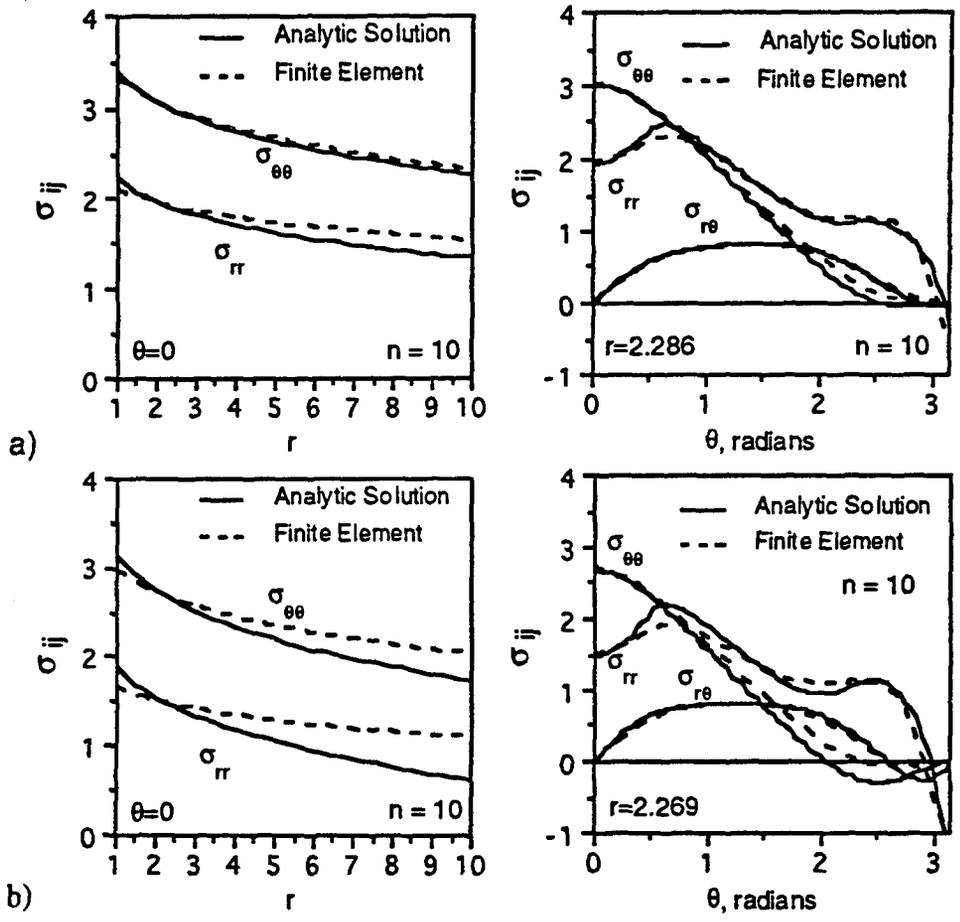

FIG. 3.19— Comparison of a six term analytic solution with finite element predictions for the in-plane stresses of the SENB specimen with an a/W=0.1: a) $J/b\sigma_o = 0.000530$, b) $J/b\sigma_o = 0.002478$.

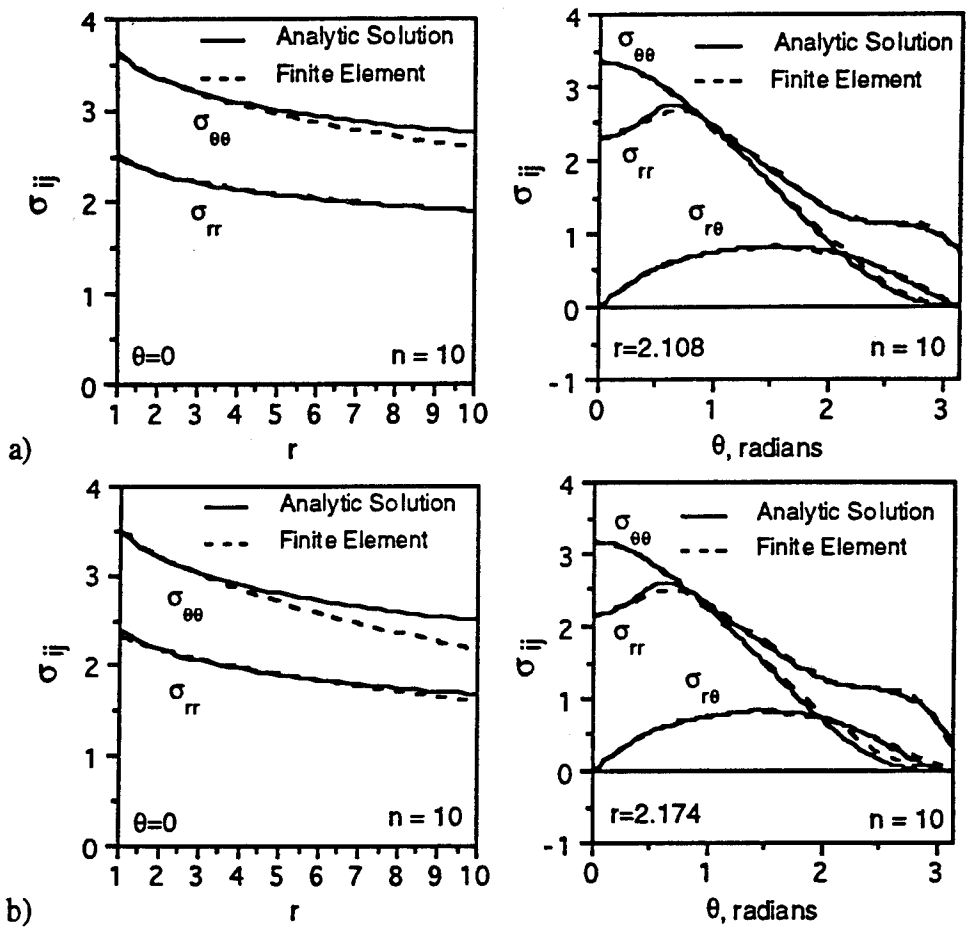

FIG. 3.20— Comparison of a six term analytic solution with finite element predictions for the in-plane stresses of the SENB specimen with an a/W=0.5: a) $J/b\sigma_0 = 0.001462$, b) $J/b\sigma_0 = 0.01111$.

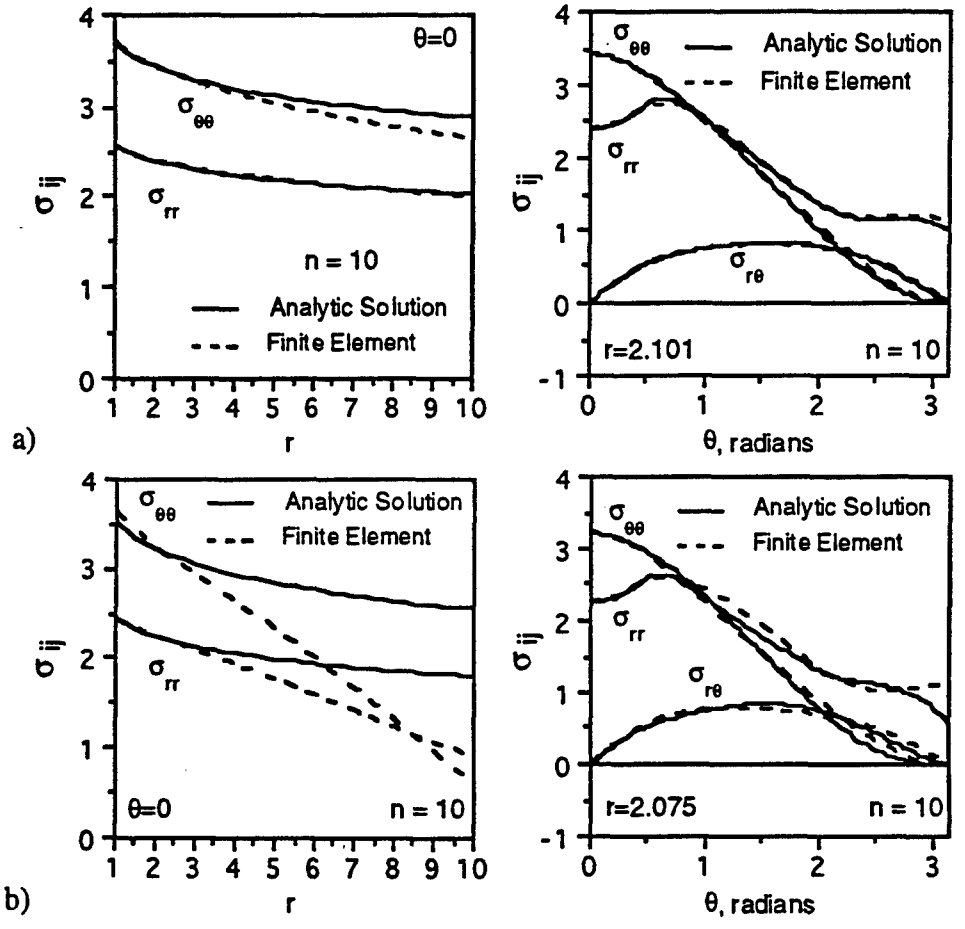

FIG. 3.21— Comparison of a six term analytic solution with finite element predictions for the in-plane stresses of the SENB specimen with an a/W=0.9: a) $J/b\sigma_o = 0.003881$, b) $J/b\sigma_o = 0.032058$.

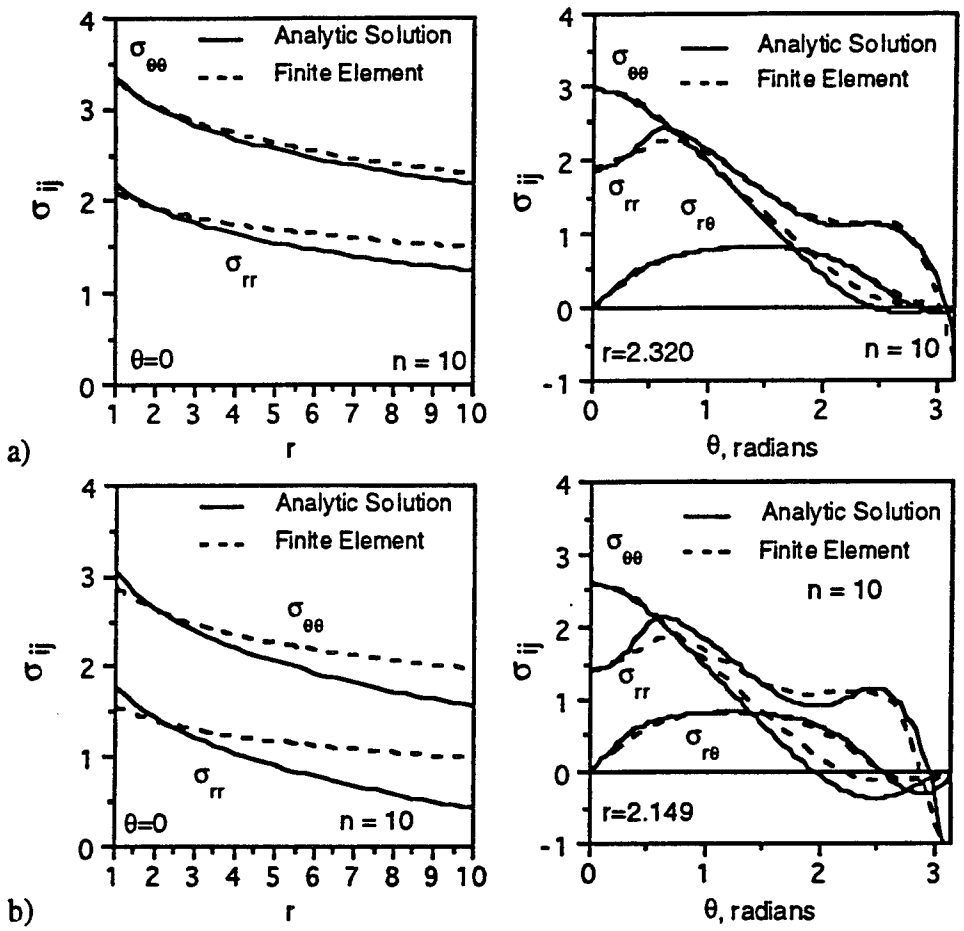

FIG. 3.22— Comparison of a six term analytic solution with finite element predictions for the in-plane stresses of the CCT specimen with an a/W=0.1: a) $J/b\sigma_0 = 0.000092$, b) $J/b\sigma_0 = 0.000421$.

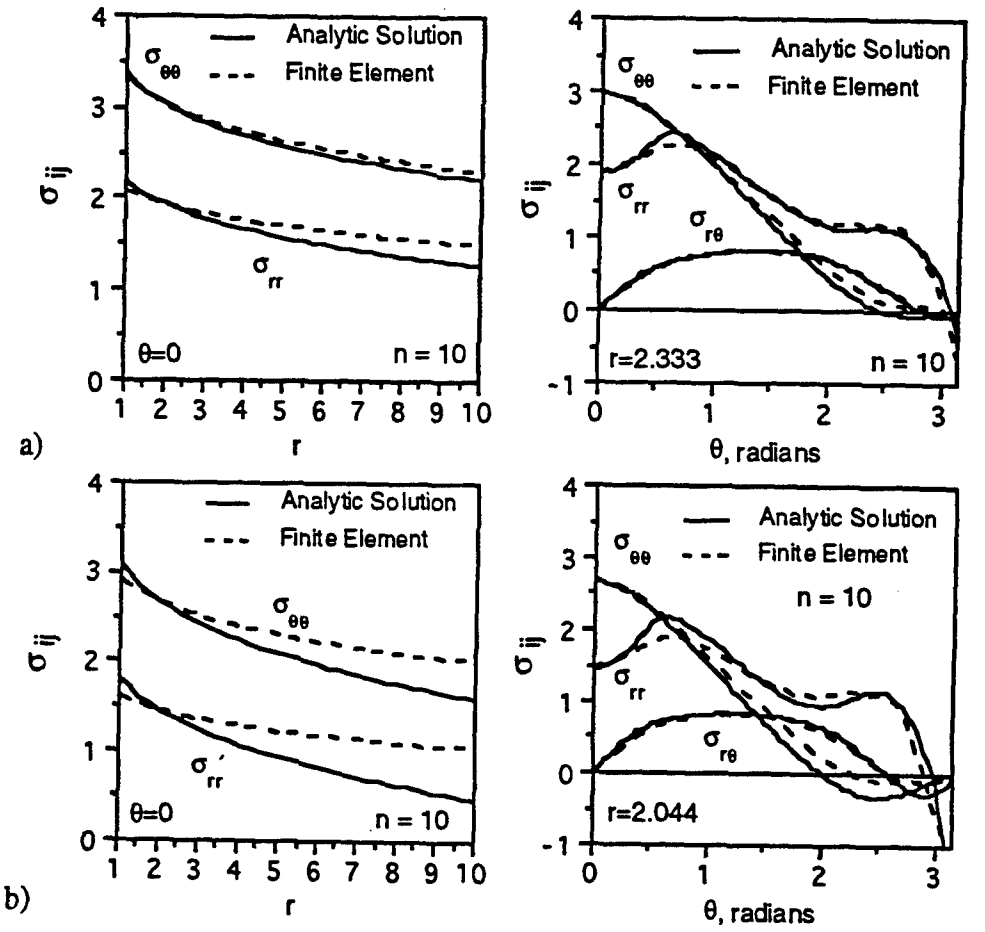

FIG. 3.23— Comparison of a six term analytic solution with finite element predictions for the in-plane stresses of the CCT specimen with an a/W=0.5: a) $J/b\sigma_o = 0.00071$, b) $J/b\sigma_o = 0.00259$.

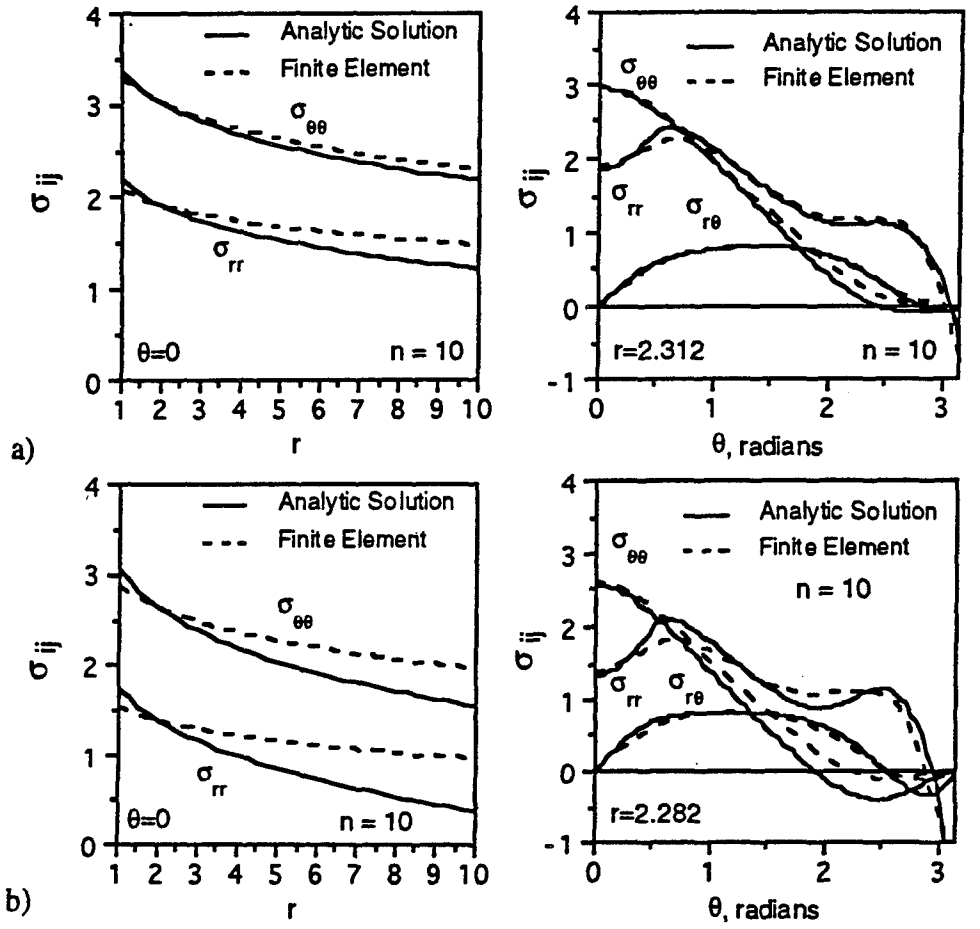

FIG. 3.24— Comparison of a six term analytic solution with finite element predictions for the in-plane stresses of the CCT specimen with an a/W=0.9: a) $J/b\sigma_0 = 0.001927$, b) $Jb/\sigma_0 = 0.006356$.

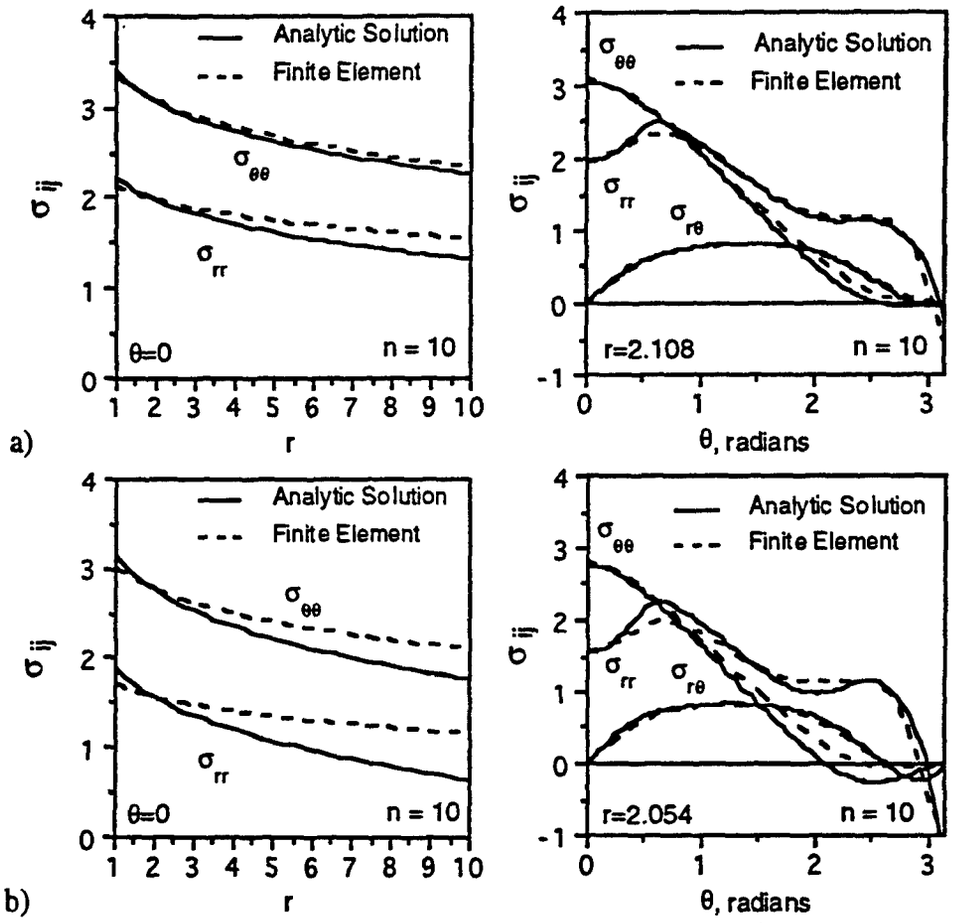

FIG. 3.25— Comparison of a six term analytic solution with finite element predictions for the in-plane stresses of the DENT specimen with an a/W=0.1: a) $J/b\sigma_o = 0.000319$, b) $J/b\sigma_o = 0.001039$.

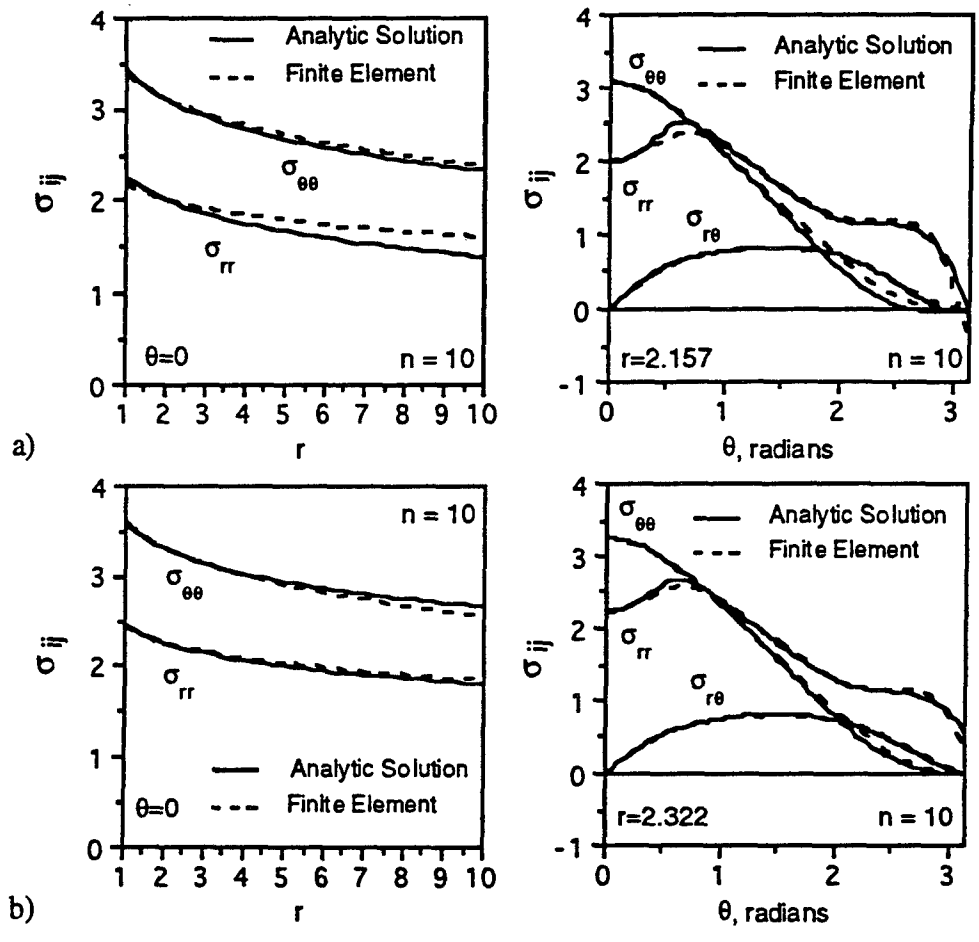

FIG. 3.26— Comparison of a six term analytic solution with finite element predictions for the in-plane stresses of the DENT specimen: a) $a/W = 0.5$, $J/b\sigma_o = 0.00245$, b) $a/W = 0.9$, $J/b\sigma_o = 0.001638$.

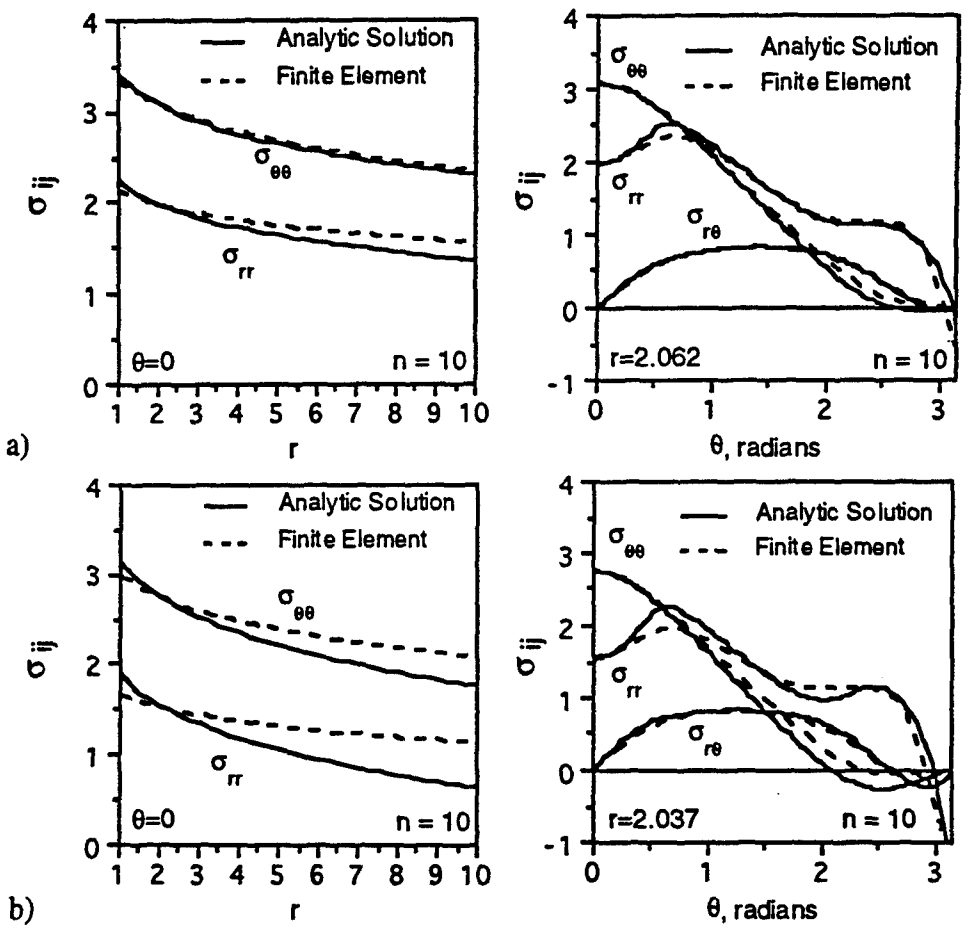

FIG. 3.27— Comparison of a six term analytic solution with finite element predictions for the in-plane stresses of the SENT specimen with an a/W=0.1: a) $J/b\sigma_0 = 0.000326$, b) $J/b\sigma_0 = 0.001205$.

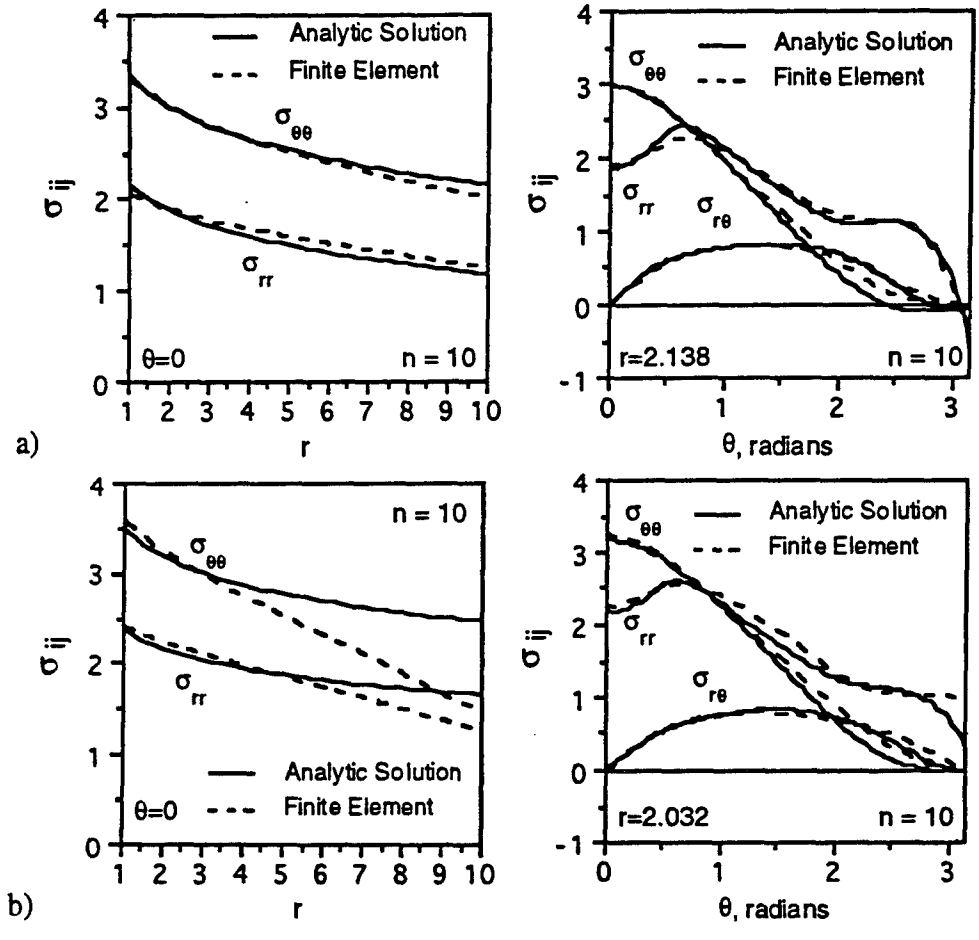

FIG. 3.28— Comparison of a six term analytic solution with finite element predictions for the in-plane stresses of the SENT specimen: a) $a/W = 0.5$, $J/b\sigma_o = 0.02230$, b) $a/W = 0.9$, $J/b\sigma_o = 0.024900$.

TABLE 3.4— Coefficients obtained for the analytic solution at r = 2.14, θ = 0.0 by matching with the finite element results for the MBL geometry with n = 10.

$\sigma_{PL} = 0.85\,\sigma_o$				$\sigma_{PL} = 0.95\,\sigma_o$				$\sigma_{PL} = 0.95\,\sigma_o$			
T/σ_o	J (J/cm^3)	K2	K4	T/σ_o	J (J/cm^3)	K2	K4	S/σ_o	J (J/cm^3)	K2	K4
-1.00	1.296	-0.0600	-0.5747	-1.00	1.296	-0.0596	-0.3900				
-0.90	1.310	-0.0570	-0.5197	-0.90	1.310	-0.0573	-0.4050				
-0.80	1.313	-0.0530	-0.4862	-0.80	1.313	-0.0534	-0.4250				
-0.70	1.317	-0.0480	-0.4750	-0.70	1.317	-0.0480	-0.4550				
-0.60	1.319	-0.0420	-0.4714	-0.60	1.319	-0.0422	-0.4714				
-0.50	1.321	-0.0350	-0.4882	-0.50	1.321	-0.0350	-0.4882				
-0.40	1.322	-0.0280	-0.4932	-0.40	1.322	-0.0280	-0.4932				
-0.30	1.322	-0.0210	-0.4876	-0.30	1.322	-0.0210	-0.4876				
-0.20	1.323	-0.0130	-0.4708	-0.20	1.323	-0.0130	-0.4708				
-0.10	1.324	-0.0070	-0.4435	-0.10	1.324	-0.0070	-0.4435	-0.01	0.336	-0.0020	-0.3889
0.00	1.324	0.0000	-0.3968	0.00	1.324	0.0000	-0.3968	0.00	0.332	0.0004	-0.3970
0.10	1.324	0.0070	-0.3100	0.10	1.324	0.0070	-0.3100	0.01	0.327	0.0132	-0.2442
0.20	1.324	0.0120	-0.2400	0.20	1.324	0.0120	-0.2400				
0.30	1.325	0.0200	-0.1545	0.30	1.325	0.0200	-0.1545				

TABLE 3.5— Coefficients obtained for the analytic solution at r = 2.14, θ = 0.0 by matching with the finite element results for the SENB geometry with n = 10.

a/W=0.1				a/W=0.5				a/W=0.9			
Load (KN)	J/b σ_0	K2	K4	Load (KN)	J/b σ_0	K2	K4	Load (KN)	J/b σ_0	K2	K4
8.89	0.0000061	-0.0020	-0.4030	4.44	0.0000282	0.0006	-0.3904	0.18	0.0000308	-0.0067	-0.3294
17.78	0.0000245	-0.0050	-0.4160	8.89	0.0001135	0.0002	-0.3806	0.36	0.0001250	0.0010	-0.3471
26.67	0.0000552	-0.0070	-0.4240	13.33	0.0002567	0.0008	-0.3589	0.53	0.0002833	0.0037	-0.3557
35.56	0.0000987	-0.0090	-0.4350	17.78	0.0004597	0.0011	-0.3783	0.71	0.0005075	0.0050	-0.3400
44.44	0.0001552	-0.0120	-0.4440	22.22	0.0007252	0.0014	-0.3770	0.89	0.0008008	0.0061	-0.3263
53.33	0.0002256	-0.0140	-0.4500	26.67	0.0010572	0.0016	-0.3763	1.07	0.0011667	0.0070	-0.3108
62.22	0.0003106	-0.0170	-0.4560	31.11	0.0014623	0.0018	-0.3767	1.24	0.0016133	0.0076	-0.2974
71.11	0.0004115	-0.0200	-0.4590	35.56	0.0019700	0.0019	-0.3788	1.42	0.0021733	0.0079	-0.2835
80.00	0.0005300	-0.0230	-0.4600	40.00	0.0026217	0.0019	-0.3837	1.60	0.0028983	0.0080	-0.2714
88.89	0.0006685	-0.0270	-0.4570	44.44	0.0034800	0.0017	-0.3924	1.78	0.0038808	0.0079	-0.2617
97.78	0.0008333	-0.0310	-0.4500	48.89	0.0046817	0.0012	-0.4090	1.96	0.0053042	0.0074	-0.2579
106.67	0.0010333	-0.0350	-0.4360	53.33	0.0068900	-0.0009	-0.4623	2.13	0.0077225	0.0059	-0.2727
115.56	0.0012815	-0.0390	-0.4170	57.78	0.0111083	-0.0034	-0.5621	2.31	0.0120667	0.0046	-0.3181
124.44	0.0015907	-0.0420	-0.3920	62.22	0.0189167	-0.0037	-0.7361	2.49	0.0193167	0.0040	-0.4098
133.33	0.0019806	-0.0460	-0.3660	66.67	0.0333833	-0.0014	-1.0387	2.67	0.0320583	0.0052	-0.6193
142.22	0.0024778	-0.0490	-0.3350	71.11	0.0600000	0.0015	-1.5910	2.84	0.0535500	0.0082	-1.0981
151.11	0.0031417	-0.0530	-0.3030	75.56	0.1078333	0.0028	-2.6076	3.02	0.0902500	0.0103	-2.2243
160.00	0.0040676	-0.0560	-0.2730					3.20	0.1523333	0.0136	-6.0907
168.89	0.0055583	-0.0590	-0.2540					3.38	0.2562500	0.0135	-11.6579
177.78	0.0079491	-0.0620	-0.2300								

TABLE 3.6— Coefficients obtained for the analytic solution at r = 2.14, θ = 0.0 by matching with the finite element results for the CCT geometry with n = 10.

a/W=0.1				a/W=0.5				a/W=0.9			
Load (MPa)	J/b σ_0	K2	K4	Load (MPa)	J/b σ_0	K2	K4	Load (MPa)	J/b σ_0	K2	K4
25.86	0.0000025	-0.0080	-0.3800	15.09	0.0000107	-0.0090	-0.4232	4.31	0.0000372	-0.0090	-0.3670
51.72	0.0000101	-0.0100	-0.4040	30.17	0.0000427	-0.0081	-0.3895	8.62	0.0001492	-0.0080	-0.4130
77.59	0.0000227	-0.0130	-0.4470	45.26	0.0000968	-0.0095	-0.4370	12.93	0.0003369	-0.0100	-0.4450
103.45	0.0000405	-0.0170	-0.4660	60.34	0.0001725	-0.0121	-0.4530	17.24	0.0006023	-0.0140	-0.4610
129.31	0.0000635	-0.0210	-0.4830	75.43	0.0002705	-0.0150	-0.4672	21.55	0.0009500	-0.0170	-0.4740
155.17	0.0000920	-0.0250	-0.4920	90.52	0.0003915	-0.0179	-0.4801	25.86	0.0013867	-0.0210	-0.4820
181.03	0.0001264	-0.0290	-0.4940	105.60	0.0005360	-0.0210	-0.4879	30.17	0.0019275	-0.0260	-0.4830
206.90	0.0001671	-0.0330	-0.4880	120.69	0.0007063	-0.0242	-0.4924	34.48	0.0026000	-0.0310	-0.4700
232.76	0.0002153	-0.0380	-0.4750	135.78	0.0009043	-0.0276	-0.4936	38.79	0.0034525	-0.0380	-0.4390
258.62	0.0002720	-0.0420	-0.4520	150.86	0.0011345	-0.0312	-0.4888	43.10	0.0045692	-0.0450	-0.3790
284.48	0.0003396	-0.0470	-0.4210	165.95	0.0014040	-0.0352	-0.4789	47.41	0.0063567	-0.0560	-0.2880
310.34	0.0004216	-0.0510	-0.3830	181.03	0.0017217	-0.0395	-0.4594	51.72	0.0099083	-0.0660	-0.1930
336.21	0.0005236	-0.0560	-0.3440	196.12	0.0021067	-0.0443	-0.4283				
362.07	0.0006591	-0.0600	-0.3030	211.21	0.0025883	-0.0496	-0.3857				
387.93	0.0008966	-0.0640	-0.2580	226.29	0.0032600	-0.0557	-0.3299				
413.79	0.0015120	-0.0690	-0.2100	241.38	0.0045367	-0.0631	-0.2576				
439.66	0.0025444	-0.0730	-0.1690								
465.52	0.0041556	-0.0770	-0.1270								

TABLE 3.7— Coefficients obtained for the analytic solution at r = 2.14, θ = 0.0 by matching with the finite element results for the DENT geometry with n = 10.

a/W=0.1				a/W=0.5				a/W=0.9			
Load (MPa)	$J/b\sigma_o$	K2	K4	Load (MPa)	$J/b\sigma_o$	K2	K4	Load (MPa)	$J/b\sigma_o$	K2	K4
28.45	0.0000038	-0.0060	-0.3500	11.21	0.0000057	-0.0038	-0.3500	3.45	0.0000158	-0.0208	-0.2817
56.90	0.0000150	-0.0070	-0.3776	22.41	0.0000230	-0.0040	-0.3808	5.17	0.0000358	-0.0076	-0.3413
85.34	0.0000339	-0.0078	-0.4218	33.62	0.0000518	-0.0044	-0.3939	6.90	0.0000642	-0.0024	-0.3876
113.79	0.0000605	-0.0097	-0.4350	44.83	0.0000922	-0.0046	-0.4115	8.62	0.0001000	-0.0030	-0.3755
142.24	0.0000949	-0.0121	-0.4437	56.03	0.0001442	-0.0053	-0.4167	10.34	0.0001442	-0.0029	-0.3788
170.69	0.0001375	-0.0146	-0.4498	67.24	0.0002078	-0.0061	-0.4223	12.07	0.0001967	-0.0020	-0.3985
199.14	0.0001887	-0.0173	-0.4526	78.45	0.0002832	-0.0070	-0.4277	13.79	0.0002567	-0.0018	-0.4003
227.59	0.0002491	-0.0202	-0.4522	89.66	0.0003705	-0.0078	-0.4327	15.52	0.0003258	-0.0020	-0.3997
256.03	0.0003194	-0.0235	-0.4471	100.86	0.0004700	-0.0088	-0.4368	17.24	0.0004025	-0.0021	-0.3998
284.48	0.0004010	-0.0272	-0.4394	112.07	0.0005817	-0.0097	-0.4407	18.97	0.0004875	-0.0021	-0.4012
312.93	0.0004964	-0.0314	-0.4260	123.28	0.0007058	-0.0107	-0.4441	20.69	0.0005817	-0.0022	-0.4033
341.38	0.0006100	-0.0361	-0.4067	134.48	0.0008428	-0.0117	-0.4472	22.41	0.0006833	-0.0022	-0.4042
369.83	0.0007535	-0.0414	-0.3763	145.69	0.0009928	-0.0127	-0.4496	24.14	0.0007933	-0.0023	-0.4049
398.28	0.0010398	-0.0485	-0.3217	156.90	0.0011563	-0.0137	-0.4520	25.86	0.0009117	-0.0025	-0.4053
426.72	0.0017704	-0.0571	-0.2384	168.10	0.0013337	-0.0148	-0.4539	27.59	0.0010400	-0.0025	-0.4070
455.17	0.0030657	-0.0630	-0.1827	179.31	0.0015253	-0.0159	-0.4552	29.31	0.0011758	-0.0026	-0.4079
483.62	0.0051519	-0.0670	-0.1527	190.52	0.0017317	-0.0169	-0.4563	31.03	0.0013208	-0.0027	-0.4087
				201.72	0.0019550	-0.0181	-0.4570	32.76	0.0014750	-0.0028	-0.4098
				212.93	0.0021933	-0.0193	-0.4566	34.48	0.0016383	-0.0029	-0.4112
				224.14	0.0024533	-0.0206	-0.4570				

TABLE 3.8— Coefficients obtained for the analytic solution at r = 2.14, θ = 0.0 by matching with the finite element results for the SENT geometry with n = 10.

a/W=0.1				a/W=0.5				a/W=0.9			
Load (MPa)	$J/b\sigma_0$	K2	K4	Load (MPa)	$J/b\sigma_0$	K2	K4	Load (MPa)	$J/b\sigma_0$	K2	K4
34.48	0.0000006	-0.0024	-0.4318	24.14	0.0001568	-0.0022	-0.3969	0.38	0.0000517	-0.0003	-0.3679
68.97	0.0000251	-0.0068	-0.4426	48.28	0.0006440	-0.0032	-0.4193	0.76	0.0002092	0.0026	-0.3634
103.45	0.0000568	-0.0095	-0.4605	72.41	0.0015252	-0.0042	-0.4436	1.14	0.0004750	0.0044	-0.3472
137.93	0.0001016	-0.0124	-0.4733	96.55	0.0029533	-0.0092	-0.4600	1.52	0.0008567	0.0057	-0.3329
172.41	0.0001606	-0.0156	-0.4811	120.69	0.0053133	-0.0114	-0.4686	1.90	0.0013608	0.0067	-0.3168
206.90	0.0002347	-0.0193	-0.4822	144.83	0.0099417	-0.0177	-0.4807	2.28	0.0020233	0.0073	-0.3013
241.38	0.0003265	-0.0235	-0.4773	168.97	0.0223000	-0.0278	-0.4695	2.66	0.0027325	0.0076	-0.2882
275.86	0.0004402	-0.0283	-0.4683	193.10	0.0611167	-0.0342	-0.4418	3.03	0.0042750	0.0073	-0.2800
310.34	0.0005858	-0.0343	-0.4463	217.24	0.1809000	-0.0400	-0.3900	3.41	0.0065567	0.0061	-0.2851
344.83	0.0007964	-0.0415	-0.4071					3.79	0.0121000	0.0032	-0.3672
379.31	0.0012056	-0.0503	-0.3386					4.17	0.0249000	0.0029	-0.5879
413.79	0.0021935	-0.0585	-0.2608					4.55	0.0541667	0.0067	-1.2287
448.28	0.0043046	-0.0640	-0.2147								
482.76	0.0081898	-0.0672	-0.1918								

series coefficients as a function of deformation level for each specimen geometry. The coefficients were obtained as a function of position within an annulus bounded by a normalized radius of $1.0 \le r \le 15$. this region excludes the finite strain zone near the crack-tip. It was found that at low to medium deformations levels, the value of coefficients did not have any significant spatial variation within this annulus except for very near the crack surfaces. The coefficients that are reported were determined at a spatial coordinate of $r = 2.148$ and $\theta = 0$. Table 3.9 contains the coefficients, deformation levels and location for the analytic/numerical comparison given in Figs. 3.17-3.28.

3.4 Influence of Second and Third Williams Terms

To insure that the boundaries in the MBL had no influence on the stress field at the crack-tip, the displacements associated with the first Williams term were applied for two different values of applied K. A comparison of the normalized hoop stress are given in Fig. 3.29. The stress fields after being normalized by σ_0 are self similar in nature indicating that the stresses at the crack-tip have not felt the influence of the boundaries. Further, the *J*-integral values obtained from the numerical study agree to within a one half of one percent to that of the applied J value.

A comparison of the crack-tip stresses for the second and third Williams terms are given in Figs. 3.30 and 3.31. The MBL was ran first with the third Williams term (S/σ_0) set to zero while varying the second term (T/σ_0) and then the second term was set to zero while the third term was varied. The values of the second and third coefficients reported in these figures correspond to plastic zones that measure approximately 8% of the MBL radius. The first fringe plot in each of the figures shows the hoop stress within the annulus of interest. The second plot in the figures shows the portion of the hoop stress which is associated with the second and third term, respectfully. The last fringe plot shows the global hoop stress associated with the second and third term, respectfully. The contribution of the second and third Williams term were determined by subtracting the full field solutions for $T/\sigma_0,\ S/\sigma_0 = 0$ from the cases for $T/\sigma_0 = \alpha,\ S/\sigma_0 = \beta$.

TABLE 3.9— Coefficients and radial value used to compare finite element results with analytic solution.

Specimen	Geometry	Load	r	J	K2	K4
		T/σ_o		(J/cm^2)		
MBL	low yield	-0.70	2.900	1.32	-0.0480	-0.4750
	high yield	-0.70	2.900	1.32	-0.0480	-0.4550
	high yield	-0.40	2.867	1.32	-0.0280	-0.4932
	high yield	0.30	2.862	1.32	0.0200	-0.1545
		(KN)		$J/b\sigma_o$		
SENB	a/w = 0.1	80.00	2.286	0.0005300	-0.0230	-0.4600
		142.22	2.269	0.0024778	-0.0490	-0.3350
	a/w = 0.5	26.67	2.108	0.0014623	0.0016	-0.3763
		57.78	2.174	0.0111083	-0.0034	-0.5621
	a/w = 0.9	1.78	2.101	0.0038808	0.0079	-0.2617
		2.67	2.075	0.0320583	0.0052	-0.6193
		(MPa)				
CCT	a/w = 0.1	155.17	2.320	0.0000920	-0.0250	-0.4920
		310.34	2.149	0.0004216	-0.0510	-0.3830
	a/w = 0.5	120.69	2.333	0.0007063	-0.0242	-0.4924
		211.21	2.044	0.0025883	-0.0496	-0.3857
	a/w = 0.9	30.17	2.312	0.0019275	-0.0260	-0.4830
		47.41	2.282	0.0063567	-0.0560	-0.2880
DENT	a/w = 0.1	256.03	2.108	0.0003194	-0.0235	-0.4471
		398.28	2.054	0.0010398	-0.0485	-0.3217
	a/w = 0.5	224.14	2.157	0.0024533	-0.0206	-0.4570
	a/w = 0.9	34.48	2.322	0.0016383	-0.0029	-0.4112
SENT	a/w = 0.1	241.38	2.062	0.0003265	-0.0235	-0.4773
		379.31	2.037	0.0012056	-0.0503	-0.3386
	a/w = 0.5	168.97	2.138	0.0223000	-0.0278	-0.4695
	a/w = 0.9	4.17	2.032	0.0249000	0.0029	-0.5879

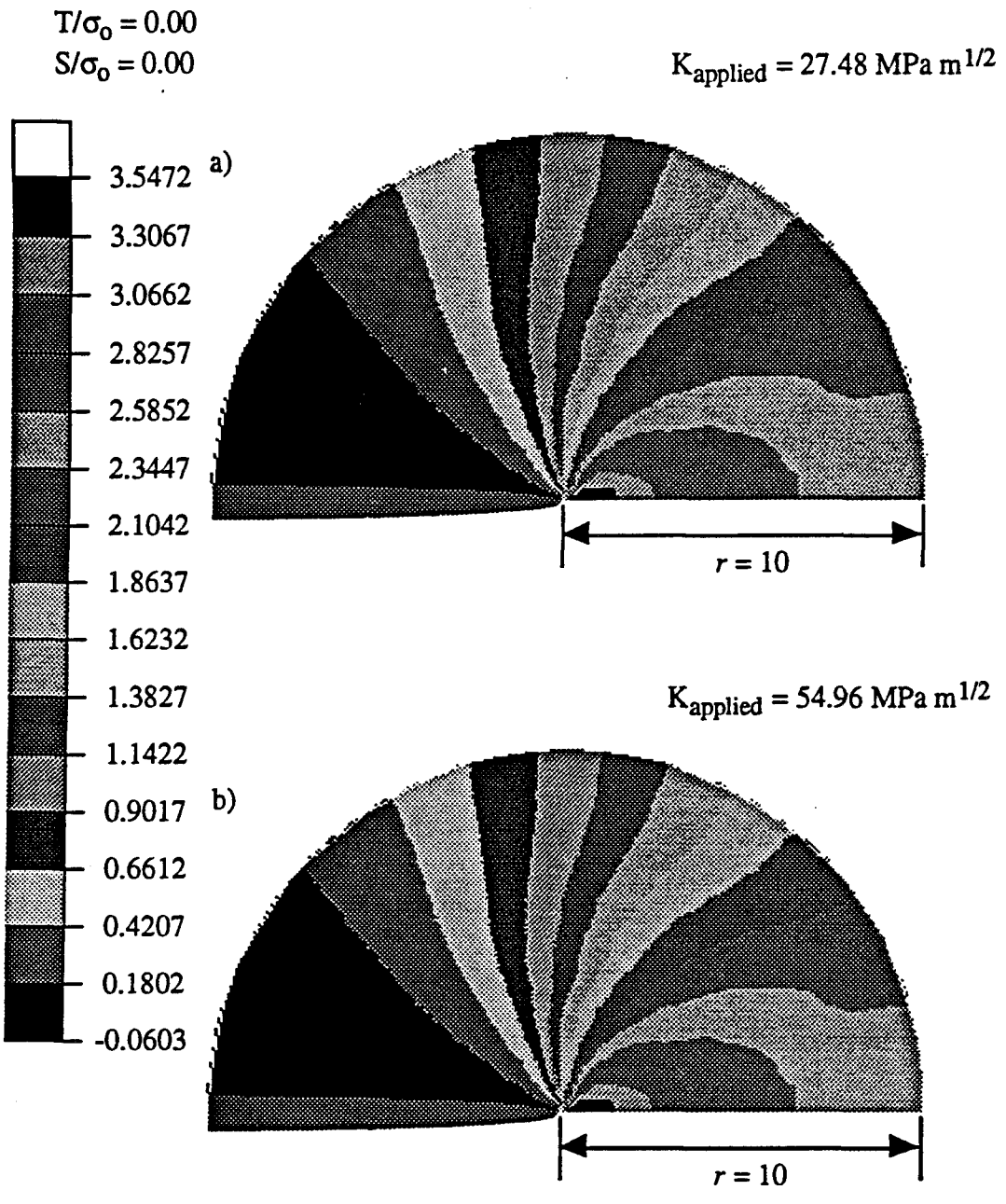

FIG. 3.29— Hoop stress for first term of modified boundary layer: a) $K_{applied}$ = 27.48 MPa $m^{1/2}$ b) $K_{applied}$ = 54.96 MPa $m^{1/2}$.

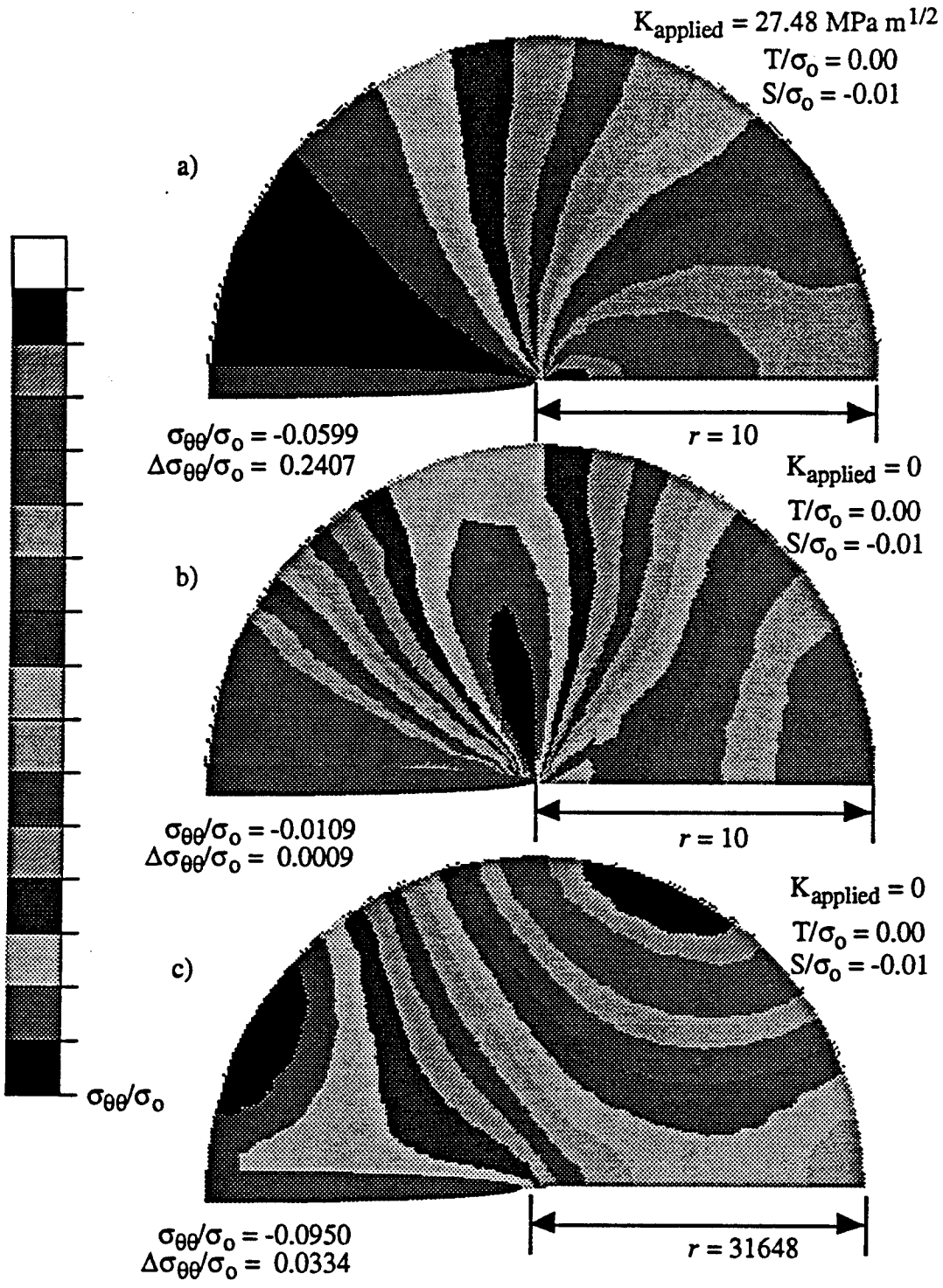

FIG. 3.30— Modified boundary layer for first two Williams terms: a) normalized hoop stress, b) contribution from second term near crack-tip, c) global contribution.

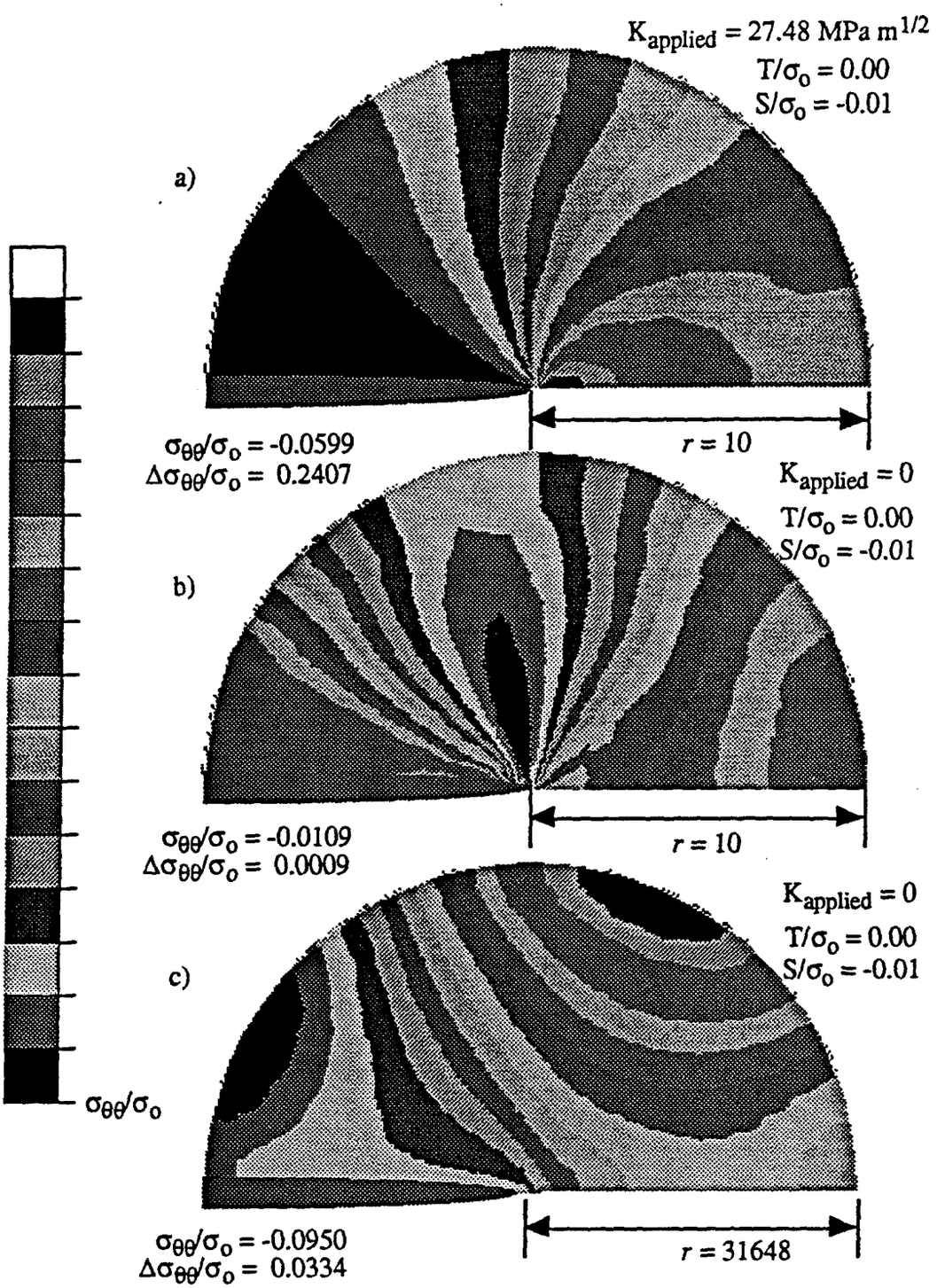

FIG. 3.31— Modified boundary layer for first and third Williams terms: a) normalized hoop stress, b) contribution from third term near crack-tip, c) global contribution.

3.5 Assumption in Constitutive Equation for the Out-of-Plane Stress

The analytical derivation for plane strain presumed that the out-of-plane stress σ_{zz} was related to the in plane stresses by

$$\sigma_{zz}(r,\theta)=\lambda(r,\theta)\left[\sigma_{rr}(r,\theta)+\sigma_{\theta\theta}(r,\theta)\right]$$

where

$$\lambda(r,\theta)=\frac{\left[\nu+\frac{\alpha}{2}\sigma_e^{n-1}(r,\theta)\right]}{\left[1+\alpha\sigma_e^{n-1}(r,\theta)\right]}.$$

The assumption was made that within a fully developed plastic region, as would exist at the crack-tip, $\nu << \sigma_e^{n-1}$ resulting in a limiting value of $\lambda \rightarrow 0.5$.

Figs. 3.32 and 3.33 show the value of $\lambda(r,\theta)$ obtained from the MBL results for different values of the second and third Williams term. The annulus of this study is contained within a normalized radius of ten. The results indicate that the region in which λ is approaching the limiting value of 0.5 depends on the second Williams term. Setting the second Williams term equal to zero results in the second fringe plot in Fig. 3.32. The region in which $\lambda \rightarrow 0.5$ is at $\theta \approx \pi/2$. Applying negative T/σ_0 values rotates this region towards the crack plane (first fringe plot) while positive values of T/σ_0 rotate the region towards the crack faces (third fringe plot). The region on the crack plane that corresponds to values of $\lambda > 0.4$ resides within a normalized radius of approximately four. As noted previously, the third Williams term has little influence on the crack-tip region for values of S/σ_0 which do not cause plastic flow beyond 10% of the MBL radius. Fig. 3.33 shows $\lambda(r,\theta)$ for values of S/σ_0 that satisfy the above condition in all three fringe plots the region is at $\theta \approx \pi/2$.

3.6 Evolution of the Second and Third Independent Amplitudes

The evolution of the second (K_2) and third (K_4) independent parameters (Tables 3.4-3.8) are shown in Figs. 3.34-3.36 as a function of the

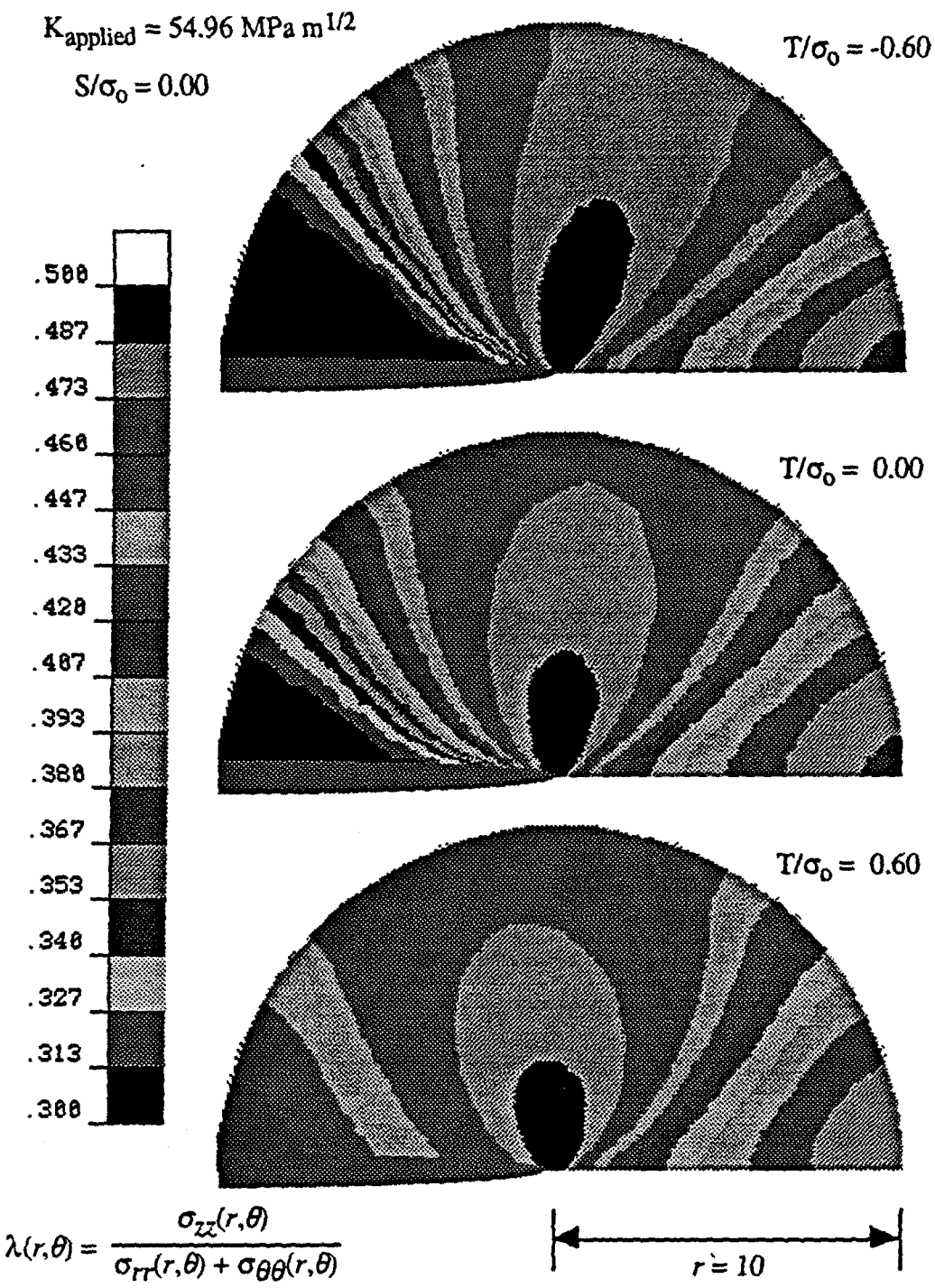

FIG. 3.32— Lambda as a function of T/σ_o and position for the MBL.

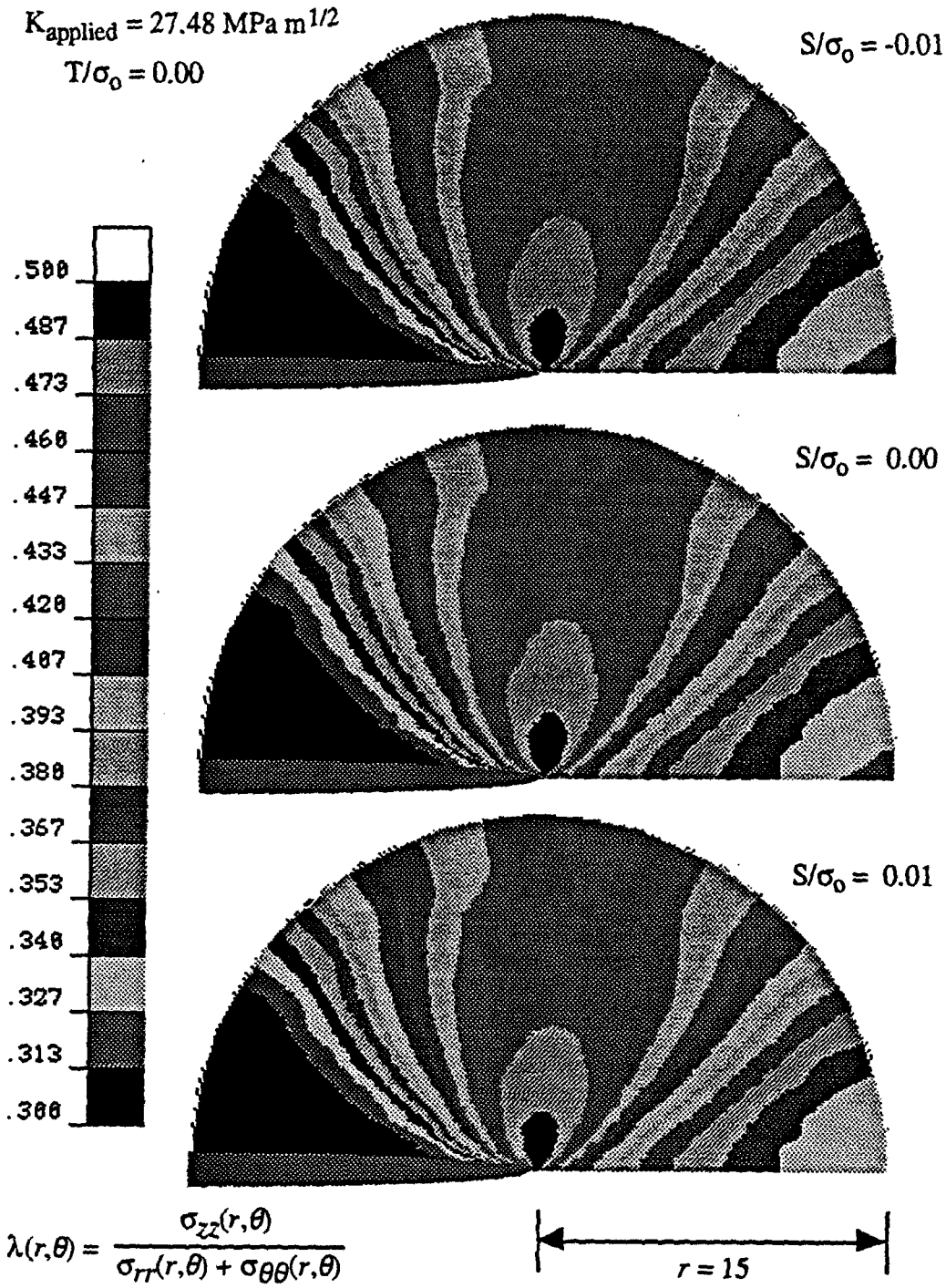

FIG. 3.33— Lambda as a function of S/σ_o and position for the MBL.

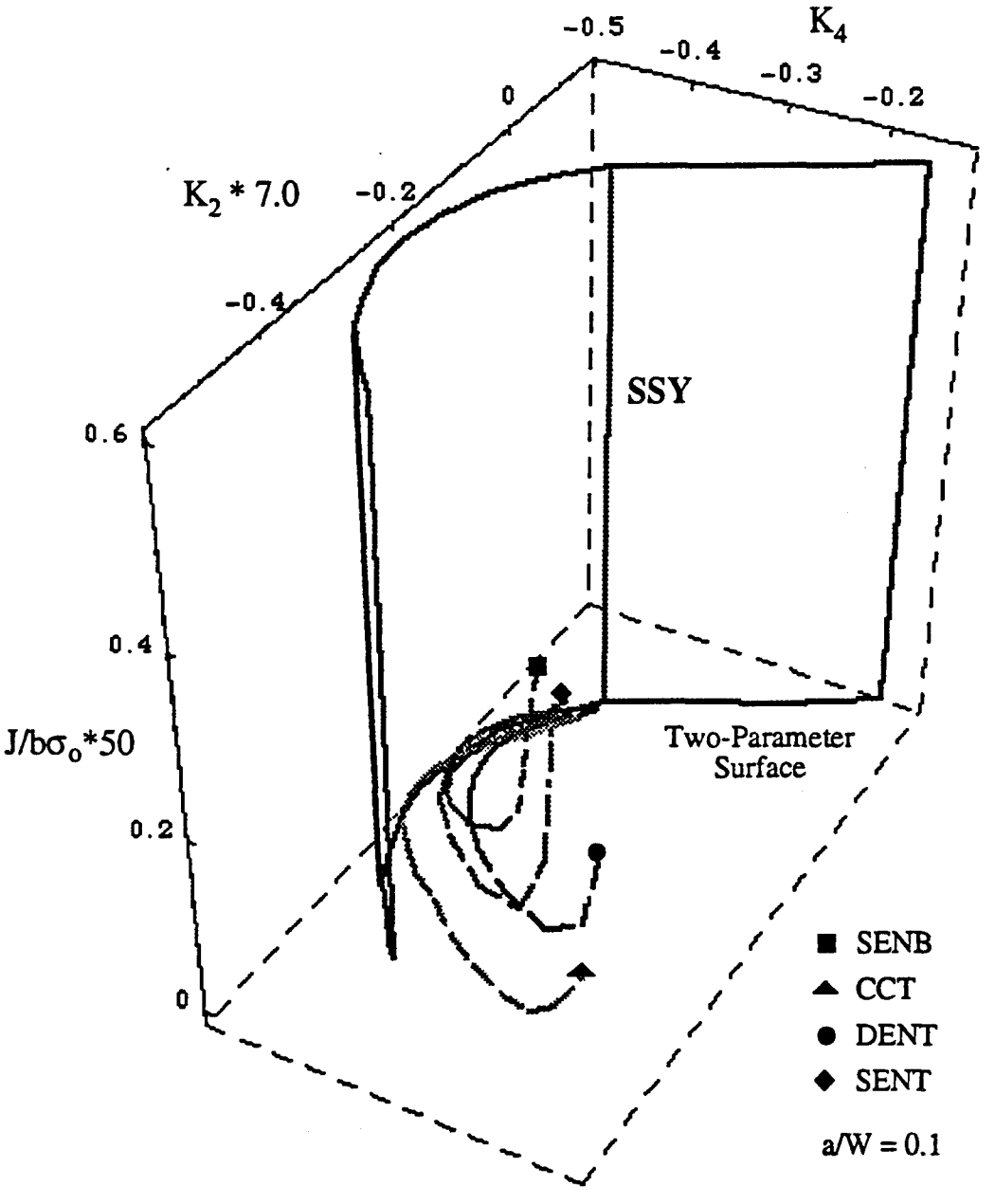

FIG. 3.34— Parameter evolution as a function of deformation level for a/W = 0.1.

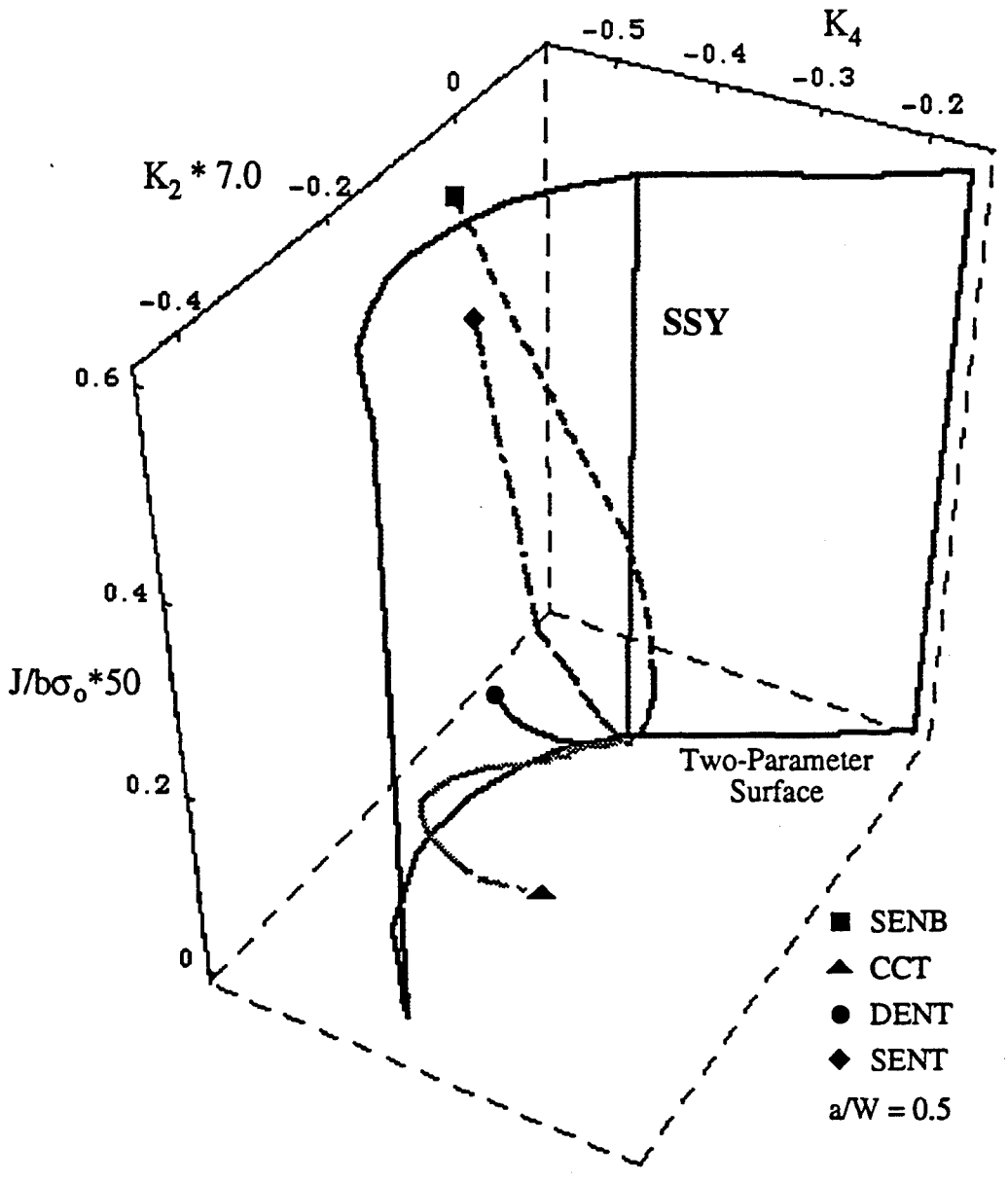

FIG. 3.35— Parameter evolution as a function of deformation level for a/W = 0.5.

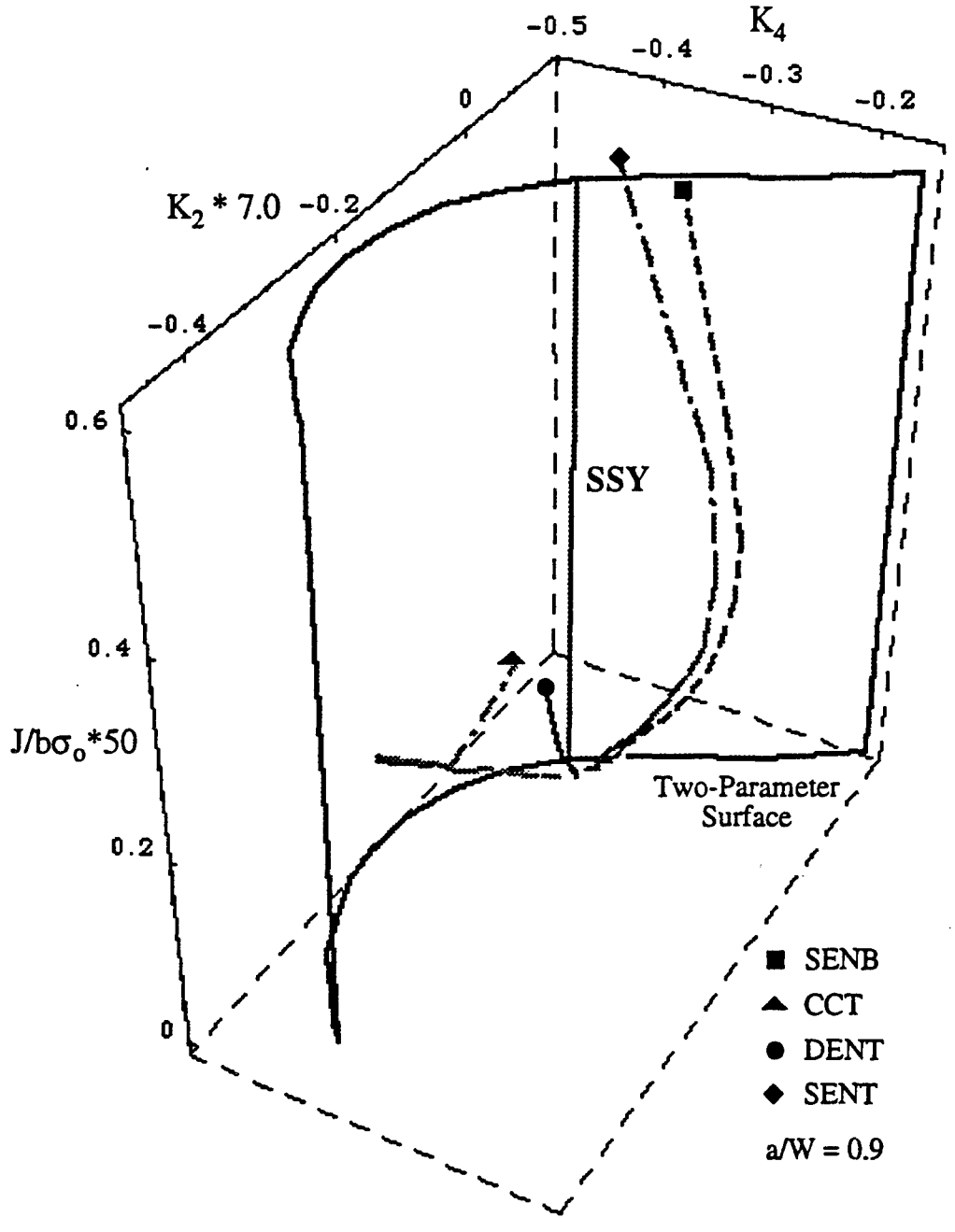

FIG. 3.36— Parameter evolution as a function of deformation level for a/W = 0.9.

deformation level ($J/b\sigma_0$) and a/W for the SENB, CCT, DENT, and SENT specimens, respectfully. These data are compared with the Williams two-parameter surface obtained for the MBL. Dashed lines indicate when the finite geometry results have significantly deviated from the MBL surface. The two-parameter surface is constructed from the K_2 and K_4 relation obtained for the MBL. The K_2 and K_4 relation can be extruded in the vertical direction as a result of the self similarity in the normalized stress field for increasing deformation level as shown in Fig. 3.29. This surface by the definition of the boundary displacements applied to the MBL is only dependent on two-parameters (K, T).

The evolution of the second independent coefficient for each of the geometries is plotted as a function of deformation level ($J/b\sigma_0$) in Figs. 3.37-3.39 for a/W=0.1, 0.5, and 0.9, respectfully. Also included is the value of the second coefficient obtained for the SSY model (MBL -> T = 0). Fig. 3.40 compares the relationship between the second and third independent parameters for the second and then the third Williams term MBL results. Two sets of the second Williams term MBL are shown. The first corresponds to a linear, elliptic, power-law constitutive relation with a proportional limit of 85% of the flow stress. The second of the MBL results is based on a proportional limit of 95% of the flow stress. For values of the proportional limit less than about 92% σ_0, boundary plasticity occurred at highly negative values of T/σ_0 Hence, the plastic zone was influenced by the proximity of the MBL boundary. At values greater than 92% the plasticity was contained within a radius that was 10% of the MBL radius. The relationship between K_2 and K_4 did not vary for highly negative values of T/σ_0 values.

The relationship between K_2 and K_4 are given in Figs. 3.41-3.44 for each of the specimen geometries. The two-parameter MBL results based on the T -stress are also plotted. Figs. 3.45-3.47 compare the second and third independent parameter relation for different specimens at a/W ratios of 0.1, 0.5, and 0.9, respectfully.

The magnitude of the difference field as given in Eq. (1.10) is determined by computing the difference between the third independent coefficient K_4 for the finite geometry specimens with that of the second Williams term two-parameter MBL value of K_4 for a fixed K_2 value. The

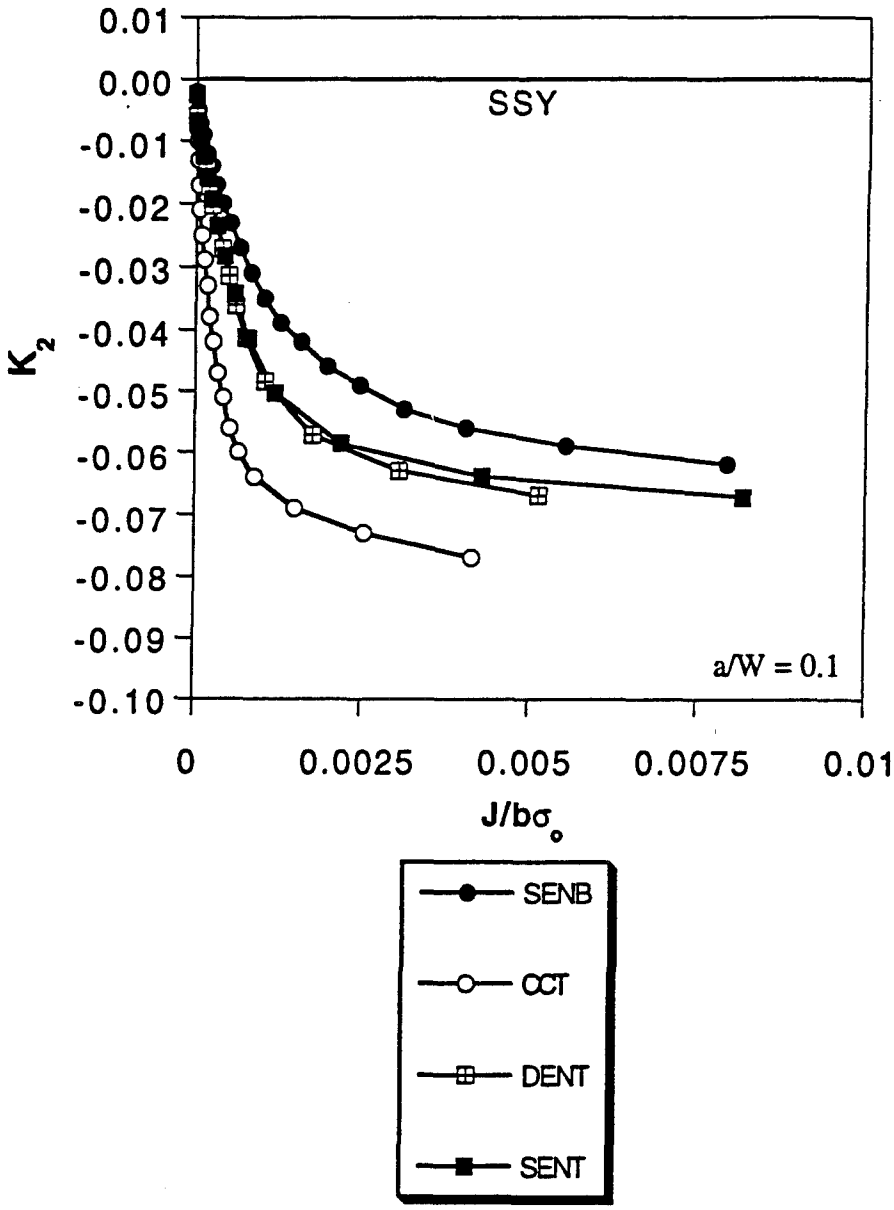

FIG. 3.37— Comparison of the second independent amplitude with that obtained for the SSY model for the specimens with a/W =0.1.

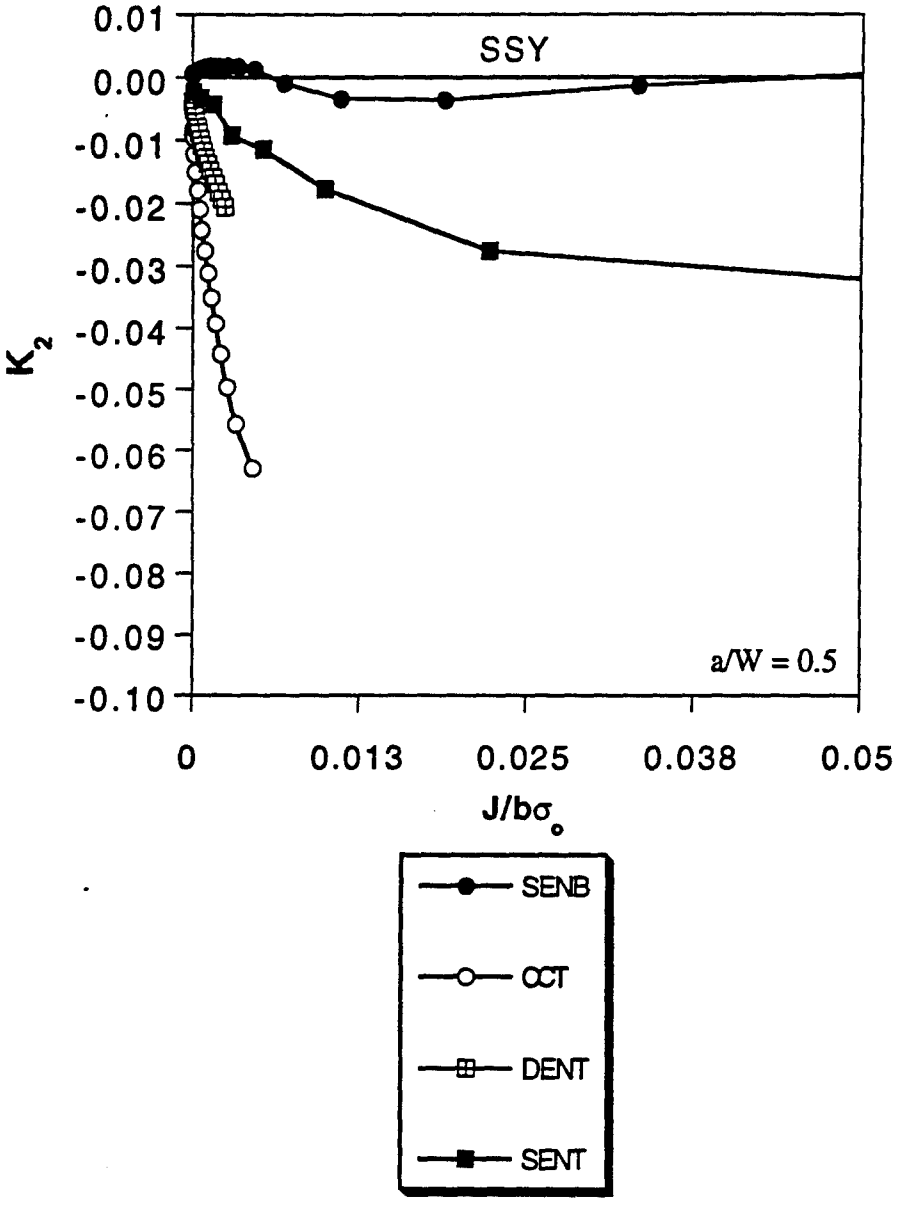

FIG. 3.38— Comparison of the second independent amplitude with that obtained for the SSY model for the specimens with a/W =0.5.

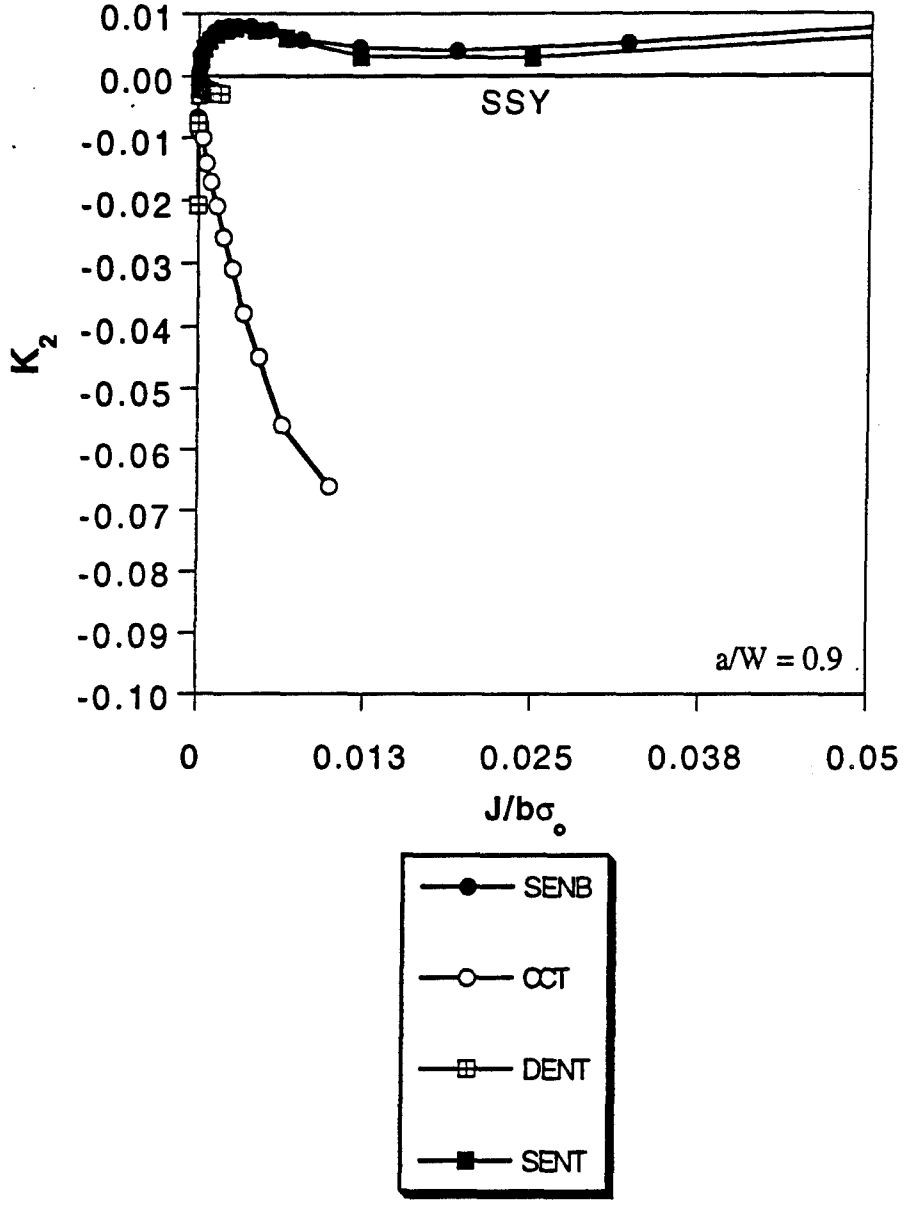

FIG. 3.39— Comparison of the second independent amplitude with that obtained for the SSY model for the specimens with a/W =0.9.

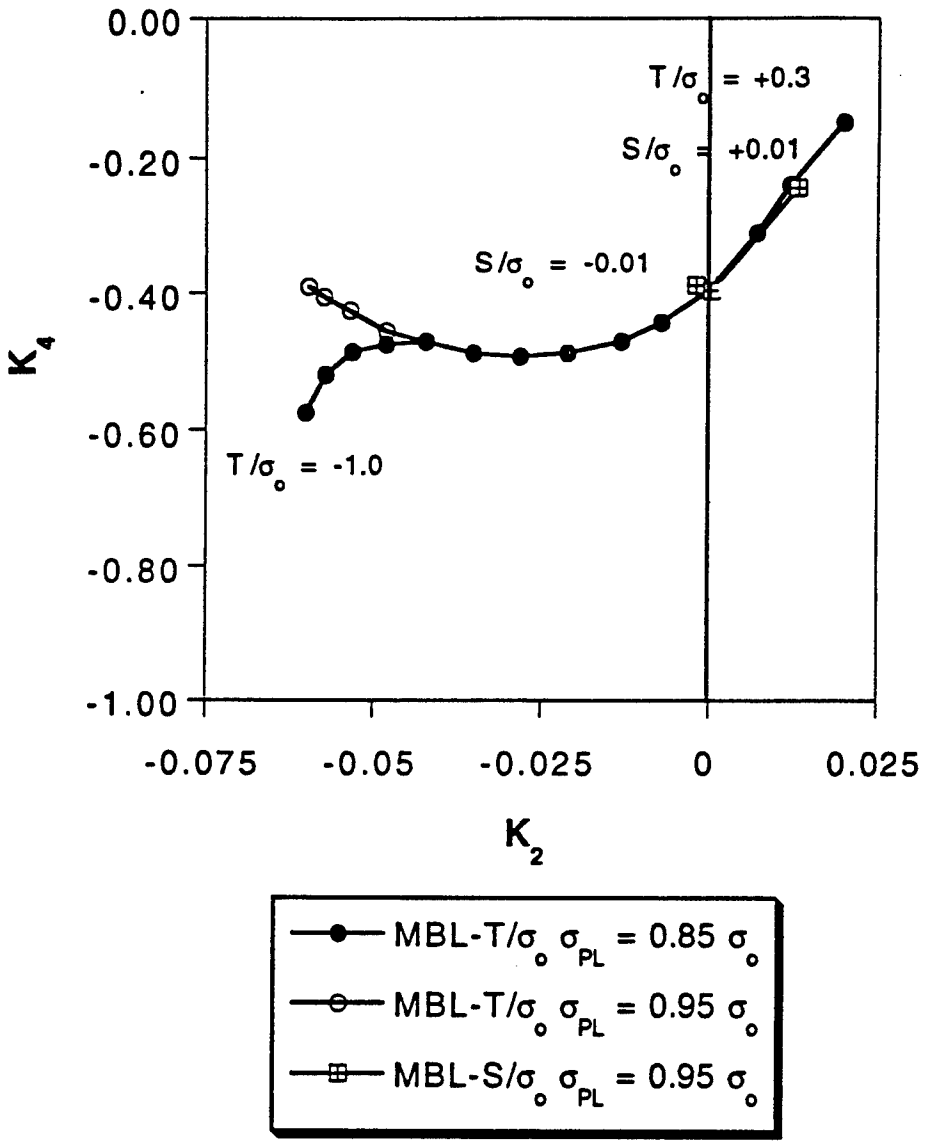

FIG. 3.40— Comparison of the normalized amplitudes for the MBL between the first and second Williams terms and different proportional limits in the constitutive relation.

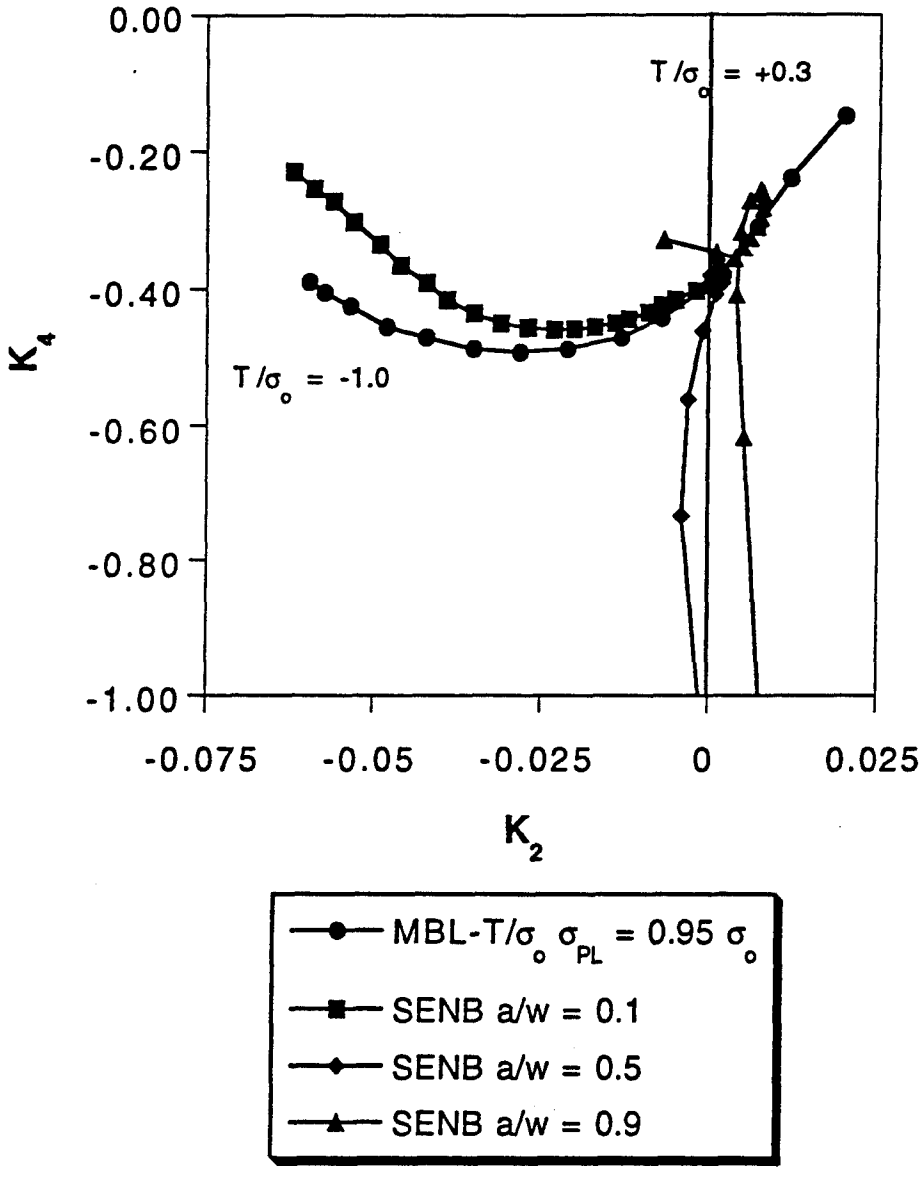

FIG. 3.41— Comparison of the normalized amplitudes for the SENB specimen with those for the two-parameter MBL.

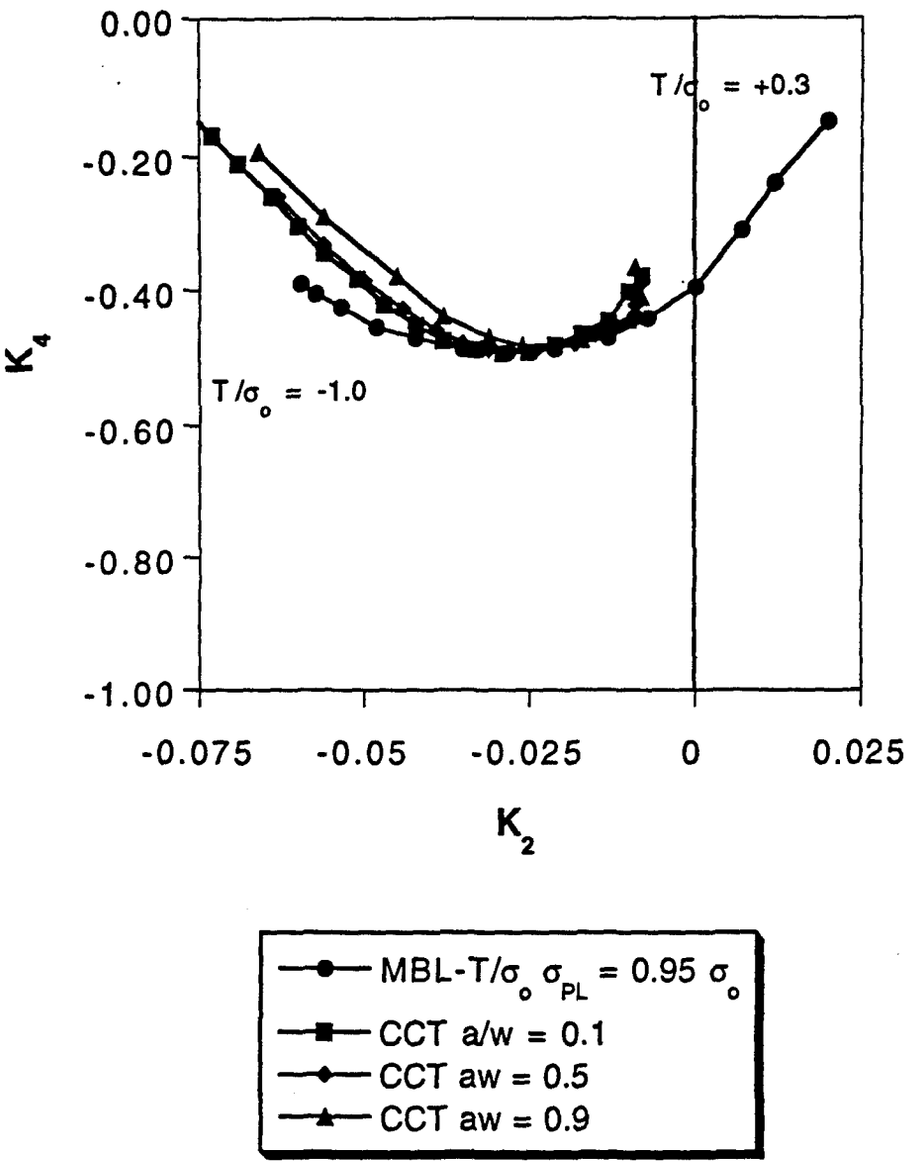

FIG. 3.42— Comparison of the normalized amplitudes for the CCT specimen with those for the two-parameter MBL.

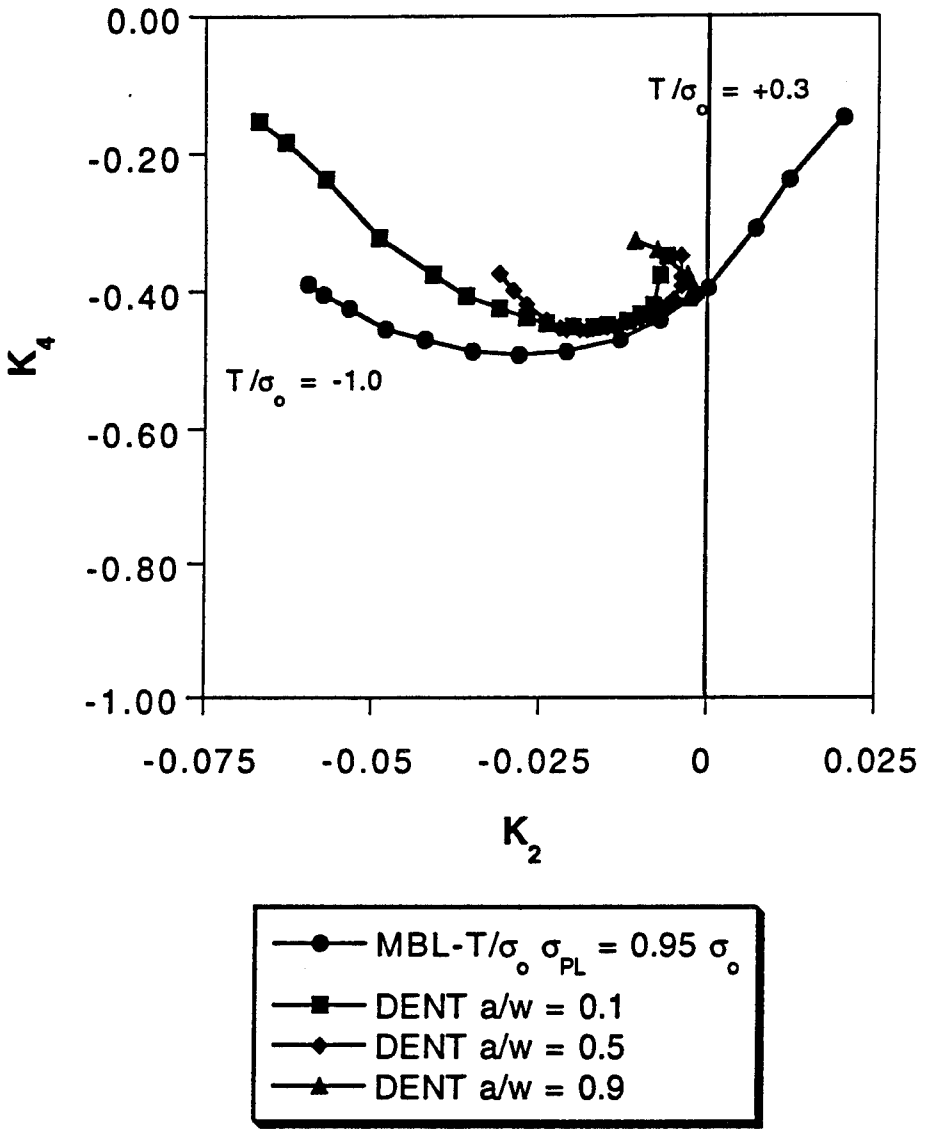

FIG. 3.43— Comparison of the normalized amplitudes for the DENT specimen with those for the two-parameter MBL.

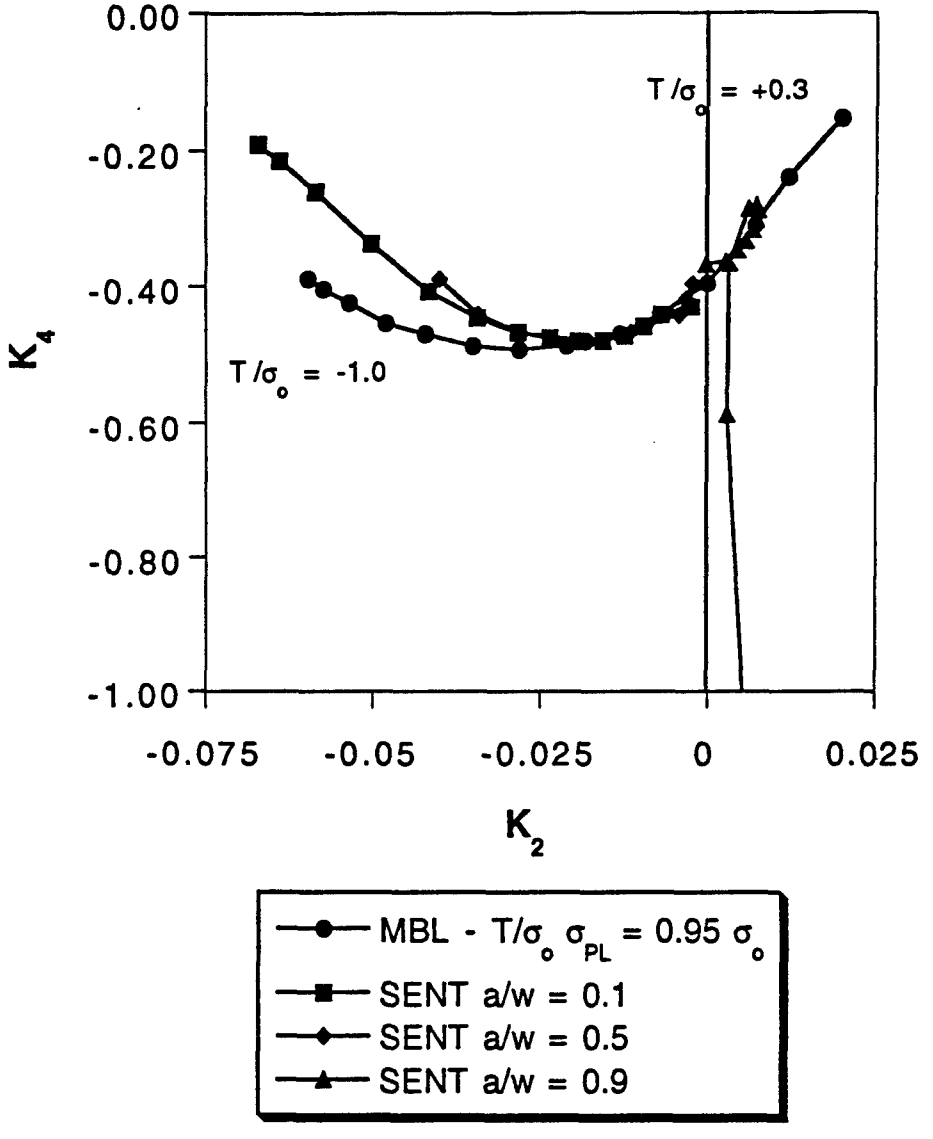

FIG. 3.44— Comparison of the normalized amplitudes for the SENT specimen with those for the two-parameter MBL.

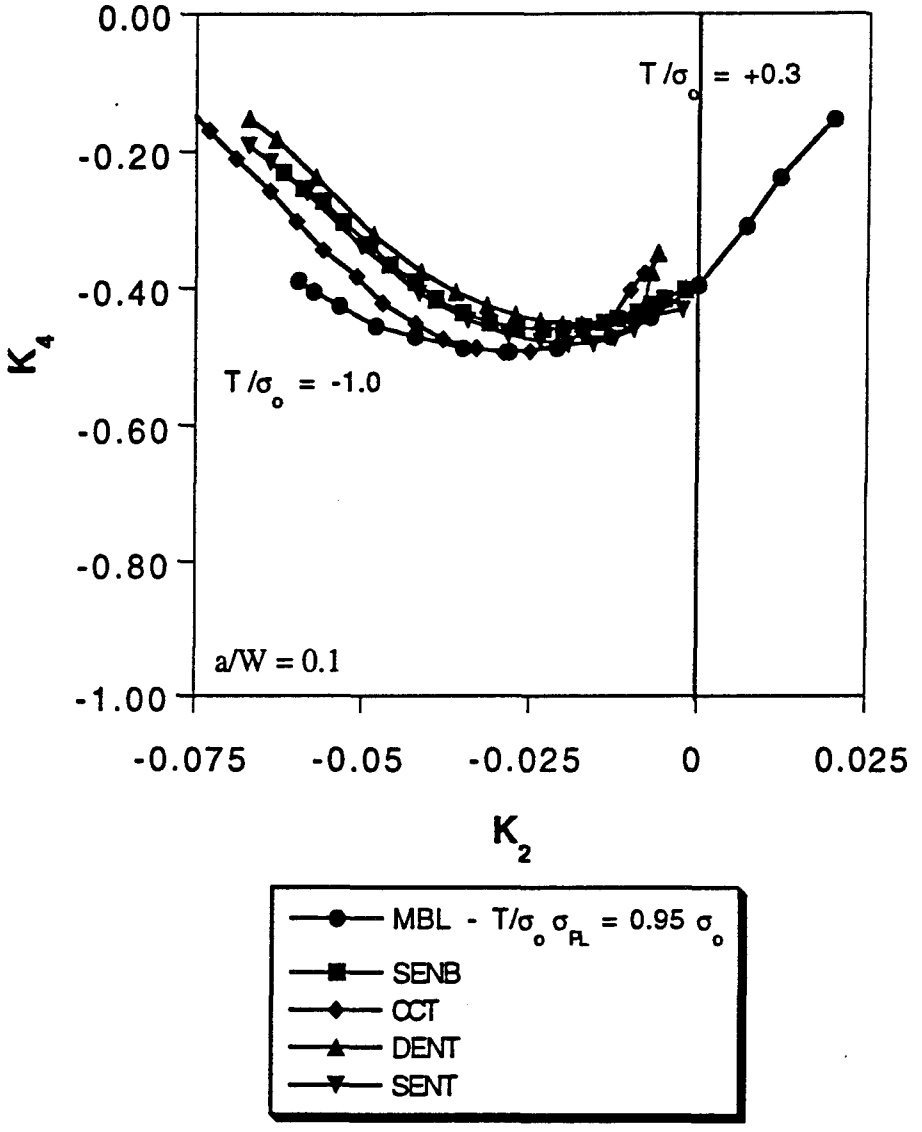

FIG. 3.45— Comparison of the normalized amplitudes for the specimens having a/W = 0.1 with those for the two-parameter MBL.

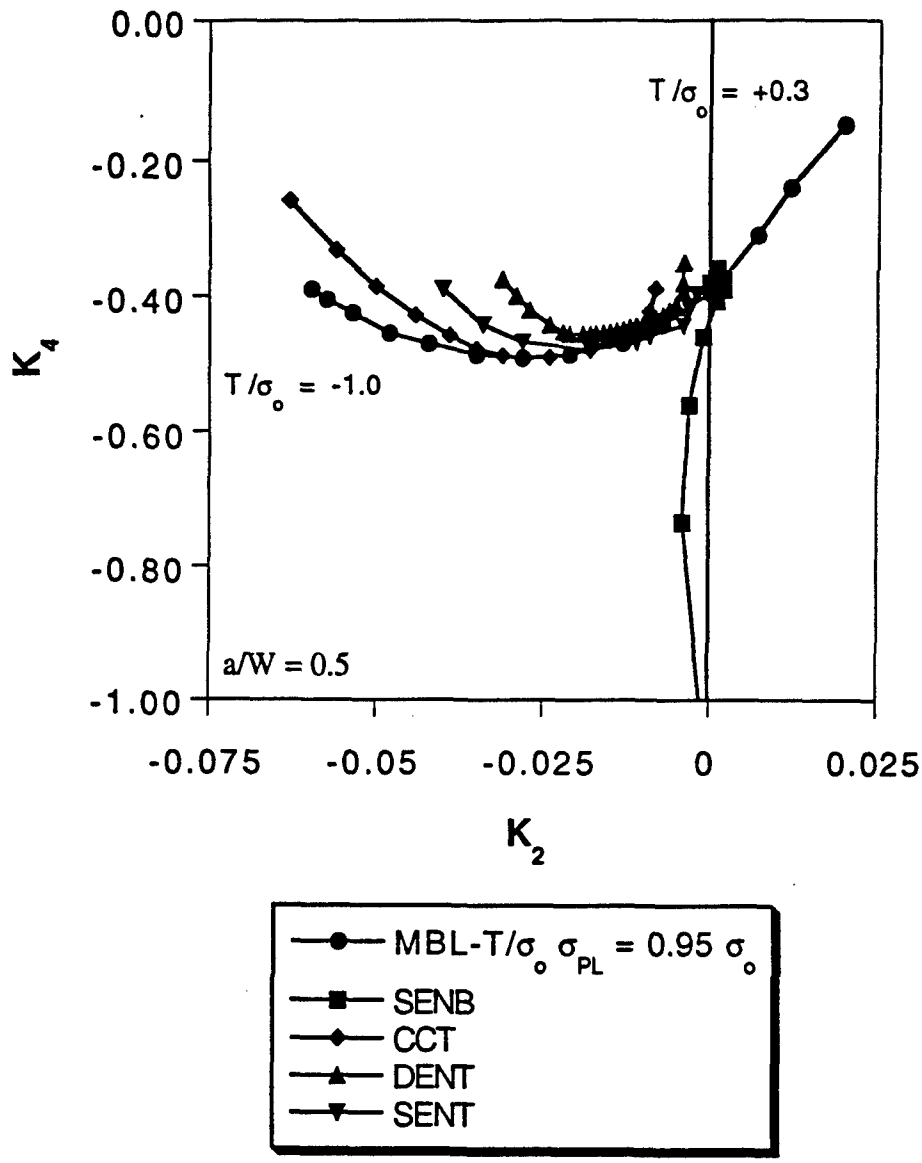

FIG. 3.46— Comparison of the normalized amplitudes for the specimens having a/W = 0.5 with those for the two-parameter MBL.

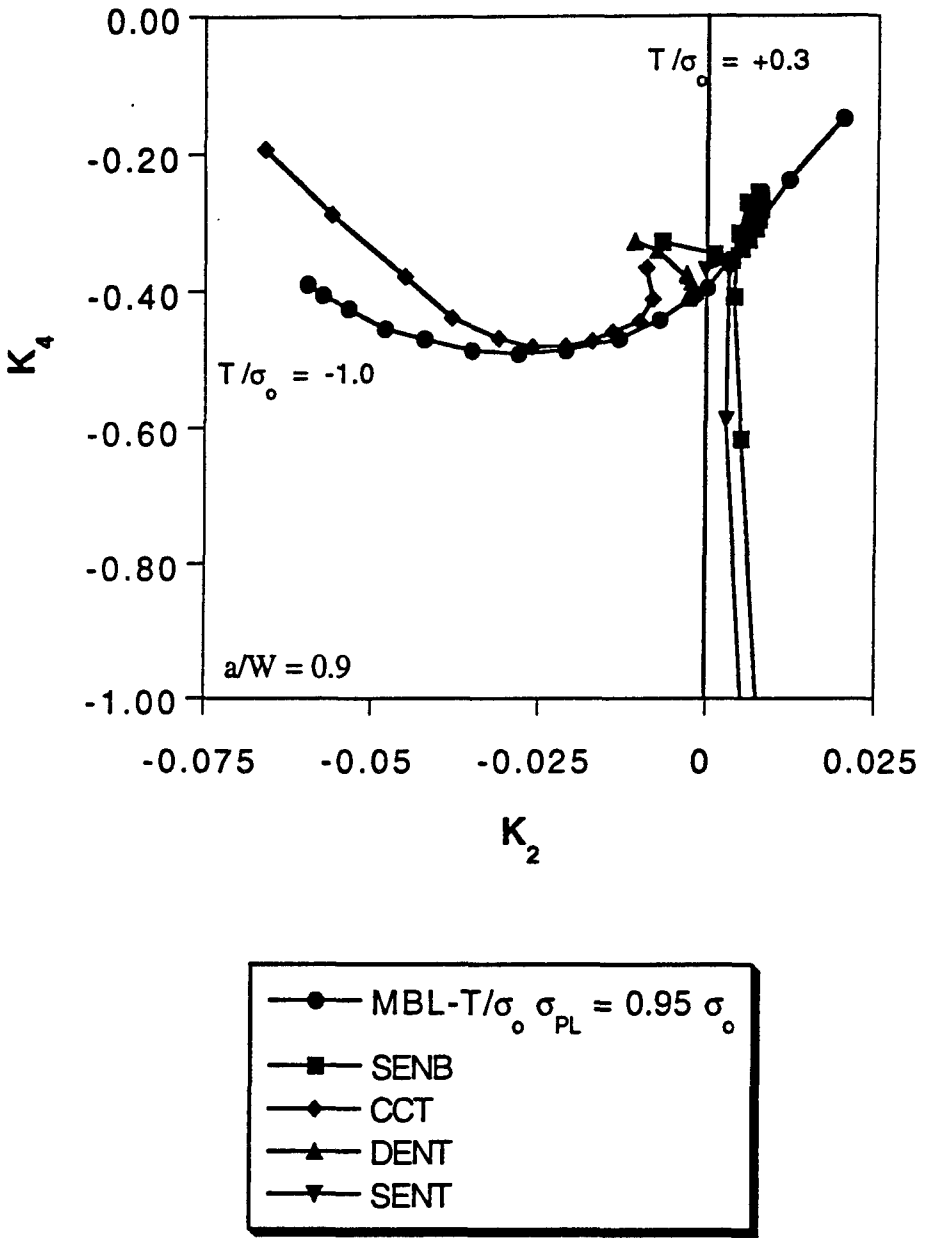

FIG. 3.47— Comparison of the normalized amplitudes for the specimens having a/W = 0.9 with those for the two-parameter MBL.

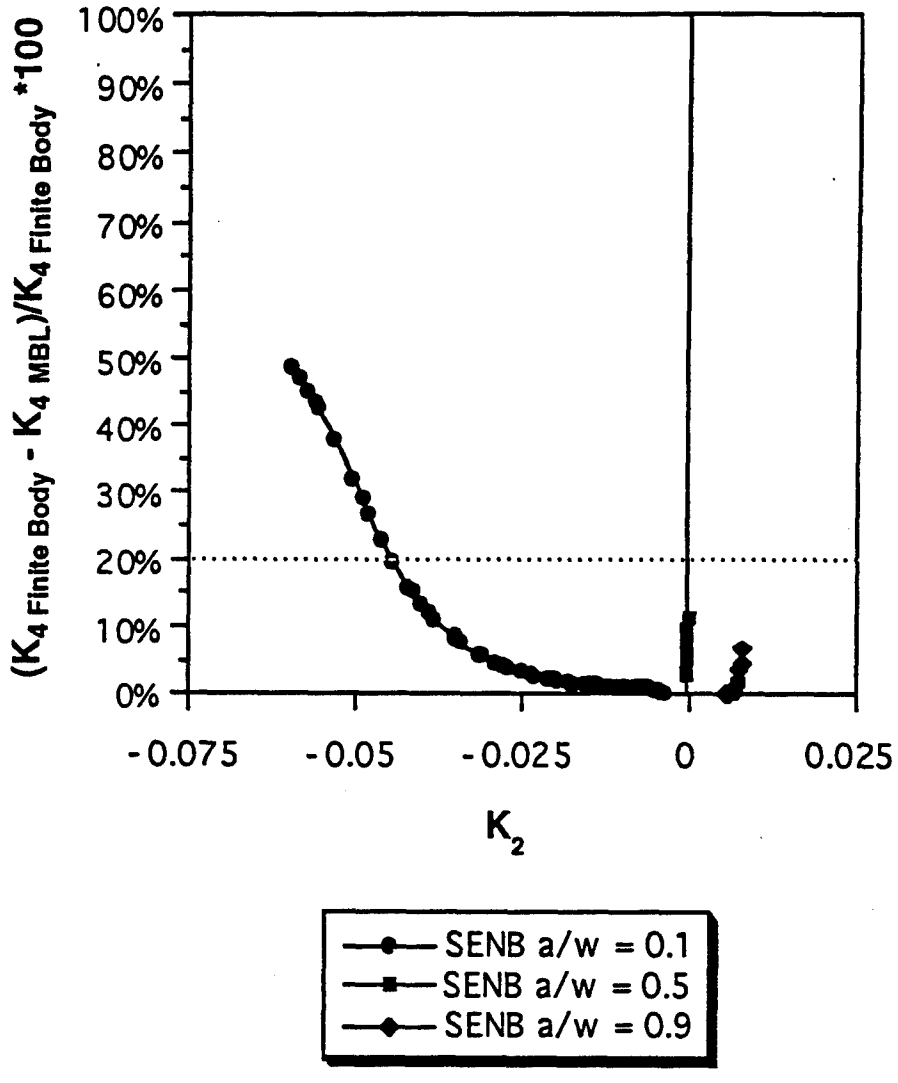

FIG. 3.48— Difference in the third independent coefficients between the SENB and MBL.

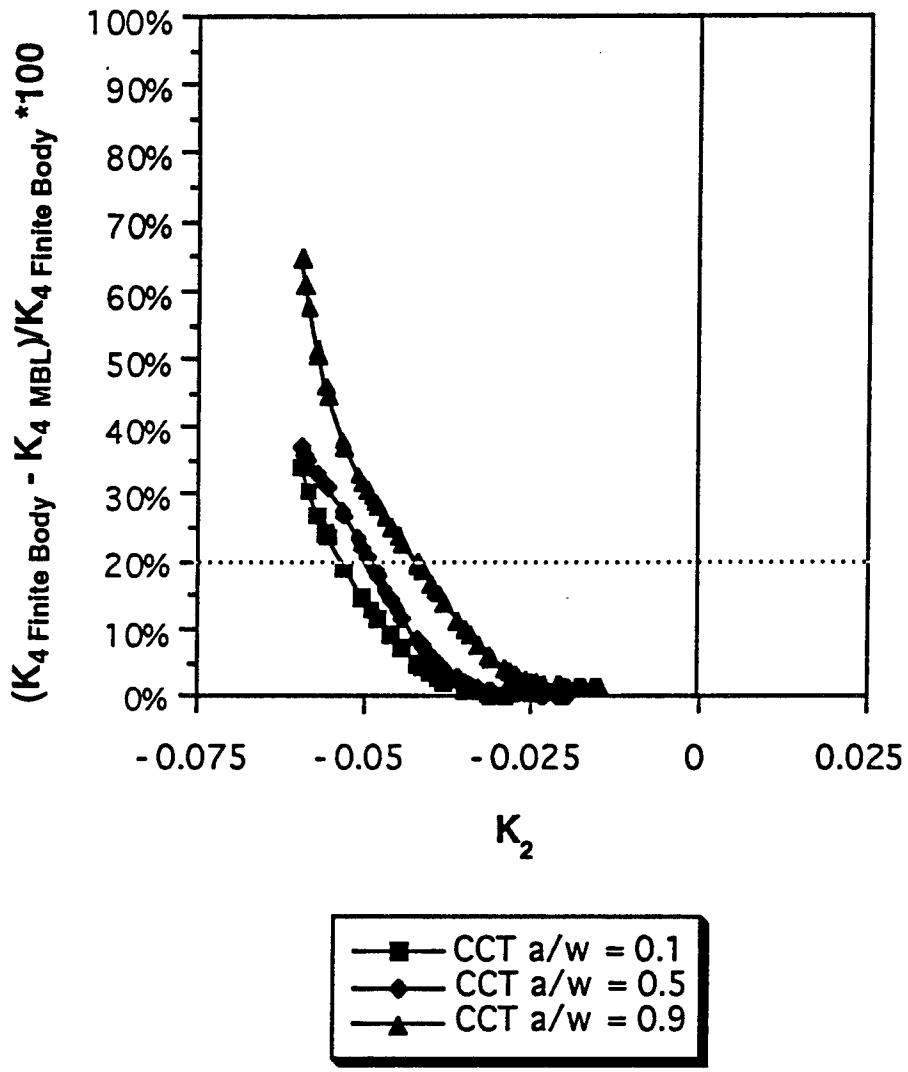

FIG. 3.49— Difference in the third independent coefficients between the CCT and MBL.

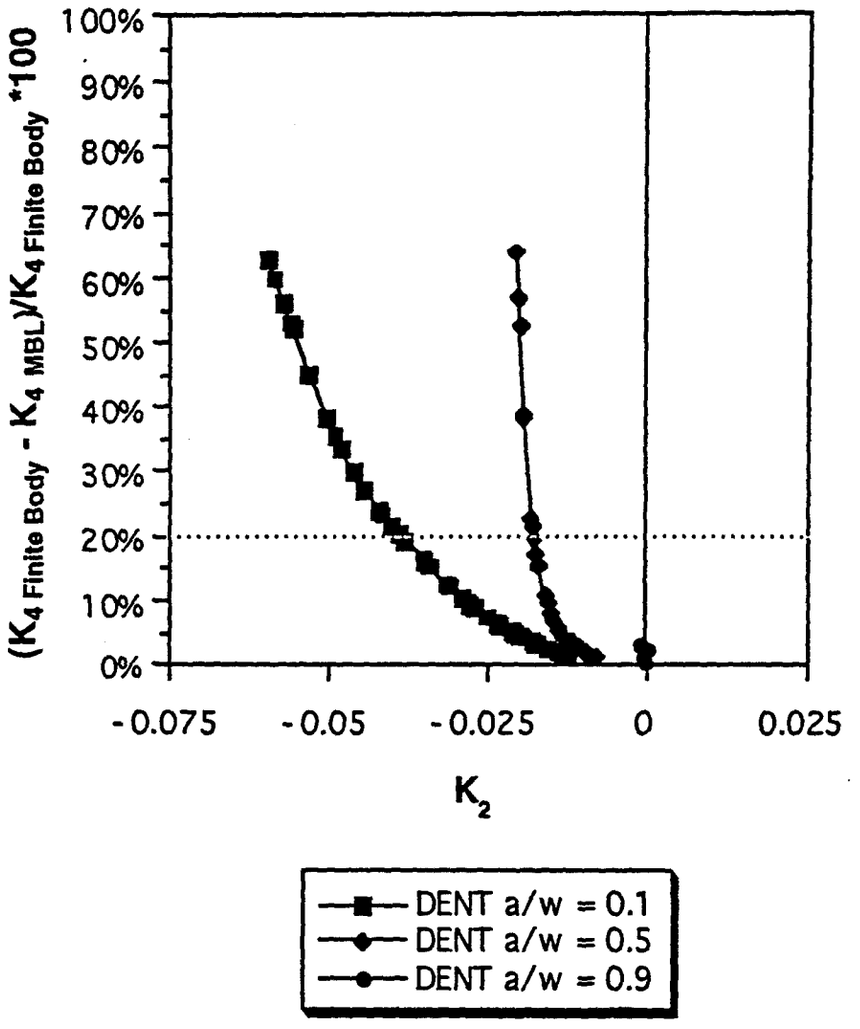

FIG. 3.50— Difference in the third independent coefficients between the DENT and MBL.

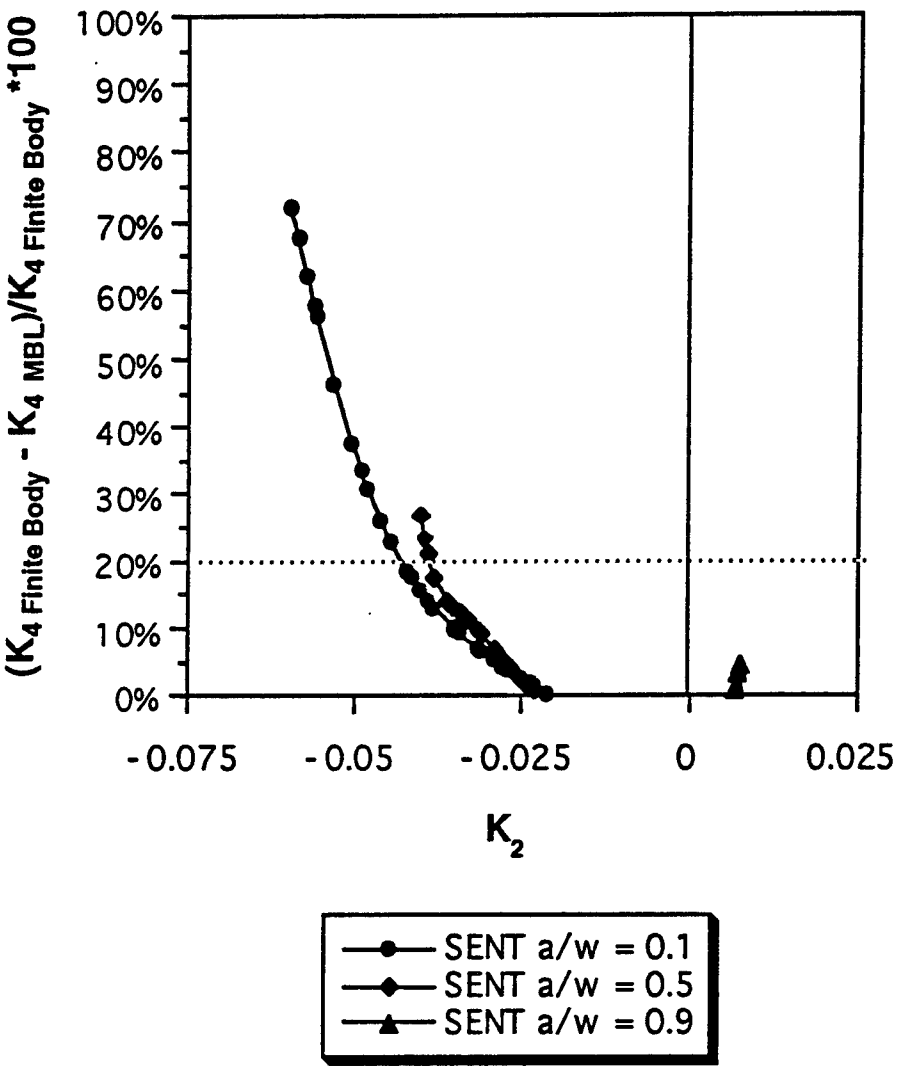

FIG. 3.51— Difference in the third independent coefficients between the SENT and MBL.

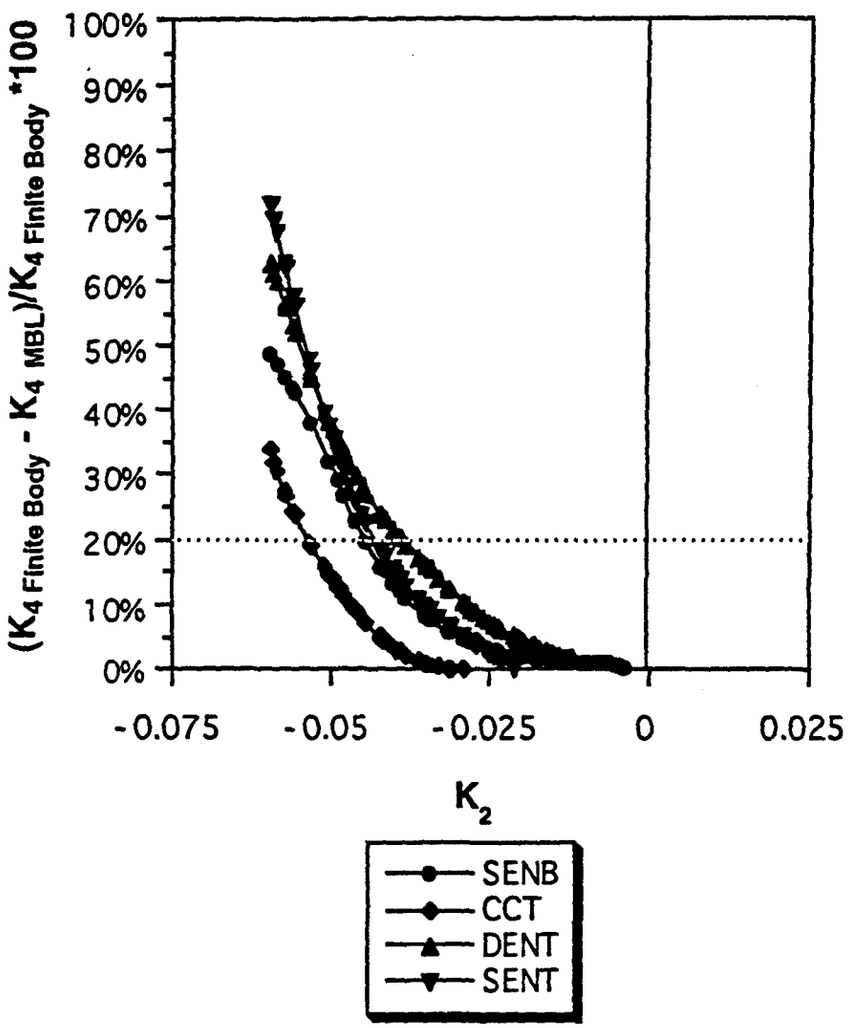

FIG. 3.52— Difference between the third independent coefficients for the specimens having a/W = 0.1 with those for the two-parameter MBL.

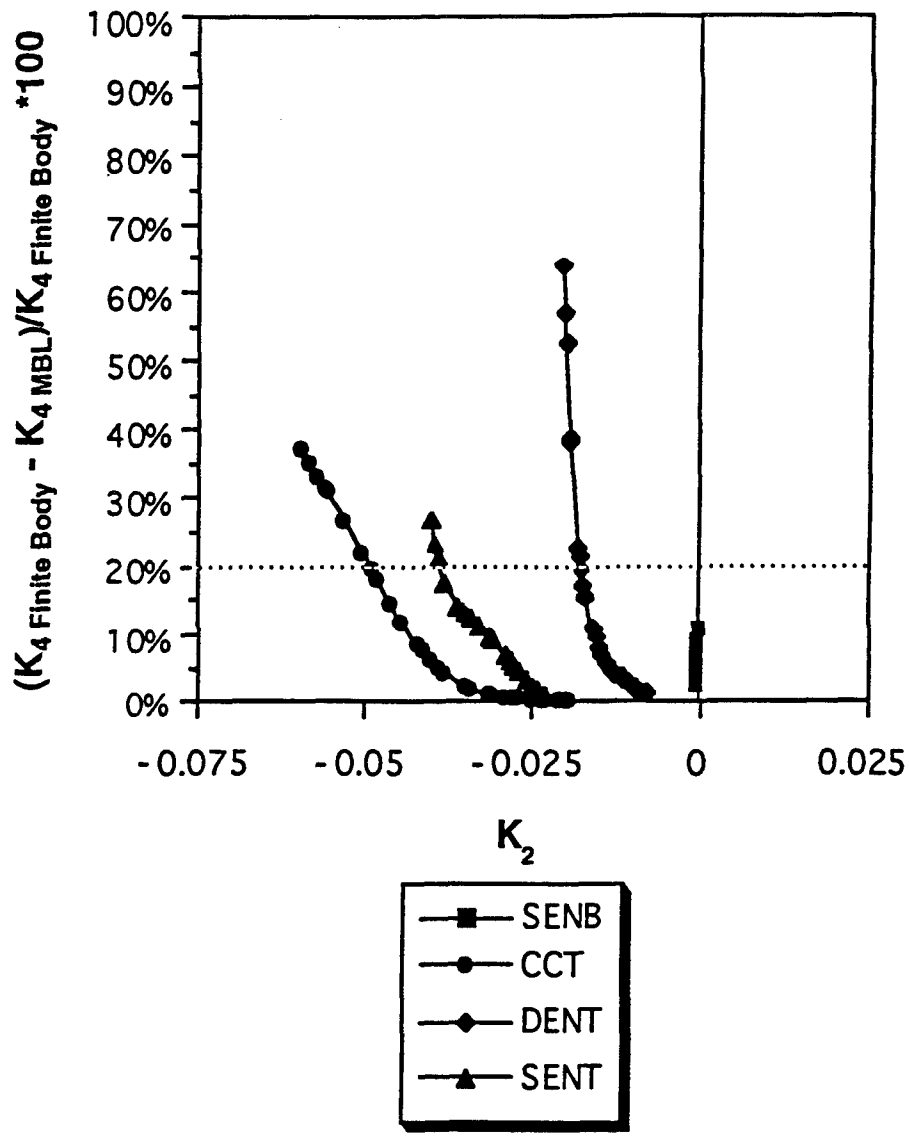

FIG. 3.53— Difference between the third independent coefficients for the specimens having a/W = 0.5 with those for the two-parameter MBL.

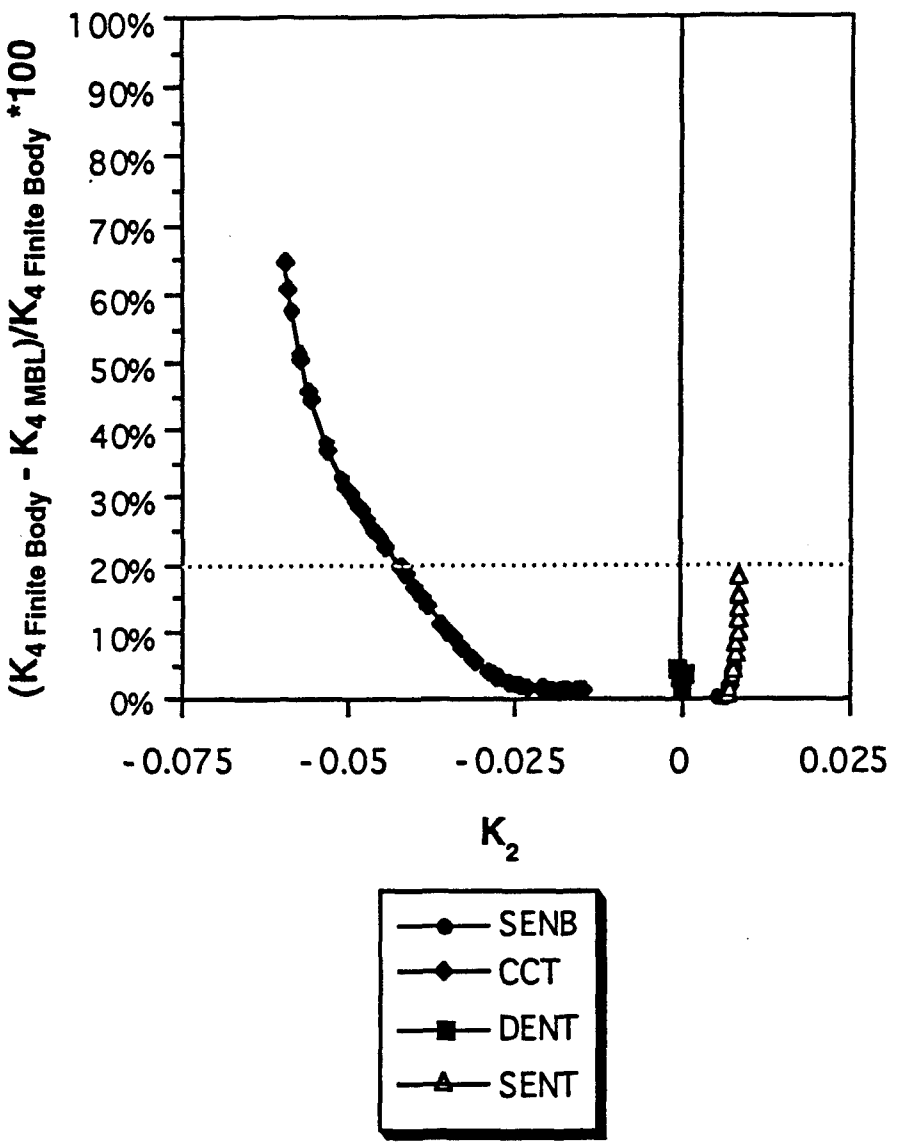

FIG. 3.54— Difference between the third independent coefficients for the specimens having a/W = 0.9 with those for the two-parameter MBL.

percent error is given in Figs. 3.48-3.51 for the SENB, CCT, DENT, and SENT, respectfully Figs. 3.52-3.54 show the percent error between K_4 for a/W values of 0.1, 0.5 and 0.9, respectfully. A dashed line has been added to indicate when the finite body stresses have deviated more than 20% from the two-parameter MBL stresses. The corresponding deformation levels as measured by $J/b\sigma_0$ are tabulated in Table 3.10.

The error in the stress field as given in Eq. (1.10) associated with a 20% difference between the finite geometry third parameter and the MBL third parameter are given in Figs. 3.55 and 3.56 for the SENB and CCT specimens having a/W=0.5. Fig. 3.55 shows the corresponding errors along the crack plane while Fig. 3.56 shows the error in the angular direction at a normalized radius of five.

TABLE 3.10— Deformation levels for 20% difference between the stress fields in the two-parameter MBL and the finite geometries.

$J/b\sigma_0$	a/w		
	0.1	0.5	0.9
SENB	0.00198	0.00026	0.00772
CCT	0.00052	0.00259	0.00457
DENT	0.00061	0.00195	---
SENT	0.00079	---	0.00273

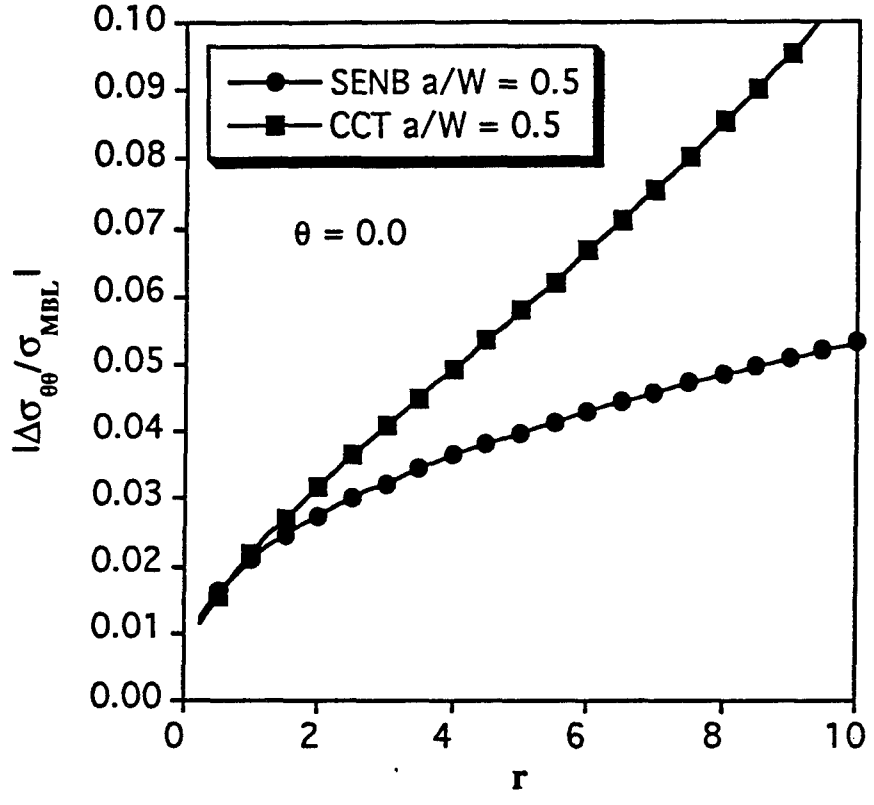

FIG. 3.55— Error field as a function of the radial coordinate for the SENB and CCT specimens at deformations corresponding to a 20% error in the third independent parameter K_4.

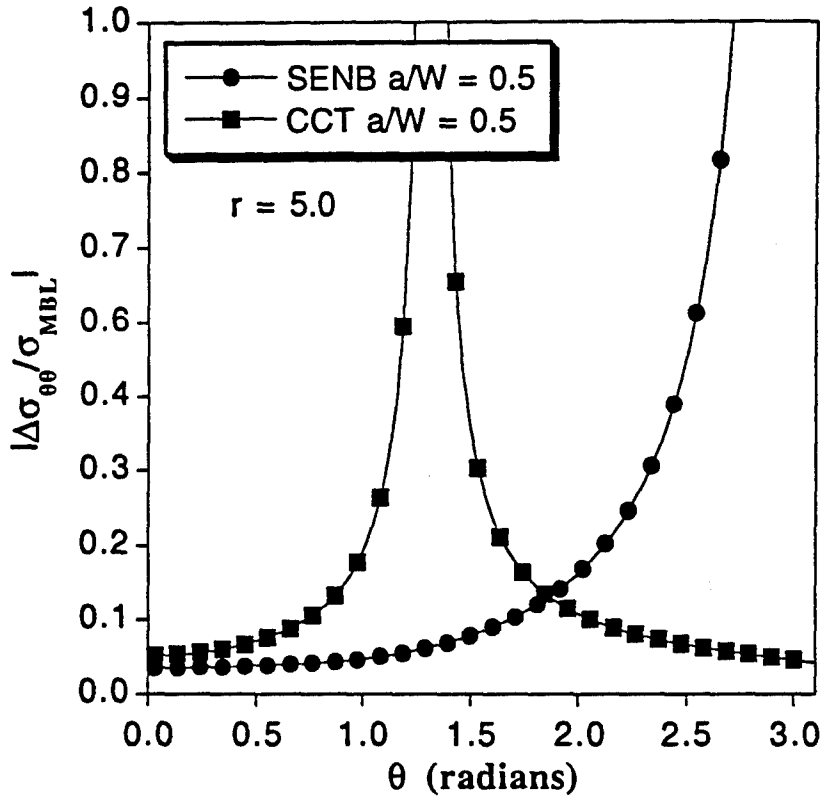

FIG. 3.56— Error field as a function of theta for the SENB and CCT specimens at deformations corresponding to a 20% error in the third independent parameter K_4.

CHAPTER IV

DISCUSSION

In this work we determine when the stresses in the plastic zone deviate from those characterized by a two-parameter methodology. In so doing, we utilize the general power series representation for the stress potential. As far as the analytic analysis for the series representation of the crack-tip stress fields, it is impossible to transition from the plastic region to the elastic region without assuming the material is elastic incompressible (i.e., $\nu = 0.3 \rightarrow \lambda(r,\theta) = 0.5$). The sixth field for the case of plane strain with a hardening coefficient of n=5 is the first elastic term (Table 3.1). Fig. 3.15f shows the sixth integration constant (I_6^E- Appendix F) for the *J*-integral. The constant must integrate to zero to preserve the path independence of *J*. The integration constant is shown for both ν=0.3 and ν=0.5. The integral is not zero for ν=0.3 leaving the *J*-integral path dependent. This discrepancy arises as a result of setting $\lambda(r,\theta) = 0.5$ in the third constitutive equation, Eq. (2.51). This assumption was necessary to make the problem mathematically tractable. The validity of this assumption was addressed by looking at the distribution of $\lambda(r,\theta)$ in the MBL. Figs. 3.32 and 3.33 indicate the region were $\lambda(r,\theta) \rightarrow 0.5$ is at $\theta = \pi/2$ and within a normalized radius of approximately four. Hence, some error is introduced with this assumption.

The comparison of the analytic solutions with the finite element results in Figs. 3.17-3.28 indicate that the six term series representation for the stress field seems to do an adequate job in describing the stress field in the annular region bounded by a normalized radius of five.

The two-parameter solution that we base our analysis is that for the MBL with a two term Williams displacement field applied on its elastic boundary. Comparison of the second fringe plot in Figs. 3.30 and 3.31 clearly indicates that the second Williams term has a greater influence on the stresses in the plastic zone then that of the third term. The reason for this is that the stress associated with the second Williams term has no dependence on the radial coordinate while the third term has a $r^{1/2}$ dependence. Hence, the

nearer the crack-tip, the smaller the stress associated with the third term. In general, this would indicate that if the elastic field outside the plastic region can be characterized by the Williams solution, then the higher order terms have a diminishing effect on the crack-tip plasticity.

The evolution of the independent coefficients for the series representation of the stresses in Figs. 3.34-3.36 clearly indicate that the shallow cracked geometries (a/W=0.1) maintain a two-parameter field description longer then that of some of the medium and deeply cracked geometries. The second parameter can be incorporated in a failure locus at the onset of cleavage by determining its value at J_c in Figs. 3.37-3.39.

The relation between the second and third independent coefficients in the analytic elastic-plastic solution for both the MBL and finite geometries are shown in Figs. 3.45-3.47. For a/W=0.1, the CCT geometry maintains a two-parameter description to higher deformation levels then those associated with the SENB, DENT, and SENT specimens. This result can best be seen in Figs. 3.34 and 3.45 were the coefficient for the difference field between the MBL and finite geometries with an a/W = 0.1 are shown.

The CCT also maintains a two-parameter field to higher deformation levels then the other finite geometries for both a/W = 0.5 and 0.9. The SENB specimen, as shown in Figs. 3.35, 3.47, and 3.40, deviates from the two-parameter description at quite low deformation levels when a/W = 0.5 and 0.9, respectfully. The SENT behaves similar in nature to the SENB specimens at a/W = 0.9 because of the presence of the large global bending field common in the SENB specimens at high a/W values. One difference between the SENB specimen with an a/W = 0.9 and the remaining geometries, is that there is an increase in constraint before the global bending field becomes dominate. The bending field can be seen to dominate in the finite element results shown in Figs. 3.20 and 3.21 for a/W = 0.5 and a/W = 0.9, respectfully.

The third Williams term was originally added to the boundary of the MBL in an attempt to account for the global bending field present in the SENB (a/W = 0.5 and 0.9) and SENT (a/W = 0.9) finite geometries. The third term as previously mentioned had little influence on the stress field within the plastic zone for S/σ_0 values for which the plastic zone did not feel the influence of the boundaries of the MBL.

The results for the difference fields in Figs. 3.48-3.54 show that of the finite geometries modeled, all but the SENB (a/W = 0.5, 0.9) and SENT (a/W = 0.9) have stress field within the plastic zone that can be characterized by two parameters at low to moderate deformation levels. What are the implications drawn from these results? The best specimens for two-parameter characterization of the stress field would appear to be the CCT, SENT (a/W = 0.1 and 0.5) and CCT (a/W = 0.9). Although, since the deep notched SENB and SENT specimens exhibit single-parameter dominance by remaining closer to the SSY solution at low to moderate deformation levels, the difference in a higher parameter description may be insignificant. The error in the difference field (Eq. 1.10) for 20% deviation from the SSY surface for the SENB (a/W=0.5) is less then that for the corresponding CCT specimen as seen in Figs. 3.55 and 3.56.

CHAPTER V

SUMMARY AND CONCLUSIONS

In the course of this study, the fifth and sixth angular functions and corresponding radial exponents for the generalized power series representation of the stress potential were determined for a Ramberg-Osgood material having hardening exponents of n=5 and 10. The leading coefficients for each term were determined for four common laboratory specimen geometries as a function of deformation level by matching the analytic solution with full field finite element results.

The general power series representation of the stress field can only be determined up to the fifth term for a hardening exponent of n=5 and up to the tenth term for a hardening exponent of n=10. The next terms in the series correspond to the elastic portion of the strain. The angular coefficient for the *J*-integral does not integrate to zero for these terms unless an elastic incompressible material is assumed. This difficulty arises due to the fact that the effective plastic poisson ratio λ in the third constitutive equation is assumed to be 0.5 for the case of plane strain. When an elastic incompressible material having a poisson ratio of 0.5 is assumed, the sixth angular coefficient integrates to zero preserving the path independence of the *J*-integral.

A criterion was established by which it is possible to determine when the near tip stress fields deviate from characterization by two-parameter descriptions. Comparisons of the evolution of the independent parameters in the general power series representation of the stress field for the laboratory specimen geometries with those for the two-parameter MBL solution indicate that all but the SENB (a/W = 0.5 and 0.9) and SENT (a/W = 0.9) lend themselves to a two-parameter description for low to moderate deformation levels. The SENB and SENT geometries that do not stay in the two-parameter surface of the MBL at low and moderate deformation levels however stay near the SSY solution. Consequently, a single parameter description is a good approximation. As the a/W ratio of the specimens increases, we find the path determined by the first three independent coefficients leaves the two-parameter MBL surface at lower deformation levels.

The results indicate that for a 20% difference in the third independent coefficient for the SENB and CCT as compared with the MBL geometry, the error in the stress field as predicted by the general power series representation of the stress field is less for the SENB as compared to the CCT specimen. The reason for this is that the SENB specimen is at a lower deformation level then the CCT specimen when there is a 20% difference between the two-parameter surface and the finite geometry results.

The laboratory specimens studied in this work did not include the compact tension specimen (CT). Future work along the same line as the present research could include determining the evolution path of the first three independent coefficients in the general power series representation for the stress field. Because this specimen demonstrates predominately a global bending field on the crack plane it is fortuitous to expect the results to be similar to that of the SENB specimen.

REFERENCES

[1] Inglis, C.E., Stresses in a Plate due to the Presence of Cracks and Sharp Corners, *Transactions of the Institution of Naval Architects*, Vol. 55, 1913, pp. 219-230.

[2] Griffith, A.A., The Phenomena of Rupture and Flow in Solids, *Philosophical Transactions*, Series A, Vol. 221, 1920, pp. 163-198.

[3] Irwin, G.R., Onset of Fast Crack Propagation in High Strength Steel and Aluminum Alloys, *Sagamore Research Conference Proceedings*, Vol. 2, 1956, pp. 289-305.

[4] Williams, M.L., On the Stress Distribution at the Base of a Stationary Crack, *Journal of Applied Mechanics*, Vol. 24, 1957, pp. 109-114.

[5] Irwin, G.R., Analysis of Stresses and Strains Near the End of a Crack Traversing a Plate, *Journal of Applied Mechanics*, Vol. 24, 1957, pp. 361-364.

[6] Westergaard, H.M., Bearing Pressures and Cracks, *Journal of Applied Mechanics*, Vol. 61, 1939, pp. 49-53.

[7] Hutchinson, J.W., Singular Behavior at the End of a Tensile Crack in a Hardening Material, *Journal of the Mechanics and Physics of Solids*, Vol. 16, 1968, pp. 13-31.

[8] Rice, J.R. and Rosengren, G.F., Plane Strain Deformation Near a Crack Tip in a Power-Law Hardening Material, *Journal of the Mechanics and Physics of Solids*, Vol. 16, 1968, pp. 1-12.

[9] Rice, J.R., A Path Independent Integral and the Approximate Analysis of Strain Concentration by Notches and Cracks, *Journal of Applied Mechanics*, Vol. 35, 1968, pp. 379-386.

[10] Rice, J.R., Paris, P.C. and Merkle, J.G., Some Further Results of *J*-Integral Analysis and Estimates, *Progress in Flaw Growth and Fracture Toughness Testing, American Society for Testing and Materials Special Technical Publication 536*, 1973, pp. 231-245.

[11] Begley, J.A. and Landes, J.D., A Comparison of the *J*-Integral Fracture Criterion with the Equivalent Energy Concept, *Progress in Flaw Growth and Fracture Toughness Testing, American Society for Testing and Materials Special Technical Publication 536*, 1973, pp. 246-263.

[12] Merkle, J.G., Analytical Applications of the *J*-Integral, *Progress in Flaw Growth and Fracture Toughness Testing, American Society for Testing and Materials Special Technical Publication 536*, 1973, pp. 264-280.

[13] Yaochen, L. and Wang, Z., Higher-Order Asymptotic Field of Tensile Plane Strain Nonlinear Crack Problems, *Scientia Sinica*, Series A, Vol. 29, No. 9, 1986, pp. 941-955.

[14] Sharma, S.M. and Aravas, N., Determination of Higher-Order Terms in Asymptotic Elastoplastic Crack Tip Solutions, *Journal of the Mechanics and Physics of Solids*, Vol. 39, 1991, pp. 1043-1072.

[15] O'Dowd, N.P, and Shih, C.F., A Family of Crack Tip Fields Characterized by a Triaxiality Parameter: Part I - Structure of Fields, *Journal of the Mechanics and Physics of Solids*, Vol. 39, 1991, pp. 989-1015.

[16] O'Dowd, N.P, and Shih, C.F., A Family of Crack Tip Fields Characterized by a Triaxiality Parameter: Part II - Fracture Applications, *Journal of the Mechanics and Physics of Solids*, Vol. 40, 1992, pp. 939-963.

[17] Xia, L., Wang, T.C. and Shih, C.F., Higher-Order Analysis of Crack-Tip Fields in Elastic Power-Law Hardening Materials, *Journal of the Mechanics and Physics of Solids*, Vol. 41, 1993, pp. 665-687.

[18] Yang, S., Chao, Y.J. and Sutton, M.A., Higher Order Asymptotic Crack Tip Fields in a Power-Law Hardening Material, *Engineering Fracture Mechanics*, Vol. 45, 1993, pp. 1-20.

[19] Yang, S., Chao, Y.J. and Sutton, M.A., Complete Theoretical Analysis of Higher Order Asymptotic Terms and the HRR Zone at a Crack Tip for Mode I and Mode II Loading of a Hardening Material, to appear in *Acta Mechanica.*

[20] Sharma, S.M., Aravas, N. and Zelman, M.G., Two-Parameter Characterization of Crack Tip Fields in Edge-Cracked Geometries: Plasticity and Creep Solutions, unpublished manuscript, Department of Mechanical Engineering, University of Pennsylvania.

[21] McMeeking, R.M., Finite Deformation Analysis of Crack Tip Opening in Elastic-Plastic Materials and Implications for Fracture, *Journal of the Mechanics and Physics of Solids*, Vol. 25, 1977, pp. 357-383.

[22] McMeeking, R.M. and Parks, D.M., On Criteria for *J*-Dominance of Crack-Tip Fields in Large-Scale Yielding, *Elastic-Plastic Fracture, American Society for Testing and Materials Special Technical Publication 668*, 1979, pp. 175-194.

[23] Shih, C.F., Relationships Between the *J*-Integral and the Crack Opening Displacement for Stationary and Extending Cracks, *Journal of the Mechanics and Physics of Solids*, Vol. 21, 1981, pp. 305-326.

[24] Shih, C.F. and German, M.D., Requirements for a One Parameter Characterization of Crack Tip Fields by the HRR Singularity, *International Journal of Fracture*, Vol. 17, 1981, pp. 27-43.

[25] Needleman, A. and Tvergaard, V., Crack-Tip Stress and Deformation Fields in a Solid with a Vertex on Its Yield Surface, *Elastic-Plastic Fracture, American Society for Testing and Materials Special Technical Publication 803*, Vol. 1, 1983, pp. 80-135.

[26] Yang, S., Chao, Y.J. and Sutton, M.A., On the Size and Shape of the HRR Fields at a Crack Tip, *Proceedings of the Society for Experimental Mechanics*, Vol. 1, 1991, pp. 16-20.

[27] Dadkhah, M.S., Kobayashi, A.S., Wang, F.X. and Graesser, D.L., *J*-Integral Measurement Using Moiré Interferometry, *Proceedings of the Society for Experimental Mechanics*, Vol. 1, 1988, pp. 227-34.

[28] Dadhkah, M.S. and Kobayashi, A.S., HRR Field of a Moving Crack, An Experimental Analysis, *Engineering Fracture Mechanics*, Vol. 34, 1989, pp. 253-263.

[29] Gang, H., Sutton, M.A. and Chao, Y.J., Crack Tip Deformation Fields Obtained by Computer Vision, *Proceedings of the Society for Experimental Mechanics*, Vol. 1, 1991, pp. 701-706.

[30] Chao, Y.J., Yang, S. and Sutton, M.A., Asymptotic Analysis of the Crack Tip Fields to Determine the Region of Dominance of the HRR Solutions, *Manuscript presented at the 28th Annual Technical Meeting, Society of Engineering Science*, Gainesville, Florida, 1991.

[31] Sih, G.C., On the Westergaard Method of Crack Analysis, *International Journal of Fracture Mechanics*, Vol. 2, 1966, pp. 628-631.

[32] Rice, J.R. and Tracey, D.M., *Numerical and Computer Methods in Structural Mechanics*, S.J. Fenves, Ed., Academic Press, New York, 1968, pp. 585-623.

[33] Anderson, T.L. and Dodds, R.H., Specimen Size Requirements for Fracture Toughness Testing in the Ductile-Brittle Transition Region, *Journal of Testing and Evaluation*, Vol. 19, 1991, pp. 123-134.

[34] Dodds, R.H., Anderson, T.L. and Kirk, M.T., A Framework to Correlate a/W Effects on Elastic-Plastic Fracture Toughness (J_c), *International Journal of Fracture*, Vol. 88, 1991, pp. 1-22.

[35] Anderson, T.L. and Dodds, R.H., Simple Constraint Corrections for Subsize Fracture Toughness Specimens, *Presented at the American Society for Testing and Materials International Symposium on Small Specimen Test Techniques*, New Orleans, Louisiana, 1992.

[36] Sorem, W.A., The Effect of Specimen Size and Crack Depth on the Elastic-Plastic Fracture Toughness of a Low-Strength High Strain Hardening Steel, Ph.D. thesis, University of Kansas, Lawrence, Kansas, May 1989.

[37] Joyce, J.A., Upper Shelf J_{Ic}-Q and T-Q Locus Results for Structural Steels, Presented at Nuclear Reglatory Commission Workshop #2, U.S. Naval Academy, Annapolis, Maryland, April 20-21, 1994.

[38] Argon, A.S., Im, J. and Safoglu, R., Cavity Formation from Inclusions in Ductile Fracture, *Metallurgical Transactions*, Vol. 6A, 1975, pp. 825-837.

[39] Rice, J.R., and Tracy, D.M., On the Ductile Enlargement of Voids in Triaxial Stress Fields, *Journal of the Mechanics and Physics of Solids*, Vol. 17, 1969, pp. 201-217.

[40] IMSL Problem-Solving Software Systems, *MATH/LIBRARY–FORTRAN Subroutines for Mathematical Applications*, Version 1.0, Houston, Texas, 1987.

[41] Hibbitt, J.T., Karlsson, D.C. and Sorenson, A.S., *ABAQUS*, Version 5.2, Pawtucket, Rhode Island, 1992.

[42] *PATRAN*, Version 2.5, PATRAN Division of PDA Engineering, Costa Mesa, California, 1990.

[43] Larsson, S.G., and Carlsson, A.J., Influence of Non-Singular Stress Terms and Specimen Geometry on Small-Scale Yielding at Crack Tips in Elastic-Plastic Materials, *Journal of the Mechanics and Physics of Solids*, Vol. 21, 1973, pp. 263-277.

[44] Kumar, V., German, M.D., and Shih, C.F., An Engineering Approach for Elastic-Plastic Fracture Analysis. EPRI Report NP-1931, Electric Power Research Institute, Palo Alto, California, 1981.

[45] Eshelby, J.D., The Continuum Theory of Lattice Defects, *Solid State Physics*, Vol. 3, 1956, pp. 67-86.

APPENDIX A

FORTRAN USER SUBROUTINE FOR NUMERICAL CONSTITUTIVE MODEL

```
C     ****************************************************************
      SUBROUTINE UMAT(STRESS,STATEV,DDSDDE,SSE,SPD,SCD,
     & RPL,DDSDDT,DRPLDE,DRPLDT,
     & STRAN,DSTRAN,TIME,DTIME,TEMP,DTEMP,PREDEF,DPRED,CMNAME,
     & NDI,NSHR,NTENS,NSTATV,PROPS,NPROPS,COORDS,DROT,PNEWDT,
     & CELENT)
C     ****************************************************************
C
      IMPLICIT REAL*8 (A-H,O-Z)
      PARAMETER(NPRECD=2)
      CHARACTER*8 CMNAME
      DIMENSION STRESS(NTENS),STATEV(NSTATV),
     & DDSDDE(NTENS,NTENS),DDSDDT(NTENS),DRPLDE(NTENS),
     & STRAN(NTENS),DSTRAN(NTENS),TIME(2),PREDEF(1),DPRED(1),
     & PROPS(NPROPS),COORDS(3),DROT(3,3)
C
      DIMENSION AA(4,4),BB(4,4),FF(4),DD(4)
      DIMENSION STRANEW(6),EDEV(6)
C
C     Define material constants
C
      SO=PROPS(1)
      EO=PROPS(2)
      RN=PROPS(3)
      RNU=PROPS(4)
      EMOD=SO/EO
C
C     Constants for the transition region
C
      ONE=1.00000000000000000000000
      ZERO=0.00000000000000000000000
      TOLERANCE=0.0000000001
      PI=4.0*ATAN(ONE)
      PI2=PI/2.0
      RK2=1.1
      RK1=0.85
      EE_1=2.0*(1+RNU)*RK1*EO/3.0
      EE_2=(RK2**RN+2.0*(1.0+RNU)*RK2/3.0)*EO
      C1=RK1
      C2=1.0
      C3=RK2+RK2**RN
      C4=1.0+RN*RK2**(RN-1.0)
      QNC=(C2/C4*RK2-RK1)/(C2/C4-1.0)-0.01
      R2=((RK2-QNC)**2.0*(1.0-C2**2.0/C4**2.0)
     &   /(1.0-C2**2.0/C4**2.0*(RK2-QNC)**2.0
     &   /(RK1-QNC)**2.0))**0.5
C
      III=1
C
  100 FF(1)=-(R2**2.0*((RK1-QNC)**2.0-C2**2.0/C4**2.0*(RK2QNC)**2.0)
     &      -(RK1-QNC)**2.0*(RK2-QNC)**2.0*(1.0-C2**2.0/C4**2.0))
      FF(2)=-(C4*(R2**2.0-(RK2-QNC)**2.0)-
     &     C4*(R2**2.0-(RK2-QNC)**2.0)**0.5*
     &     (R2**2.0-(RK1-QNC)**2.0)**0.5-(C1-C3)*(RK2-QNC))
C
```

```
      AA(1,1)=-2.0*R2**2.0*(RK1-QNC)
     &       +2.0*R2**2.0*C2**2.0/C4**2.0*(RK2-QNC)
     &       +2.0*(1.0-C2**2.0/C4**2.0)*(RK1-QNC)*(RK2-QNC)
     &       *((RK1-QNC)+(RK2-QNC))
      AA(1,2)=(RK1-QNC)**2.0-C2**2.0/C4**2.0*(RK2-QNC)**2.0
      AA(2,1)=2.0*C4*(RK2-QNC)-C4*
     &       ((RK1-QNC)*(R2**2.0-(RK2-QNC)**2.0)**0.5
     &       /(R2**2.0-(RK1-QNC)**2.0)**0.5
     &       +(RK2-QNC)*(R2**2.0-(RK1-QNC)**2.0)**0.5
     &       /(R2**2.0-(RK2-QNC)**2.0)**0.5)+(C1-C3)
      AA(2,2)=2.0*C4*R2-C4*R2*
     &       ((R2**2.0-(RK2-QNC)**2.0)**0.5
     &       /(R2**2.0-(RK1-QNC)**2.0)**0.5
     &       +(R2**2.0-(RK1-QNC)**2.0)**0.5
     &       /(R2**2.0-(RK2-QNC)**2.0)**0.5)
C
      BB(1,1)=AA(2,2)/(AA(1,1)*AA(2,2)-AA(1,2)*AA(2,1))
      BB(1,2)=-AA(1,2)/(AA(1,1)*AA(2,2)-AA(1,2)*AA(2,1))
      BB(2,1)=-AA(2,1)/(AA(1,1)*AA(2,2)-AA(1,2)*AA(2,1))
      BB(2,2)=AA(1,1)/(AA(1,1)*AA(2,2)-AA(1,2)*AA(2,1))
C
      DD(1)=BB(1,1)*FF(1)+BB(1,2)*FF(2)
      DD(2)=BB(2,1)*FF(1)+BB(2,2)*FF(2)
C
      RMAXDIFF=ZERO
      IF(ABS(DD(1)).GT.RMAXDIFF)RMAXDIFF=ABS(DD(1))
      IF(ABS(DD(2)).GT.RMAXDIFF)RMAXDIFF=ABS(DD(2))
C
      QNC2=QNC+DD(1)
      R22=R2+DD(2)
C
      QNC=QNC2
      R2=R22
C
      IF(RMAXDIFF.GT.TOLERANCE)THEN
        IF(III.GT.300)THEN
          WRITE(7,*) 'Number of ellipse',
     &               ' iterations to high!'
          STOP
        ENDIF
        III=III+1
        GOTO 100
      ENDIF
C
      R2=((RK2-QNC)**2.0*(1.0-C2**2.0/C4**2.0)
     &   /(1.0-C2**2.0/C4**2.0*(RK2-QNC)**2.0
     &   /(RK1-QNC)**2.0))**0.5
      R1=C4*R2*(1.0-((RK2-QNC)/R2)**2.0)**0.5
     &   /((RK2-QNC)/R2)
      EENC=C1+R1*(1.0-((RK1-QNC)/R2)**2.0)**0.5
C
C     Calculate total strain from begining strain and strain
C     increment
C
      DO I=1,NTENS,1
```

```
            STRANEW(I)=STRAN(I)+DSTRAN(I)
         ENDDO
C
C     Calculate volumetric strain and deviatoric strain
C
         EV=(STRANEW(1)+STRANEW(2)+STRANEW(3))/3.0
         DO I=1,NDI,1
            EDEV(I)=STRANEW(I)-EV
         ENDDO
         DO I=1,NSHR,1
            EDEV(NDI+I)=STRANEW(NDI+I)
         ENDDO
C
C     Calculate equivalent strain
C
         EE=0.00000
         DO I=1,NDI,1
            EE=EE+EDEV(I)**2.0
         ENDDO
         DO I=1,NSHR,1
            EE=EE+2.0*(EDEV(NDI+I)/2.0)**2.0
         ENDDO
         EE=(2.0*EE/3.0)**(0.5)
C
C     Zero stress array (given strains there is only one stress
C     tensor)
C
         DO I=1,NTENS,1
            STRESS(I)=ZERO
         ENDDO
C
C     Zero jacobian
C
         DO I=1,NTENS,1
            DO J=1,NTENS,1
               DDSDDE(I,J)=ZERO
            ENDDO
         ENDDO
C
C     ****************************************************************
C     Linear elastic segment
C     ****************************************************************
C
         IF(EE.LE.EE_1)THEN
C
C        Equivalent stress
C
           SENEW=3.0/2.0*EMOD/(1.0+RNU)*EE
C
C        Stress tensor
C
           DO I=1,NDI,1
              DO J=1,NDI,1
                 STRESS(I)=STRESS(I)+DDSDDE(I,J)*STRANEW(J)
              ENDDO
```

```
      ENDDO
      DO I=1,NSHR,1
         STRESS(I+NDI)=DDSDDE(I+NDI,I+NDI)*STRANEW(I+NDI)
      ENDDO
C
C     Elastic jacobian
C
      DO I=1,NDI,1
         DO J=1,NDI,1
            DDSDDE(I,J)=EMOD/(1.0+RNU)*RNU/(1.0-2.0*RNU)
         ENDDO
      ENDDO
      DO I=1,NDI,1
         DDSDDE(I,I)=DDSDDE(I,I)+EMOD/(1.0+RNU)
      ENDDO
      DO I=1,NSHR,1
         DDSDDE(I+NDI,I+NDI)=EMOD/(1.0+RNU)/2.0
      ENDDO

C
C     Update state variables
C
      STATEV(1)=EE
      STATEV(2)=SENEW
      STATEV(3)=EE*SENEW
C
C     Update strain energy, plastic dissipation, and creep
C     dissipation
C
      PRESS=ZERO
      DO I=1,NDI,1
         PRESS=PRESS+STRESS(I)/3.0
      ENDDO
      SSE=((1+RNU)*SENEW**2.0/3.0+3.0*(1.0-2.0*RNU)
     &       *PRESS**2.0/2.0)/EMOD
      SPD=ZERO
      SCD=ZERO
C
C     ****************************************************************
C     Transitional Segment
C     ****************************************************************
C
      ELSEIF((EE.GT.EE_1).AND.(EE.LT.EE_2))THEN
C
C       Equivalent stress by Newtons method
C
        III=1
        SE=STATEV(2)
        SESO=SE/SO
        IF(SESO.LT.RK1)THEN
          SESO=RK1
        ENDIF
        EEEO=EE/EO
        D=EENC-R1*(1.0-((SESO-QNC)/R2)**2.0)**0.5+
     &    (2.0*RNU-1.0)/3.0*SESO-EEEO
```

```
  200   STIFF=R1/R2*(SESO-QNC)/R2/(1.0-((SESO-QNC)/R2)**2.0)**0.5
     &    +(2.0*RNU-1.0)/3.0
        SESONEW=SESO-D/STIFF
        IF(SESONEW.GT.RK2)SESONEW=RK2
        DNEW=EENC-R1*(1.0-((SESONEW-QNC)/R2)**2.0)**0.5+
     &    (2.0*RNU-1.0)/3.0*SESONEW-EEEO
        IF(III.GT.300)THEN
           WRITE(7,*) 'To many iterations in the material subroutine'
           STOP
        ENDIF
        IF(ABS(DNEW).LT.TOLERANCE)THEN
          SENEW=SESONEW*SO
        ELSE
          IF(SESONEW.LT.RK1)THEN
            SESONEW=(RK1+SESO)/2.0
            DNEW=EENC-R1*(1.0-((SESONEW-QNC)/R2)**2.0)**0.5+
     &           (2.0*RNU-1.0)/3.0*SESONEW-EEEO
          ENDIF
          SESO=SESONEW
          D=DNEW
          III=III+1
          GOTO 200
        ENDIF
C
C       Stress tensor
C
        IF(EE.NE.ZERO)THEN
           DO I=1,NDI,1
              STRESS(I)=2.0/3.0*SENEW/EE*EDEV(I)
     &                  +EMOD/(1.0-2.0*RNU)*EV
           ENDDO
           DO I=1,NSHR,1
              STRESS(I+NDI)=2.0/3.0*SENEW/EE*EDEV(I+NDI)/2.0
           ENDDO
        ENDIF
C
C       Transitional jacobian
C
        STIFF=R1/R2*(SESONEW-QNC)/R2/
     &    (1.0-((SESONEW-QNC)/R2)**2.0)**0.5+(2.0*RNU-1.0)/3.0
        F=2.0/3.0*SENEW/EE
        G=1.0/3.0*(EMOD/(1.0-2.0*RNU)-2.0/3.0*SENEW/EE)
        IF(EE.NE.ZERO)THEN
          H=4.0/9.0*SENEW/EE**2.0*(EMOD/(SENEW*STIFF)-1.0/EE)
        ELSE
          H=ZERO
        ENDIF
C
C       Calculate first part of jacobian while also changing
C       from engineering to tensor strains
C
        DO I=1,NDI+NSHR,1
           DO J=1,NDI+NSHR,1
              IF((I.LE.NDI).AND.(J.LE.NDI))THEN
                DDSDDE(I,J)=H*EDEV(I)*EDEV(J)
```

```
            ELSEIF((I.LE.NDI).AND.(J.GT.NDI))THEN
              DDSDDE(I,J)=H*EDEV(I)*EDEV(J)/2.0
            ELSEIF((I.GT.NDI).AND.(J.LE.NDI))THEN
              DDSDDE(I,J)=H*EDEV(I)*EDEV(J)/2.0
            ELSEIF((I.GT.NDI).AND.(J.GT.NDI))THEN
              DDSDDE(I,J)=H*EDEV(I)*EDEV(J)/2.0/2.0
            ELSE
              WRITE(7,*)'Did not add first jacobian'
            ENDIF
         ENDDO
      ENDDO
C
C     Calculate second part of jacobian
C
      DO I=1,NDI,1
         DO J=1,NDI,1
            DDSDDE(I,J)=DDSDDE(I,J)+G
         ENDDO
      ENDDO
C
C     Calculate third part of jacobian
C
      DO I=1,NDI+NSHR,1
         DDSDDE(I,I)=DDSDDE(I,I)+F
      ENDDO
C
C     Change jacobian to engineering strain (2eps = gamma)
C
      DO I=1,NDI+NSHR,1
         DO J=1,NDI+NSHR,1
            IF((I.GT.NDI).OR.(J.GT.NDI))THEN
              DDSDDE(I,J)=DDSDDE(I,J)/2.0
            ENDIF
         ENDDO
      ENDDO
C
C     Update state variables
C
      STATEV(1)=EE
      STATEV(2)=SENEW
      STATEV(3)=EE*SENEW
C
C     Update strain energy, plastic dissipation, and creep
C     dissipation
C
      PRESS=ZERO
      DO I=1,NDI,1
         PRESS=PRESS+STRESS(I)/3.0
      ENDDO
      SS_1=RK1*SO
      THETA1=ASIN((SS_1/SO-QNC)/R2)
      THETA2=ASIN((SENEW/SO-QNC)/R2)
      SSE_PRESS=3.0*(1.0-2.0*RNU)/2.0*PRESS**2.0
      SSE_ELASTIC=(1.0+RNU)/3.0*SS_1**2.0
      SSE_TRANS=(R1*R2*SO**2.0*(1.0/2.0*THETA2-1.0/4.0
```

```
     &           *SIN(2.0*THETA2)
     &           -QNC/R2*(1.0-((SENEW/SO-QNC)/R2)**2.0)**0.5))
     &           -(R1*R2*SO**2.0*(1.0/2.0*THETA1-1.0/4.0
     &           *SIN(2.0*THETA1)
     &           -QNC/R2*(1.0-((SS_1/SO-QNC)/R2)**2.0)**0.5))
         SSE=(SSE_PRESS+SSE_ELASTIC+SSE_TRANS)/EMOD
         SPD=ZERO
         SCD=ZERO
C
C     ****************************************************************
C     Power law Segment
C     ****************************************************************
C
      ELSEIF(EE.GE.EE_2)THEN
C
C       Equivalent stress by Newtons method
C
         III=1
         TOLERANCE=0.0000000001
         SE=STATEV(2)
         SESO=SE/SO
         EEEO=EE/EO
         D=SESO**RN+2.0*(1+RNU)/3.0*SESO-EEEO
  300    STIFF=RN*SESO**(RN-1.0)+2.0/3.0*(1.0+RNU)
         SESONEW=SESO-D/STIFF
         DNEW=SESONEW**RN+2.0*(1+RNU)/3.0*SESONEW-EEEO
         IF(III.GT.300)THEN
            WRITE(7,*) 'To many iterations in the material subroutine'
            STOP
         ENDIF
         IF(ABS(DNEW).LT.TOLERANCE)THEN
           SENEW=SESONEW*SO
         ELSE
           SESO=SESONEW
           D=DNEW
           III=III+1
           GOTO 300
         ENDIF
C
C       Stress tensor
C
         IF(EE.NE.ZERO)THEN
            DO I=1,NDI,1
               STRESS(I)=2.0/3.0*SENEW/EE*EDEV(I)
     &                   +EMOD/(1.0-2.0*RNU)*EV
            ENDDO
            DO I=1,NSHR,1
               STRESS(I+NDI)=2.0/3.0*SENEW/EE*EDEV(I+NDI)/2.0
            ENDDO
         ENDIF
C
C       Powerlaw jacobian
C
         F=EMOD/(1.0+RNU+3.0/2.0*(SENEW/SO)**(RN-1.0))
         G=EMOD/3.0*(1.0/(1.0-2.0*RNU)-1.0/(1.0+RNU
```

```
     &     +3.0/2.0*(SENEW/SO)**(RN-1.0)))
           IF(EE.NE.ZERO)THEN
             H=2.0/3.0*EMOD/EE/(1.0+RNU+3.0/2.0*(SENEW/SO)**(RN-1.0))
     &         *(1.0/(EE+(RN+1.0)*(SENEW/SO)**(RN-1.0)
     &         *(SENEW/EMOD))-1.0/EE)
           ELSE
             H=ZERO
           ENDIF
C
C          Calculate first part of jacobian while also changing
C          from engineering to tensor strains
C
           DO I=1,NDI+NSHR,1
              DO J=1,NDI+NSHR,1
                 IF((I.LE.NDI).AND.(J.LE.NDI))THEN
                   DDSDDE(I,J)=H*EDEV(I)*EDEV(J)
                 ELSEIF((I.LE.NDI).AND.(J.GT.NDI))THEN
                   DDSDDE(I,J)=H*EDEV(I)*EDEV(J)/2.0
                 ELSEIF((I.GT.NDI).AND.(J.LE.NDI))THEN
                   DDSDDE(I,J)=H*EDEV(I)*EDEV(J)/2.0
                 ELSEIF((I.GT.NDI).AND.(J.GT.NDI))THEN
                   DDSDDE(I,J)=H*EDEV(I)*EDEV(J)/2.0/2.0
                 ELSE
                   WRITE(7,*)'Did not add first jacobian'
                 ENDIF
              ENDDO
           ENDDO
C
C          Calculate second part of jacobian
C
           DO I=1,NDI,1
              DO J=1,NDI,1
                 DDSDDE(I,J)=DDSDDE(I,J)+G
              ENDDO
           ENDDO
C
C          Calculate third part of jacobian
C
           DO I=1,NDI+NSHR,1
              DDSDDE(I,I)=DDSDDE(I,I)+F
           ENDDO
C
C          Change jacobian to engineering strain (2eps = gamma)
C
           DO I=1,NDI+NSHR,1
              DO J=1,NDI+NSHR,1
                 IF((I.GT.NDI).OR.(J.GT.NDI))THEN
                   DDSDDE(I,J)=DDSDDE(I,J)/2.0
                 ENDIF
              ENDDO
           ENDDO
C
C          Update state variables
C
           STATEV(1)=EE
```

```
      STATEV(2)=SENEW
      STATEV(3)=EE*SENEW
C
C     Update strain energy, plastic dissipation, and creep
C     dissipation
C
      PRESS=ZERO
      DO I=1,NDI,1
         PRESS=PRESS+STRESS(I)/3.0
      ENDDO
      SS_1=RK1*SO
      SS_2=RK2*SO
      THETA1=ASIN((SS_1/SO-QNC)/R2)
      THETA2=ASIN((SS_2/SO-QNC)/R2)
      SSE_PRESS=3.0*(1.0-2.0*RNU)/2.0*PRESS**2.0
      SSE_ELASTIC=(1.0+RNU)/3.0*SS_1**2.0
      SSE_TRANS=(R1*R2*SO**2.0*(1.0/2.0*THETA2-1.0/4.0
     &          *SIN(2.0*THETA2)
     &          -QNC/R2*(1.0-((SS_2/SO-QNC)/R2)**2.0)**0.5))
     &          -(R1*R2*SO**2.0*(1.0/2.0*THETA1-1.0/4.0
     &          *SIN(2.0*THETA1)
     &          -QNC/R2*(1.0-((SS_1/SO-QNC)/R2)**2.0)**0.5))
      SSE_POWER=((1.0+RNU)/3.0*SENEW**2.0
     &             +RN*SO**2.0/(RN+1.0)*(SENEW/SO)**(RN+1.0))
     &             -((1.0+RNU)/3.0*SS_2**2.0
     &             +RN*SO**2.0/(RN+1.0)*(SS_2/SO)**(RN+1.0))
      SSE=(SSE_PRESS+SSE_ELASTIC+SSE_TRANS+SSE_POWER)/EMOD
      SPD=ZERO
      SCD=ZERO
    ENDIF
C
    RETURN
    END
```

APPENDIX B

CONSTANTS FOR SIXTH ORDER

RUNGE-KUTTA-VERNER INTEGRATION

$$k_i^{\ell,1} = h f_i^{\ell}\left[\theta, Y_i^{\ell}(\theta)\right]$$

$$k_i^{\ell,2} = h f_i^{\ell}\left[\theta + \frac{h}{6}, Y_i^{\ell}(\theta) + \frac{k_i^{\ell,1}}{6}\right]$$

$$k_i^{\ell,3} = h f_i^{\ell}\left[\theta + \frac{4h}{15}, Y_i^{\ell}(\theta) + \frac{4k_i^{\ell,1}}{75} + \frac{16k_i^{\ell,2}}{75}\right]$$

$$k_i^{\ell,4} = h f_i^{\ell}\left[\theta + \frac{2h}{3}, Y_i^{\ell}(\theta) + \frac{5k_i^{\ell,1}}{6} - \frac{8k_i^{\ell,2}}{3} + \frac{5k_i^{\ell,3}}{2}\right]$$

$$k_i^{\ell,5} = h f_i^{\ell}\left[\theta + \frac{5h}{6}, Y_i^{\ell}(\theta) - \frac{165k_i^{\ell,1}}{64} + \frac{55k_i^{\ell,2}}{6} - \frac{425k_i^{\ell,3}}{64} + \frac{85k_i^{\ell,4}}{96}\right]$$

$$k_i^{\ell,6} = h f_i^{\ell}\left[\theta + h, Y_i^{\ell}(\theta) + \frac{12k_i^{\ell,1}}{5} - 8k_i^{\ell,2} + \frac{4015k_i^{\ell,3}}{612} - \frac{11k_i^{\ell,4}}{36} + \frac{88k_i^{\ell,5}}{255}\right]$$

$$k_i^{\ell,7} = h f_i^{\ell}\left[\theta + \frac{h}{15}, Y_i^{\ell}(\theta) - \frac{8263k_i^{\ell,1}}{15000} + \frac{124k_i^{\ell,2}}{75} - \frac{4501k_i^{\ell,3}}{4760} - \frac{81k_i^{\ell,4}}{250} + \frac{2484k_i^{\ell,5}}{10625}\right]$$

$$k_i^{\ell,8} = h f_i^{\ell}\left[\theta + h, Y_i^{\ell}(\theta) + \frac{3501k_i^{\ell,1}}{1720} - \frac{300k_i^{\ell,2}}{43} + \frac{2972751k_i^{\ell,3}}{52632} - \frac{319k_i^{\ell,4}}{2322} + \frac{24068k_i^{\ell,5}}{84065} + 0k_i^{\ell,6} + \frac{3850k_i^{\ell,7}}{26703}\right]$$

The functions $f_i^{\ell}(\,)$ are the derivatives of $Y_i^{\ell}(\theta)$. The value h in these constants is the step size for integration.

APPENDIX C

FORTRAN PROGRAM FOR SOLUTION OF NONLINEAR DIFFERENTIAL EQUATIONS WITH A SHOOTING TECHNIQUE

```
C     ****************************************************************
      PROGRAM SHOOTTWO_FIRSTORDER
C     ****************************************************************
C
      IMPLICIT    NONE
      CHARACTER*3 CERR,PRI
      INTEGER     I,J,K,ITERATION
      REAL*8      ONE,PIE,PIE2,ZERO,STEP1,STEP2,TOL,ERRF
      REAL*8      DELTA,PERCENT
      REAL*8      GUESS(5),YL(5),YR(5),PARAM(50),FEND(5),ENDL(5)
      REAL*8      FENDINIT(5),DELTAGUESS(5),ENDR(5)
      REAL*8      JAC(5,5),INVJAC(5,5)
C
      INTEGER     NHARD,COUNT,IU1,IU2,IU3,IU4,IU5,IU6,IU7
      REAL*8      RLAMBDA,S1,ALPHA,BETA,MAXMIS
      REAL*8      POTENTIAL1(7,2000),CONSTANT1(3,4000)
      COMMON/MAINC/S1,RLAMBDA,ALPHA,BETA,NHARD,COUNT,MAXMIS
      COMMON/MAINA/POTENTIAL1,CONSTANT1
      COMMON/OUT/IU1,IU2,IU3,IU4,IU5,IU6,IU7
C
      CALL INPUT            (TOL,PARAM,STEP1,STEP2,ERRF,DELTA,NHARD,
     &                       RLAMBDA,PERCENT,GUESS)

      S1       = -1.0/(NHARD+1)              ! First eigen value
      ALPHA    = RLAMBDA**2-RLAMBDA+1
      BETA     = 2*RLAMBDA**2-2*RLAMBDA-1
      ZERO     =  0.0
      ONE      =  1.0
      PIE      =  4*DATAN(ONE)
      PIE2     =  PERCENT*PIE
      COUNT    = 0
      MAXMIS   = -1000000.0
C
      ITERATION = 1
      CALL OPENUNIT         (ITERATION,IU1,IU2,IU3,IU4,IU5,IU6,IU7)
   10 CALL FIRSTTRY         (CERR,PRI,ITERATION,PIE,PIE2,ZERO,STEP1,
     &                       STEP2,TOL,ERRF,GUESS,YL,YR,PARAM,FEND,
     &                       ENDL,FENDINIT,ENDR)
      CALL NORMALIZE        (COUNT,MAXMIS,POTENTIAL1)
      CALL SORT             (COUNT,POTENTIAL1,7,2000)
      CALL OUTPUT
      CALL SORT             (2*COUNT,CONSTANT1,3,4000)
      CALL INTEGCONST       (2*COUNT,CONSTANT1)
      IF(CERR(1:1).EQ.'N')  GOTO 20
C
      CALL IMPROVE          (CERR,PRI,ITERATION,PIE,PIE2,ZERO,STEP1,
     &                       STEP2,TOL,ERRF,GUESS,YL,YR,PARAM,FEND,
     &                       ENDL,FENDINIT,ENDR,DELTA,JAC)
      CALL INVERTJACOBIAN   (JAC,INVJAC)
      CALL FINDDELTAGUESS   (INVJAC,FENDINIT,DELTAGUESS)
      CALL ADDGUESSANDDELTA (GUESS,DELTAGUESS)
      CALL CLOSEUNIT        (IU1,IU2,IU3,IU4,IU5,IU6,IU7)
      CALL OPENUNIT         (1,IU1,IU2,IU3,IU4,IU5,IU6,IU7)
      ITERATION = ITERATION+1
      COUNT=0
```

```
      MAXMIS=-1000000.0
      GOTO 10
C
   20 CALL CLOSEUNIT        (IU1,IU2,IU3,IU4,IU5,IU6,IU7)
C
      STOP
      END
C
C     ****************************************************************
      SUBROUTINE INPUT(TOL,PARAM,STEP1,STEP2,ERRF,DELTA,NHARD,
     &                 RLAMBDA,PERCENT,GUESS)
C     ****************************************************************
C
      IMPLICIT    NONE
      INTEGER     NHARD
      REAL*8      STEP1,STEP2,TOL,ERRF,DELTA,PERCENT,RLAMBDA
      REAL*8      PARAM(50),GUESS(5)
C
      OPEN (UNIT=1,FILE='INPUT.DAT',STATUS='OLD')
C
      READ(1,*) TOL       ! Global error tolerence < 0.001
      READ(1,*) PARAM(1)  ! Initial guess of step size
      READ(1,*) PARAM(2)  ! Absolute value of minimum step size
      READ(1,*) PARAM(3)  ! Absolute value of maximum step size
      READ(1,*) PARAM(10)! Type of error control
      READ(1,*) STEP1     ! Number of increments for zero to pie/2
      READ(1,*) STEP2     ! Number of increments for pie to pie/2
      READ(1,*) ERRF      ! Acceptable difference at pie/2
      READ(1,*) DELTA     ! Increment for guesses
      READ(1,*) NHARD     ! Ramberg-Osgood hardening coefficient
      READ(1,*) RLAMBDA   ! Measure of the degree of plasticity
      READ(1,*) PERCENT   ! Percent of pie to shoot too
      READ(1,*) GUESS(1)  ! Five initial guess for boundary conditions
      READ(1,*) GUESS(2)
      READ(1,*) GUESS(3)
      READ(1,*) GUESS(4)
      READ(1,*) GUESS(5)
C
      CLOSE (UNIT=1)
C
      RETURN
      END
C
C     ****************************************************************
      SUBROUTINE FIRSTTRY (CERR,PRI,ITERATION,PIE,PIE2,ZERO,STEP1,
     &                     STEP2,TOL,ERRF,GUESS,YL,YR,PARAM,FEND,
     &                     ENDL,FENDINIT,ENDR)
C     ****************************************************************
C
      IMPLICIT    NONE
      CHARACTER*3 CERR,PRI
      INTEGER     ITERATION
      REAL*8      PIE,PIE2,ZERO,STEP1,STEP2,TOL,ERRF
      REAL*8      GUESS(5),YL(5),YR(5),PARAM(50),FEND(5),ENDL(5)
      REAL*8      FENDINIT(5),ENDR(5)
```

```
C
      PRI = 'YES'
      CALL LEFTBOUND         (GUESS,YL)
      CALL RIGHTBOUND        (GUESS,YR)
      CALL INTEGRATZEROPIE2 (ZERO,PIE2,STEP1,TOL,PARAM,YL,PRI)
      CALL INTEGRATPIEPIE2  (PIE,PIE2,STEP2,TOL,PARAM,YR,PRI)
      CALL SAVEENDPOINTS     (YL,YR,ENDL,ENDR)
      CALL FENDPOINTS        (YL,YR,FENDINIT)
      CALL FERROR            (ITERATION,FENDINIT,ERRF,CERR)
C
      RETURN
      END
C
C     ****************************************************************
      SUBROUTINE IMPROVE (CERR,PRI,ITERATION,PIE,PIE2,ZERO,STEP1,
     &                    STEP2,TOL,ERRF,GUESS,YL,YR,PARAM,FEND,
     &                    ENDL,FENDINIT,ENDR,DELTA,JAC)
C     ****************************************************************
C
      IMPLICIT    NONE
      CHARACTER*3 CERR,PRI
      INTEGER     I,ITERATION
      REAL*8      PIE,PIE2,ZERO,STEP1,STEP2,TOL,ERRF,DELTA
      REAL*8      GUESS(5),YL(5),YR(5),PARAM(50),FEND(5),ENDL(5)
      REAL*8      FENDINIT(5),ENDR(5)
      REAL*8      JAC(5,5)
C
      PRI = 'NOO'
      DO I=1,5,1
         CALL INCREMENTGUESS   (DELTA,GUESS(I))
         CALL LEFTBOUND        (GUESS,YL)
         CALL RIGHTBOUND       (GUESS,YR)
         CALL INTEGRATZEROPIE2 (ZERO,PIE2,STEP1,TOL,PARAM,YL,PRI)
         CALL INTEGRATPIEPIE2  (PIE,PIE2,STEP2,TOL,PARAM,YR,PRI)
         CALL FENDPOINTS       (YL,YR,FEND)
         CALL JACOBIAN         (I,DELTA,FENDINIT,FEND,JAC)
         CALL UNINCREMENTGUESS (DELTA,GUESS(I))
      ENDDO
C
      RETURN
      END
C
C     ****************************************************************
      SUBROUTINE LEFTBOUND (GUESS,YL)
C     ****************************************************************
C
      IMPLICIT    NONE
      INTEGER     I
      REAL*8      GUESS(5),YL(5)
C
      WRITE(11,*) 'Setting left boundary conditions'
C

      YL(1) =  1.0
      YL(2) =  0
```

```
      YL(3) =  GUESS(1)
      YL(4) =  0.0
      YL(5) =  GUESS(2)
C
      RETURN
      END
C
C     ****************************************************************
      SUBROUTINE RIGHTBOUND (GUESS,YR)
C     ****************************************************************
C
      IMPLICIT    NONE
      INTEGER     I
      REAL*8      GUESS(5),YR(5)
C
      WRITE(11,*) 'Setting right boundary conditions'
C
      YR(1) =  0
      YR(2) =  0
      YR(3) =  GUESS(3)
      YR(4) =  GUESS(4)
      YR(5) =  GUESS(5)
C
      RETURN
      END
C
C     ****************************************************************
      SUBROUTINE INTEGRATZEROPIE2 (ZERO,PIE2,STEP1,TOL,PARAM,YL,PRI)
C     ****************************************************************
C
      IMPLICIT    NONE
      CHARACTER*3 PRI
      INTEGER     I
      REAL*8      ZERO,PIE2,STEP1,X,TOL,RINCREMENT1,OVER
      REAL*8      YL(5),PARAM(50),DYDX(5)
C
      WRITE(11,*) 'Integrating from zero to pie/2'
C
      RINCREMENT1 = (PIE2-ZERO)/INT(STEP1)
      IF (PRI(1:1).EQ.'Y') THEN
          CALL SAVE (ZERO,YL)
      ENDIF
      OVER = RINCREMENT1/2
      DO X=ZERO,PIE2-RINCREMENT1+OVER,RINCREMENT1
         CALL INTEGRATE (X,X+RINCREMENT1,RINCREMENT1,TOL,PARAM,YL)
         IF (PRI(1:1).EQ.'Y') THEN
             CALL SAVE(X+RINCREMENT1,YL)
         ENDIF
      ENDDO
C
      RETURN
      END
C
```

```
C     ****************************************************************
      SUBROUTINE INTEGRATPIEPIE2 (PIE,PIE2,STEP2,TOL,PARAM,YR,PRI)
C     ****************************************************************
C
      IMPLICIT    NONE
      CHARACTER*3 PRI
      INTEGER     I
      REAL*8      PIE,PIE2,STEP2,X,TOL,RINCREMENT2,OVER
      REAL*8      YR(5),PARAM(50),DYDX(5)
C
      WRITE(11,*) 'Integrating from pie to pie/2'
C
      RINCREMENT2 = (PIE2-PIE)/INT(STEP2)
      IF (PRI(1:1).EQ.'Y') THEN
         CALL SAVE(PIE,YR)
      ENDIF
      OVER = RINCREMENT2/2
      DO X=PIE,PIE2-RINCREMENT2+OVER,RINCREMENT2
         CALL INTEGRATE (X,X+RINCREMENT2,RINCREMENT2,TOL,PARAM,YR)
         IF (PRI(1:1).EQ.'Y') THEN
            CALL SAVE(X+RINCREMENT2,YR)
         ENDIF
      ENDDO
C
      RETURN
      END
C
C     ****************************************************************
      SUBROUTINE INTEGRATE (BEGIN,END,STEP,TOL,PARAM,Y)
C     ****************************************************************
C
      IMPLICIT    NONE
      INTEGER     IDO,NEQ
      REAL*8      BEGIN,END,STEP,XEND,X,TOL,OVER
      REAL*8      Y(5),YJUNK(5),FCN,PARAM(50)
      EXTERNAL    FCN,DIVPRK
C
      IDO = 1
      NEQ = 5
      OVER = STEP/2
      DO X=BEGIN,END-STEP+OVER,STEP
         XEND = X+STEP
         CALL DIVPRK (IDO,NEQ,FCN,X,XEND,TOL,PARAM,Y)
      ENDDO
C
      IDO = 3
      CALL DIVPRK (IDO,NEQ,FCN,X,XEND,TOL,PARAM,YJUNK)
C
      RETURN
      END
C
C     ****************************************************************
      SUBROUTINE SAVEENDPOINTS (YL,YR,ENDL,ENDR)
C     ****************************************************************
C
```

```
      IMPLICIT    NONE
      INTEGER     I
      REAL*8      YL(5),YR(5),ENDL(5),ENDR(5)
C
      WRITE(11,*) 'Saving endpoints'
C
      DO I=1,5,1
         ENDL(I) = YL(I)
         ENDR(I) = YR(I)
      ENDDO
C
      RETURN
      END
C
C     ****************************************************************
      SUBROUTINE FENDPOINTS (YL,YR,FEND)
C     ****************************************************************
C
      IMPLICIT NONE
      INTEGER  I
      REAL*8   YL(5),YR(5),FEND(5)
C
      WRITE(11,*) 'Determining error in the endpoints'
C
      DO I=1,5,1
         FEND(I) = YR(I)-YL(I)
      ENDDO
C
      RETURN
      END
C
C     ****************************************************************
      SUBROUTINE FERROR (ITERATION,FEND,ERRF,CERR)
C     ****************************************************************
C
      IMPLICIT    NONE
      CHARACTER*3 CERR
      INTEGER     I,ITERATION
      REAL*8      ERRMAX,ERRF,ERR
      REAL*8      FEND(5)
C
      INTEGER    IU1,IU2,IU3,IU4,IU5,IU6,IU7
      COMMON/OUT/IU1,IU2,IU3,IU4,IU5,IU6,IU7
C
      WRITE(11,*) 'Determining maximum error in F at pie/2'
C
      ERRMAX = 0
      DO I=1,5,1
         ERR    = DABS(FEND(I))
         ERRMAX = MAX(ERR,ERRMAX)
      ENDDO
      WRITE(*,*) 'Max error for iteration ',ITERATION,' is ',ERRMAX
      WRITE(11,*) 'Max error for iteration ',ITERATION,' is ',ERRMAX
      IF (ERRMAX.LE.ERRF) THEN
         CERR = 'NOO'
```

```
      ELSE
         CERR = 'YES'
      ENDIF
C
      RETURN
      END
C
C     ****************************************************************
      SUBROUTINE INCREMENTGUESS (DELTA,G)
C     ****************************************************************
C
      IMPLICIT    NONE
      REAL*8      DELTA,G
C
      G = G + DELTA
C
      RETURN
      END
C
C     ****************************************************************
      SUBROUTINE UNINCREMENTGUESS (DELTA,G)
C     ****************************************************************
C
      IMPLICIT    NONE
      REAL*8      DELTA,G
C
      G = G - DELTA
C
      RETURN
      END
C
C
C     ****************************************************************
      SUBROUTINE JACOBIAN (ICOL,DELTA,FENDINIT,FEND,JAC)
C     ****************************************************************
C
      IMPLICIT    NONE
      INTEGER     I,ICOL
      REAL*8      DELTA
      REAL*8      FENDINIT(5),FEND(5)
      REAL*8      JAC(5,5)
C
      DO I=1,5,1
         JAC(I,ICOL)=(FEND(I)-FENDINIT(I))/DELTA
      ENDDO
C
      RETURN
      END
C
C
C     ****************************************************************
      SUBROUTINE INVERTJACOBIAN (JAC,INVJAC)
C     ****************************************************************
C
      IMPLICIT    NONE
```

```
      INTEGER     I,J
      REAL*8      JAC(5,5),INVJAC(5,5)
C
      CALL DLINRG (5,JAC,5,INVJAC,5)
C
      RETURN
      END
C
C     ****************************************************************
      SUBROUTINE FINDDELTAGUESS (INVJAC,FENDINIT,DELTAGUESS)
C     ****************************************************************
C
      IMPLICIT    NONE
      INTEGER     I,J
      REAL*8      FENDINIT(5),DELTAGUESS(5)
      REAL*8      INVJAC(5,5)
C
      WRITE(11,*) 'Determine change in guesses'
C
      DO I=1,5,1
         DELTAGUESS(I) = 0
         DO J=1,5,1
            DELTAGUESS(I) = DELTAGUESS(I)-INVJAC(I,J)*FENDINIT(J)
         ENDDO
      ENDDO
C
      RETURN
      END
C
C     ****************************************************************
      SUBROUTINE ADDGUESSANDDELTA (GUESS,DELTAGUESS)
C     ****************************************************************
C
      IMPLICIT    NONE
      INTEGER     I
      REAL*8      GUESS(5),DELTAGUESS(5)
C
      WRITE(11,*) 'Adding the change in guesses to previous guesses'
C
      GUESS(1) = GUESS(1)+DELTAGUESS(1)
      GUESS(2) = GUESS(2)+DELTAGUESS(2)
      GUESS(3) = GUESS(3)+DELTAGUESS(3)
      GUESS(4) = GUESS(4)+DELTAGUESS(4)
      GUESS(5) = GUESS(5)+DELTAGUESS(5)
C
      RETURN
      END
C
C     ****************************************************************
      SUBROUTINE FCN(NEQ,XX,Y,DYDX)
C     ****************************************************************
C
      IMPLICIT    NONE
      INTEGER     NEQ,I
      REAL*8      XX,Y(NEQ),DYDX(NEQ),MEAN
```

```
      REAL*8       SIG(4),DSIG(4),DDSIG(4),S(4),MIS(5)
      REAL*8       C11,C12
      REAL*8       CN11,CN12,CN13,CN14,CN15
      REAL*8       CL11,CL12,CL13,CL14,CL15
      REAL*8       C21,C22,C23,C24,C25
C
      INTEGER      NHARD,COUNT
      REAL*8       RLAMBDA,S1,ALPHA,BETA,MAXMIS
      REAL*8       POTENTIAL1(7,2000),CONSTANT1(3,4000)
      COMMON/MAINC/S1,RLAMBDA,ALPHA,BETA,NHARD,COUNT,MAXMIS
      COMMON/MAINA/POTENTIAL1,CONSTANT1
C
C     Find the values of the last field at X
C
      CALL STRESS(Y(5),Y,SIG)
      CALL DSTRESS(Y(5),Y,DSIG)
      CALL DDSTRESS(Y(5),Y,DDSIG)
      CALL DEV(SIG,S,MEAN)
      CALL SIGMIS(SIG,SIG,DSIG,DSIG,DDSIG,DDSIG,MIS)
      MIS(1)=MIS(1)**0.5
C
      C11 = 2*ALPHA*(DSIG(1)**2+SIG(2)*DDSIG(2)+DSIG(2)**2)
     &      + BETA*(SIG(1)*DDSIG(2)+2*DSIG(1)*DSIG(2))
     &      + 6*(SIG(3)*DDSIG(3)+DSIG(3)**2)
     &      + (Y(5)+2)*(2*ALPHA*SIG(1)+BETA*SIG(2))*Y(3)
      C12 = 2*ALPHA*SIG(1)+BETA*SIG(2)
C
C     Linear coefficients of the differential equation
C
      CL11 = NHARD*Y(5)*(((1+RLAMBDA)/3+(NHARD*Y(5)+1)
     &       *(2-RLAMBDA)/3)*(Y(5)+1)-((2-RLAMBDA)/3
     &       +(NHARD*Y(5)+1)*(1+RLAMBDA)/3))*(Y(5)+2)
      CL12 = 0.0
      CL13 = (2-RLAMBDA)/3*(Y(5)+2)
     &       -(1+RLAMBDA)/3*(Y(5)+2)*(Y(5)+1)
     &       +2*(NHARD*Y(5)+1)*(Y(5)+1)
     &       -NHARD*Y(5)*((2-RLAMBDA)/3+(NHARD*Y(5)+1)
     &       *(1+RLAMBDA)/3)
      CL14 = 0.0
      CL15 = (2-RLAMBDA)/3
C
C     Nonlinear coefficients of the differential equation
C
      CN11 = (NHARD-1)*(Y(5)+2)*MIS(1)**(-2)
     &       *(C11/2+(NHARD-3)*MIS(3)**2)
     &       *((2-RLAMBDA)/3-(1+RLAMBDA)/3*(Y(5)+1))
      CN12 = 2*(NHARD-1)*MIS(1)**(-1)*MIS(3)
     &       *((2-RLAMBDA)/3*(Y(5)+2)
     &       -(1+RLAMBDA)/3*(Y(5)+2)*(Y(5)+1)
     &       +(NHARD*Y(5)+1)*(Y(5)+1))
      CN13 = (2-RLAMBDA)/3*(NHARD-1)*MIS(1)**(-2)
     &       *(C11/2+(NHARD-3)*MIS(3)**2)
      CN14 = 2*(NHARD-1)*(2-RLAMBDA)/3*MIS(1)**(-1)*MIS(3)
      CN15 = C12*(NHARD-1)/2*MIS(1)**(-2)*S(1)
C
```

```
C     Coefficients for the differential equation
C
      C21 = CL11+CN11
      C22 = CL12+CN12
      C23 = CL13+CN13
      C24 = CL14+CN14
      C25 = CL15+CN15
C
C     Set of first order differential equations
C
      DYDX(1) = Y(2)
      DYDX(2) = Y(3)
      DYDX(3) = Y(4)
      DYDX(4) = -(C24*Y(4)+C23*Y(3)+C22*Y(2)+C21*Y(1))/C25
      DYDX(5) = 0.0
C
      RETURN
      END
C
C     ****************************************************************
      SUBROUTINE STRESS(SI,F,SIG)
C     ****************************************************************
C
      IMPLICIT    NONE
      REAL*8      SI
      REAL*8      F(5),SIG(4)
C
      INTEGER     NHARD,COUNT
      REAL*8      RLAMBDA,S1,ALPHA,BETA,MAXMIS
      REAL*8      POTENTIAL1(7,2000),CONSTANT1(3,4000)
      COMMON/MAINC/S1,RLAMBDA,ALPHA,BETA,NHARD,COUNT,MAXMIS
      COMMON/MAINA/POTENTIAL1,CONSTANT1
C
C     Determine the stresses
C
      SIG(1)=F(3)+(SI+2)*F(1)
      SIG(2)=(SI+2)*(SI+1)*F(1)
      SIG(3)=-(SI+1)*F(2)
      SIG(4)=RLAMBDA*(SIG(1)+SIG(2))
C
      RETURN
      END
C
C     ****************************************************************
      SUBROUTINE DSTRESS(SI,F,DSIG)
C     ****************************************************************
C
      IMPLICIT    NONE
      REAL*8      SI
      REAL*8      F(5),DSIG(4)
C
      INTEGER     NHARD,COUNT
      REAL*8      RLAMBDA,S1,ALPHA,BETA,MAXMIS
      REAL*8      POTENTIAL1(7,2000),CONSTANT1(3,4000)
      COMMON/MAINC/S1,RLAMBDA,ALPHA,BETA,NHARD,COUNT,MAXMIS
```

```
      COMMON/MAINA/POTENTIAL1,CONSTANT1
C
C     Determine the first derivative of the stresses
C
      DSIG(1)=F(4)+(SI+2)*F(2)
      DSIG(2)=(SI+2)*(SI+1)*F(2)
      DSIG(3)=-(SI+1)*F(3)
      DSIG(4)=RLAMBDA*(DSIG(1)+DSIG(2))
C
      RETURN
      END
C
C     ****************************************************************
      SUBROUTINE DDSTRESS(SI,F,DDSIG)
C     ****************************************************************
C
      IMPLICIT    NONE
      REAL*8      SI
      REAL*8      F(5),DDSIG(4)
C
      INTEGER     NHARD,COUNT
      REAL*8      RLAMBDA,S1,ALPHA,BETA,MAXMIS
      REAL*8      POTENTIAL1(7,2000),CONSTANT1(3,4000)
      COMMON/MAINC/S1,RLAMBDA,ALPHA,BETA,NHARD,COUNT,MAXMIS
      COMMON/MAINA/POTENTIAL1,CONSTANT1
C
C     Determine the second derivative of the stresses
C
      DDSIG(1)=F(5)+(SI+2)*F(3)
      DDSIG(2)=(SI+2)*(SI+1)*F(3)
      DDSIG(3)=-(SI+1)*F(4)
      DDSIG(4)=RLAMBDA*(DDSIG(1)+DDSIG(2))
C
      RETURN
      END
C
C     ****************************************************************
      SUBROUTINE DEV(SIG,S,MEAN)
C     ****************************************************************
C
      IMPLICIT    NONE
      REAL*8      MEAN
      REAL*8      SIG(4),S(4)
C
      INTEGER     NHARD,COUNT
      REAL*8      RLAMBDA,S1,ALPHA,BETA,MAXMIS
      REAL*8      POTENTIAL1(7,2000),CONSTANT1(3,4000)
      COMMON/MAINC/S1,RLAMBDA,ALPHA,BETA,NHARD,COUNT,MAXMIS
      COMMON/MAINA/POTENTIAL1,CONSTANT1
C
C     Determine the deviatoric stresses
C
      S(1) = (2-RLAMBDA)/3*SIG(1)-(1+RLAMBDA)/3*SIG(2)
      S(2) = (2-RLAMBDA)/3*SIG(2)-(1+RLAMBDA)/3*SIG(1)
      S(3) = SIG(3)
```

```
      S(4) = (2*RLAMBDA-1)/3*(SIG(1)+SIG(2))
      MEAN = (1+RLAMBDA)/3*(SIG(1)+SIG(2))
C
      RETURN
      END
C
C     ****************************************************************
      SUBROUTINE DDEV(DSIG,DS)
C     ****************************************************************
C
      IMPLICIT    NONE
      REAL*8      DSIG(4),DS(4)
C
      INTEGER     NHARD,COUNT
      REAL*8      RLAMBDA,S1,ALPHA,BETA,MAXMIS
      REAL*8      POTENTIAL1(7,2000),CONSTANT1(3,4000)
      COMMON/MAINC/S1,RLAMBDA,ALPHA,BETA,NHARD,COUNT,MAXMIS
      COMMON/MAINA/POTENTIAL1,CONSTANT1
C
C     Determine the first derivative of the deviatoric stresses
C
      DS(1) = (2-RLAMBDA)/3*DSIG(1)-(1+RLAMBDA)/3*DSIG(2)
      DS(2) = (2-RLAMBDA)/3*DSIG(2)-(1+RLAMBDA)/3*DSIG(1)
      DS(3) = DSIG(3)
      DS(4) = (2*RLAMBDA-1)/3*(DSIG(1)+DSIG(2))
C
      RETURN
      END
C
C     ****************************************************************
      SUBROUTINE DDDEV(DDSIG,DDS)
C     ****************************************************************
C
      IMPLICIT    NONE
      REAL*8      DDSIG(4),DDS(4)
C
      INTEGER     NHARD,COUNT
      REAL*8      RLAMBDA,S1,ALPHA,BETA,MAXMIS
      REAL*8      POTENTIAL1(7,2000),CONSTANT1(3,4000)
      COMMON/MAINC/S1,RLAMBDA,ALPHA,BETA,NHARD,COUNT,MAXMIS
      COMMON/MAINA/POTENTIAL1,CONSTANT1
C
C     Determine the second derivative of the deviatoric stresses
C
      DDS(1) = (2-RLAMBDA)/3*DDSIG(1)-(1+RLAMBDA)/3*DDSIG(2)
      DDS(2) = (2-RLAMBDA)/3*DDSIG(2)-(1+RLAMBDA)/3*DDSIG(1)
      DDS(3) = DDSIG(3)
      DDS(4) = (2*RLAMBDA-1)/3*(DDSIG(1)+DDSIG(2))
C
      RETURN
      END
C
```

```
C     ****************************************************************
      SUBROUTINE SIGMIS(SIG1,SIG2,DSIG1,DSIG2,DDSIG1,DDSIG2,MIS)
C     ****************************************************************
C
      IMPLICIT    NONE
      REAL*8      SIG1(4),DSIG1(4),DDSIG1(4),MIS(5)
      REAL*8      SIG2(4),DSIG2(4),DDSIG2(4)
C
      INTEGER     NHARD,COUNT
      REAL*8      RLAMBDA,S1,ALPHA,BETA,MAXMIS
      REAL*8      POTENTIAL1(7,2000),CONSTANT1(3,4000)
      COMMON/MAINC/S1,RLAMBDA,ALPHA,BETA,NHARD,COUNT,MAXMIS
      COMMON/MAINA/POTENTIAL1,CONSTANT1
C
C     Determine the angular functions for the effective stress
C
      MIS(1) = ALPHA*(SIG1(1)*SIG2(1)+SIG1(2)*SIG2(2))
     &         +BETA/2*(SIG1(1)*SIG2(2)+SIG2(1)*SIG1(2))
     &         +3*SIG1(3)*SIG2(3)
      MIS(2) = ALPHA*(SIG1(1)*DSIG2(1)+DSIG1(1)*SIG2(1)
     &         +SIG1(2)*DSIG2(2)+DSIG1(2)*SIG2(2))
     &         +BETA/2*(SIG1(1)*DSIG2(2)+DSIG1(1)*SIG2(2)
     &         +SIG2(1)*DSIG1(2)+DSIG2(1)*SIG1(2))
     &         +3*(SIG1(3)*DSIG2(3)+DSIG1(3)*SIG2(3))
      IF(MIS(1).GT.0)THEN
        MIS(3) = MIS(2)/2/MIS(1)**0.5
      ENDIF
      MIS(4) = ALPHA*(SIG1(1)*DDSIG2(1)+DSIG1(1)*DSIG2(1)
     &               +DSIG1(1)*DSIG2(1)+DDSIG1(1)*SIG2(1)
     &               +SIG1(2)*DDSIG2(2)+DSIG1(2)*DSIG2(2)
     &               +DSIG1(2)*DSIG2(2)+DDSIG1(2)*SIG2(2))
     &        +BETA/2*(SIG1(1)*DDSIG2(2)+DSIG1(1)*DSIG2(2)
     &               +DSIG1(1)*DSIG2(2)+DDSIG1(1)*SIG2(2)
     &               +SIG2(1)*DDSIG1(2)+DSIG2(1)*DSIG1(2)
     &               +DSIG2(1)*DSIG1(2)+DDSIG2(1)*SIG1(2))
     &        +3*(SIG1(3)*DDSIG2(3)+DSIG1(3)*DSIG2(3)
     &           +DSIG1(3)*DSIG2(3)+DDSIG1(3)*SIG2(3))
      IF(MIS(1).GT.0)THEN
        MIS(5) = (MIS(4)-MIS(2)**2/2/MIS(1))/2/MIS(1)**0.5
      ENDIF
C
      RETURN
      END
C
C     ****************************************************************
      SUBROUTINE STRAIN(MIS,S,EPS)
C     ****************************************************************
C
      IMPLICIT    NONE
      REAL*8      MIS(5),S(4),EPS(4)
C
      INTEGER     NHARD,COUNT
      REAL*8      RLAMBDA,S1,ALPHA,BETA,MAXMIS
      REAL*8      POTENTIAL1(7,2000),CONSTANT1(3,4000)
      COMMON/MAINC/S1,RLAMBDA,ALPHA,BETA,NHARD,COUNT,MAXMIS
```

```
      COMMON/MAINA/POTENTIAL1,CONSTANT1
C
C     Determine the angular strain functions
C
      EPS(1) = 3*MIS(1)**(NHARD-1)*S(1)/2
      EPS(2) = 3*MIS(1)**(NHARD-1)*S(2)/2
      EPS(3) = 3*MIS(1)**(NHARD-1)*S(3)/2
      EPS(4) = 0
C
      RETURN
      END
C
C     ****************************************************************
      SUBROUTINE DSTRAIN(MIS,S,DS,DEPS)
C     ****************************************************************
C
      IMPLICIT    NONE
      REAL*8      MIS(5),S(4),DS(4),DEPS(4)
C
      INTEGER     NHARD,COUNT
      REAL*8      RLAMBDA,S1,ALPHA,BETA,MAXMIS
      REAL*8      POTENTIAL1(7,2000),CONSTANT1(3,4000)
      COMMON/MAINC/S1,RLAMBDA,ALPHA,BETA,NHARD,COUNT,MAXMIS
      COMMON/MAINA/POTENTIAL1,CONSTANT1
C
C     Determine the first derivative of the angular strain functions
C
      DEPS(1) = 3*(MIS(1)**(NHARD-1)*DS(1)+(NHARD-1)*MIS(1)**(NHARD-
2)
     &          *MIS(3)*S(1))/2
      DEPS(2) = 3*(MIS(1)**(NHARD-1)*DS(2)+(NHARD-1)*MIS(1)**(NHARD-
2)
     &          *MIS(3)*S(2))/2
      DEPS(3) = 3*(MIS(1)**(NHARD-1)*DS(3)+(NHARD-1)*MIS(1)**(NHARD-
2)
     &          *MIS(3)*S(3))/2
      DEPS(4) = 0
C
      RETURN
      END
C
C     ****************************************************************
      SUBROUTINE DDSTRAIN(MIS,S,DS,DDS,DDEPS)
C     ****************************************************************
C
      IMPLICIT    NONE
      REAL*8      MIS(5),S(4),DS(4),DDS(4),DDEPS(4)
C
      INTEGER     NHARD,COUNT
      REAL*8      RLAMBDA,S1,ALPHA,BETA,MAXMIS
      REAL*8      POTENTIAL1(7,2000),CONSTANT1(3,4000)
      COMMON/MAINC/S1,RLAMBDA,ALPHA,BETA,NHARD,COUNT,MAXMIS
      COMMON/MAINA/POTENTIAL1,CONSTANT1
C
C     Determine the second derivative of the angular
```

```
C     strain functions
C
      DDEPS(1) = 3*(MIS(1)**(NHARD-1)*DDS(1)+
     &           (NHARD1)*MIS(1)**(NHARD-2)
     &           *MIS(3)*DS(1)+(NHARD-1)*(MIS(1)**(NHARD-2)
     &           *(MIS(3)*DS(1)+MIS(5)*S(1))+
     &           (NHARD2)*MIS(1)**(NHARD-3)
     &           *MIS(3)**2*S(1)))/2
      DDEPS(2) = 3*(MIS(1)**(NHARD-1)*DDS(2)+
     &           (NHARD1)*MIS(1)**(NHARD-2)
     &           *MIS(3)*DS(2)+(NHARD-1)*(MIS(1)**(NHARD-2)
     &           *(MIS(3)*DS(2)+MIS(5)*S(2))+
     &           (NHARD2)*MIS(1)**(NHARD-3)
     &           *MIS(3)**2*S(2)))/2
      DDEPS(3) = 3*(MIS(1)**(NHARD-1)*DDS(3)+
     &           (NHARD1)*MIS(1)**(NHARD-2)
     &           *MIS(3)*DS(3)+(NHARD-1)*(MIS(1)**(NHARD-2)
     &           *(MIS(3)*DS(3)+MIS(5)*S(3))+
     &           (NHARD2)*MIS(1)**(NHARD-3)
     &           *MIS(3)**2*S(3)))/2
      DDEPS(4) = 0
C
      RETURN
      END
C
C     ****************************************************************
      SUBROUTINE DISPLACE(EIGEN,MIS,EPS,DEPS,U)
C     ****************************************************************
C
      IMPLICIT    NONE
      REAL*8      EIGEN
      REAL*8      U(2),EPS(4),MIS(5),DEPS(4)
C
      INTEGER     NHARD,COUNT
      REAL*8      RLAMBDA,S1,ALPHA,BETA,MAXMIS
      REAL*8      POTENTIAL1(7,2000),CONSTANT1(3,4000)
      COMMON/MAINC/S1,RLAMBDA,ALPHA,BETA,NHARD,COUNT,MAXMIS
      COMMON/MAINA/POTENTIAL1,CONSTANT1
C
C     Determine the angular displacement functions
C
      U(1) = EPS(1)/(NHARD*EIGEN+1)
      U(2) = (2*EPS(3)-DEPS(1)/(NHARD*EIGEN+1))/(NHARD*EIGEN)
C
      RETURN
      END
C
C     ****************************************************************
      SUBROUTINE DDISPLACE(EIGEN,MIS,EPS,DEPS,DDEPS,DU)
C     ****************************************************************
C
      IMPLICIT    NONE
      REAL*8      EIGEN
      REAL*8      DU(2),EPS(4),MIS(5),DEPS(4),DDEPS(4)
C
```

```
      INTEGER      NHARD,COUNT
      REAL*8       RLAMBDA,S1,ALPHA,BETA,MAXMIS
      REAL*8       POTENTIAL1(7,2000),CONSTANT1(3,4000)
      COMMON/MAINC/S1,RLAMBDA,ALPHA,BETA,NHARD,COUNT,MAXMIS
      COMMON/MAINA/POTENTIAL1,CONSTANT1
C
C     Determine the derivative of the angular displacement functions
C
      DU(1) = DEPS(1)/(NHARD*EIGEN+1)
      DU(2) = (2*DEPS(3)-DDEPS(1)/(NHARD*EIGEN+1))/(NHARD*EIGEN)
C
      RETURN
      END
C
C     ****************************************************************
      SUBROUTINE INTEGRAND(X,EIGEN,MIS,SIG1,U1,DU1,KOUNT)
C     ****************************************************************
C
      IMPLICIT     NONE
      INTEGER      KOUNT
      REAL*8       X,EIGEN
      REAL*8       MIS(5),SIG1(4),U1(2),DU1(2)
C
      INTEGER      NHARD,COUNT
      REAL*8       RLAMBDA,S1,ALPHA,BETA,MAXMIS
      REAL*8       POTENTIAL1(7,2000),CONSTANT1(3,4000)
      COMMON/MAINC/S1,RLAMBDA,ALPHA,BETA,NHARD,COUNT,MAXMIS
      COMMON/MAINA/POTENTIAL1,CONSTANT1
C
C     Integrand for the J-integral
C
      CONSTANT1(1,KOUNT)=X
      CONSTANT1(2,KOUNT)=NHARD*MIS(1)**(NHARD+1)*DCOS(X)/(NHARD+1)
     &       -DSIN(X)*(SIG1(1)*(U1(2)-DU1(1))-SIG1(3)*(U1(1)+DU1(2)))
     &       -DCOS(X)*(NHARD*EIGEN+1)*(SIG1(1)*U1(1)+SIG1(3)*U1(2))
      CONSTANT1(1,KOUNT+1)=-X
      CONSTANT1(2,KOUNT+1)=NHARD*MIS(1)**(NHARD+1)*DCOS(-X)/(NHARD+1)
     &       -DSIN(-X)*(SIG1(1)*(U1(2)+DU1(1))
     &       +SIG1(3)*(U1(1)+DU1(2)))
     &       -DCOS(-X)*(NHARD*EIGEN+1)*(SIG1(1)*U1(1)+SIG1(3)*U1(2))
C
   10 FORMAT(1X,5(1X,E14.7))
C
      RETURN
      END
C
C     ****************************************************************
      SUBROUTINE SAVE(X,YINC)
C     ****************************************************************
C
      IMPLICIT     NONE
      INTEGER      I
      REAL*8       X
      REAL*8       YINC(5),Y(5),DYDX(5),MIS11(5)
      REAL*8       SIG1(4),DSIG1(4),DDSIG1(4)
```

```
C
      INTEGER      NHARD,COUNT
      REAL*8       RLAMBDA,S1,ALPHA,BETA,MAXMIS
      REAL*8       POTENTIAL1(7,2000),CONSTANT1(3,4000)
      COMMON/MAINC/S1,RLAMBDA,ALPHA,BETA,NHARD,COUNT,MAXMIS
      COMMON/MAINA/POTENTIAL1,CONSTANT1
C
      COUNT=COUNT+1
      DO I=1,5,1
         Y(I)=YINC(I)
      ENDDO
      POTENTIAL1(1,COUNT)=X
      POTENTIAL1(7,COUNT)=YINC(5)
      CALL FCN (5,X,Y,DYDX)
      POTENTIAL1(6,COUNT)=DYDX(4)
      DO I=1,4,1
         POTENTIAL1(I+1,COUNT)=Y(I)
      ENDDO
      Y(5)=DYDX(4)
      CALL STRESS (YINC(5),Y,SIG1)
      CALL DSTRESS (YINC(5),Y,DSIG1)
      CALL DDSTRESS (YINC(5),Y,DDSIG1)
      CALL SIGMIS(SIG1,SIG1,DSIG1,DSIG1,DDSIG1,DDSIG1,MIS11)
      MIS11(1)=MIS11(1)**0.5
      IF(MAXMIS.LT.MIS11(1))THEN
         MAXMIS=MIS11(1)
      ENDIF
C
   10 FORMAT (1X,6E12.4)
C
      RETURN
      END
C
C     ****************************************************************
      SUBROUTINE OUTPUT
C     ****************************************************************
C
      IMPLICIT     NONE
      INTEGER      I,J,KOUNT
      REAL*8       X,MEAN1
      REAL*8       YINC(5),Y(5),MIS11(5)
      REAL*8       SIG1(4),DSIG1(4),DDSIG1(4),SS1(4),DSS1(4),DDSS1(4)
      REAL*8       EPS1(4),DEPS1(4),DDEPS1(4),U1(2),DU1(2)
C
      INTEGER      NHARD,COUNT,IU1,IU2,IU3,IU4,IU5,IU6,IU7
      REAL*8       RLAMBDA,S1,ALPHA,BETA,MAXMIS
      REAL*8       POTENTIAL1(7,2000),CONSTANT1(3,4000)
      COMMON/MAINC/S1,RLAMBDA,ALPHA,BETA,NHARD,COUNT,MAXMIS
      COMMON/MAINA/POTENTIAL1,CONSTANT1
      COMMON/OUT/IU1,IU2,IU3,IU4,IU5,IU6,IU7
C
      KOUNT=1
      DO I=1,COUNT,1
         X=POTENTIAL1(1,I)
         DO J=1,5,1
```

```
            Y(J)=POTENTIAL1(J+1,I)
          ENDDO
          CALL STRESS (POTENTIAL1(7,I),Y,SIG1)
          CALL DSTRESS (POTENTIAL1(7,I),Y,DSIG1)
          CALL DDSTRESS (POTENTIAL1(7,I),Y,DDSIG1)
          CALL SIGMIS(SIG1,SIG1,DSIG1,DSIG1,DDSIG1,DDSIG1,MIS11)
          MIS11(1)=MIS11(1)**0.5
          CALL DEV(SIG1,SS1,MEAN1)
          CALL DDEV(DSIG1,DSS1)
          CALL DDDEV(DDSIG1,DDSS1)
          CALL STRAIN(MIS11,SS1,EPS1)
          CALL DSTRAIN(MIS11,SS1,DSS1,DEPS1)
          CALL DDSTRAIN(MIS11,SS1,DSS1,DDSS1,DDEPS1)
          CALL DISPLACE(POTENTIAL1(7,I),MIS11,EPS1,DEPS1,U1)
          CALL DDISPLACE(POTENTIAL1(7,I),MIS11,EPS1,DEPS1,DDEPS1,DU1)
          CALL INTEGRAND(X,POTENTIAL1(7,I),MIS11,SIG1,U1,DU1,KOUNT)
          KOUNT=KOUNT+2
C
          WRITE(IU2,15) X,(Y(J),J=1,5,1),POTENTIAL1(7,I)
          WRITE(IU3,10) X,(SIG1(J),J=1,4,1),MIS11(1)
          WRITE(IU4,10) X,(SS1(J),J=1,4,1),MEAN1
          WRITE(IU5,10) X,(EPS1(J),J=1,4,1)
          WRITE(IU6,10) X,U1(1),U1(2),DU1(1),DU1(2)
C
        ENDDO
C
        WRITE(11,*) 'For faster convergence use the following guesses:'
        WRITE(11,*) 'GUESS(1) = ',POTENTIAL1(4,1)/POTENTIAL1(2,1)
        WRITE(11,*) 'GUESS(2) = ',POTENTIAL1(7,1)
        WRITE(11,*) 'GUESS(3) = ',POTENTIAL1(4,COUNT)/POTENTIAL1(2,1)
        WRITE(11,*) 'GUESS(4) = ',POTENTIAL1(5,COUNT)/POTENTIAL1(2,1)
        WRITE(11,*) 'GUESS(5) = ',POTENTIAL1(7,COUNT)
C
   10 FORMAT (1X,6E18.10)
   15 FORMAT (1X,7E18.10)
C
        RETURN
        END
C
C       ****************************************************************
        SUBROUTINE SORT(NREC,ARRAY,NDIM1,NDIM2)
C       ****************************************************************
C
        IMPLICIT REAL*8 (A-H,O-Z)
        DIMENSION   TEMP(6)
        DIMENSION   ARRAY(NDIM1,NDIM2)
C
C       Sort data
C
        DO I=2,NREC,1
           DO J=2,NREC,1
              IF(ARRAY(1,J).LT.ARRAY(1,J-1))THEN
                DO K=1,NDIM1,1
                   TEMP(K)=ARRAY(K,J-1)
                ENDDO
```

```
                DO K=1,NDIM1,1
                   ARRAY(K,J-1)=ARRAY(K,J)
                ENDDO
                DO K=1,NDIM1,1
                   ARRAY(K,J)=TEMP(K)
                ENDDO
             ENDIF
          ENDDO
       ENDDO
C
       RETURN
       END
C
C      ****************************************************************
       SUBROUTINE INTEGCONST(COUNT,CONSTANT1)
C      ****************************************************************
C
       IMPLICIT     NONE
       INTEGER      I,COUNT
       REAL*8       CONSTANT1(3,4000)
C
       INTEGER     IU1,IU2,IU3,IU4,IU5,IU6,IU7
       COMMON/OUT/IU1,IU2,IU3,IU4,IU5,IU6,IU7

C
C      Integrate data
C
       DO I=1,COUNT,1
          CONSTANT1(3,I)=0
       ENDDO
       DO I=2,COUNT,1
          CONSTANT1(3,I)=(CONSTANT1(2,I-1)+CONSTANT1(2,I))/2
     &                    *(CONSTANT1(1,I)-CONSTANT1(1,I-1))
     &                    +CONSTANT1(3,I-1)
       ENDDO
C
       WRITE(IU7,10) CONSTANT1(1,1),CONSTANT1(2,1),
     &               CONSTANT1(3,1),CONSTANT1(3,COUNT)
       DO I=2,COUNT,1
          WRITE(IU7,10) CONSTANT1(1,I),CONSTANT1(2,I),CONSTANT1(3,I)
       ENDDO
C
   10  FORMAT(1X,4E15.7)
C
       RETURN
       END
C
C      ****************************************************************
       SUBROUTINE OPENUNIT(ITERATION,IU1,IU2,IU3,IU4,IU5,IU6,IU7)
C      ****************************************************************
C
       IMPLICIT NONE
       INTEGER  ITERATION,IU1,IU2,IU3,IU4,IU5,IU6,IU7
C
       IU1 = 11+(ITERATION-1)*7      ! Program output file
```

```
      IU2 = 12+(ITERATION-1)*7      ! Potential and derivatives
      IU3 = 13+(ITERATION-1)*7      ! Stresses
      IU4 = 14+(ITERATION-1)*7      ! Deviatoric and mean stresses
      IU5 = 15+(ITERATION-1)*7      ! Strains
      IU6 = 16+(ITERATION-1)*7      ! displacements and derivatives
      IU7 = 17+(ITERATION-1)*7      ! integrand and constant
C
      OPEN (UNIT=IU1,STATUS='NEW')
      OPEN (UNIT=IU2,STATUS='NEW')
      OPEN (UNIT=IU3,STATUS='NEW')
      OPEN (UNIT=IU4,STATUS='NEW')
      OPEN (UNIT=IU5,STATUS='NEW')
      OPEN (UNIT=IU6,STATUS='NEW')
      OPEN (UNIT=IU7,STATUS='NEW')
C
      WRITE(IU1,1)
      WRITE(IU2,2)
      WRITE(IU3,3)
      WRITE(IU4,4)
      WRITE(IU5,5)
      WRITE(IU6,6)
      WRITE(IU7,7)
C
    1 FORMAT(1X'Program output')
    2 FORMAT(5X,'Theta',7X,'f0',9X,'f1',9X,'f2',
     &       9X,'f3',9X,'f4',3X,'eigenvalue')
    3 FORMAT(5X,'Theta',8X,'sigrr',7X,'sigtt',7X,'sigrt',
     &       7X,'sigzz',6X,'sigmis')
    4 FORMAT(5X,'Theta',6X,'devsigrr',4X,'devsigtt',
     &       4X,'devsigrt',4X,'devsigzz',5X,'meansig')
    5 FORMAT(5X,'Theta',7X,'epsrr',7X,'epstt',
     &       7X,'epsrt',7X,'epszz')
    6 FORMAT(5X,'Theta',8X,'Ur',10X,'Ut',10X,'dUr',9X,'dUt')
    7 FORMAT(7X,'Theta',8X,'integrand',6X,'integral',
     &       7X,'constant')
C
      RETURN
      END
C     ****************************************************************
      SUBROUTINE NORMALIZE(COUNT,MAXMIS,POTENTIAL1)
C     ****************************************************************
C
      IMPLICIT NONE
      INTEGER  I,J,COUNT
      REAL*8   MAXMIS
      REAL*8   POTENTIAL1(7,2000)
C
      DO I=1,COUNT,1
         DO J=2,6,1
            POTENTIAL1(J,I)=POTENTIAL1(J,I)/MAXMIS
         ENDDO
      ENDDO
C
      RETURN
      END
```

```
C
C     ****************************************************************
      SUBROUTINE CLOSEUNIT(IU1,IU2,IU3,IU4,IU5,IU6,IU7)
C     ****************************************************************
C
      IMPLICIT NONE
      INTEGER  IU1,IU2,IU3,IU4,IU5,IU6,IU7
C
      CLOSE(UNIT=IU1)
      CLOSE(UNIT=IU2)
      CLOSE(UNIT=IU3)
      CLOSE(UNIT=IU4)
      CLOSE(UNIT=IU5)
      CLOSE(UNIT=IU6)
      CLOSE(UNIT=IU7)
C
      RETURN
      END
C
```

APPENDIX D

SHAPE FUNCTIONS USED FOR FINITE ELEMENT SOLUTIONS

Shape functions for eight node quadratic element;

$$\hat{\psi}_1(\xi_1,\xi_2)=\frac{1}{4}(1-\xi_1)(1-\xi_2)(-1-\xi_1-\xi_2)$$

$$\hat{\psi}_2(\xi_1,\xi_2)=\frac{1}{4}(1+\xi_1)(1-\xi_2)(-1+\xi_1-\xi_2)$$

$$\hat{\psi}_3(\xi_1,\xi_2)=\frac{1}{4}(1+\xi_1)(1+\xi_2)(-1+\xi_1+\xi_2)$$

$$\hat{\psi}_4(\xi_1,\xi_2)=\frac{1}{4}(1-\xi_1)(1+\xi_2)(-1-\xi_1+\xi_2)$$

$$\hat{\psi}_5(\xi_1,\xi_2)=\frac{1}{2}(1-\xi_1^2)(1-\xi_2)$$

$$\hat{\psi}_6(\xi_1,\xi_2)=\frac{1}{2}(1+\xi_1)(1-\xi_2^2)$$

$$\hat{\psi}_7(\xi_1,\xi_2)=\frac{1}{2}(1-\xi_1^2)(1+\xi_2)$$

$$\hat{\psi}_6(\xi_1,\xi_2)=\frac{1}{2}(1-\xi_1)(1-\xi_2^2)$$

Coordinates of 3×3 Gauss quadrature integration points and corresponding quadrature weights:

$$(\xi_1^1,\xi_2^1)=\left(-\sqrt{\frac{3}{5}},-\sqrt{\frac{3}{5}}\right),\quad \overline{w}_1=\frac{25}{81}$$

$$(\xi_1^2,\xi_2^2)=\left(0,-\sqrt{\frac{3}{5}}\right),\quad \overline{w}_2=\frac{40}{81}$$

$$(\xi_1^3,\xi_2^3)=\left(+\sqrt{\frac{3}{5}},-\sqrt{\frac{3}{5}}\right),\quad \overline{w}_3=\frac{25}{81}$$

$$(\xi_1^4,\xi_2^4)=\left(-\sqrt{\frac{3}{5}},0\right),\quad \overline{w}_4=\frac{40}{81}$$

$$(\xi_1^5,\xi_2^5)=(0,0),\quad \overline{w}_5=\frac{64}{81}$$

$$(\xi_1^6,\xi_2^6)=\left(+\sqrt{\frac{3}{5}},0\right),\quad \overline{w}_6=\frac{40}{81}$$

$$(\xi_1^7,\xi_2^7)=\left(-\sqrt{\frac{3}{5}},+\sqrt{\frac{3}{5}}\right),\quad \overline{w}_7=\frac{25}{81}$$

$$(\xi_1^8,\xi_2^8)=\left(0,+\sqrt{\frac{3}{5}}\right),\quad \overline{w}_8=\frac{40}{81}$$

$$(\xi_1^9,\xi_2^9)=\left(+\sqrt{\frac{3}{5}},+\sqrt{\frac{3}{5}}\right),\quad \overline{w}_9=\frac{25}{81}$$

APPENDIX E

ABAQUS FINITE ELEMENT INPUT FILE

```
*HEADING
CCT_AW_01_300000
** NEUTRAL FILE GENERATED ON:06-Jan-94 14:51:44 PATABA VERSION: 3.1A
**
**  NODE DEFINITIONS
**
*NODE
       1,  0.000000000E-00,  0.000000000E-00,  0.000000000E+00
       2, -0.122028234E-11,  0.591932803E-05,  0.000000000E+00
       3,  0.000000000E-00,  0.000000000E-00,  0.000000000E+00

                                     *
                                     *
                                     *

    3688,  0.135783806E+00, -0.135783881E+00,  0.000000000E+00
    3689,  0.132622838E+00, -0.161601558E+00,  0.000000000E+00
    3690,  0.106684595E+00, -0.159664989E+00,  0.000000000E+00
**
**  NODE SETS FROM NAMED COMPONENTS
**
*NSET, NSET=CRACK
   1   3   5   6   8   9  11  12  14  15  17  18  20  21  23  24
  26  27  29  30  32  33  35  36  38  39  41  42  44  45  48  49
  50
**
**  ELEMENT DEFINITIONS
**
*ELEMENT, TYPE=CPE8     , ELSET=PID1
    1, 2565, 2497, 2500, 2568, 2496, 2499, 2498, 2566
    2, 2622, 2565, 2568, 2625, 2567, 2566, 2569, 2623
    3, 2667, 2622, 2625, 2670, 2624, 2623, 2626, 2668

                          *
                          *
                          *

 1132, 3638, 3644, 3605, 3599, 3640, 3607, 3601, 3600
 1133, 3645, 3641, 3602, 3606, 3642, 3604, 3603, 3609
 1134, 3644, 3645, 3606, 3605, 3647, 3609, 3608, 3607
*ELEMENT, TYPE=CPE8     , ELSET=PID2
  865, 2772, 2770, 2736, 2738, 2769, 2735, 2734, 2737
  866, 2775, 2772, 2738, 2741, 2773, 2737, 2739, 2740
  867, 2778, 2775, 2741, 2744, 2776, 2740, 2742, 2743
  868, 2781, 2778, 2744, 2747, 2779, 2743, 2745, 2746
  869, 2784, 2781, 2747, 2750, 2782, 2746, 2748, 2749
  870, 2787, 2784, 2750, 2753, 2785, 2749, 2751, 2752
  871, 2790, 2787, 2753, 2756, 2788, 2752, 2754, 2755
  872, 2796, 2790, 2756, 2762, 2791, 2755, 2757, 2761
  873, 2794, 2799, 2766, 2760, 2793, 2764, 2759, 2758
  874, 2800, 2796, 2762, 2767, 2797, 2761, 2763, 2765
  875, 2799, 2800, 2767, 2766, 2802, 2765, 2768, 2764
**
**  ELEMENT PROPERTIES
**
```

```
**
*SOLID SECTION,ELSET=PID1,MATERIAL=PLASTIC,ORIENTATION=CYLINDER
 1.0
*SOLID SECTION,ELSET=PID2,MATERIAL=ELASTIC,ORIENTATION=CYLINDER
 1.0
**
**  DEFINE A CYLINDRICAL COORDINATE SYSTEM TO GET OUTPUT
**
*ORIENTATION,NAME=CYLINDER,DEFINITION=COORDINATES,SYSTEM=CYLINDRICAL
0.0,0.0,0.0,0.0,0.0,1.0
**
**  MATERIAL DEFINITIONS
**
*MATERIAL,NAME=ELASTIC
*ELASTIC
30000000,0.3
**
**
*MATERIAL,NAME=PLASTIC
*USER MATERIAL,CONSTANTS=4
60000,0.002,10,0.3
**
**
**
**  LOAD CASE     1
**
*STEP,AMPLITUDE=RAMP,INC=500
LOAD CASE     1
*STATIC
0.1, 1.0, 0.0000001, 1
**
*DLOAD, OP=NEW
     865, P3,  -3750.0
     866, P3,  -3750.0
     867, P3,  -3750.0
     868, P3,  -3750.0
     869, P3,  -3750.0
     870, P3,  -3750.0
     871, P3,  -3750.0
     872, P3,  -3750.0
     873, P3,  -3750.0
     874, P3,  -3750.0
     875, P3,  -3750.0
**
** Zero displacements on planes of symmetry
**
*BOUNDARY, OP=NEW
      10,  1,,   0.0
      12,  1,,   0.0
      61,  1,,   0.0

           *
           *
           *
```

```
    3615,  1,,   0.0
    3617,  1,,   0.0
    3618,  1,,   0.0
**
**  Fracture Mechanics
**
*J-INTEGRAL,CONTOURS=50,FREQUENCY=1,OUTPUT=BOTH,SYMM
1.0,0.0
CRACK
**
**  Output
**
*PRINT,CONTACT=NO,FREQUENCY=1,RESIDUAL=YES,SOLVE=YES
**
*NODE FILE,FREQUENCY=500,GLOBAL=YES
U
*NODE PRINT,FREQUENCY=500,GLOBAL=YES
U
RF
*EL FILE, FREQUENCY=500,POSITION=INTEGRATION POINTS
S
SINV
E
*EL PRINT,FREQ=500,POS=INTEGRATION POINTS,SUMMARY=NO,TOTALS=NO
S
SINV
E
*FILE FORMAT, ASCII
*END STEP
**
**
*STEP,AMPLITUDE=RAMP,INC=500
LOAD CASE     2
*STATIC
0.1, 1.0, 0.0000001, 1
**
*DLOAD, OP=NEW
     865, P3,  -7500.0
     866, P3,  -7500.0
     867, P3,  -7500.0
     868, P3,  -7500.0
     869, P3,  -7500.0
     870, P3,  -7500.0
     871, P3,  -7500.0
     872, P3,  -7500.0
     873, P3,  -7500.0
     874, P3,  -7500.0
     875, P3,  -7500.0
**
**  Fracture Mechanics
**
*J-INTEGRAL,CONTOURS=50,FREQUENCY=1,OUTPUT=BOTH,SYMM
1.0,0.0
CRACK
**
```

```
**  Output
**
*PRINT,CONTACT=NO,FREQUENCY=1,RESIDUAL=YES,SOLVE=YES
**
*NODE FILE,FREQUENCY=500,GLOBAL=YES
U
*NODE PRINT,FREQUENCY=500,GLOBAL=YES
U
RF
*EL FILE, FREQUENCY=500,POSITION=INTEGRATION POINTS
S
SINV
E
*EL PRINT,FREQ=500,POS=INTEGRATION POINTS,SUMMARY=NO,TOTALS=NO
S
SINV
E
*FILE FORMAT, ASCII
*END STEP
**
**
                    *
                    *
                    *
                    *
                    *
                    *

*STEP,AMPLITUDE=RAMP,INC=500
LOAD CASE     20
*STATIC
0.1, 1.0, 0.0000001, 1
**
*DLOAD, OP=NEW
     865, P3,  -75000.0
     866, P3,  -75000.0
     867, P3,  -75000.0
     868, P3,  -75000.0
     869, P3,  -75000.0
     870, P3,  -75000.0
     871, P3,  -75000.0
     872, P3,  -75000.0
     873, P3,  -75000.0
     874, P3,  -75000.0
     875, P3,  -75000.0
**
**  Fracture Mechanics
**
*J-INTEGRAL,CONTOURS=50,FREQUENCY=1,OUTPUT=BOTH,SYMM
1.0,0.0
CRACK
**
**  Output
**
```

```
*PRINT,CONTACT=NO,FREQUENCY=1,RESIDUAL=YES,SOLVE=YES
**
*NODE FILE,FREQUENCY=500,GLOBAL=YES
U
*NODE PRINT,FREQUENCY=500,GLOBAL=YES
U
RF
*EL FILE, FREQUENCY=500,POSITION=INTEGRATION POINTS
S
SINV
E
*EL PRINT,FREQ=500,POS=INTEGRATION POINTS,SUMMARY=NO,TOTALS=NO
S
SINV
E
*FILE FORMAT, ASCII
*END STEP
**
```

APPENDIX F

INTEGRATION CONSTANTS FOR ANALYTICAL *J*-INTERGAL

Tildes indicate the function is only dependent on the angular coordinate and the upper indices are the field numbers. The constants that follow are for the case of n=10 for which fields 1, 2, and 4 are derived from homogeneous fourth order equations and fields 3, 5, and 6 are derived from nonhomogeneous fourth order equations.

$$I_1 = \int_{-\pi}^{\pi}\left[\frac{n}{n+1}\tilde{\sigma}_{e_1}^{n+1}\cos\theta - \sin\theta\left\{\tilde{\sigma}_{rr}^{1}\left\langle\tilde{u}_{\theta}^{1} - \frac{\partial\tilde{u}_{r}^{1}}{\partial\theta}\right\rangle - \tilde{\sigma}_{r\theta}^{1}\left\langle\tilde{u}_{r}^{1} + \frac{\partial\tilde{u}_{\theta}^{1}}{\partial\theta}\right\rangle\right\} - \cos\theta\left(ns_1+1\right)\left\{\tilde{\sigma}_{rr}^{1}\tilde{u}_{r}^{1} + \tilde{\sigma}_{r\theta}^{1}\tilde{u}_{\theta}^{1}\right\}\right]d\theta$$

$$I_2 = \int_{-\pi}^{\pi}\left[n\tilde{\sigma}_{e_1}^{n-1}\tilde{\sigma}_{e_{12}}\cos\theta - \sin\theta\left\{\tilde{\sigma}_{rr}^{1}\left\langle\tilde{u}_{\theta}^{2} - \frac{\partial\tilde{u}_{r}^{2}}{\partial\theta}\right\rangle + \tilde{\sigma}_{rr}^{2}\left\langle\tilde{u}_{\theta}^{1} - \frac{\partial\tilde{u}_{r}^{1}}{\partial\theta}\right\rangle - \tilde{\sigma}_{r\theta}^{1}\left\langle\tilde{u}_{r}^{2} + \frac{\partial\tilde{u}_{\theta}^{2}}{\partial\theta}\right\rangle - \tilde{\sigma}_{r\theta}^{2}\left\langle\tilde{u}_{r}^{1} + \frac{\partial\tilde{u}_{\theta}^{1}}{\partial\theta}\right\rangle\right\}\right.$$
$$\left. - \cos\theta\left\{\left(ns_1+1\right)\left\langle\tilde{\sigma}_{rr}^{2}\tilde{u}_{r}^{1} + \tilde{\sigma}_{r\theta}^{2}\tilde{u}_{\theta}^{1}\right\rangle + \left(ns_1+\Delta s_2+1\right)\left\langle\tilde{\sigma}_{rr}^{1}\tilde{u}_{r}^{2} + \tilde{\sigma}_{r\theta}^{1}\tilde{u}_{\theta}^{2}\right\rangle\right\}\right]d\theta$$

$$I_3 = \int_{-\pi}^{\pi}\left[n\tilde{\sigma}_{e_1}^{n-3}\left\{\tilde{\sigma}_{e_1}^{2}\tilde{\sigma}_{e_{13}} + \frac{1}{2}\tilde{\sigma}_{e_1}^{2}\tilde{\sigma}_{e_{22}} + \frac{(n-1)}{2}\tilde{\sigma}_{e_{12}}^{2}\right\}\cos\theta\right.$$
$$- \sin\theta\left\{\tilde{\sigma}_{rr}^{1}\left\langle\tilde{u}_{\theta}^{22} + \tilde{u}_{\theta}^{3} - \frac{\partial\tilde{u}_{r}^{22}}{\partial\theta} - \frac{\partial\tilde{u}_{r}^{3}}{\partial\theta}\right\rangle + \tilde{\sigma}_{rr}^{2}\left\langle\tilde{u}_{\theta}^{2} - \frac{\partial\tilde{u}_{r}^{2}}{\partial\theta}\right\rangle + \tilde{\sigma}_{rr}^{3}\left\langle\tilde{u}_{\theta}^{1} - \frac{\partial\tilde{u}_{r}^{1}}{\partial\theta}\right\rangle\right.$$
$$\left. - \tilde{\sigma}_{r\theta}^{1}\left\langle\tilde{u}_{r}^{22} + \tilde{u}_{r}^{3} + \frac{\partial\tilde{u}_{\theta}^{22}}{\partial\theta} + \frac{\partial\tilde{u}_{\theta}^{3}}{\partial\theta}\right\rangle - \tilde{\sigma}_{r\theta}^{2}\left\langle\tilde{u}_{r}^{2} + \frac{\partial\tilde{u}_{\theta}^{2}}{\partial\theta}\right\rangle - \tilde{\sigma}_{r\theta}^{3}\left\langle\tilde{u}_{r}^{1} + \frac{\partial\tilde{u}_{\theta}^{1}}{\partial\theta}\right\rangle\right\}$$
$$- \cos\theta\left\{\left(ns_1+2\Delta s_2+1\right)\tilde{\sigma}_{rr}^{1}\left\langle\tilde{u}_{r}^{22} + \tilde{u}_{r}^{3}\right\rangle + \left(ns_1+\Delta s_2+1\right)\tilde{\sigma}_{rr}^{2}\tilde{u}_{r}^{2} + \left(ns_1+1\right)\tilde{\sigma}_{rr}^{3}\tilde{u}_{r}^{1}\right.$$
$$\left. + \left(ns_1+2\Delta s_2+1\right)\tilde{\sigma}_{r\theta}^{1}\left\langle\tilde{u}_{\theta}^{22} + \tilde{u}_{\theta}^{3}\right\rangle + \left(ns_1+\Delta s_2+1\right)\tilde{\sigma}_{r\theta}^{2}\tilde{u}_{\theta}^{2} + \left(ns_1+1\right)\tilde{\sigma}_{r\theta}^{3}\tilde{u}_{\theta}^{1}\right\}\left.\right]d\theta$$

$$I_4 = \int_{-\pi}^{\pi}\Bigg[n\tilde{\sigma}_{e_1}^{n-1}\tilde{\sigma}_{e_{14}}\cos\theta - \sin\theta\Bigg\{\tilde{\sigma}_{rr}^{1}\left\langle \tilde{u}_{\theta}^{4} - \frac{\partial\tilde{u}_{r}^{4}}{\partial\theta}\right\rangle + \tilde{\sigma}_{rr}^{4}\left\langle \tilde{u}_{\theta}^{1} - \frac{\partial\tilde{u}_{r}^{1}}{\partial\theta}\right\rangle - \tilde{\sigma}_{r\theta}^{1}\left\langle \tilde{u}_{r}^{4} + \frac{\partial\tilde{u}_{\theta}^{4}}{\partial\theta}\right\rangle - \tilde{\sigma}_{r\theta}^{4}\left\langle \tilde{u}_{r}^{1} + \frac{\partial\tilde{u}_{\theta}^{1}}{\partial\theta}\right\rangle\Bigg\}$$
$$- \cos\theta\Big\{\left(ns_1+1\right)\left\langle\tilde{\sigma}_{rr}^{4}\tilde{u}_{r}^{1} + \tilde{\sigma}_{r\theta}^{4}\tilde{u}_{\theta}^{1}\right\rangle + \left(ns_1+\Delta s_4+1\right)\left\langle\tilde{\sigma}_{rr}^{1}\tilde{u}_{r}^{4} + \tilde{\sigma}_{r\theta}^{1}\tilde{u}_{\theta}^{4}\right\rangle\Big\}\Bigg]d\theta$$

$$I_5 = \int_{-\pi}^{\pi}\Bigg[n\tilde{\sigma}_{e_1}^{n-5}\Bigg\{\tilde{\sigma}_{e_1}^{4}\left\langle\tilde{\sigma}_{e_{15}} + \tilde{\sigma}_{e_{23}}\right\rangle + (n-1)\tilde{\sigma}_{e_1}^{2}\tilde{\sigma}_{e_{12}}\left\langle\tilde{\sigma}_{e_{13}} + \frac{1}{2}\tilde{\sigma}_{e_{22}}\right\rangle + \frac{(n-1)(n-3)}{6}\tilde{\sigma}_{e_{12}}^{3}\Bigg\}\cos\theta$$
$$- \sin\theta\Bigg\{\tilde{\sigma}_{rr}^{1}\left\langle \tilde{u}_{\theta}^{5} + \tilde{u}_{\theta}^{23} + \tilde{u}_{\theta}^{222} - \frac{\partial\tilde{u}_{r}^{5}}{\partial\theta} - \frac{\partial\tilde{u}_{r}^{23}}{\partial\theta} - \frac{\partial\tilde{u}_{r}^{222}}{\partial\theta}\right\rangle + \tilde{\sigma}_{rr}^{2}\left\langle \tilde{u}_{\theta}^{3} + \tilde{u}_{\theta}^{22} - \frac{\partial\tilde{u}_{r}^{3}}{\partial\theta} - \frac{\partial\tilde{u}_{r}^{22}}{\partial\theta}\right\rangle + \tilde{\sigma}_{rr}^{3}\left\langle \tilde{u}_{\theta}^{2} - \frac{\partial\tilde{u}_{r}^{2}}{\partial\theta}\right\rangle + \tilde{\sigma}_{rr}^{5}\left\langle \tilde{u}_{\theta}^{1} - \frac{\partial\tilde{u}_{r}^{1}}{\partial\theta}\right\rangle$$
$$- \tilde{\sigma}_{r\theta}^{1}\left\langle \tilde{u}_{r}^{5} + \tilde{u}_{r}^{23} + \tilde{u}_{r}^{222} + \frac{\partial\tilde{u}_{\theta}^{5}}{\partial\theta} + \frac{\partial\tilde{u}_{\theta}^{23}}{\partial\theta} + \frac{\partial\tilde{u}_{\theta}^{222}}{\partial\theta}\right\rangle - \tilde{\sigma}_{r\theta}^{2}\left\langle \tilde{u}_{r}^{3} + \tilde{u}_{r}^{22} + \frac{\partial\tilde{u}_{\theta}^{3}}{\partial\theta} + \frac{\partial\tilde{u}_{\theta}^{22}}{\partial\theta}\right\rangle - \tilde{\sigma}_{r\theta}^{3}\left\langle \tilde{u}_{r}^{2} + \frac{\partial\tilde{u}_{\theta}^{2}}{\partial\theta}\right\rangle - \tilde{\sigma}_{r\theta}^{5}\left\langle \tilde{u}_{r}^{1} + \frac{\partial\tilde{u}_{\theta}^{1}}{\partial\theta}\right\rangle\Bigg\}$$
$$- \cos\theta\Big\{\left(ns_1+\Delta s_5+1\right)\tilde{\sigma}_{rr}^{1}\left\langle\tilde{u}_{r}^{5} + \tilde{u}_{r}^{23} + \tilde{u}_{r}^{222}\right\rangle + \left(ns_1+\Delta s_3+1\right)\tilde{\sigma}_{rr}^{2}\left\langle\tilde{u}_{r}^{3} + \tilde{u}_{r}^{22}\right\rangle + \left(ns_1+\Delta s_2+1\right)\tilde{\sigma}_{rr}^{3}\tilde{u}_{r}^{2} + \left(ns_1+1\right)\tilde{\sigma}_{rr}^{5}\tilde{u}_{r}^{1}$$
$$+ \left(ns_1+\Delta s_5+1\right)\tilde{\sigma}_{r\theta}^{1}\left\langle\tilde{u}_{\theta}^{5} + \tilde{u}_{\theta}^{23} + \tilde{u}_{\theta}^{222}\right\rangle + \left(ns_1+\Delta s_3+1\right)\tilde{\sigma}_{r\theta}^{2}\left\langle\tilde{u}_{\theta}^{3} + \tilde{u}_{\theta}^{22}\right\rangle + \left(ns_1+\Delta s_2+1\right)\tilde{\sigma}_{r\theta}^{3}\tilde{u}_{\theta}^{2} + \left(ns_1+1\right)\tilde{\sigma}_{r\theta}^{5}\tilde{u}_{\theta}^{1}\Big\}\Bigg]d\theta$$

$$I_6 = \int_{-\pi}^{\pi}\Bigg[n\tilde{\sigma}_{e_1}^{n-3}\left\{\tilde{\sigma}_{e_1}^2\left\langle\tilde{\sigma}_{e_{16}}+\tilde{\sigma}_{e_{24}}\right\rangle+(n-1)\tilde{\sigma}_{e_{12}}\tilde{\sigma}_{e_{14}}\right\}\cos\theta$$

$$-\sin\theta\left\{\tilde{\sigma}_{rr}^1\left\langle\tilde{u}_\theta^6+\tilde{u}_\theta^{24}-\frac{\partial\tilde{u}_r^6}{\partial\theta}-\frac{\partial\tilde{u}_r^{24}}{\partial\theta}\right\rangle+\tilde{\sigma}_{rr}^2\left\langle\tilde{u}_\theta^4-\frac{\partial\tilde{u}_r^4}{\partial\theta}\right\rangle+\tilde{\sigma}_{rr}^4\left\langle\tilde{u}_\theta^2-\frac{\partial\tilde{u}_r^2}{\partial\theta}\right\rangle+\tilde{\sigma}_{rr}^6\left\langle\tilde{u}_\theta^1-\frac{\partial\tilde{u}_r^1}{\partial\theta}\right\rangle\right.$$

$$\left.-\tilde{\sigma}_{r\theta}^1\left\langle\tilde{u}_r^6+\tilde{u}_r^{24}+\frac{\partial\tilde{u}_\theta^6}{\partial\theta}+\frac{\partial\tilde{u}_\theta^{24}}{\partial\theta}\right\rangle-\tilde{\sigma}_{r\theta}^2\left\langle\tilde{u}_r^4+\frac{\partial\tilde{u}_\theta^4}{\partial\theta}\right\rangle-\tilde{\sigma}_{r\theta}^4\left\langle\tilde{u}_r^2+\frac{\partial\tilde{u}_\theta^2}{\partial\theta}\right\rangle-\tilde{\sigma}_{r\theta}^6\left\langle\tilde{u}_r^1+\frac{\partial\tilde{u}_\theta^1}{\partial\theta}\right\rangle\right\}$$

$$-\cos\theta\Big\{(ns_1+\Delta s_6+1)\tilde{\sigma}_{rr}^1\left\langle\tilde{u}_r^6+\tilde{u}_r^{24}\right\rangle+(ns_1+\Delta s_4+1)\tilde{\sigma}_{rr}^2\tilde{u}_r^4+(ns_1+\Delta s_2+1)\tilde{\sigma}_{rr}^4\tilde{u}_r^2+(ns_1+1)\tilde{\sigma}_{rr}^6\tilde{u}_r^1$$

$$+(ns_1+\Delta s_6+1)\tilde{\sigma}_{r\theta}^1\left\langle\tilde{u}_\theta^6+\tilde{u}_\theta^{24}\right\rangle+(ns_1+\Delta s_4+1)\tilde{\sigma}_{r\theta}^2\tilde{u}_\theta^4+(ns_1+\Delta s_2+1)\tilde{\sigma}_{r\theta}^4\tilde{u}_\theta^2+(ns_1+1)\tilde{\sigma}_{r\theta}^6\tilde{u}_\theta^1\Big\}\Bigg]d\theta$$

The next constant is for the first elastic field. The first elastic influence is felt in the fourth, sixth, and eleventh fields for n=3, 5, 10 respectfully. The following expression is for n=5 but by changing the indices six to four or eleven can be used for n=3 or 10.

$$I_6^E = \int_{-\pi}^{\pi}\Bigg[\left\{n\tilde{\sigma}_{e_1}^{n-1}\tilde{\sigma}_{e_{16}}+\frac{1}{2}\left(\lambda^2-2\nu\lambda+1\right)\left\langle\tilde{\sigma}_{rr}^1\tilde{\sigma}_{rr}^1+\tilde{\sigma}_{\theta\theta}^1\tilde{\sigma}_{\theta\theta}^1\right\rangle+\left(\lambda^2-2\nu\lambda-\nu\right)\tilde{\sigma}_{rr}^1\tilde{\sigma}_{\theta\theta}^1+(1+\nu)\tilde{\sigma}_{r\theta}^1\tilde{\sigma}_{r\theta}^1\right\}\cos\theta$$

$$-\sin\theta\left\{\tilde{\sigma}_{rr}^1\left\langle\tilde{u}_\theta^6+\tilde{u}_\theta^{E1}-\frac{\partial\tilde{u}_r^6}{\partial\theta}-\frac{\partial\tilde{u}_r^{E1}}{\partial\theta}\right\rangle+\tilde{\sigma}_{rr}^6\left\langle\tilde{u}_\theta^1-\frac{\partial\tilde{u}_r^1}{\partial\theta}\right\rangle-\tilde{\sigma}_{r\theta}^1\left\langle\tilde{u}_r^6+\tilde{u}_r^{E1}+\frac{\partial\tilde{u}_\theta^6}{\partial\theta}+\frac{\partial\tilde{u}_\theta^{E1}}{\partial\theta}\right\rangle-\tilde{\sigma}_{r\theta}^6\left\langle\tilde{u}_r^1+\frac{\partial\tilde{u}_\theta^1}{\partial\theta}\right\rangle\right\}$$

$$-\cos\theta\left\{(s_1+1)\left\langle\tilde{\sigma}_{rr}^1\tilde{u}_r^{E1}+\tilde{\sigma}_{r\theta}^1\tilde{u}_\theta^{E1}\right\rangle+(ns_1+\Delta s_6+1)\left\langle\tilde{\sigma}_{rr}^1\tilde{u}_r^6+\tilde{\sigma}_{r\theta}^1\tilde{u}_\theta^6\right\rangle+(ns_1+1)\left\langle\tilde{\sigma}_{rr}^6\tilde{u}_r^1+\tilde{\sigma}_{r\theta}^6\tilde{u}_\theta^1\right\rangle\right\}\Bigg]d\theta$$

APPENDIX G

FORTRAN PROGRAM TO EXTRACT AND NORMALIZE THE FINITE ELEMENT STRESSES AND DETERMINE THE ANALYTICAL AMPLITUDES

```
C     ****************************************************************
      PROGRAM EXTRACTSTRESS
C     ****************************************************************
C
      IMPLICIT REAL*8 (A-H,O-Z)
      CHARACTER*80 FILE(50),FIELDFILE(10)
      DIMENSION OUTPUT1(4),OUTPUT2(4),RJINT(100),NUMANGLES(10)
      DIMENSION EIGEN(10),ATWO(3),AFOUR(3),SDIFF1(3)
      DIMENSION NRAYS(17,300),COORDINATES(5000,4),VARIABLES(5000,100)
      DIMENSION NRINGS(55,300),ASYMSTRESS(10,10),RL(10,3),RG(6)
      DIMENSION STRESSFIELD(10,2000,10)
C
C     Enter needed constants
C
      SIGNOT=60000
      EMOD=30000000
      EPSNOT=0.002
C
C     Get the names of the PATRAN.NOD files with stresses
C
      CALL FILENAMES(NFILES,FILE)
C
C     Get the groups of nodes for the individual rays
C
      CALL RAYS(NSET1,NUMNODES1,NRAYS)
C
C     Get the groups of nodes for the individual rings
C
      CALL RINGS(NSET2,NUMNODES2,NRINGS)
C
C     Get the coordinates of the nodes
C
      CALL COORDS(NUM,COORDINATES)
C
C     Get the J-integral values for the load steps corresponding
C     to the results in the PATRAN.NOD files
C
      CALL JINTEGRALS(NUMJINT,RJINT)
C
C     Get the filenames which the analytic angular solutions
C     are stored in
C
      CALL FIELDFILENAMES(NFIELDFILES,FIELDFILE)
C
C     Read in the analytic angular solutions
C
      CALL FIELDS(NFIELDFILES,FIELDFILE,NUMANGLES,STRESSFIELD)
C
C     Get the eigenvalues for the analytic solution
C
      CALL EIGENVALUES(NEIGEN,EIGEN,FIRSTCONSTANT)
C
      DO J=1,NFILES,1
         CALL VARIABLE(FILE(J),NUM,VARIABLES)
         DO MMM=1,3,1
```

```
            WRITE(20,*)
            WRITE(30,*)
         ENDDO
         WRITE(20,2)FILE(J)
         WRITE(30,2)FILE(J)
C
C        Find variables for given nodes in node sets in rays
C
         DO K=1,NSET1,1
            WRITE(20,*)
            WRITE(20,*)'Ray: ',K
            WRITE(20,*)
            WRITE(20,*)'Normalized_Quantities:'
            WRITE(20,*)
            WRITE(20,3)
            WRITE(20,*)
            WRITE(30,*)
            WRITE(30,*)'Ray:',K
            WRITE(30,*)
            WRITE(30,*)'Normalized_Quantities:'
            WRITE(30,*)
            WRITE(30,4)
            WRITE(30,*)
            A2=0.0
            A4=0.0
            DO I=1,NUMNODES1,1
               CALL SEARCHRAYS(I,NUM,K,COORDINATES,NRAYS,VARIABLES,
     &                         RR,THETA,OUTPUT1)
               RNORM=RR*SIGNOT/RJINT(J)
               IF((RNORM.LT.15.0).AND.(RNORM.GT.0.0))THEN
                  IF(THETA.LT.3.1415)THEN
                     CALL INTERPOLATESTRESS(THETA,NFIELDFILES,
     &                                NUMANGLES,STRESSFIELD,ASYMSTRESS)
                     CALL COEFF1(SIGNOT,EPSNOT,FIRSTCONSTANT,
     &                           ASYMSTRESS,RR,RJINT(J),EIGEN,RL)
                     CALL COEFF2(RL,RG,OUTPUT1(1),OUTPUT1(2))
                     CALL NEWTON(RG,RL,OUTPUT1(1),OUTPUT1(4),
     &                           A2,A4,ATWO,AFOUR,SDIFF1)
                  ENDIF
                  RLAMBDA=OUTPUT1(3)/(OUTPUT1(1)+OUTPUT1(2))
                  WRITE(20,1) RR*SIGNOT/RJINT(J),THETA,
     &                        OUTPUT1(1)/SIGNOT,
     &                        OUTPUT1(2)/SIGNOT,
     &                        OUTPUT1(3)/SIGNOT,
     &                        OUTPUT1(4)/SIGNOT,RLAMBDA
                  WRITE(30,5) RR*SIGNOT/RJINT(J),THETA,RLAMBDA,
     &                        (ATWO(LL),LL=1,3,1),
     &                        (AFOUR(LL),LL=1,3,1)
               ENDIF
            ENDDO
         ENDDO
C
C        Find variables for given nodes in node sets in rings
C
         DO NNN=1,2,1
```

```
            WRITE(20,*)
            WRITE(30,*)
         ENDDO
         WRITE(20,*)
         WRITE(20,*)'Ring: First_with_normalized_radius_less_than_15'
         WRITE(20,*)
         WRITE(20,*)'Normalized_Quantities:'
         WRITE(20,*)
         WRITE(20,3)
         WRITE(20,*)
         WRITE(30,*)
         WRITE(30,*)'Ring: First_with_normalized_radius_less_than_15'
         WRITE(30,*)
         WRITE(30,*)'Normalized_Quantities:'
         WRITE(30,*)
         WRITE(30,4)
         WRITE(30,*)
         DO K=1,NSET2,1
            A2=0.0
            A4=0.0
            DO I=1,NUMNODES2,1
               CALL SEARCHRINGS(I,NUM,K,COORDINATES,NRINGS,
     &                          VARIABLES,RR,THETA,OUTPUT2)
               RNORM=RR*SIGNOT/RJINT(J)
               IF((RNORM.LT.15.0).AND.(RNORM.GT.0.0))THEN
                  IF(THETA.LT.3.1415)THEN
                     CALL INTERPOLATESTRESS(THETA,NFIELDFILES,
     &                           NUMANGLES,STRESSFIELD,ASYMSTRESS)
                     CALL COEFF1(SIGNOT,EPSNOT,FIRSTCONSTANT,
     &                           ASYMSTRESS,RR,RJINT(J),EIGEN,RL)
                     CALL COEFF2(RL,RG,OUTPUT2(1),OUTPUT2(2))
                     CALL NEWTON(RG,RL,OUTPUT2(1),OUTPUT2(4),
     &                           A2,A4,ATWO,AFOUR,SDIFF1)
                  ENDIF
                  RLAMBDA=OUTPUT2(3)/(OUTPUT2(1)+OUTPUT2(2))
                  WRITE(20,1) RR*SIGNOT/RJINT(J),THETA,
     &                        OUTPUT2(1)/SIGNOT,
     &                        OUTPUT2(2)/SIGNOT,
     &                        OUTPUT2(3)/SIGNOT,
     &                        OUTPUT2(4)/SIGNOT,RLAMBDA
                  WRITE(30,5) RR*SIGNOT/RJINT(J),THETA,RLAMBDA,
     &                        (ATWO(LL),LL=1,3,1),
     &                        (AFOUR(LL),LL=1,3,1)
               ENDIF
            ENDDO
            IF((RNORM.LT.15.0).AND.(RNORM.GT.0.0))THEN
               IF(K.LE.(NSET2-2))THEN
                  WRITE(20,*)
                  WRITE(20,*)'Ring:',K+1
                  WRITE(20,*)
                  WRITE(20,*)'Normalized_Quantities:'
                  WRITE(20,*)
                  WRITE(20,3)
                  WRITE(20,*)
                  WRITE(30,*)
```

```
                WRITE(30,*)'Ring:',K+1
                WRITE(30,*)
                WRITE(30,*)'Normalized_Quantities:'
                WRITE(30,*)
                WRITE(30,4)
                WRITE(30,*)
              ENDIF
            ENDIF
          ENDDO

        ENDDO
C
     1 FORMAT(10(TR1,E12.4))
     2 FORMAT(A80)
     3 FORMAT(TR6,'rbar',TR8,'theta',TR8,'sigrr',TR8,'sigtt',TR8,
      &       'sigzz',TR8,'sigrt',TR7,'lambda')
     4 FORMAT(TR6,'rbar',TR8,'theta',TR7,'lambda',TR9,'A2_1',TR9,
      &       'A2_2',TR9,'A2_3',TR9,'A4_1',TR9,'A4_2',TR9,'A4_3')
     5 FORMAT(9(TR1,E12.4))
C
        STOP
        END
C
C     ****************************************************************
        SUBROUTINE FILENAMES(NFILES,FILE)
C     ****************************************************************
C
        IMPLICIT REAL*8 (A-H,O-Z)
        CHARACTER*80 FILE(50)
C
        OPEN(UNIT=14,FILE='filenames.dat',STATUS='old')
C
        KKK=1
  100   READ(14,1,END=200)FILE(KKK)
        KKK=KKK+1
        GOTO 100
C
  200   KKK=KKK-1
        NFILES=KKK
C
        CLOSE(UNIT=14)
C
     1  FORMAT(A80)
C
        RETURN
        END
C
C     ****************************************************************
        SUBROUTINE FIELDFILENAMES(NFIELDFILES,FIELDFILE)
C     ****************************************************************
C
        IMPLICIT REAL*8 (A-H,O-Z)
        CHARACTER*80 FIELDFILE(10)
C
        OPEN(UNIT=16,FILE='fieldfilenames.dat',STATUS='old')
```

```
C
      KKK=1
  100 READ(16,1,END=200)FIELDFILE(KKK)
      KKK=KKK+1
      GOTO 100
C
  200 KKK=KKK-1
      NFIELDFILES=KKK
C
      CLOSE(UNIT=16)
C
    1 FORMAT(A80)
C
      RETURN
      END
C
C     ******************************************************************
      SUBROUTINE RAYS(NSET1,NUMNODES1,NRAYS)
C     ******************************************************************
C
      IMPLICIT REAL*8 (A-H,O-Z)
      DIMENSION NRAYS(17,300)
C
      OPEN(UNIT=13,FILE='rays.dat',STATUS='old')
C
    1 FORMAT(16(I5))
C
      READ(13,*)NUMNODES1
      III=1
  100 READ(13,1,ERR=200,END=300)(NRAYS(III,J),J=1,NUMNODES1)
      III=III+1
  200 GOTO 100
  300 III=III-1
      NSET1=III
C
      CLOSE(UNIT=13)
C
      RETURN
      END
C
C     ******************************************************************
      SUBROUTINE RINGS(NSET2,NUMNODES2,NRINGS)
C     ******************************************************************
C
      IMPLICIT REAL*8 (A-H,O-Z)
      DIMENSION NRINGS(55,300)
C
      OPEN(UNIT=13,FILE='rings.dat',STATUS='old')
C
    1 FORMAT(16(I5))
C
      READ(13,*)NUMNODES2
      III=1
  100 READ(13,1,ERR=200,END=300)(NRINGS(III,J),J=1,NUMNODES2)
      III=III+1
```

```
  200 GOTO 100
  300 III=III-1
      NSET2=III
C
      CLOSE(UNIT=13)
C
      RETURN
      END
C
C     ****************************************************************
      SUBROUTINE COORDS(NUM,COORDINATES)
C     ****************************************************************
C
      IMPLICIT REAL*8 (A-H,O-Z)
      DIMENSION COORDINATES(5000,4)
C
      OPEN(UNIT=10,FILE='coordinates.dat',STATUS='old')
C
    1 FORMAT(I8,1X,E17.9,1X,E17.9,1X,E17.9)
C
      NUM=1
  100 READ(10,1,ERR=200) NODENUMBER,COORDINATES(NUM,2),
     &                   COORDINATES(NUM,3),COORDINATES(NUM,4)
      COORDINATES(NUM,1)=NODENUMBER
      NUM=NUM+1
      GOTO 100
  200 NUM=NUM-1
C
      CLOSE(UNIT=10)
C
      RETURN
      END
C
C     ****************************************************************
      SUBROUTINE VARIABLE(NAME,NUM,VARIABLES)
C     ****************************************************************
C
      IMPLICIT REAL*8 (A-H,O-Z)
      CHARACTER*80 NAME
      DIMENSION VARIABLES(5000,100)
C
    1 FORMAT(I8,5(E13.7))
    2 FORMAT(5(E13.7))
    3 FORMAT(E13.7)
C
      OPEN(UNIT=11,FILE=NAME,STATUS='old')
C
      READ(11,*)
      READ(11,*)
      READ(11,*)
      READ(11,*)
      DO I=1,NUM,1
         READ(11,1) NODENUMBER,(VARIABLES(I,J),J=2,6,1)
         VARIABLES(I,1)=NODENUMBER
         DO K=1,17,1
```

```
            NSTART=7+(K-1)*5
            NEND=11+(K-1)*5
            READ(11,2) (VARIABLES(I,J),J=NSTART,NEND,1)
         ENDDO
         READ(11,3) VARIABLES(I,NEND+1)
      ENDDO
C
      CLOSE(UNIT=11)
C
      RETURN
      END
C
C     ****************************************************************
      SUBROUTINE JINTEGRALS(NUMJINT,RJINT)
C     ****************************************************************
C
C
      IMPLICIT REAL*8 (A-H,O-Z)
      DIMENSION RJINT(100)
C
      OPEN(UNIT=15,FILE='jintegral.dat',STATUS='old')
C
      III=1
  100 READ(15,1,END=200) RJINT(III)
      III=III+1
      GOTO 100
C
  200 III=III-1
      NUMJINT=III
C
      CLOSE(UNIT=15)
C
    1 FORMAT(F10.2)
C
      RETURN
      END
C
C     ****************************************************************
      SUBROUTINE SEARCHRAYS(I,NUM,NSET1,COORDINATES,NRAYS,
     &                      VARIABLES,RR,THETA,OUTPUT1)
C     ****************************************************************
C
C
      IMPLICIT REAL*8 (A-H,O-Z)
      DIMENSION OUTPUT1(4)
      DIMENSION COORDINATES(5000,4),NRAYS(17,300),VARIABLES(5000,100)
C
C     Find node coordinates
C
      ZERO=0.00000000000
      ONE=1.000000000000
      PIE=4.0*ATAN(ONE)
      DO J=1,NUM,1
         IF(NRAYS(NSET1,I).EQ.INT(COORDINATES(J,1)))THEN
           XX=COORDINATES(J,2)
```

```
            YY=COORDINATES(J,3)
            RR=(XX**2.0+YY**2.0)**0.5
            IF(YY.EQ.ZERO)THEN
              THETA=PIE
              GOTO 100
            ENDIF
            THETA=ATAN(ABS(XX)/ABS(YY))
            IF(YY.GT.ZERO)THETA=PIE-THETA
            GOTO 100
          ENDIF
        ENDDO
C
C       Find variables
C
  100 DO J=1,NUM,1
        IF(NRAYS(NSET1,I).EQ.INT(VARIABLES(J,1)))THEN
          OUTPUT1(1)=VARIABLES(J,2)
          OUTPUT1(2)=VARIABLES(J,3)
          OUTPUT1(3)=VARIABLES(J,4)
          OUTPUT1(4)=VARIABLES(J,5)
          GOTO 200
        ENDIF
      ENDDO
C
  200 RETURN
      END
C
C     ****************************************************************
      SUBROUTINE SEARCHRINGS(I,NUM,NSET2,COORDINATES,NRINGS,
     &                       VARIABLES,RR,THETA,OUTPUT2)
C     ****************************************************************
C
C
      IMPLICIT REAL*8 (A-H,O-Z)
      DIMENSION OUTPUT2(4)
      DIMENSION COORDINATES(5000,4),NRINGS(55,300)
      DIMENSION VARIABLES(5000,100)
C
C     Find node coordinates
C
      ZERO=0.00000000000
      ONE=1.000000000000
      PIE=4.0*ATAN(ONE)
      DO J=1,NUM,1
        IF(NRINGS(NSET2,I).EQ.INT(COORDINATES(J,1)))THEN
          XX=COORDINATES(J,2)
          YY=COORDINATES(J,3)
          RR=(XX**2.0+YY**2.0)**0.5
          IF(YY.EQ.ZERO)THEN
            THETA=PIE
            GOTO 100
          ENDIF
          THETA=ATAN(ABS(XX)/ABS(YY))
          IF(YY.GT.ZERO)THETA=PIE-THETA
          GOTO 100
```

```
         ENDIF
      ENDDO
C
C     Find variables
C
  100 DO J=1,NUM,1
         IF(NRINGS(NSET2,I).EQ.INT(VARIABLES(J,1)))THEN
           OUTPUT2(1)=VARIABLES(J,2)
           OUTPUT2(2)=VARIABLES(J,3)
           OUTPUT2(3)=VARIABLES(J,4)
           OUTPUT2(4)=VARIABLES(J,5)
           GOTO 200
         ENDIF
      ENDDO
C
  200 RETURN
      END
C
C     ****************************************************************
      SUBROUTINE FIELDS(NFIELDFILES,FIELDFILE,NUMANGLES,STRESSFIELD)
C     ****************************************************************
C
C
      IMPLICIT REAL*8 (A-H,O-Z)
      CHARACTER*80 FIELDFILE(10)
      DIMENSION NUMANGLES(10)
      DIMENSION STRESSFIELD(10,2000,10)
C
      DO I=1,NFIELDFILES,1
         OPEN(UNIT=17,FILE=FIELDFILE(I),STATUS='old')
         KKK=1
  100    READ(17,1,ERR=200,END=300)(STRESSFIELD(I,KKK,J),J=1,6,1)
c         IF(I.EQ.6)THEN
c           DO LLL=2,6,1
c              STRESSFIELD(I,KKK,LLL)=0.0
c           ENDDO
c         ENDIF
         KKK=KKK+1
  200    GOTO 100
  300    KKK=KKK-1
         NUMANGLES(I)=KKK
         CLOSE(UNIT=17)
      ENDDO
C
    1 FORMAT(6(E18.10))
C
      RETURN
      END
C
C     ****************************************************************
      SUBROUTINE INTERPOLATESTRESS(THETA,NFIELDFILES,NUMANGLES,
     &                             STRESSFIELD,ASYMSTRESS)
C     ****************************************************************
C
C
```

```
      IMPLICIT REAL*8 (A-H,O-Z)
      DIMENSION NUMANGLES(10)
      DIMENSION ASYMSTRESS(10,10)
      DIMENSION STRESSFIELD(10,2000,10)
C
      DO I=1,NFIELDFILES,1
         DO J=2,NUMANGLES(I),1
            IF((STRESSFIELD(I,J-1,1).LE.THETA).AND.
     &          (STRESSFIELD(I,J,1).GE.THETA))THEN
               DO K=1,5,1
                  ASYMSTRESS(I,K)=STRESSFIELD(I,J-1,K+1)+
     &                 (THETA-STRESSFIELD(I,J-1,1))/
     &                 (STRESSFIELD(I,J,1)-STRESSFIELD(I,J-1,1))*
     &                 (STRESSFIELD(I,J,K+1)-STRESSFIELD(I,J-1,K+1))
               ENDDO
               GOTO 100
            ENDIF
         ENDDO
  100 ENDDO
C
      RETURN
      END
C
C     ****************************************************************
      SUBROUTINE EIGENVALUES(NEIGEN,EIGEN,FIRSTCONSTANT)
C     ****************************************************************
C
      IMPLICIT REAL*8 (A-H,O-Z)
      DIMENSION EIGEN(10)
C
      OPEN(UNIT=18,FILE='eigenvalues.dat',STATUS='old')
C
  100 READ(18,1,ERR=100,END=400)FIRSTCONSTANT
      KKK=1
  200 READ(18,1,ERR=300,END=400)EIGEN(KKK)
      KKK=KKK+1
  300 GOTO 200
  400 KKK=KKK-1
      NEIGEN=KKK
C
      CLOSE(UNIT=18)
C
    1 FORMAT(F11.7)
C
      RETURN
      END
C
C     ****************************************************************
      SUBROUTINE COEFF1(SIGNOT,EPSNOT,FIRSTCONSTANT,ASYMSTRESS,RR,
     &                  RJINTEGRAL,EIGEN,RL)
C     ****************************************************************
C
      IMPLICIT REAL*8 (A-H,O-Z)
      DIMENSION EIGEN(10)
      DIMENSION ASYMSTRESS(10,10),RL(10,3)
```

```
C
      RBAR=SIGNOT*EPSNOT*RR/RJINTEGRAL
      BETA=RJINTEGRAL/(SIGNOT*EPSNOT)
C
      RL(1,1)=SIGNOT*FIRSTCONSTANT**EIGEN(1)*ASYMSTRESS(1,1)*
     &        RBAR**EIGEN(1)
      RL(1,2)=SIGNOT*FIRSTCONSTANT**EIGEN(1)*ASYMSTRESS(1,2)*
     &        RBAR**EIGEN(1)
      RL(1,3)=SIGNOT*FIRSTCONSTANT**EIGEN(1)*ASYMSTRESS(1,3)*
     &        RBAR**EIGEN(1)
      RL(2,1)=SIGNOT*BETA**EIGEN(2)*ASYMSTRESS(2,1)*RBAR**EIGEN(2)
      RL(2,2)=SIGNOT*BETA**EIGEN(2)*ASYMSTRESS(2,2)*RBAR**EIGEN(2)
      RL(2,3)=SIGNOT*BETA**EIGEN(2)*ASYMSTRESS(2,3)*RBAR**EIGEN(2)
      RL(3,1)=SIGNOT*BETA**EIGEN(3)*(BETA/FIRSTCONSTANT)**EIGEN(1)*
     &        ASYMSTRESS(3,1)*RBAR**EIGEN(3)
      RL(3,2)=SIGNOT*BETA**EIGEN(3)*(BETA/FIRSTCONSTANT)**EIGEN(1)*
     &        ASYMSTRESS(3,2)*RBAR**EIGEN(3)
      RL(3,3)=SIGNOT*BETA**EIGEN(3)*(BETA/FIRSTCONSTANT)**EIGEN(1)*
     &        ASYMSTRESS(3,3)*RBAR**EIGEN(3)
      RL(4,1)=SIGNOT*BETA**EIGEN(4)*ASYMSTRESS(4,1)*RBAR**EIGEN(4)
      RL(4,2)=SIGNOT*BETA**EIGEN(4)*ASYMSTRESS(4,2)*RBAR**EIGEN(4)
      RL(4,3)=SIGNOT*BETA**EIGEN(4)*ASYMSTRESS(4,3)*RBAR**EIGEN(4)
      RL(5,1)=SIGNOT*BETA**EIGEN(5)*(BETA/FIRSTCONSTANT)
     &        **(2*EIGEN(1))*ASYMSTRESS(5,1)*RBAR**EIGEN(5)
      RL(5,2)=SIGNOT*BETA**EIGEN(5)*(BETA/FIRSTCONSTANT)
     &        **(2*EIGEN(1))*ASYMSTRESS(5,2)*RBAR**EIGEN(5)
      RL(5,3)=SIGNOT*BETA**EIGEN(5)*(BETA/FIRSTCONSTANT)
     &        **(2*EIGEN(1))*ASYMSTRESS(5,3)*RBAR**EIGEN(5)
      RL(6,1)=SIGNOT*BETA**EIGEN(6)*(BETA/FIRSTCONSTANT)**EIGEN(1)*
     &        ASYMSTRESS(6,1)*RBAR**EIGEN(6)
      RL(6,2)=SIGNOT*BETA**EIGEN(6)*(BETA/FIRSTCONSTANT)**EIGEN(1)*
     &        ASYMSTRESS(6,2)*RBAR**EIGEN(6)
      RL(6,3)=SIGNOT*BETA**EIGEN(6)*(BETA/FIRSTCONSTANT)**EIGEN(1)*
     &        ASYMSTRESS(6,3)*RBAR**EIGEN(6)
C
      RETURN
      END
C
C     ****************************************************************
      SUBROUTINE COEFF2(RL,RG,SIGRR,SIGTT)
C     ****************************************************************
C
      IMPLICIT REAL*8 (A-H,O-Z)
      DIMENSION RG(6)
      DIMENSION RL(10,3)
C
      RG(1)=RL(6,2)*RL(5,1)-RL(6,1)*RL(5,2)
      RG(2)=RL(4,2)*RL(5,1)+RL(6,2)*RL(3,1)-RL(4,1)*RL(5,2)
     &      -RL(6,1)*RL(3,2)
      RG(3)=RL(4,2)*RL(3,1)+RL(6,2)*RL(2,1)-RL(4,1)*RL(3,2)
     &      -RL(6,1)*RL(2,2)
      RG(4)=RL(4,2)*RL(2,1)+RL(6,2)*RL(1,1)-RL(4,1)*RL(2,2)
     &      -RL(6,1)*RL(1,2)-RL(6,2)*SIGRR+RL(6,1)*SIGTT
      RG(5)=RL(4,2)*RL(1,1)-RL(4,2)*SIGRR-RL(4,1)*RL(1,2)
     &      +RL(4,1)*SIGTT
```

```
C
      RETURN
      END
C
C     ****************************************************************
      SUBROUTINE NEWTON(RG,RL,SIGRR,SIGRT,A2,A4,ATWO,AFOUR,SDIFF1)
C     ****************************************************************
C
      IMPLICIT REAL*8 (A-H,O-Z)
      DIMENSION RG(6),ATWO(3),AFOUR(3),SDIFF1(3)
      DIMENSION RL(10,3)
C
      TOL=0.0000000000001
      ITERATION=1
      SDIFF=0.0
      A2=0.0
      I=1
  100 FNOT=RG(1)*A2**4.0+RG(2)*A2**3.0+RG(3)*A2**2.0+RG(4)*A2+RG(5)
      STIFF=4.0*RG(1)*A2**3.0+3.0*RG(2)*A2**2.0+2.0*RG(3)*A2+RG(4)
      A2NEW=A2-FNOT/STIFF
      DIFF=ABS(A2-A2NEW)
      IF(DIFF.GT.TOL)THEN
        A2=A2NEW
        ITERATION=ITERATION+1
        IF(ITERATION.GT.300)THEN
          A2=-1000000000000000000
          A4=-1000000000000000000
          GOTO 200
        ENDIF
        GOTO 100
      ENDIF
      A2=A2NEW
      A4=(SIGRR-(RL(1,1)+RL(2,1)*A2+RL(3,1)*A2**2.0+
     &    RL(5,1)*A2**3.0))/(RL(4,1)+RL(6,1)*A2)
  200 ATWO(I)=A2
      AFOUR(I)=A4
C
      SDIFF1(I)=SIGRT-(RL(1,3)+RL(2,3)*A2+RL(3,3)*A2**2.0+RL(4,3)*A4
     &                 +RL(5,3)*A2**3.0+RL(6,3)*A2*A4)
      IF(I.EQ.1)THEN
        I=I+1
        A2=10.0
        GOTO 100
      ELSEIF(I.EQ.2)THEN
        I=I+1
        A2=-10.0
        GOTO 100
      ELSEIF(I.EQ.3)THEN
        RMAX=10000000000000000
        NUNU=0
        DO JJ=1,3,1
          IF(ATWO(JJ).LT.RMAX)THEN
            RMAX=ATWO(JJ)
            NUNU=NUNU+1
            SDIFF=SDIFF1(JJ)
```

```
              A2=ATWO(JJ)
              A4=AFOUR(JJ)
            ENDIF
          ENDDO
        ENDIF
C
    1 FORMAT(I10,E15.7)
C
        RETURN
        END
C
```

APPENDIX H

FORTRAN PROGRAM TO CALCULATE STRESSES FROM ANALYTIC SOLUTIONS

```
C     ****************************************************************
      PROGRAM PRINCIPLE_STRESSES
C     ****************************************************************
C
      IMPLICIT NONE
      CHARACTER*80 FILENAME(10),NAME
      INTEGER      NUMFILE,NHARD,J
      INTEGER      TEMP(10)
      REAL*8       R,THETA,DELTHETA
      REAL*8       THETAMAX,ZERO,PIE,RT
      REAL*8       STRESSRTHETA(3),DSTRESSRTHETA(3)
      REAL*8       STRESSTEMP(10,2000),EIGENCOEF(10,2),STRESSK(10,10)
      REAL*8       STRESS(10,7,2000)
C
C     Define the data files to be read in
C
      NAME='eigen.dat'
      NUMFILE    = 6
      FILENAME(1)='f1_n10_lambda5_stress.dat'
      FILENAME(2)='f2_n10_lambda5_stress.dat'
      FILENAME(3)='f3_n10_lambda5_stress.dat'
      FILENAME(4)='f4_n10_lambda5_stress.dat'
      FILENAME(5)='f5_n10_lambda5_stress.dat'
      FILENAME(6)='f6_n10_lambda5_stress.dat'
C
      NHARD=10
      WRITE(*,*)'Please enter the normalized radius?'
      read(*,*)R
      R=R*0.002
      THETAMAX=3.141592654
      DELTHETA=3.141592654/90
C
      PIE=4*ACOS((2.0)**(-0.5))
      RT=360.0/(2.0*PIE)
      ZERO=0.00000000000000000000000000000000
C
C     Get angular stress functions
C
      CALL GETALLSTRESSES    (NUMFILE,FILENAME,STRESS)
C
C     Get eigen values and coefficients
C
      CALL GETEIGENCOE (NAME,EIGENCOEF,NUMFILE)
C
C     Define Coefficients
C
      EIGENCOEF(1,2)=(EIGENCOEF(1,2))**EIGENCOEF(1,1)
      EIGENCOEF(3,2)=EIGENCOEF(2,2)**2/EIGENCOEF(1,2)
      EIGENCOEF(5,2)=EIGENCOEF(2,2)**3/EIGENCOEF(1,2)**2
      EIGENCOEF(6,2)=EIGENCOEF(2,2)*EIGENCOEF(4,2)/EIGENCOEF(1,2)
C
C     Initialize angle
C
      THETA=0
C
```

```
C     Get angular stress functions at theta
C
   10 CALL STRESSK_AT_THETA (THETA,NUMFILE,STRESS,STRESSK)
C
C     Get stress at angle
C
      CALL STRESS_R_THETA (NUMFILE,1,R,EIGENCOEF,STRESSK,
     &                     STRESSRTHETA,DSTRESSRTHETA)
C
C     Write angle and stress to output file
C
      WRITE(99,1) THETA,(STRESSRTHETA(J),J=1,3)
C
C     Increment theta
C
      THETA=THETA+DELTHETA
      IF(THETA.LE.THETAMAX) GOTO 10
C
    1 FORMAT(1X,4(F15.7))
C
      STOP
      END
C
C     ****************************************************************
      SUBROUTINE STRESS_R_THETA(NUMFILE,BEGIN,R,EIGENCOEF,STRESSK,
     &                          STRESSRTHETA,DSTRESSRTHETA)
C     ****************************************************************
C
      IMPLICIT NONE
      INTEGER  I,J,NUMFILE,BEGIN
      REAL*8   R
      REAL*8   STRESSRTHETA(3),DSTRESSRTHETA(3)
      REAL*8   EIGENCOEF(10,2),STRESSK(10,10)
C
      DO I=1,3,1
         STRESSRTHETA(I)=0
         DSTRESSRTHETA(I)=0
         DO J=BEGIN,NUMFILE,1
            STRESSRTHETA(I)=STRESSRTHETA(I)+
     &                 EIGENCOEF(J,2)*STRESSK(J,I)*R**EIGENCOEF(J,1)
            DSTRESSRTHETA(I)=DSTRESSRTHETA(I)+
     &                 EIGENCOEF(J,2)*EIGENCOEF(J,1)*STRESSK(J,I)*
     &                 R**(EIGENCOEF(J,1)-1)
         ENDDO
      ENDDO
C
      RETURN
      END
C
C     ****************************************************************
      SUBROUTINE STRESSK_AT_THETA (THETA,NUMFILE,STRESS,STRESSK)
C     ****************************************************************
C
      IMPLICIT NONE
      INTEGER  NUMFILE,I,J,K
```

```
      REAL*8   THETA,PERCENT
      REAL*8   STRESSK(10,10)
      REAL*8   STRESS(10,7,2000)
C
      DO I=1,NUMFILE,1
         DO J=2,STRESS(I,1,1),1
            IF((STRESS(I,2,J).GE.THETA).AND.
     &          (STRESS(I,2,J-1).LE.THETA))THEN
               PERCENT=(THETA-STRESS(I,2,J-1))
     &                 /(STRESS(I,2,J)-STRESS(I,2,J-1))
               DO K=1,5,1
                  STRESSK(I,K)=STRESS(I,K+2,J-1)+PERCENT
     &                       *(STRESS(I,K+2,J)-STRESS(I,K+2,J-1))
               ENDDO
               GOTO 1000
            ENDIF
         ENDDO
 1000 ENDDO
C
      RETURN
      END
C
C     ****************************************************************
      SUBROUTINE GETEIGENCOE(NAME,EIGEN,NUMFILE)
C     ****************************************************************
C
      IMPLICIT NONE
      CHARACTER*80 NAME
      INTEGER I,NUMFILE
      REAL*8  EIGEN(10,2)
C
      OPEN(UNIT=1,FILE=NAME,STATUS='OLD')
C
      WRITE(*,*)'getting eigenvalues'
      DO I=1,NUMFILE,1
         READ(1,*) EIGEN(I,1),EIGEN(I,2)
      ENDDO
C
      CLOSE (UNIT=1)
C
      RETURN
      END
C
C     ****************************************************************
      SUBROUTINE GETALLSTRESSES (NUMFILE,FILENAME,STRESS)
C     ****************************************************************
C
      IMPLICIT      NONE
      INTEGER       I,J,K,NREC,NUMFILE
      CHARACTER*80 FILENAME(10)
      REAL*8        FACTOR
      REAL*8        STRESSTEMP(10,2000)
      REAL*8        STRESS(10,7,2000)
C
      WRITE(*,*)'getting angular distributions'
```

```
      DO I=1,NUMFILE,1
         NREC=0
         CALL ZERO              (STRESSTEMP,10,2000)
         CALL LAST              (FILENAME(I),NREC,STRESSTEMP,6)
C         CALL SORT               (NREC,STRESSTEMP,10,2000)
         STRESS(I,1,1)=NREC
         DO J=2,7,1
            DO K=1,NREC,1
               FACTOR=1.0
C
C              Using Wang's convention
C
c               IF((I.GT.1).AND.(J.GE.3).AND.(J.LE.6))THEN
c                 FACTOR=-1.0
c               ELSE
c                 FACTOR=1.0
c               ENDIF
               STRESS(I,J,K)=FACTOR*STRESSTEMP(J-1,K)
            ENDDO
         ENDDO
      ENDDO
C
      RETURN
      END
C
C     ****************************************************************
      SUBROUTINE LAST(FILENAME,NREC,POTENTIAL,NDIM1)
C     ****************************************************************
C
      IMPLICIT NONE
      CHARACTER*80 FILENAME
      INTEGER I,NREC,NDIM1
      REAL*8  POTENTIAL(10,2000)
C
      OPEN(UNIT=1,FILE=FILENAME,STATUS='OLD')
C
      WRITE(*,*)'reading in data'
      NREC = 1
      READ(1,*)
   10 READ(1,*,ERR=20,END=20) (POTENTIAL(I,NREC),I=1,NDIM1,1)
      NREC = NREC+1
      GOTO 10
   20 NREC = NREC-1
C
      CLOSE (UNIT=1)
C
      RETURN
      END
C
C     ****************************************************************
      SUBROUTINE SORT(NUM,ARRAY,NDIM1,NDIM2)
C     ****************************************************************
C
      IMPLICIT REAL*8 (A-H,O-Z)
      DIMENSION   TEMP(10)
```

```
      DIMENSION   ARRAY(NDIM1,NDIM2)
C
C     Sort data
C
      WRITE(*,*)'sorting'
      DO I=2,NUM,1
         DO J=2,NUM,1
            IF(ARRAY(1,J).LT.ARRAY(1,J-1))THEN
              DO K=1,NDIM1,1
                 TEMP(K)=ARRAY(K,J-1)
              ENDDO
              DO K=1,NDIM1,1
                 ARRAY(K,J-1)=ARRAY(K,J)
              ENDDO
              DO K=1,NDIM1,1
                 ARRAY(K,J)=TEMP(K)
              ENDDO
            ENDIF
         ENDDO
      ENDDO
C
      RETURN
      END
C
C     ****************************************************************
      SUBROUTINE ZERO(ARRAY,NDIM1,NDIM2)
C     ****************************************************************
C
      IMPLICIT REAL*8 (A-H,O-Z)
      DIMENSION   ARRAY(NDIM1,NDIM2)
C
C     zero data
C
      DO I=1,NDIM1,1
         DO J=1,NDIM2,1
            ARRAY(I,J)=0
         ENDDO
      ENDDO
C
      RETURN
      END
C
```

INITIAL DISTRIBUTION

OUTSIDE CENTER

Copies

1 DDRE/Lib

1 CNO/OP 098T

2 OCNR
- 1 332 (Rajapakse)
- 1 332 (Vasudivan)
- 1 0225
- 1 432S
- 1 Lib

1 NAVPGSCOL

1 USNROTCU
NAVADMINU MIT

2 NRL
- 1 Code 6380
- 1 Code 6384

8 NAVSEA
- 1 (SEA03M)
- 1 (SEA03M2)
- 1 (SEA03P)
- 1 (SEA03P1)
- 1 (SEA03P2)
- 1 (SEA03P3)
- 2 (SEA08S)

2 DTIC

5 USNRC
- 1 (M. Mayfield)
- 2 (Dr. S.N. Malik)
- 1 (A. Hiser)
- 1 (Dr. E.M. Hackett)

1 DOE, Oak Ridge

2 NIST, Boulder
- 1 Lib
- 1 (J. Berger)

4 NIST, Washington
- 1 Lib
- 1 (R. Fields)
- 1 (R. DeWitt)
- 1 (J.T. Fong)

1 Brown Univ.
- 1 (Dr. C.F. Shih)

1 Univ. of Illinois
- 1 (Dr. R.H. Dodds, Jr.)

1 Texas A&M Univ.
- 1 (Dr. T.L. Anderson)

2 NASA/Langley
- 1 Lib
- 1 (Dr. J.C. Newman)

1 Hibbit, Karlsson and Sorenson, Inc.

1 University of Washington
- 1 (Dr. A.S. Kobayashi)

1 Univ. of Dayton Research Institute
- 1 (J. Gallagher)

CENTER DISTRIBUTION

Copies

1	0115
1	60
1	60D
1	601
1	602
1	603
1	65
2	65.4
1	66
2	66.3
1	68.
1	68.3
5	61
1	612
1	613
12	614
5	614 (R. Link)
1	615
1	3421
1	3422

NAVSSES

1	62
1	624
1	625

REPORT DOCUMENTATION PAGE

Form Approved
OMB No. 0704-0188

Public reporting burden for this collection of information is estimated to average 1 hour per response, including the time for reviewing instructions, searching existing data sources, gathering and maintaining the data needed, and completing and reviewing the collection of information. Send comments regarding this burden estimate or any other aspect of this collection of information, including suggestions for reducing this burden, to Washington Headquarters Services, Directorate for Information Operations and Reports, 1215 Jefferson Davis Highway, Suite 1204, Arlington, VA 22202-4302, and to the Office of Management and Budget, Paperwork Reduction Project (0704-0188), Washington, DC 20503.

1. AGENCY USE ONLY (Leave blank)	2. REPORT DATE	3. REPORT TYPE AND DATES COVERED
		Final 1/92 - 9/94

4. TITLE AND SUBTITLE

Deformation Limits on Two-Parameter Fracture Mechanics in Terms of Higher Order Asymptotics

5. FUNDING NUMBERS

WU: 1-6140-654
1-6140-654

6. AUTHOR(S)

D.L. Crane
T.L. Anderson

7. PERFORMING ORGANIZATION NAME(S) AND ADDRESS(ES)

Texas A&M University
Department of Mechanical Engineering
College Station, TX 77848

Under contract to:
NSWC
Carderock Division
Annapolis MD 21402

8. PERFORMING ORGANIZATION REPORT NUMBER

CARDIVNSWC-TR-61-CR-94/06

9. SPONSORING / MONITORING AGENCY NAME(S) AND ADDRESS(ES)

Division of Engineering
Office of Nuclear Regulatory Research
U.S. Nuclear Regulatory Commission
Washington DC 2055-0001

10. SPONSORING / MONITORING AGENCY REPORT NUMBER

NUREG/CR-6271

11. SUPPLEMENTARY NOTES

12a. DISTRIBUTION / AVAILABILITY STATEMENT

Approved for public release; distribution is unlimited

12b. DISTRIBUTION CODE

A

13. ABSTRACT *(Maximum 200 words)*

This report addresses the limitations of two-parameter fracture mechanics. We performed an asymptotic analysis of the general power series representation of the crack tip stress potential in an elastic plastic material that obeys a Ramberg-Osgood constitutive law. Expansion of the power series over a substantial number of terms yields only three independent coefficients for low- and medium-hardening materials. The first independent coefficient is uniquely related to the J-integral. The second and third independent coefficients, K2 and K4, are a function of geometry and loading level. A two-parameter theory implies that the crack tip stress fields have two degrees of freedom, but the asymptotic analysis implies that three parameters are required to characterize near-tip conditions. Thus two-parameter fracture theory is a valid engineering model only when there is an approximately unique relationship between K2 and K4.

We performed elastic-plastic finite element analyses on several geometries and evaluated K2 and K4 as a function of deformation level. A reference two-parameter solution (which gives a unique relation between K2 and K4) was provided by the modified boundary layer (MBL) geometry.

Results indicate that the near tip stresses in all but the deeply cracked SENB (a/W=0.5,0.9) and SENT (a/W=0.9) lend themselves to a two-parameter characterization. However, the deeply cracked SENB and SENT specimens maintain a high level of constraint to relatively large deformation levels. Thus single-parameter fracture mechanics is fairly robust for these high constraint geometries, but two-parameter theory is of little value when constraint loss eventually occurs.

14. SUBJECT TERMS

HRR field, J-Q theory, fracture toughness, finite element fracture specimen

15. NUMBER OF PAGES

16. PRICE CODE

17. SECURITY CLASSIFICATION OF REPORT	18. SECURITY CLASSIFICATION OF THIS PAGE	19. SECURITY CLASSIFICATION OF ASSTRACT	20. LIMITATION OF ABSTRACT
Unclassified	Unclassified	Unclassified	Unlimited